NUCLEAR WASTE MANAGEMENT ORGANIZATION
SOCIÉTÉ DE GESTION DES DÉCHETS NUCLÉAIRES

Phase 2 Geoscientific Preliminary Assessment
Geological Mapping

TOWNSHIP OF MANITOUWADGE AND AREA, ONTARIO

APM-REP-01332-0215

NOVEMBER 2017

For more information, please contact:
Nuclear Waste Management Organization
22 St. Clair Avenue East, Sixth Floor
Toronto, Ontario M4T 2S3 Canada
Tel 416.934.9814
Toll Free 1.866.249.6966
Email contactus@nwmo.ca
www.nwmo.ca

Phase 2 Geoscientific Preliminary Assessment
Geological Mapping, Township of Manitouwadge and Area, Ontario

Report Prepared for

Nuclear Waste Management Organization

NWMO Report Number APM-REP-01332-0215

nwmo
NUCLEAR WASTE MANAGEMENT ORGANIZATION
SOCIÉTÉ DE GESTION DES DÉCHETS NUCLÉAIRES

.

Report Prepared by

srk consulting

SRK Consulting (Canada) Inc.
3CN020.005
November 20, 2017

Phase 2 Geoscientific Preliminary Assessment Geological Mapping, Township of Manitouwadge and Area, Ontario

Nuclear Waste Management Organization

22 St. Clair Avenue East, 6th Floor
Toronto, Ontario
M4T 2S3
e-mail: contactus@nwmo.ca
website: www.nwmo.ca
Tel: +1 416 934 9814
Fax: +1 416 934 9526

SRK Consulting (Canada) Inc.
Suite 1300, 151 Yonge Street
Toronto, Ontario, Canada
M5C 2W7
e-mail: toronto@srk.com
website: www.srk.com
Tel: +1 416 601 1445
Fax: +1 416 601 9046

Project Number 3CN020.005

November 20, 2017

Authored by:

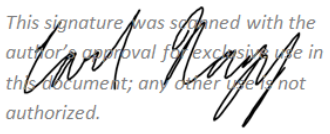

Carl Nagy, MSc, PGeo
Consultant (Structural Geology)
SRK Consulting (Canada) Inc.

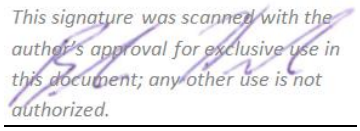

Blair Hrabi, MSc, PGeo
Principal Consultant (Structural Geology)
SRK Consulting (Canada) Inc.

Peer Reviewed by:

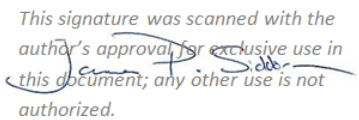

James Siddorn, PhD, PGeo
Principal Consultant (Structural Geology)
SRK Consulting (Canada) Inc.

Cover: Landscape of the Manitouwadge area, Ontario, along Gaffhook Lake road.

EXECUTIVE SUMMARY

This technical report documents the results of the Phase 2 Geological Mapping activity completed in 2016 as part of the Phase 2 Geoscientific Preliminary Assessment, to further assess the suitability of the Manitouwadge area to safely host a deep geological repository. This study followed the successful completion of the Phase 1 Geoscientific Desktop Preliminary Assessment (AECOM, 2014), which identified four withdrawal areas for further field studies. The four withdrawal areas include one in the metasedimentary dominated Quetico Subprovince (Quetico area) and three in the metavolcanic-granitoid dominated Wawa Subprovince (Fourbay Lake pluton area, Black-Pic batholith area - west, and Black-Pic batholith area - east). Geological mapping was completed within and around these withdrawal areas.

The purpose of the Phase 2 Geological Mapping is to advance understanding of the bedrock geology of the withdrawal areas, with an emphasis on observation and analysis of bedrock structure and lithology. Information collected during Phase 2 Geological Mapping also helps to identify areas of exposed bedrock, assess overburden thickness, and identify surface constraints within and around the withdrawal areas, which might affect suitability.

Observations were conducted at select locations that were accessed using existing secondary roads, trail networks and waterbodies, as well as some off-trail hiking. The four areas were mapped over a total period of 57 days by up to three mapping teams, using a consistent workflow and standardized digital data collection system. Observations were made at a total of 551 locations in and around the four withdrawal areas, including 106 stations in the Quetico area, 76 stations in the Fourbay Lake pluton area, 242 stations in the Black-Pic batholith area - west and 127 stations in the Black-Pic batholith area - east.

A digital data collection protocol was applied and observations were compiled into a GIS-compatible database. This includes information on bedrock character (lithology, magnetic susceptibility, gamma ray spectrometry, structure, rock strength), fracture character, bedrock exposure and surface constraints. This report details the field observation for the withdrawal areas.

Table of Contents

List of Tables

List of Appendices

List of Figures

IMPORTANT NOTICE

The Nuclear Waste Management Organization (NWMO) commissioned SRK Consulting (Canada) Inc. (SRK) to conduct a field program to collect observations of general geological features and to conduct detailed mapping in the Manitouwadge area in Ontario. SRK and NWMO retain all rights to methodology, knowledge, and data brought to the work and used therein. No rights to proprietary interests existing prior to the start of the work are passed hereunder other than rights to use same as provided for below. All title and beneficial ownership interests to all intellectual property, including copyright, of any form, including, without limitation, discoveries (patented or otherwise), software, data (hard copies and machine readable) or processes, conceived, designed, written, produced, developed or reduced to practice in the course of the work, shall vest in and remain with NWMO. For greater certainty, all rights, title and interest in the work or deliverables will be owned by NWMO and all intellectual property created, developed or reduced to practice in the course of creating a deliverable or performing the work will be exclusively owned by NWMO.

1 Introduction

This report presents the results of Observations of General Geological Features (OGGF) and Detailed Geological Mapping (collectively to be referred to as Phase 2 Geological Mapping) conducted in 2016 as part of the Phase 2 Geoscientific Preliminary Assessment, to assess the suitability of the Township of Manitouwadge area (the Manitouwadge area) in northwestern Ontario (Figure 1.1), to safely host a deep geological repository as part of NWMO's Adaptive Phased Management (APM) Site Selection process. The Phase 2 Geological Mapping was completed by SRK Consulting (Canada) Inc. (SRK). The results of the Phase 2 Geological Mapping are intended to build on those of the Initial Screening (Geofirma, 2013) and the Phase 1 Geoscientific Desktop Preliminary Assessment (AECOM, 2014).

The Phase 1 Geoscientific Desktop Preliminary Assessment (AECOM, 2014) used available geophysical surveys and geological mapping to identify a number of large potentially suitable areas within the Manitouwadge area warranting further study, including Phase 2 high-resolution geophysical surveys and geological mapping. These subsequent Phase 2 geophysical studies included the results of high-resolution airborne magnetic and gravity geophysical surveys completed by Sander Geophysics Limited (SGL, 2017), that were followed by detailed lineament interpretations completed by SRK Consulting (Canada) Inc. (SRK, 2017) over three large blocks that included four potentially suitable areas. Four rectangular blocks, centred on the potentially suitable areas, identified by the Phase 1 Geoscientific Desktop Preliminary Assessment (AECOM, 2014), were temporarily withdrawn from mineral staking (withdrawal areas) to provide an opportunity for the Phase 2 Geological Mapping field studies to be conducted. The Phase 2 Geological Mapping in the Manitouwadge area focussed on these four withdrawal areas.

The objective of the Phase 2 Geological Mapping was to advance the understanding of the bedrock geology of the four withdrawal areas, with an emphasis on observation and analysis of the bedrock structure and lithology, in the context of the results from the Phase 2 Airborne Geophysical Assessment (SGL, 2017) and the Phase 2 Lineament Assessment (SRK, 2017). Information collected during the Phase 2 Geological Mapping also helped identify areas of exposed bedrock, assess overburden thickness, and identify surface constraints affecting accessibility within withdrawal areas.

The observations were conducted at select locations that were accessed using existing primary and secondary roads, trail networks and waterbodies, in addition to extensive off-trail hiking (Figure 1.2).

1.1 Scope of Work and Work Program

The scope of work for the Phase 2 Geological Mapping comprised three stages, including:

- Stage 1: Pre-mapping planning
- Stage 2: Geological mapping
  (Observation of General Geological Features and Detailed Geological Mapping)
- Stage 3: Synthesis and reporting

During the pre-mapping planning stage, a plan for the observation of general geological features and detailed mapping was developed for the four withdrawal areas identified in the Phase 1 Preliminary

Assessment report (AECOM, 2014) and initial results of the Phase 2 Lineament Interpretation (SRK, in press). These included one area in the Quetico metasedimentary rocks, one area in the Fourbay Lake pluton, and two areas in the Black-Pic batholith (Figure 1.2). During the geological mapping stage, geological information was collected in accordance with the work plan defined during Stage 1 (See Section 4 and Appendix A), and during Stage 3 the information was analysed, compiled and documented in this report.

The four areas were mapped in the summer and fall of 2016 over a total period of approximately 57 mapping days by up to three mapping teams, assisted as-needed by two local guides. Each team consisted of one lead mapping structural geologist and one geotechnical mapper. Several GIS datasets were used as base maps for planning and undertaking the Phase 2 Geological Mapping, including predictive outcrop mapping generated by NWMO using remote sensing data (See Appendix B), high-resolution satellite imagery, recently-acquired high-resolution geophysical data (SGL, 2017), and interpreted lineaments (SRK, 2017).

1.2 Qualifications of the Team

The SRK Group comprises over 1,400 professionals, offering expertise in a wide range of resource engineering disciplines. The SRK Group's independence is ensured by the fact that it holds no equity in any project and that its ownership rests solely with its staff. This fact permits SRK to provide its clients with conflict-free and objective recommendations on crucial judgment issues. SRK has a demonstrated track record in undertaking independent assessments of mineral resources and mineral reserves, project evaluations and audits, technical reports and independent feasibility evaluations to bankable standards on behalf of exploration and mining companies and financial institutions worldwide. The SRK Group has also worked with a large number of major international mining companies and their projects, providing mining industry consultancy service inputs.

The investigations and compilation of the data presented in this report were completed by Mr. Blair Hrabi, Mr. Carl Nagy, Dr. Julia Kramer Bernhard, Mr. Choong Lee, Mr. Ryan Williams, Mr. Ed Saunders, Mr. Matthew Clark, Dr. Lars Weiershäuser, Dr. Alexander Mitrofanov, and Mr. Dominic Chartier. Additional contributions were provided by Dr. James Siddorn. A brief description of their roles and qualifications is provided below.

Mr. Blair Hrabi, MSc, PGeo (APGO #1723) is a Principal Consultant (Structural Geology) with SRK, based in the Toronto office. He is a structural geologist with 22 years of experience gained in the exploration industry, government geological surveys, and academic settings. He has extensive experience in field mapping and structural analysis of Archean and Proterozoic terranes from regional to detailed scales. Mr. Hrabi was the project manager to NWMO, a lead mapping geologist, and second author of this report.

Mr. Carl Nagy, MSc, PGeo (APGO #2551), is a Consultant (Structural Geology) with SRK, based in the Toronto office. He is a structural geologist with over 7 years of experience in the exploration industry, government geological surveys, and academic settings, focused on the study of complex tectonic environments and the evaluation of structural controls on mineral deposits. Mr. Nagy was a lead mapping geologist and the lead author of this report.

Dr. Julia Bernhard Kramer, is a Senior Consultant (Structural Geology) with SRK, based in the Vancouver office. She is a structural geologist with over 19 years of experience gained in the exploration industry, academia, and government geological surveys. She has extensive experience in regional to deposit-scale field mapping and structural analysis of polyphase deformed and

polymetamorphic regions from Archean terranes to active tectonic settings. Dr. Kramer Bernhard was a lead mapping geologist.

Mr. Choong Lee, Mr. Ryan Williams, Mr. Ed Saunders, Mr. Matthew Clark, Dr. Alexander Mitrofanov, Dr. Lars Weiershäuser, and **Mr. Dominic Chartier** are all Consultants or Senior Consultants with the SRK Toronto and Vancouver offices. All individuals have a minimum of 5 years of experience in geological and/or geotechnical studies, and all acted as geotechnical mappers for this project. Dr. Weiershäuser also performed quality control checks on the GIS mapping data.

Dr. James P. Siddorn, PGeo (Practice Leader; APGO #1314) served as a technical advisor and reviewed a draft of this report prior to its delivery to the NWMO as per SRK internal quality management procedures.

1.3 Report Organization

This report was prepared by SRK. A general description of the Manitouwadge area, including location and physiography is provided in Section 2. Section 3 summarizes the regional and local geological setting for the Manitouwadge area. The methodology employed to undertake the Phase 2 Geological Mapping activity is provided in Section 4. Results of the mapping are summarized in Section 5. A summary of the results is included in Section 6, followed by references cited in Section 7. Accompanying figures and appendices are included at the end of the report.

2 Description of the Manitouwadge Area

2.1 Location

The Township of Manitouwadge is located within the District of Thunder Bay in northwestern Ontario, approximately 265 kilometres northeast of Thunder Bay and 310 kilometres north-northwest of Sault Ste. Marie (Figure 1.1). The town site of Manitouwadge (referred to simply as Manitouwadge in the remainder of report) is located on the shore of Manitouwadge Lake, approximately in the centre of the township. Manitouwadge is located at the end of Highway 614, approximately 55 kilometres north of the Trans-Canada Highway (Highway 17).

The four withdrawal area are all located within approximately 50 kilometres of Manitouwadge. One withdrawal area is located within metasedimentary rocks of the Quetico Subprovince, centred approximately 42 kilometres north-northwest of Manitouwadge (Quetico area). A second withdrawal area is located within the Fourbay Lake pluton, centred approximately 24 kilometres southwest of Manitouwadge (Fourbay Lake pluton area). The third and fourth withdrawal areas are located within the Black-Pic batholith, one adjacent to and centred approximately 12 kilometres south of Manitouwadge (Black-Pic batholith area - west), and the other centred approximately 30 kilometres east-southeast of Manitouwadge (Black-Pic batholith area - east). These four areas comprised the main regions of focus during the field visits for this assignment (Figure 1.1).

2.2 Physiography

The Manitouwadge area is located in the Abitibi Uplands physiographic regions (Thurston, 1991), and is characterized by abundant bedrock outcrop overlain by a discontinuous mantle of unconsolidated glacial deposits. The resultant physiography forms low to moderate relief with undulating land surfaces. Locally, elevated terrain and intervening valleys form areas of rugged terrain (Figure 1.2).

Locally, glacial and post-glacial derived overburden form significant areas of overburden. In particular, the majority of the Quetico area within the metasedimentary rocks of the Quetico Subprovince is dominated by significant morainal and organic terrains, accounting for the subdued topography within this area. Within the Black-Pic batholith, in the Black-Pic batholith area - west, south of Manitouwadge, a domain of northeast-trending glaciolacustrine and morainal material is present along the southern portion of the Black River. Within the Black-Pic batholith area - east, to the east-southeast of Manitouwadge, a north-trending domain of glaciofluvial terrain is present in the southeast corner of the area. Beyond these domains of overburden, the areas of interest are dominated by exposed bedrock with a thin veneer of overburden. The bedrock is resistant to weathering and contributes to the rolling to rugged topography and numerous lakes that characterize much of the three areas of interest south of Manitouwadge.

The land surface elevation in the Manitouwadge area ranges from around 485 metres above sea level (masl) just north of Manitouwadge, down to approximately 195 masl in the Pic River valley west of the township (Figure 1.2). In general, the topography of all withdrawal areas is moderately rugged with the exception of the western half of the Quetico area and the southern portion of the Black River valley directly south of Manitouwadge, which are dominated by overburden and have subdued topography. Particularly rugged relief and significant scarps are present along northeast and northwest trends in the Fourbay Lake pluton and within the Black-Pic batholith southwest of

Agonzon Lake (Figure 1.2). These topographic features likely result from preferential erosion along bedrock structures.

2.3 Accessibility

The Manitouwadge area is accessible via Ontario Highway 614, which ends at Manitouwadge after trending northward approximately 50 kilometres from Highway 17 (Trans-Canada Highway). The Caramat Industrial Road is a gravel road that is maintained year-round, and exits Manitouwadge on its west side before heading north and then northwest, near the east and north boundaries of the Quetico area, eventually connecting with Ontario Highway 11. A rail line, operated by Canadian National Railways (CNR), runs northwest through Hillsport and cuts through the northern edge of the Quetico area. An airport with a single, paved 1,050 metre runway is located 5 kilometres south of Manitouwadge.

Access to the Manitouwadge withdrawal areas are provided by a network of secondary and tertiary roads and trails primarily developed during forestry operations (Figure 1.1). Certain of these roads and trails are currently accessible only by all-terrain vehicles (ATVs) or on foot. Greater detail regarding the accessibility of each of the areas of interest is provided in Section 5.

3 Summary of Geology

The geology of the Manitouwadge area is described in detail in the Phase 1 Geoscientific Desktop Preliminary Assessment (AECOM, 2014) which is summarized below. The following sections provide a brief description of the geologic setting, bedrock geology, structural history and mapped structures, metamorphism, and Quaternary geology of the Manitouwadge area.

3.1 Geological Setting

The Manitouwadge area is located within the Superior Province of northern Ontario. The Superior Province is a stable craton created from a collage of ancient plates and accreted juvenile arc terranes that were progressively amalgamated over a period of more than 2 billion years ago (Ga; e.g., Percival et al., 2006). The Superior Province covers an area of approximately 1,500,000 square kilometres and is divided into east-trending subprovinces, including the Wawa and Quetico subprovinces. The Quetico area is located entirely within the Quetico Subprovince, whereas the other three withdrawal areas are located entirely within the Wawa Subprovince (Figure 1.2).

The Wawa Subprovince is composed of a series of narrow belts of metamorphosed volcanic rocks and associated metasedimentary rocks (greenstone belts), separated by granitoid rock units. These volcanic and metasedimentary units typically occur in elongate narrow geometries and represent a relatively minor percentage of the rocks volumetrically. The granitoids consist of massive, foliated and gneissic tonalite-granodiorite, which is cut by massive to foliated granodiorite and granite, and together they represent the vast majority of the rock present throughout the area. The majority of the granitoids were emplaced during or after the deposition of the greenstone belts with which they are associated (Williams et al., 1991).

The Quetico Subprovince consists of variably metamorphosed and migmatized metasedimentary rocks (Zaleski et al., 1995). Granitic intrusions are widely present throughout the Quetico Subprovince, whereas mafic to ultramafic intrusions occur sporadically (Williams, 1989; Sutcliffe, 1991).

3.2 Bedrock Geology

The main bedrock geology units present within the Manitouwadge area include the metasedimentary rocks of the Quetico Subprovince and predominantly gneissic tonalite rocks of the Black-Pic batholith of the Wawa Subprovince. Additional relevant geological units include the Fourbay Lake pluton to the southwest of Manitouwadge, and two gabbroic intrusions, a granite-granodiorite intrusion and a unit of mafic metavolcanic rocks located east of Manitouwadge (Figure 1.2). The southern boundary of a granite-granodiorite intrusion is located along the northern boundary of the northern survey block, but is not considered significant as only a minor amount of this intrusion is located within the interpretation area (see Section 5.1.3).

Three generations of Paleoproterozoic diabase dyke swarms, ranging in age from circa 2.473 to 2.121 Ga, intruded all bedrock units in the Manitouwadge area (Hamilton et al., 2002; Buchan and Ernst, 2004; Halls et al., 2006).

The bedrock in the Manitouwadge area has experienced several generations of ductile and brittle deformation, and the individual rock units have been subjected to varying amounts of metamorphism.

3.2.1 Quetico Subprovince

Metasedimentary Rocks

Metasedimentary rocks of the Quetico Subprovince underlie the majority of the Quetico area, with the exception of the northernmost boundary, which is located along the contact of a granite-granodiorite intrusion (Figure 1.2).

Metasedimentary rocks of the Quetico Subprovince include wacke-pelite-arenite rocks, as well as varying amounts of ironstone, conglomerate, and siltstone (Williams and Breaks, 1996; Zaleski et al., 1999). The Quetico Subprovince is interpreted to be an accretionary prism of an Archean volcanic island-arc system, which developed where the Wawa and Wabigoon belts formed converging arcs (Percival and Williams, 1989). The timing of the Quetico-Wawa belt accretion is constrained to between circa 2.689 Ga and 2.684 Ga (Percival, 1989), and the metasedimentary rocks are dated at 2.700 to 2.688 Ga (Percival, 1989; Zaleski et al., 1999).

Rocks within the Quetico Subprovince have experienced varying degrees of metamorphism and deformation, and commonly exhibit gneissic and migmatitic textures (Percival, 1989; Zaleski et al., 1999). Extensive deformation can be observed in numerous small-scale folds, shear zones, and boudinaged units (Williams and Breaks, 1996). Evidence of extensive metamorphism includes significant volumes of leucosome, resulting from partial melting and segregation during high-grade metamorphism (Williams and Breaks, 1996).

The thickness of the metasedimentary rocks of the Quetico Subprovince have been modelled using gravity and aeromagnetic data with results suggesting that the metasedimentary rocks extend to a depth of about seven and a half kilometres below mean sea level, in the Manitouwadge area. The depth shallows to a minimum of 4.5 km if density variations within the metasedimentary rocks are removed (SGL, 2017).

Granite - Granodiorite Intrusion

The southern boundary of a granite-granodiorite intrusion straddles the northern boundary of the Quetico area (Figure 1.2). Similar intrusions have been mapped elsewhere in the region, and are described as quartzofeldspathic gneisses (Coates, 1970) and biotite leucogranite (Percival, 1989). In general, granitic rocks in the Quetico Subprovince are typically medium- to coarse-grained and massive (Percival, 1989). Crust-derived granitic plutons and pegmatites in the Quetico include circa 2.67 Ga peraluminous granite and circa 2.65 Ga biotite granite (Percival et al., 2006).

3.2.2 Wawa Subprovince

Black-Pic Batholith

The Black-Pic batholith is a regionally extensive intrusion located within the Wawa Subprovince, encompassing an area of approximately 3,000 square kilometres. With the exception of several relatively small, younger intrusions, the bedrock underlying the Black-Pic batholith areas (west and east) is entirely contained within this batholith (Figure 1.2).

The Black-Pic batholith comprises a multi-phase suite of hornblende-biotite monzodiorite, foliated tonalite, and pegmatitic granite, with subordinate foliated diorite, granodiorite, granite and cross-cutting aplitic to pegmatitic dykes (Williams and Breaks, 1989; Zaleski and Peterson, 1993). Local

lithological variations occur throughout the batholith, including upper levels of the tonalite, which are frequently cut by granitic sheets of pegmatite and aplite, and are generally more massive (Williams and Breaks, 1989). Also present throughout the batholith are zones of migmatized sedimentary rocks and massive granodiorite to granite. The contact between these rocks and the tonalitic rocks is gradational and associated with extensive sheeting of the tonalitic unit (Williams and Breaks, 1989; Williams et al., 1991).

The Black-Pic batholith is a structural dome with foliation dips that are shallow to moderate outward from the centre (Williams and Breaks, 1989; 1990). Structurally deeper levels of the tonalite suite contain a strong sub-horizontal foliation and a weak north-trending mineral elongation lineation (Williams and Breaks, 1989).

The age of emplacement of the Black-Pic batholith is constrained by U-Pb (zircon) dating of the oldest recognized phase of the tonalite at circa 2.720 Ga (Jackson et al., 1998). A younger monzodiorite phase is also dated at circa 2.689 Ga (Zaleski et al., 1999). The thickness of the batholith in the Manitouwadge area is not known, but previous regional geologic models of the area (e.g., Lin and Beakhouse, 2013) suggest it may extend to a considerable depth. More recently, the thickness of the Black-Pic batholith has been modelled using gravity and aeromagnetic data with results suggesting that the batholith extends to a depth of about seven and a half kilometres below mean sea level, in the Manitouwadge area (SGL, 2017).

Fourbay Lake Pluton

The Fourbay Lake pluton is an approximately 69 square kilometre elliptical-shaped intrusion located southwest of Manitouwadge and underlies most of the Fourbay Lake pluton area (Figure 1.2). The pluton is mapped as a pyroxene-hornblende-biotite granodiorite (Milne, 1967), and as a hornblende–biotite±clinopyroxene quartz monzodiorite with a massive, medium-grained texture (Beakhouse, 2001).

The Fourbay Lake pluton is evident in geophysical data, and is clearly distinguished from the Black-Pic batholith by a prominent aeromagnetic anomaly with clearly defined boundaries (Milne, 1967; PGW, 2014; SGL, 2017). The elevated magnetic signature relative to the surrounding Black-Pic batholith, may be due to the abundance of iron and iron-titanium oxides (approximately one to two percent) within the pluton (Williams and Breaks, 1996).

U-Pb (zircon) age dating of the Fourbay Lake pluton yielded an age of circa 2.678 Ga (Beakhouse, 2001). The pluton is interpreted as an intrusion in a series of late-stage, likely post-tectonic plutons situated along the central axis of the Black-Pic batholith (Williams and Breaks, 1996). No previous information was available on the depth of the Fourbay Lake intrusion; however, it was expected to extend to considerable depths based on the interpretation of regional gravity data (PGW, 2014) and the regional geological model for the area (Santaguida, 2001; Muir, 2003). More recently, the thickness of the Fourbay Lake pluton has been modelled using gravity and aeromagnetic data with results suggesting that the pluton extends to a depth of around one kilometre below mean sea level (SGL, 2017).

Granite-Granodiorite Intrusion

An unnamed, northeast-trending granite-granodiorite pluton is depicted in the central portion of the Black-Pic batholith area - east (Figure 1.2). This geological unit is present in the compilation map of the area (Johns and McIlraith, 2003), and is based on previous geological maps (Giguere, 1972). No aeromagnetic anomaly is visible based on historic geophysical data (PGW, 2014; Figure 4).

Faries-Moshkinabi Intrusion

The Faries-Moshkinabi intrusion is an east-northeast–trending linear intrusion located between two Black-Pic batholith withdrawal areas (Figure 1.2). The intrusion comprises a series of mafic rocks including websterite, hornblendite, metagabbro, gabbro, anorthositic gabbro, gabbroic anorthosite, and anorthosite (Giguere, 1972). The Faries-Moshkinabi intrusion is in contact to the north with a relatively narrow unit of metavolcanic rocks of the Manitouwadge greenstone belt. The contact between the Faries-Moshkinabi intrusion and the Black-Pic batholith is interpreted to be a thrust-modified tectonic breccia, composed of centimetre- to metre-scale blocks of anorthosite, metawacke, and granitic rocks (Williams and Breaks, 1996).

Based on a previous interpretation of historic geophysical data the Faries-Moshkinabi intrusion is marked by a zone of moderate magnetic intensity that strikes northeastward (PGW, 2014). No data are available on the thickness or age of this intrusion.

Bulldozer Lake Intrusion

The informally named Bulldozer Lake intrusion (AECOM, 2014) is an ellipsoidal gabbroic intrusion, approximately 15 by 10 kilometres, located on the southern boundary of the Black-Pic batholith area – east, to the northeast of the Dotted Lake pluton (Figure 1.2). The Bulldozer Lake intrusion is apparent in geophysical data, and can be differentiated from the surrounding Black-Pic batholith by an elevated magnetic signature (PGW, 2014).

Supracrustal Rocks

Supracrustal rocks of the Wawa Subprovince, proximal to the Manitouwadge Phase 2 Geological Mapping area, include the Manitouwadge and the Schreiber-Hemlo greenstone belts.

The Manitouwadge greenstone belt comprises a semi-continuous suite of metavolcanic and meta-sedimentary rocks and associated intrusions situated along the northern boundary of the Wawa Subprovince (Figure 1.2). The greenstone belt is located completely outside the Phase 2 Geological Mapping areas, and is therefore only summarized briefly within this report.

The Manitouwadge greenstone belt comprises strongly metamorphosed wacke and siltstone metasedimentary rocks, mafic to felsic volcanic rocks, iron formations, and volcanogenic massive sulphide deposits (Zaleski et al., 1999). Locally, sedimentary and volcanic rocks are interwoven both along strike and down dip. East of Manitouwadge, the Faries-Moshkinabi gabbroic intrusion is in contact with the volcanic rocks of the Manitouwadge greenstone belt. Throughout the greenstone belt, bedding is rarely observed, and is typically transposed into planar fabrics due to extensive deformation. The Manitouwadge greenstone belt has been modelled using gravity and aeromagnetic data with results suggesting that it extends to approximately two and a half kilometres below mean sea level (SGL, 2017).

The western part of the Schreiber-Hemlo greenstone belt occurs to the west of the Fourbay Lake pluton area. The belt in this location comprises mafic metavolcanic rocks and associated intrusions of the Schreiber assemblage (Williams et al., 1991). The Schreiber-Hemlo greenstone belt has been modelled using gravity and aeromagnetic data with results suggesting that it extends to a depth of just over one kilometre below mean sea level (SGL, 2017).

3.2.3 Mafic Dykes

Three diabase dyke swarms are known to cross-cut the Manitouwadge area (Figure 1.2), including:

- Northwest-trending Matachewan dykes (circa 2.473 Ga; Buchan and Ernst, 2004). This dyke swarm is one of the largest in the Canadian Shield. Individual dykes are generally up to 10 metres wide, and have vertical to subvertical dips. Matachewan dykes are mainly quartz-diabase dominated by plagioclase, augite, and quartz (Osmani, 1991).
- North-northeast–trending Marathon dykes (circa 2.121 Ga; Buchan et al., 1996; Hamilton et al., 2002). These dykes form a fan-shaped distribution pattern around the northern, eastern, and western flanks of Lake Superior. The dykes vary in orientation from northwest to northeast, and occur as steep to subvertical sheets, typically a few metres to tens of metres thick, but occasionally up to 75 metres thick (Hamilton et al., 2002). The Marathon dykes are quartz-diabase dominated by equigranular to subophitic clinopyroxene and plagioclase (Osmani, 1991).
- Northeast-trending Biscotasing dykes (circa 2.167 Ga; Hamilton et al., 2002). Locally, Marathon dykes also trend northeast and cannot be separated with confidence from the Biscotasing Suite dykes.

The three dyke swarms in the Manitouwadge area are generally distinguishable by their characteristic trend directions, cross-cutting relationships and, to a lesser degree, by their magnetic intensity.

3.3 Structural History

Information on the structural history of the Manitouwadge area is based primarily on structural investigations of the Manitouwadge and Dayohessarah greenstone belts (Polat, 1998; Peterson and Zaleski, 1999) and the Hemlo gold deposit and surrounding region (Muir, 2003). Additional studies by Lin (2001), Percival et al. (2006), and Williams and Breaks (1996) have also contributed to the structural understanding of the area. The aforementioned studies were performed at various scales and with a variety of objectives. Consequently, the following summary of the structural history of the Manitouwadge area should be considered as a best-fit compilation that incorporates relevant findings from all studies. The structural history of the Manitouwadge area is described below and summarized in Table 3.3.1.

The Manitouwadge area straddles a structurally complex boundary between the metasedimentary-migmatitic Quetico Subprovince and the volcano-plutonic Wawa Subprovince within the Archean Superior Province. The structural history of the Manitouwadge and nearby Schreiber-Hemlo greenstone belts is generally well-characterized and includes multiple phases of deformation (Polat et al., 1998; Peterson and Zaleski, 1999; Lin, 2001; and Muir, 2003). Polat et al. (1998) interpreted that the Schreiber-Hemlo and surrounding greenstone belts represent collages of oceanic plateaus, oceanic arcs, and subduction-accretion complexes amalgamated through subsequent episodes of compressional and transpressional collision.

On the basis of overprinting relationships between different structures, Polat et al. (1998) suggested that the Schreiber-Hemlo greenstone belt underwent at least two main episodes of deformation. These deformation events can be correlated with observations from Peterson and Zaleski (1999) and Muir (2003), who reported at least five and six generations of structural elements, respectively. Two of these generations of structures account for most of the ductile strain, and although others can be distinguished on the basis of cross-cutting relationships, they are likely the products of progressive strain events. Integration of the structural histories detailed in Williams and Breaks (1996), Polat et al. (1998), Peterson and Zaleski (1999), Lin (2001), and Muir (2003) suggest that six deformation events occurred within the Manitouwadge area. The first four deformation events (D_1-D_4) are associated with brittle-ductile deformation of the greenstone belts. D_5 and D_6 were associated with a

combination of brittle deformation and fault propagation through all rock units in the Manitouwadge area. The main characteristics of each deformation event are summarized below.

The earliest recognizable deformation phase (D_1) is associated with rarely preserved small-scale isoclinal (F_1) folds, ductile shear zones, and a general lack of penetrative foliation development. Peterson and Zaleski (1999) reported that an S_1 foliation is only preserved locally in outcrop and in thin section. D_1 deformation is poorly constrained to between ca. 2.719 and ca. 2.691 Ga (Muir, 2003).

Table 3.3.1: Summary of the Geological and Structural History of the Manitouwadge Area (adapted from AECOM, 2014)

Approximate Time Period (years before present)	Geological Event
2.89 to 2.77 Ga	Progressive growth and early evolution of the Wawa-Abitibi terrane by collision, and ultimately accretion, of distinct geologic terranes
2.770 – 2.673 Ga	- ca. 2.720 Ga: Volcanism and subordinate sedimentation associated with the formation of the Manitouwadge greenstone belt - ca. <2.693: Deposition of sedimentary rocks in the Manitouwadge greenstone belt and the Quetico Subprovince - ca. 2.720-2.678 Ga: Inferred emplacement of granitoid intrusions in the Manitouwadge area Emplacement of the Pukaskwa and Black-Pic gneissic complexes at ca. 2.72 Ga Emplacement of Loken Lake pluton (ca. 2.687 Ga), Nama Creek pluton (2.680 Ga), and Fourbay Lake pluton (ca. 2.678 Ga) - ca. 2.719 to 2.673 Ga: Four generations of ductile to brittle deformation (D_1-D_4) D1: ca. 2.719 – 2.691 Ga D2: ca. 2.691 – 2.683 Ga D3: ca. 2.682 – 2.679 Ga D4: ca. 2.679 – 2.673 Ga
2.675 to 2.669 Ga	Peak metamorphism of the Manitouwadge greenstone belt
2.666 to 2.650 Ga	Peak metamorphism of the Quetico Subprovince
2.5 to 2.100 Ga	- ca. 2.5 Ga: Supercontinent fragmentation and rifting in Lake Superior area; development of the Southern Province - ca. 2.473 Ga: Emplacement of the Matachewan dyke swarm - ca. 2.167 Ga: Emplacement of Biscotasing dyke swarm - ca. 2.121 Ga: Emplacement of the Marathon dyke swarm
1.9 to 1.7 Ga	Penokean Orogeny in Lake Superior and Lake Huron areas; possible deposition and subsequent erosion in the Manitouwadge area
1.150 to 1.090 Ga	Rifting and formation of the Midcontinent Rift structure - ca. 1.1 Ga
540 to 355 Ma	Possible coverage of the area by marine seas and deposition of carbonate and clastic rocks subsequently removed by erosion
145 to 66 Ma	Possible deposition of marine and terrestrial sediments of Cretaceous age, subsequently removed by erosion
2.6 to 0.01 Ma	Periods of glaciation and deposition of glacial sediments

D_2 structural elements include prevalent open to isoclinal F_2 folds, an axial planar S_2 foliation, and L_2 mineral elongation lineations (Peterson and Zaleski, 1999). Muir (2003) interpreted D_2 to have resulted from progressive north-northeast- to northeast-directed compression that was coeval with the intrusion of various plutons. The S_2 foliation is the dominant meso- to macro-scale regional

fabric evident across the study area. Ductile flow of volcano-sedimentary rocks between more competent batholiths may also have occurred during D_2 deformation. This generation of deformation is constrained to between circa 2.691 and circa 2.683 Ga (Muir, 2003).

D_3 deformation was the result of northwest-southeast shortening during regional dextral transpression. D_3 structural elements include macroscale F_3 folds, including the regional scale isoclinal fold developed within the Manitouwadge greenstone belt, and local shear fabrics that exhibit a dextral sense of motion and overprint D_2 structures (Peterson and Zaleski, 1999; Muir, 2003). D_3 deformation did not develop an extensive penetrative axial planar nor a crenulation cleavage. D_3 deformation is constrained to between circa 2.682 and circa 2.679 Ga (Muir, 2003).

D_4 structural elements include isolated northeast-plunging F_4 kink folds with a Z-asymmetry, and associated small-scale fractures and faults overprinting D_3 structures. D_3-D_4 interference relationships are best developed in the Manitouwadge greenstone belt and in rocks of the Quetico Subprovince. D_4 deformation is roughly constrained to between circa 2.679 and circa 2.673 Ga (Muir, 2003).

Details of structural features associated with the D_5 and D_6 deformation events are limited in the literature to brittle and brittle-ductile shear zones of various scales and orientations (Lin, 2001; Muir, 2003). Within the Hemlo greenstone belt, Muir (2003) suggested that locally D_5 and D_6 faults offset the Marathon and Biscotasing dyke swarms (circa 2.12 -2.17 Ga), and as such, suggested that in the Hemlo region D_5 and D_6 faults propagated after circa 2.1 Ga. However, since there are no absolute age constraints on specific events, the entire D_5-D_6 interval of brittle deformation can only be constrained to a post-2.673 Ga timeframe that may include many periods of re-activation attributable to any of several post-Archean tectonic events.

3.3.1 Mapped Structures and Named Faults

In the Manitouwadge area, in both the Quetico and Wawa subprovinces, numerous faults are indicated on public domain geological maps (Figure 1.2). These faults display four dominant orientations: north, northeast, northwest, and east. Despite the interpretation of multiple mapped faults, few of these structures are named.

Surrounding the Manitouwadge withdrawal areas, several named structures are present, including the north-trending Cadawaja, Slim Lake, and Fox Creek faults, and the northwest-trending Mose Lake fault, all of which offset folded stratigraphy within the Manitouwadge greenstone belt (Chown, 1957; Peterson and Zaleski, 1999). The southern portions of the Cadawaja and Fox Creek faults extend into the northern portion of the Black-Pic batholith area - west (Figure 1.2). A previously mapped, strong north-trending lineament passing through Barehead Lake (Milne, 1967) is named the Barehead Lake fault for this report and projects to the north into the Cadawaja fault. Several named east-trending structures are also present in the area surrounding the withdrawal areas (Figure 1.2), including the Agam Lake, Rabbitskin Lake, and Little Nama Lake faults, which parallel the outline of the Manitouwadge greenstone belt and subprovince boundary, and are typically offset by north-trending faults. Mapping and interpretation of aeromagnetic data (e.g., Miles, 1998), indicates that all mapped faults offset the regional fabric throughout the Manitouwadge area.

Of the aforementioned mapped structures, the north-trending Cadajwa, Slim Lake and Fox Creek faults were mapped as sinistral strike-slip faults (Miles, 1998). The Fox Creek fault exhibits a 60-metre sinistral strike-separation of the Geco volcanogenic massive sulphide (VMS) deposit combined with a minor east-side-up vertical displacement (Milne, 1969). The Cadawaja fault offsets the stratigraphy on the southern edge of the Manitouwadge greenstone belt by 500 metres (Miles, 1998). The east-trending Agam Lake fault was mapped primarily as a brittle strike-slip fault (Chown,

1957). This structure in part follows the volcanic-sedimentary contact and locally may represent a reactivated ductile shear zone (Peterson and Zaleski, 1999).

The north-, northwest- and northeast-trending faults are subparallel and locally adjacent to Marathon, Matachewan, and Biscotasing dykes. Locally, these dykes are offset by younger generations of brittle faulting (e.g., Miles, 1998).

3.4 Metamorphism

In the Manitouwadge area, the metamorphic grade of the exposed rocks of the Manitouwadge greenstone belt ranges from greenschist to upper amphibolite facies (James et al., 1978; Petersen, 1984; Pan and Fleet, 1992). To the north, metasedimentary rocks of the Quetico Subprovince exhibit granulite facies metamorphic conditions close to the boundary between the Wawa and Quetico subprovinces (Williams and Breaks, 1989, 1990; Zaleski and Peterson 1995; Pan et al., 1994). The area overprinted by granulite facies metamorphism is defined by an orthopyroxene isograd approximately 10 kilometres wide that extends from the western portion of the Manitouwadge area westward for over 100 kilometres (Pan et al., 1998). Outside the orthopyroxene isograd, the granulite facies grades into regional upper amphibolite facies metamorphic grade typical of this part of the Quetico Subprovince (Pan et al., 1998).

Geothermobarometric and geochronological calculations by Pan et al. (1994) and Pan et al. (1998) in the Manitouwadge area and surroundings, indicate that low pressure-high temperature, amphibolite facies metamorphism in metasedimentary rocks of the Quetico Subprovince took place before circa 2.666 Ga, in agreement with the period circa 2.671 to 2.665 Ga estimated by Percival and Sullivan (1988). In the Manitouwadge area, this prograde amphibolite facies regional metamorphism would have been initiated circa 2.675 Ga, increased after circa 2.666 Ga and reached granulite facies under a thermal peak of 680 to 700 degrees Celsius (°C) and 4 to 6 Kbar perhaps circa 2.658 Ga. Granulite facies metamorphism would have lasted until circa 2.650 Ga, after which a retrograde event would have occurred at 550 to 660°C, 3 to 4 Kbar. After the retrogression, hydrothermal alteration occurred at 200 to 400°C, 1 to 2 Kbar.

To the south of the Manitouwadge greenstone belt, the Black-Pic batholith and other smaller plutons typically display greenschist facies metamorphism (AECOM, 2014). Locally, higher metamorphic grades up to upper amphibolite facies are recorded in rocks along the margins of plutons. No records exist that suggest that rocks in the Manitouwadge area may have been affected by thermotectonic overprints related to post-Archean events.

3.5 Quaternary Geology

The Quaternary geology of the Manitouwadge area is described in detail in the remote sensing and terrain evaluation completed as part of the Phase 1 Geoscientific Desktop Preliminary assessment (AECOM, 2014). An overview of the relevant Quaternary features are summarized below.

The Quaternary sediments in the Manitouwadge area comprise glacial and post-glacial materials that overlie the bedrock. All glacial landforms and related materials are associated with the Wisconsinan glaciation, which began approximately 115,000 years ago (Barnett, 1992). Throughout the majority of the Manitouwadge area, bedrock outcrops are common and the terrain is dominantly classified, for surficial purposes, as a bedrock-drift complex (i.e. thin drift cover that only locally achieves thicknesses that mask or subdue the bedrock topography). When present, drifts overlying bedrock are typically limited in thickness and the ground surface reflects the bedrock topography (Kristjansson and Geddes, 1985). Beyond bedrock-drift complexes, valleys and lowland areas are

present, which typically exhibit extensive and thick surficial deposits, frequently in a linear geometry.

In the Quetico area, and to a limited extent within the other withdrawal areas, significant areas are covered by ground moraine (till). Two styles of till are documented: moderately loose, stony, sandy till of local derivation that forms a discontinuous veneer over the bedrock, and a calcareous, silt dominated till that contains abundant non-local pebble clasts derived from the James Bay Lowland (Geddes and Kristjansson, 1984; Geddes et al., 1985). Till thickness in the Manitouwadge area is variable and while depths of several metres are present locally; thicknesses are typically less than 3 metres (AECOM, 2014).

In the Fourbay Lake pluton area only a small area in the northwest corner of the withdrawal area is covered by glaciolacustrine deposits and the remainder was mapped as a bedrock terrain

In the Black-Pic batholith area - west, and to a limited extent within the other withdrawal areas, glaciolacustrine sediments cover significant area and trend dominantly to the northeast. These sediments comprise stratified to laminated sand, silt and clay that were deposited during the incursion of glacial lakes into the Manitouwadge area (Prest, 1970; Gartner and McQuay, 1980; Kettles and Way Nee, 1998). The thickness of glaciolacustrine deposits is variable, ranging from several tens of metres to a relative thin drape over bedrock (Kettles and Way Nee, 1998).

In the Black-Pic batholith area - east, and to a limited extent within the other blocks, glaciofluvial outwash deposits cover significant areas. Deposits are generally well-sorted and consist predominantly of stratified sand (Kristjansson and Geddes, 1986). The thicknesses of the outwash deposits are anticipated to be variable.

Minor organic-rich alluvial deposits and eolian deposits are also locally present throughout the Manitouwadge area, and have limited extents. Alluvial deposits are organic-rich, consist of sand, silt and clay, and are typically present along water courses. Eolian deposits consist of sand and are present as dunes developed on certain glacial deposits (Gartner and McQuay, 1980; Kristjansson and Geddes, 1986; Kettles and Way Nee, 1998).

Glacial striae in the Manitouwadge area record that the last direction of glacial movement was toward the south-southwest (Kristjansson and Geddes, 1986).

4 Methodology

The following sections provide an overview of the methods implemented in order to fulfill the requirements of the technical scope of work for the Phase 2 Geological Mapping completed by SRK for the Manitouwadge area in Ontario. Phase 2 Geological Mapping in the Manitouwadge area focused within and around the four withdrawal areas for mapping that were identified in the Phase 1 Geoscientific Desktop Preliminary Assessment report (Figure 1.1).

The OGGF component of the Phase 2 Geological Mapping was intended to acquire a reasonably-sized initial data set at easily accessible outcrops in order to define priority areas on which to concentrate during the subsequent Detailed Outcrop Mapping component. The data collected at each outcrop for both of these components was the same. The methods described below include tasks associated with planning, implementation, and reporting.

4.1 Pre-Mapping Planning

The pre-mapping planning stage of the Phase 2 Geological Mapping was completed prior to mobilizing to the Manitouwadge area. This stage included the development of a list of available source data (Appendix A, Table A.1) and equipment requirements (Appendix A, Table A.2), including calibrations (and documentation thereof) for the planning and implementing the two components of the Phase 2 Geological Mapping. This stage also included the development of a summary list of daily field tasks allocated to each mapping team member (Appendix A, Table A.3).

The key geological attributes to be investigated, along with the methods identified to observe and capture the relevant information at each bedrock outcrop location, were also outlined in the pre-mapping planning stage. This included the use of a digital data capturing method, which for this activity included an ArcGIS compatible data-logging instrument. The instrument consisted of a Trimble (T41 or equivalent) handheld computer that included a customized version of ArcPad data collection software (SRK, 2016) and a database that was consistent with a modified version of the GanFeld database used in previous OGGF mapping projects. The GanFeld system is an Ontario Geological Survey (OGS) standard system for data collection which was originally provided in an open file format by the Geological Survey of Canada (Shimamura et al., 2008). Entry of geological information into the data collector followed a simple data collection protocol (SRK, 2016b) which directed the observer to the appropriate digital form within the database system to capture the appropriate geological information for each geological characteristic being investigated. Additional guidance relevant to the documentation of the geological characteristics is provided in Table A.4 (Appendix A), and, specifically for geomechanical characterization, in Table A.5 (Appendix A).

4.1.1 Predicted Outcrop Filtering and Defining Daily Traverses

The pre-mapping planning stage also included the task of analyzing the spatial distribution of predicted outcrop locations in relation to their distance to the existing road and trail network, and to the key geological features to be investigated during the Phase 2 Geological Mapping. The results from a remote predictive bedrock mapping exercise, provided by the NWMO, show the distribution of predicted bedrock outcrop locations within and around the withdrawal areas (Figure 1.2). The process that was used to undertake the remote predictive bedrock mapping exercise is included in Appendix B below. These predicted outcrops serve as input for the task of defining traverses for the Phase 2 Geological Mapping, as they represent potential targets for direct investigation of exposed

bedrock. The spatial distribution of predicted outcrop locations in relation to their distance to the existing road and trail network, and to the key geological features to be investigated during the Phase 2 Geological Mapping, was assessed. The key geological features include interpreted lineaments, interpreted geophysical anomalies and mapped geological bedrock unit contacts. This task involved filtering and categorizing each predicted outcrop to define target locations to visit during the OGGF and Detailed Outcrop Mapping components of the fieldwork.

The subset of easily accessible outcrops identified to be visited during the initial OGGF component of mapping included predicted outcrops located within 100 metres of existing roads and trails (and where applicable, electrical power and rail corridors) in and around the withdrawal areas. The subset of outcrops identified to be visited during the Detailed Outcrop Mapping stage included outcrops located more than 100 metres from existing roads and trails, and focused within the withdrawal areas. Prior to undertaking the OGFF component, a detailed daily traverse plan including target outcrops for each day was developed. Outcrops that were coincident with, or near to, key geological features, and in close enough proximity that they could reasonably be examined during one day of mapping, were grouped together to form daily traverses.

A simplified outline for the Detailed Outcrop Mapping component was also initially developed, and practical knowledge of the access in the area was incorporated from the OGGF mapping to define a detailed traverse plan for the Detailed Outcrop Mapping component prior to returning to the field for the second and third site visits. During the course of both the OGGF and the Detailed Outcrop Mapping stages, the daily traverses were adjusted to accommodate several considerations, including method(s) of access, weather and overall progress of the mapping.

4.2 Mapping Stage

The information included above provided the planning approach to be taken to meet the objectives of the Phase 2 Geological Mapping, including both of the OGGF and Detailed Outcrop Mapping components. Three site visits were undertaken, the first constituting the OGGF component and the following two constituting the Detailed Outcrop Mapping component. At each identified outcrop traverse location, the geological attributes identified in appendices A.4 and A.5 were investigated.

Prior to starting mapping on the first site visit, a reconnaissance fly-over of all four withdrawal areas was completed to assess the results from the remote predicted outcrop activity and to get an overall understanding of the lay of the land.

An important additional aspect of both the OGGF and Detailed Outcrop Mapping stages was the non-technical workflow that was followed on a daily basis to allow the technical work to be done to meet the required objectives. This included morning safety briefings, equipment calibration checks, data check, data back-up and next day planning (Appendix A, Table A.3). A daily log documented the completion of these tasks. A telephone conference call was held with NWMO every evening during the course of the mapping campaign in order to discuss all aspects of the on-going work. This workflow provided the mechanism for communicating progress with the NWMO during mapping and for prioritizing traverses or making changes to planned traverses.

4.2.1 Proterozoic Mafic Dyke Scanline Fracture Mapping Exercise

Along with compiling observations on Proterozoic mafic dykes that were encountered on daily OGGF and Detailed Outcrop Mapping traverses, three well-exposed examples of mafic dykes were identified as candidates for a scanline fracture mapping exercise, after the completion of the Detailed Outcrop Mapping. The emplacement of these Proterozoic mafic dykes, as outlined in Section 3, is

understood to post-date the penetrative regional ductile deformation that is characteristic of the Superior Province. However, the relationship between dyke emplacement and the brittle deformation history of the Superior Province is less well constrained. The purpose of the scanline fracture mapping exercise is to assess both the nature and extent (if any) of the damage to the bedrock caused by dyke emplacement and the nature and extent of brittle deformation overprinting the dykes themselves. The results from the scanline fracture mapping exercise completed for three Proterozoic mafic dykes are included in Section 5.5 of this report. A summary of the method employed to complete each scanline fracture mapping exercise is described below.

Where a suitable target dyke is located, a scanline is laid out perpendicular to the strike of the dyke contact. One metre intervals were marked for reference along the strike direction, shifting the line to a parallel location where necessary (e.g. overburden cover). Observations of the type and distribution (spacing) of brittle deformation features (veins, faults, joints) were collected systematically within a 1 to 2 m wide swath parallel to the scanline line perpendicular to strike of dyke contact and extending as far as possible into the adjacent bedrock beyond the dyke contacts. Very few dykes have two contacts exposed and the adjacent country rock uncovered, so the transect was defined from the centre of the dyke, across the best exposed contact, and into the bedrock for at least several metres. Additional characteristics such as fracture infill, cross-cutting relationships and offsets were noted, if present.

A sketch of the scanline was drawn, and photographs taken, to highlight key features (dyke contacts, prominent fractures, shifts in the scanline, overburden cover, etc.). Magnetic susceptibility readings were made at each 1 m interval, with five readings used to obtain an average for each measurement location. Host rock foliation on both sides of the dyke was also recorded, if present.

4.3 Synthesis and Reporting Stage

Following the completion of the Detailed Outcrop Mapping stage, the lead mappers drafted this report describing the results from the OGGF and Detailed Outcrop Mapping components of the Phase 2 Geological Mapping. The report is focussed on the objective of increasing the overall understanding of the key geological attributes for the withdrawal areas and the identified withdrawal areas. This report includes the methodologies applied and an interpretation and analysis of the field observations in terms of an update on the new state of knowledge that the observations provide, specific to the withdrawal areas.

Shapefiles delivered to NWMO are in accordance with the types of information entered into the observation database. The list of shapefiles delivered includes:

- Station.
- Lithology.
- Structure.
- Linework.
- Samples.
- Magnetic Susceptibility.
- Gamma Ray Spectrometry.
- Photographs.

All digital photographs were delivered in a zipped folder. Field notebooks were provided by means of a zipped folder of scanned pages. The data delivery also included a summary calibration report that includes copies of all calibration reports provided by third-party equipment providers and summary of results from all calibration activities undertaken during the mapping activities.

Metadata accompanying each shapefile and zipped folder, along with the calibration report, was prepared according to metadata guidelines provided by the NWMO. A summary of the mapping observations is presented in Section 5 of this report.

5 Geological Observation Findings

Geological field investigations in the Manitouwadge area were undertaken by SRK during three separate site visits in the summer and fall of 2016. All site visits focused on the four withdrawal areas based on the general potentially suitable areas identified in the Phase 1 Geoscientific Desktop Preliminary Assessment (AECOM, 2014) and displayed on Figure 1.1. The withdrawal areas include the Quetico area, the Fourbay Lake pluton area, the Black Pic batholith area - west and the Black Pic batholith area - east (Figures 1.1 and 1.2).

The SRK mapping team for the Manitouwadge area comprised:

- Blair Hrabi Lead Geological Mapper
- Julia Bernhard Kramer Lead Geological Mapper
- Carl Nagy Lead Geological Mapper
- Choong Lee Geotechnical Mapper
- Ryan Williams Geotechnical Mapper
- Ed Saunders Geotechnical Mapper
- Matthew Clark Geotechnical Mapper
- Lars Weiershäuser Geotechnical Mapper
- Dominic Chartier Geotechnical Mapper
- Alexander Mitrofanov Geotechnical Mapper

A total of 57 days were spent in the field in the Manitouwadge area over three periods:

- June 30, 2016 to July 17 2016
- August 06, 2016 – August 26, 2016
- September 27, 2016 – October 10, 2016

Geological field observations were made at a total of 551 stations that were investigated during the 57 days. This included observations from: 106 stations in the Quetico area (Section 5.1), 76 stations in the Fourbay Lake pluton area (Section 5.2.), 242 stations in the Black-Pic batholith area - west (Section 5.3), and 127 stations in the Black-Pic batholith area - east (Section 5.4).

Observations relating to Proterozoic mafic dykes and Archean felsic and mafic dykes are included in Section 5.5. A summary of the key findings is presented in Section 6.

5.1 Quetico Area

5.1.1 Accessibility and Surface Constraints

The Quetico area is located approximately 40 kilometres north of Manitouwadge, Ontario and is accessed via a network of logging roads originating from the Caramat Industrial Road (Figure 5.1.1). The Caramat Industrial Road is a primary double track gravel road that is maintained year-round, and leads west from Manitouwadge before heading north and then northwest, eventually connecting with Highway 625 at Caramat and continuing to Highway 11. A series of secondary single track mud and gravel logging roads (passable by 4x4 truck or ATV) originate from the Caramat Industrial Road, and provide partial access to the perimeter of the mapping area (e.g., Figure 5.1.2a). Locally,

the secondary logging roads are obstructed by beaver dams and deteriorated into overgrown trails, limiting access. Tertiary logging roads are locally present throughout the mapping area, and are typically overgrown, not passable by ATV, and required foot traverses. In certain instances, tertiary trails could not be located due to extensive overgrowth. Additional foot access to the Quetico area was provided by a rail corridor in the northeastern portion of the block. At the time of the 2016 field work, the central portion of the block was accessible only by helicopter.

In preparation for renewed logging operations, two east-west roads (Harkness and Bishop Lake roads) were being rebuilt and upgraded in the central and south parts of the Quetico area providing additional access during the third site visit. Access was limited and caution was exercised when working in these areas due to active forestry operations.

5.1.2 Bedrock Exposure and Overburden Thickness

The Quetico area is located in an area previously mapped as bedrock terrain with considerable surficial cover (AECOM, 2014) and generally low relief. A broad region of low topography is evident in the centre of the area. Previously mapped surficial cover consisted of large areas of roughly northeast-trending morainal terrain, and limited areas of organic terrain.

Remotely predicted outcrops for the Quetico area were identified dominantly in the west and southwest parts of the study area, and typically occurred as clusters of outcrops in areas of previous logging (Figure 5.1.1). In these areas, considerable outcrops were predicted in areas previously mapped as overburden. Rare isolated outcrops were also predicted in the central and eastern portion of the study area. In contrast to the western portion of the study area, little outcrop was predicted in areas previously mapped as bedrock in the eastern portion of the mapping area. In general, very limited outcrop was predicted in the eastern portion of the mapping Quetico area.

Of the 106 predicted outcrops visited, 88 (83%) were confirmed to be bedrock, while 18 (17%) were overburden. Field investigations confirmed that predicted outcrops in the western portion of the Quetico area are typically exposed bedrock. The best exposures occurred as elongate semi-exposed ridges and a series of slightly elevated contiguous outcrops. In the eastern portion of the Quetico area, predicted outcrops were confirmed to be small, sparse and of limited value (e.g., poor to moderate exposure, flat lying with a lack of relief, covered with a veneer of overburden). In addition, most of the predicted outcrops in the east of the Quetico area previously mapped as overburden were identified to be overburden (Figure 5.1.2). Areas of overburden are characterized by extensive thick cover (minimum greater than 1 metre).

5.1.3 Lithology and Physical Character

The descriptions below provide an overview of the main and minor bedrock lithological units observed in the Quetico area, including their main physical characteristics. Lithological units described below as main units tend to occur as the predominant rock type covering at least 60% of the exposed bedrock, by area, at any individual bedrock station, and are observed at a high frequency of bedrock stations overall. Minor lithological units described below may occasionally occur as the main rock type at individual bedrock stations, but in general they occur infrequently, and represent only a small portion overall of the bedrock in the Quetico area.

Two main lithological units are observed in the Quetico area, metasedimentary rock derived migmatite, referred to throughout the report as ‘migmatitic metasedimentary rock’, and granite (Figure 5.1.3a). The migmatitic metasedimentary rock unit includes sub-units of metatexite and diatexite (Figure 5.1.3b), as discussed below. A magnetite-rich granite, with characteristics that are

considered distinct enough to separate it from the main granite, is the one minor lithological unit identified in the Quetico area (Figure 5.1.5).

A summary of characteristics of the lithological units encountered in the Quetico area is included in Table 5.1.1 below.

Table 5.1.1: Summary of Bedrock Characteristics by Lithological Unit for the Quetico Area

Lithological Unit	# of Occurrences (% of bedrock stations)	Fabric	Magnetic Susceptibility (average S.I.)	Gamma Spectrometry (average)	Strength (range)
Migmatitic Metasedimentary Rock	70 (80%)	Strongly foliated	2.73 x10^{-3}	K = 2.3% U = 2.2 ppm Th = 12.7 ppm	R3-R5
Granite	67 (76%)	Massive	0.51 x10^{-3}	K = 3.8% U = 2.0 ppm Th = 14.7 ppm	R4-R5
Magnetite-rich Granite	3 (3%)	Massive to weakly foliated	21.44 x10^{-3}	K = 3.5% U = 1.4 ppm Th = 17.9 ppm	R5

Note: Percentages in the second column exceed 100% because more than one rock type can be found at a single station.

5.1.3.1 Migmatitic Metasedimentary Rocks

Migmatitic metasedimentary rock is present throughout all of the Quetico area, observed in 77 of the 88 bedrock outcrops investigated (80%) (Figure 5.1.3a). In these occurrences, the percentage of exposed bedrock underlain by migmatitic metasedimentary rock was observed to range between less than 10% and more than 90% by area. Overall, migmatitic metasedimentary rock is interpreted to represent approximately 70% of the underlying bedrock of the Quetico area (with the remaining 30% comprised dominantly of granite). Migmatitic metasedimentary rock includes two components, the metasedimentary rock remaining after partial melting has occurred, and the leucosome, which is the product of the partial melting. In 62 instances, the amount of leucosome accounted for less than 30% of the migmatitic metasedimentary rock by outcrop area and these occurrences were characterized as metatexites. In 8 instances, the portion of leucosome represented greater than 30% of volume of the outcrop, and the rock was therefore termed a diatexite (Figure 5.1.3b). The diatexites are similar to the metatexites in all other descriptive terms besides percentage of melt observed. A total of 39 representative samples of migmatitic metasedimentary rock were collected during the field investigations.

Typical migmatitic metasedimentary rock comprises centimetre- to metres-wide layers of strongly foliated, medium-grained metasedimentary rocks interlayered with irregular, massive leucosome bands ranging from millimetres to metres thick (Figure 5.1.4a: A-D). The mineralogy of the metasedimentary layers included quartz, feldspar, 10 to 80% biotite, and rare garnet, suggesting the protolith was a quartz-feldspar arenite (i.e., sandstone) with varying degrees of mudstone (equivalent to metamorphic psammite to pelite). The leucosome layers generally have a granitic composition, are composed primarily of medium- to coarse-grained quartz and feldspar, and locally contained less than 10% muscovite and/or biotite. Garnet is locally present, cordierite is rarely present, and a single occurrence of kyanite was noted. These leucosome layers are interpreted to have crystallized from partial melting of a metasedimentary rock protolith. The texture and contact relationships of the leucosome indicates that both in situ leucosome and intrusive leucosome derived further afield are present.

The metasedimentary portion of the migmatitic metasedimentary rock is grey when fresh and beige to brown when weathered. The leucosome portion is white to grey both when fresh and when weathered. In general, the metasedimentary rock portion is less resistant to weathering relative to the leucosome (and adjacent granites), and is preferentially eroded. This phenomenon was observed on both an outcrop and regional scale. On an outcrop scale, layers of metasedimentary rocks are preferentially eroded, while leucosome bodies protruded.

A total of 73 rock hardness measurements were made on the migmatitic metasedimentary rock in the Quetico area. In 53 instances (73%) it exhibited a very strong (R5) character, including 13 for diatexite and 40 for metatexite, in 19 instances (26%) it exhibited a strong (R4) character, including 1 for diatexite and 18 for metatexite, and in one additional instance (metatexite) it exhibited a medium strong (R3) character.

Magnetic susceptibility measurements taken from the metasedimentary portion of the migmatitic metasedimentary rock yielded a range of values from 0.01 to 43.80 $x10^{-3}$ SI (Figure 5.1.4a: E, N=69), an average value of 2.73 $x10^{-3}$ SI, and a standard deviation of 7.77 $x10^{-3}$ SI.

A total of 62 gamma-ray spectrometry measurements were taken from the metasedimentary portion of the migmatitic metasedimentary rocks in the Quetico area (Figure 5.1.4a: F). The measurements yielded the following results:

- Total Count (Range: 90 – 407 Average: 171 Std. Dev: 61)
- Potassium (%) (Range 1.2 – 4.9 Average: 2.3 Std. Dev: 0.8)
- Uranium (ppm) (Range 0 – 9.6 Average: 2.2 Std. Dev: 1.6)
- Thorium (ppm) (Range 5.1 – 40.8 Average: 12.7 Std. Dev: 7.1)

5.1.3.2 Granite

Granite is present throughout the majority of the Quetico area, and was observed in 67 of the 88 bedrock outcrops investigated (76%), with six additional outcrops of very similar composition identified as granodiorite in the field. In these occurrences, the percentage of exposed bedrock underlain by granite was observed to range between less than 10% and more than 90% by area. Overall, granite is interpreted to represent approximately 30% of the underlying bedrock within the Quetico Area (with the remaining 70% comprised dominantly of migmatitic metasedimentary rock). A total of 34 representative samples of granite were collected during the field investigations.

The typical granite is characterized by an equigranular, moderate to very coarse-grained massive texture (Figure 5.1.4b: A, B). It has a white to grey colour (weather and fresh surfaces), and typically contained biotite, and locally muscovite and garnet. The presence of two micas in the granite suggest it was derived from a sedimentary source (i.e., partial melt of sedimentary rocks). Locally, the quartz and feldspar ratios indicate a granodiorite composition.

Intrusive granite units have a number of modes of occurrence. Granite forms centimetre to multi-metre wide layers and pods that are both concordant and discordant to foliated metasedimentary rocks (commonly boudinaged or strongly folded), and is also present as separate granite intrusions cutting the metatexite. Gradational changes from predominantly metasedimentary rocks with variable leucosome percentages to outcrops dominated by intrusive granite with rafts of metasedimentary rock to domains of predominantly, or wholly, granite are common. One large granite-granodiorite intrusion was identified in multiple outcrops in the northeast corner of the Quetico area, and is characterized by medium- to coarse-grained, massive texture with up to 50-centimetre long phenocrysts, and isolated xenoliths of mostly digested metasedimentary rocks.

A total of 54 rock hardness measurements were made on the granite in the Quetico area. In 43 instances (80%) it exhibited a very strong (R5) character, in the remaining 11 instances (20%), it exhibited a strong (R4) character.

Granite yielded low magnetic values, ranging from 0.004 to 4.30 $x10^{-3}$ SI, with an average value of 0.35 $x10^{-3}$ SI (Figure 5.1.4b: C, N=54), and a standard deviation of 0.83 $x10^{-3}$ SI.

A total of 53 gamma-ray spectrometry measurements were taken from granite in the Quetico area (Figure 5.1.4b: D). The measurements yielded the following results:

- Total Count (Range: 60 – 682 Average: 218 Std. Dev: 100)
- Potassium (%) (Range 0.9 – 7.2 Average: 3.8 Std. Dev: 1.3)
- Uranium (ppm) (Range 0 – 15.1 Average: 2.0 Std. Dev: 2.3)
- Thorium (ppm) (Range 0.2 – 68.5 Average: 14.6 Std. Dev: 15.2)

5.1.3.3 Minor Lithological Units

Magnetite-rich Granite

Only one lithological unit, a magnetite-rich granite, was recognized as a minor lithology in the Quetico area (Figures 5.1.5 and 5.1.6). This magnetite-rich granite was clearly distinct from the peraluminous granite described above. Magnetite-rich granite was observed in 3 of the 88 bedrock outcrops investigated (3%). In these occurrences, the percentage of exposed bedrock underlain by magnetite-rich granite range between 30% and more than 90% by area. Overall, magnetite-rich granite is interpreted to represent less than 3% of the underlying bedrock within the Quetico Area. A total of 3 representative samples of magnetite-rich granite were collected during the field investigations.

One occurrence of magnetite-rich granite was observed in a single station southeast of the centre of the study area (Figure 5.1.5). This east-dipping sheet of granite is characterized by a medium-grained, massive texture with up to 5 centimetre long phenocrysts. The granite is grey both when fresh and when weathered. It exhibits an anomalously high magnetic signature (19.84 $x10^{-3}$ SI). The magnetite-rich granite was observed to intrude a peraluminuous granite along a sharp, shallowly dipping contact. Two additional occurrences of magnetite-rich granite, observed in the southeast portion of the study area (Figure 5.1.5), yielded anomalously high magnetic signatures (8.93 and 35.58 $x10^{-3}$ SI). These relative narrow intrusive units were characterized by a fine-grained, homogeneous, equigranular, massive, light pink granite that weathered to a light grey colour. Several other magnetite-rich granite occurrences were observed in the south of the Quetico area. The latter occurrences exhibit similar characteristics as the main granite occurrences, except for elevated magnetic signature.

A total of 3 rock hardness measurements were made on the magnetite-rich granite in the Quetico area. In all instances (100%) it exhibited a very strong (R5) character.

Magnetite-rich granite yielded high magnetic values, ranging from 8.93 to 35.58 $x10^{-3}$ SI, with an average value of 21.45 $x10^{-3}$ SI (N=3), and a standard deviation of 10.94 $x10^{-3}$ SI.

A total of 3 gamma-ray spectrometry measurements were taken from magnetite-rich granite in the Quetico area. The measurements yielded the following results:

- Total Count (Range: 180 – 230 Average: 210 Std. Dev: 22)
- Potassium (%) (Range 3.2 – 3.9 Average: 3.5 Std. Dev: 0.3)
- Uranium (ppm) (Range 0.3 – 3.0 Average: 1.4 Std. Dev: 1.2)

- Thorium (ppm) (Range 14.5 – 21.8 Average: 17.9 Std. Dev: 3.0)

5.1.4 Structure

Ductile and brittle structures that were observed throughout the Quetico area are discussed below and presented in Figures 5.1.7 to 5.1.20. Ductile structures include foliation, gneissic layering, ductile and brittle-ductile shear zones, folds, and associated mineral lineations. Brittle structures include joints, veins, faults, and any associated slickenlines. Fracture infilling minerals, alteration and the orientation of the joint sets are also discussed.

5.1.4.1 Ductile Structure

Ductile structures observed in the Quetico area include extensive penetrative planar fabrics (foliation and gneissosity), and limited folds (fold axial planes and fold axes), ductile and brittle-ductile shear zones, and associated lineations. A summary of ductile structures is presented in Table 5.1.2.

Table 5.1.2: Summary of Ductile Structures in the Quetico Area

Structure Type	Orientation Family	Peak (°)	Frequency (%)	Range (°)	Confidence
Tectonic Foliation	WSW-W	75	19.5	5	High
		90	31.1	17	
	WNW	287	8.2	5	Medium-Low
Gneissic Layering	WSW-W	080	23.5	10	High
		090	33.7	10	
	WNW	287	11.4	10	Medium-Low
	NE	057	9.0	7	Medium-Low
Mineral Foliation	WSW-W	072	17.4	18	High
		090	33.5	8	
Shear Zones	NW	330	27.3	10	High
	NNW	353	16.4	8	Medium
	NNE	015	16.0	9	Medium
	NE	047	20.2	13	High

Tectonic Foliation

Within the Quetico area, a mineral foliation and a gneissosity represented a spectrum of planar fabrics resulting from the alignment and segregation of mineral grains due to progressive deformation. These planar fabrics exhibit similar orientations and minor variations in texture (i.e., locally resided on the boundary between foliated and gneissic), and were interpreted to represent components of a composite tectonic foliation that developed during a single progressive deformation event; these fabrics are therefore discussed together.

A total of 53 mineral foliation and 20 gneissosity measurements were recorded throughout the metasedimentary rocks of the Quetico area (Figures 5.1.7 and 5.1.8). Foliated migmatitic metasedimentary rock is located throughout the entirety of the area (Figures 5.1.11A to 5.1.11D). Mineral foliation is well developed, and is defined predominantly by the alignment of biotite, and in rare instances, muscovite and cordierite. Penetrative planar fabrics are not developed in the granite intrusions or in the leucosome portions of the migmatitic metasedimentary rock. Despite exhibiting an overall consistent orientation, on an outcrop scale the mineral foliation hosted by migmatitic metasedimentary rocks locally anastomosed and was rotated in various orientations around leucosome and granite bodies.

Gneissosity is typically intense and defined by the segregation and alignment of felsic and mafic minerals. Gneissic layering was predominantly observed in the western portion of the block, suggesting that the intensity of deformation may have increased towards the west.

Tectonic foliation, including mineral foliation and gneissosity, typically strikes west to west-southwest, and dip steeply to the north with local reversal to steeply south-dipping (Figure 5.1.8A). The total tectonic foliation population (N = 53) exhibits one broad orientation that ranges between 065° and 115° and which includes one main peak trend at 090° and two lesser peak trends at 075° and 287° (Figure 5.1.8B).

The gneissic layering population (N = 20) exhibits one main broad orientation that ranges between 052° and 115° and which includes two main peak trends at 080° and 090° and one lesser peak trends at 287°. A less prominent orientation peak at 057° is also evident in the gneissic layering dataset (Figure 5.1.8C).

The mineral foliation population (N = 53) exhibits one main broad orientation that ranges between 63° and 112° and which includes one main peak trend at 090° and a lesser peak trend at 072° (Figure 5.1.8D).

A total of four mineral lineations were measured in foliated units. Where observed, lineations are well-defined by the alignment of biotite, and plunge moderately to the west-southwest (Figure 5.1.8E).

Folds (Folds Axes, Fold Axial Planes)

A total of 10 fold axes and four axial planes were measured in the Quetico area, typically within the migmatitic metasedimentary rocks where they are best developed (Figures 5.1.7 and 5.1.8F). Folds occurred on a centimetre to greater than outcrop scale, and were characterized by tight to isoclinal U-, S-, and Z-shaped geometries. Fold axes typically plunge moderately but do not have a preferred direction. A weak second axial planar foliation was measured in a small number of these folds, with axial planes striking either to the southwest and northeast and dipping steeply to the northwest and southeast (Figure 5.1.8F). Less common northwest-trending folds were locally observed.

Folding of the foliated migmatitic metasedimentary rocks indicates that these folds postdate the main deformation event responsible for the formation of the regional foliation and gneissosity.

Ductile and Brittle-Ductile Shear Zones

A total of six shear zones, including five ductile shear zones and a single brittle-ductile shear zone, were measured in the Quetico area, all within the migmatitic metasedimentary rocks in the western and southern portions of the block (Figures 5.1.9 and 5.1.10). Observed ductile shear zones are individually less than 10 centimetres wide and characterized by strong to intense foliation development (Figures 5.1.11E and 5.1.11F). The single brittle-ductile shear zone offsets migmatitic layering and is occupied by a white felsic dyke.

The total population of shear zones are moderately to steeply dipping with northeast and north-northwest trends most common (Figure 5.1.10A). Four orientation peaks, at 330°, 353°, 015° and 047°, are evident in the dataset (Figure 5.1.10B).

Dextral strike-separation was observed on north-northwest-trending ductile shear zones (peaks at 333° and 353°) and sinistral strike-separation on northeast-trending ductile shear zones (peaks at 015° and 042°). No lineations associated with ductile shear zones were observed. These ductile shear

zones are interpreted as minor structures associated with the main deformation event that formed the penetrative tectonic foliation.

5.1.4.2 Brittle Structure

Brittle structures observed in the Quetico area include joints, veins, and faults, and associated slickenlines. A summary of brittle structures is presented in Table 5.1.3 and details are shown in Figures 5.1.12 to 5.1.20.

Table 5.1.3: Summary of Brittle Structures in the Quetico Area

Structure Type	Orientation Family	Peak (°)	Peak Frequency (%)	Range (°)	Confidence
Joints - All	W-WNW	272	8.4	22	Medium-High
		302	8.5	29	Medium-High
	NW	325	5.9	6	Medium-Low
	NNW	342	6.0	5	Medium-Low
	NNE	020	9.0	30	Medium-High
	NE	042	5.6	3	Medium-Low
Joints - Subhorizontal	W	277	14.6	13	Medium
	WNW	303	15.9	11	Medium-High
	N	008	7.6	10	Medium-Low
	NNE	025	8.7	10	Medium-Low
	NE	045	8.7	10	Medium-Low
		060	12.4	14	Medium
Joints - Intermediate	W	275	10.7	14	Medium-Low
	NW	295	17.5	17	Medium-High
		308	14.3	11	Medium
	NNE	013	9.0	9	Medium-Low
	ENE	062	10.2	20	Medium-Low
Joints - Subvertical	W	272	8.0	15	Medium
	WNW	287	5.7	8	Medium-Low
		302	7.5	18	Medium
	NW	325	6.6	10	Medium-Low
	NNW	342	7.0	11	Medium-Low
	NNE	008	6.0	11	Medium-Low
		020	9.9	28	High
	NE	042	5.8	8	Medium-Low
Faults - All	W	275	25.6	11	High
	NW	328	20.7	33	Medium-High
	NNE	018	7.6	6	Medium-Low
	ENE	060	11.5	12	Medium-Low
Veins	WNW	295	25.2	10	Medium-High
	NNW	340	14.1	7	Medium
	NNE	015	24.7	13	Medium-High
	NE	032	28.4	17	Medium-High
Secondary Mineral Infill	W	275	5.9	8	Medium-Low
	WNW	292	11.4	13	Medium
	NW	314	8.1	10	Medium-Low
		325	9.6	12	Medium
	NNW	342	8.2	10	Medium-Low
		352	6.9	10	Medium-Low
	NNE	015	10.0	17	Medium
	NE	036	9.2	18	Medium-Low

Joints

A total of 280 joint measurements were recorded in the Quetico area (Figures 5.1.12 and 5.1.13). Most joint sets are found across the entire area but not necessarily at the same outcrop. Identifying a shallow dipping joint set requires sufficient outcrop topography and were more commonly measured in the more rugged parts of the area or along rock cuts in the railway.

Several steeply dipping joint sets, and one shallowly dipping joint set, are evident in the total joint dataset (Figure 5.1.13A). The total joint population includes a broad north-northeast-trending joint set that ranges between 006° and 036°, and which includes a main central peak trend at 020° (Figure 5.1.13B). It also includes a broad west to west-northwest-trending joint set that ranges between 265° and 314°, and which includes two main peak trends at 272° and 302°. Less prominent joint peak trends are evident at 325° and 342°, defining a northwest-trending joint set, and at 042°, defining a northeast-trending joint set. The north-northeast and west- to west-northwest joint sets are the most common.

Out of the total joint population, 23 joints (8%) dip between 0° and 30°, and are classified as subhorizontal, 20 joints (7%) dip between 31° and 60°, and are classified as intermediate, while the remaining 237 joints (85%) dip greater than 60° and are classified as subvertical. Subhorizontal joints exhibit northeast-trending orientation peaks at 060° and west to northwest-trending orientation peaks at 277° and 303° (Figure 5.1.13C). Intermediate joints exhibit orientation peaks at 295° and 308° (Figure 5.1.13D). Subvertical joints include a broad north-northeast-trending joint set that ranges between 005° and 045°, and which includes a main central peak trend at 020°. Subvertical joints also several west- to north-northwest joint orientation trends at 272°, 287°, 302°, 325° and 342° (Figure 5.1.13E).

Joints with 100 to 500 centimetre spacing are the most common overall in the Quetico area (Figure 5.1.14), and this average spacing is wider than observed in the other three mapping areas. The average spacing is smaller (30 to 100 centimetres) however for the east, northwest, and shallowly dipping joint sets. Figure 5.1.15 illustrates the range of joint spacing encountered and the nature of some of the joint sets in the field.

Outcrops within larger granite intrusions had some of the widest joint spacing and least amount of brittle deformation (e.g., Figures 5.1.15B and 5.1.15E). Conversely, it was commonly observed that joint spacing is tighter in granitic parts of outcrops containing both migmatitic metasedimentary rocks and granitic intrusions (Figure 5.1.15F), suggesting the rheological contrast in the units focussed brittle deformation in the granitic parts of mixed outcrops.

The majority of joints in the Quetico area did not contain any secondary mineral fill or evidence of alteration. Those that did contain fill are typically hematite stained, and less commonly can contain epidote, or quartz. Joints with fill were primarily observed in the southwest portion of the area, but did not form any coherent pattern or spatial relationship to other geological features. A discussion of secondary mineral infilling and alteration observed in association with joints is included below in Section 5.1.4.3.

Faults

A total of 14 faults (13 with a measurable dip) were recorded in the Quetico area, all within the western portion of the study area (Figures 5.1.16 and 5.1.17). Six of the faults are located in migmatitic metasedimentary rocks, and eight are located within granite.

Faults are characterized by discrete slip surfaces typically less than 5 centimetres wide, with minor (centimetre-scale) sinistral offsets (Figure 5.1.18). The majority of these faults are interpreted as minor structural features. However, certain faults are associated with series of sub-parallel joints, and are located adjacent to linear lakes and minor valleys indicating the influence of these faults beyond their immediate area.

Faults have north-northwest, east, and northeast trends and are typically steeply dipping (Figure 5.1.17A). The total fault population includes two main orientation peaks, including one at 275° and one at 328°. The latter also exhibits two lesser peaks on either side of the main peak, at 316° and 347°. Two lesser peaks, at 018° and 060°, are evident in the total fault population (Figure 5.1.17B).

Sinistral faults exhibit one main peak orientation at 327°, with a lesser adjacent peak at 337°, and two lesser peak trends at 018° and 057° (Figure 5.1.17C). Faults with unknown movement history exhibit one main orientation peak at 275°, and lesser peak trends at 315°, 330°, 350° and 062° (Figure 5.1.17D).

Two fault sets had an associated slickenline and these plunge shallowly to subhorizontal to the northwest, west and southwest respectively, suggesting strike- to oblique-slip movement (Figure 5.1.17E).

Two brittle faults contained quartz fill, and one contained hematite fill. The other brittle faults did not contain any secondary minerals. Further discussion of secondary mineral infilling and alteration observed in association with faults is included below in Section 5.1.4.3.

Veins

A total of seven veins were measured in the Quetico area, distributed throughout the area (Figures 5.1.19 and 5.1.20). Three veins are located in the migmatitic metasedimentary rocks, a single vein is located within granite, and the remaining three veins are located within a northeast-trending Proterozoic mafic dyke of the Biscotasing diabase dyke swarm.

Observed veins are typically less than 3 centimetres wide and are filled with quartz, quartz-feldspar, biotite and/or chlorite (e.g., Figures 5.1.20C and 5.1.20D). Five of the seven vein occurrences were interpreted, based on texture, as extensional veins. The other two occurrences were interpreted as shear veins.

Measured veins trend northeast and northwest, and are moderately to steeply dipping (Figure 5.1.20A). The total vein population exhibits orientation peaks at 015°, 032°, 295° and 340° (Figure 5.1.20B). Three veins located in the Biscotasing mafic dyke were oriented parallel and orthogonal to the dyke and likely represent extensional veins. The majority of the remaining veins strike south-southwest.

5.1.4.3 Secondary Minerals/Alteration

Secondary minerals were observed filling limited brittle structures throughout the Quetico area (Figure 5.1.21). In general, brittle structures throughout the Quetico area contained little fill and typically have weak or no alteration. Structures with secondary minerals and alteration are described below and summarized in Table 5.1.4 to Table 5.1.7 below, for all fractures in the Quetico area (N = 301, including 280 joints, 14 faults and 7 veins. Secondary mineral orientation information is summarized in Figure 5.1.22 and some representative field examples are illustrated in Figure 5.1.23.

Overall, 266 out of 301 total fractures (89%) observed exhibited no secondary mineral infill or alteration (Table 5.1.4), leaving 35 fractures (11%) with some evidence of secondary mineral infill or alteration. The majority of secondary mineral infillings and alteration were observed on sub-vertical structures, dipping greater than 60° (Figure 5.1.22A).

The total secondary mineral and alteration fracture population includes several trends, including peak orientations to the north-northeast at 015° and 036°, to the west at 275°, to the west-northwest at 292°, to the northwest at 314° and 325°, and to the north-northwest at 342° and 352° (Figure 5.1.22B).

The most common secondary mineral and alteration types identified within all fractures in the Quetico area are: hematite identified in 20 fractures (7%), epidote in eight fractures (3%), quartz in eight fractures (3%), and chlorite in nine fractures (3%). In some instances, more than one infilling mineral was identified within a single fracture. An additional three fractures (1%) hosted the assemblage of plagioclase+k-feldspar+biotite.

Table 5.1.4: All Fractures – Secondary Minerals and Alteration in the Quetico Area

Mineral Phase/Alteration	All Occurrences	% of Total
Hematite	20	7
Epidote	8	3
Quartz	8	3
Chlorite	9	3
Plag+KF+Bt	3	1
None	266	88
Total # of Fractures	**301**	

Hematite was observed mainly as an iron staining within joints, local veins, and a single brittle fault. Fractures with hematite stain exhibit a wide range of orientations (Figure 5.1.22C). Hematite was the dominant secondary mineral identified in the southern portion of the Quetico area. Epidote was observed mainly filling joints and a single fault along north-northwest and northeast trends (Figure 5.1.22D). Epidote was dominant in the southwestern portion of the Quetico area. Quartz was observed in northwest- to northeast-trending faults, joints and veins (Figure 5.1.22E). Quartz was observed throughout the Quetico area. Chlorite was observed as a coating primarily along west-northwest-trending joint surfaces (Figure 5.1.22F), including within a northeast-trending Biscotasing mafic dyke. Some combination of hematite+chlorite+epidote was a common secondary mineral assemblage within filled fractures.

Secondary mineral infilling and alteration was identified on 25 out of 280 (9%) total documented joints, leaving the remaining 255 occurrences (91%) unfilled (Table 5.1.5) Filled joints include occurrences of hematite (6%), chlorite (3%), epidote (2%), and quartz (<1%). The majority of secondary minerals and alteration were identified on sub-vertical joints.

Table 5.1.5: Joints – Secondary Minerals and Alteration in the Quetico Area

Mineral Phase/Alteration	All Occurrences	% of Total	Subvertical Dip (61-90°)	Intermediate Dip (31-60°)	Subhorizontal Dip (0-30°)
Hematite	17	6	14	2	1
Chlorite	7	3	6	1	0
Epidote	6	2	6	0	0
Quartz	2	<1	2	0	0
None	255	91	215	19	21

Total # of Joints	**280**

Secondary mineral infilling and alteration was identified on four out of 14 (29%) total documented faults, leaving the remaining 10 occurrences (71%) unfilled (Table 5.1.6). Filled faults include occurrences of epidote (14%), quartz (14%) and hematite (7%). All secondary minerals and alteration were identified on sub-vertical faults.

Table 5.1.6: Faults – Secondary Minerals and Alteration in the Quetico Area

Mineral Phase/Alteration	All Occurrences	% of Total	Subvertical Dip (61-90°)	Intermediate Dip (31-60°)	Subhorizontal Dip (0-30°)
Epidote	2	14	2	0	0
Quartz	2	14	2	0	0
Hematite	1	7	1	0	0
None	10	71	8	1	0
Total # of Faults	**14**				

Secondary mineral infilling and alteration for the seven observed veins is shown in Table 5.1.7 below. The most common fills were quartz, chlorite and plagioclase + K-feldspar + biotite, each with three occurrences (43%). Hematite was observed in two veins (29%). The majority of observed veins were subvertical in orientation.

Table 5.1.7: Veins – Secondary Minerals and Alteration in the Quetico Area

Mineral Phase/Alteration	All Occurrences	% of Total	Subvertical Dip (61-90°)	Intermediate Dip (31-60°)	Subhorizontal Dip (0-30°)
Hematite	2	29	2	0	0
Chlorite	3	43	3	0	0
Quartz	3	43	2	1	0
Plag+KF+Bt	3	43	1	2	0
Total # of Veins	**7**				

5.2 Fourbay Lake Pluton Area

5.2.1 Accessibility and Surface Constraints

The Fourbay Lake pluton area is located approximately 25 kilometres southwest of Manitouwadge and can be accessed via a network of logging roads and trails originating from two, well-maintained, secondary roads (Figure 5.2.1). The Gaffhook Lake road is a maintained single track gravel road that originates from the Caramat Industrial Road approximately 7 kilometres west of Manitouwadge, and links up to a series of trails accessing the northwestern portion of the area. The Barehead road is a maintained single track secondary gravel road originating from Highway 614, approximately 12 kilometres south of Manitouwadge, and provides access to a series of trails and an electric power transmission line that crosses from northwest to southeast across the central-eastern portion of the area (e.g., Figures 5.2.2A and 5.2.2B). Beyond these secondary roads, former logging roads have degraded into overgrown trails that were partially passable by ATV. Once trails degraded to an unpassable level, extensive foot traverses were required. These trails, in conjunction with foot traverses provided access to the majority of the study area, and no boat or helicopter access was required. Minor forestry operations were active in the Fourbay Lake pluton area during the final days of mapping.

5.2.2 Bedrock Exposure and Overburden Thickness

The Fourbay Lake pluton area is located in an area previously mapped as bedrock terrain with very limited surficial cover (AECOM, 2014, Figure 2.3). Remotely predicted outcrop for this area identified series of elongated northeast-trending clusters of relatively small outcrops (Figure 5.2.1), typically located along elevated ridges, and isolated outcrops located along previously excavated trails and the hydro corridor (Figures 5.2.2A and 5.2.2B). Predicted outcrop are roughly evenly spaced throughout the study area. A lack of outcrop was predicted in the south-central portion of the area, with the exception of minor outcrop along the electric power transmission line.

Of the 76 predicted outcrops visited, 68 (89%) were confirmed to be bedrock, while eight (11%) were overburden. Verification of predicted outcrop while mapping confirmed that the best outcrop exposures occur as series of large scarps and rock faces along northeast-trending topographic ridges (Figures 5.2.2C and 5.2.2D). Away from ridges, limited isolated outcrops were observed to occur in dense bush. A small number of predicted outcrops were identified as areas of exposed grey clay (Figures 5.2.2E and 5.2.2F). Mapping has confirmed that areas of no predicted outcrop are indeed characterized by extensive thick overburden (generally greater than 1 metre depth). These areas of surficial cover were often observed to occur in broad northeast-oriented valleys.

5.2.3 Lithology and Physical Character

The descriptions below provide an overview of the main and minor bedrock lithological units observed in the Fourbay Lake pluton area, including their main physical characteristics. Lithological units described below as main units tend to occur as the predominant rock type covering at least 60% of the exposed bedrock, by area, at any individual bedrock station, and are observed at a high frequency of bedrock stations overall. Minor lithological units described below may occasionally occur as the main rock type at individual bedrock stations, but in general they occur infrequently, and represent only a small portion overall of the bedrock in the Fourbay Lake pluton area.

Diorite to granodiorite of the Fourbay Lake pluton was the only main lithology type observed in the Fourbay Lake pluton area (Figures 5.2.3 and 5.2.4). Minor lithological units observed in the Fourbay Lake pluton area include several occurrences of granite and a single outcrop of tonalite (Figure 5.2.5).

A summary of characteristics of the lithological units encountered in the Fourbay Lake pluton area is included in Table 5.2.1 below.

Table 5.2.1: Summary of Bedrock Characteristics by Lithological Unit for the Fourbay Lake Pluton Area

Lithological Unit	# of Occurrences (% of bedrock stations)	Fabric	Magnetic Susceptibility (average S.I.)	Gamma Spectrometry (average)	Strength (range)
Diorite to Granodiorite	66 (97%)	Massive to weakly foliated	Diorite: 18.095 x10-3 Granodiorite: 19.866 x10^{-3}	Diorite: K = 2.7% U = 1.1 ppm Th = 7.6 ppm Granodiorite: K = 2.7% U = 1.2 ppm Th = 7.6 ppm	R5-R6
Granite	9 (13%)	Massive	5.125 x10^{-3}	K = 3.8% U = 2.1 ppm Th = 7.2 ppm	R4-R6
Tonalite	1 (1%)	Foliated	7.236 x10^{-3}	K = 1.1% U = 0.0 ppm Th = 3.1 ppm	R5

Note: Percentages in the second column exceed 100% because more than one rock type can be found at a single station.

5.2.3.1 Diorite to Granodiorite

The Fourbay Lake pluton area is located predominantly within a diorite to granodiorite pluton, understood to be the Fourbay Lake pluton (Figure 5.2.3). Dioritic to granodioritic units were observed at a total of 66 out of 68 bedrock outcrop stations (97%), including 3 stations that had multiple outcrops of diorite or granodiorite mapped (69 outcrops total). These include 26 outcrops of diorite and 43 outcrops of granodiorite. In all but three occurrences, the diorite or granodiorite accounted for more than 90% of the exposed outcrop, by area (e.g., Figure 5.2.4A). Overall, this unit is interpreted to represent greater than 90% of the underlying bedrock of the Fourbay Lake pluton area. A total of 22 and 29 representative samples of diorite and granodiorite, respectively, were collected during the field investigations.

Diorite and granodiorite were observed throughout the Fourbay Lake pluton area, with the exception of the northwest corner of the study area, which is located within the Black-Pic batholith (Figure 5.2.3). Diorite observations form a large cluster in the northern half of the study area, while granodiorite was observed in the remainder of the study area. These observations may indicate the presence of different compositional phases of the pluton, but the contact between the two was not sharply defined, and is interpreted to be gradational in nature.

Diorite to granodiorite is characterized by an equigranular, fine- to medium-grained crystal form (0.5 to 5 millimetre crystals), massive to locally weakly foliated texture (Figures 5.2.4B and 5.2.4C). Diorite to granodiorite is off-white to pink where fresh and light grey to off white where weathered. Subtle variation in quartz and feldspar content was the basis for distinguishing between the diorite and granodiorite, and accessory minerals characteristically include hornblende ± biotite and high magnetite. The intrusion is typically homogeneous, and is locally intruded by felsic dykes. Centimetre-scale, rounded xenoliths of more mafic composition are characteristic of the pluton (Figure 5.2.4D).

A total of 69 rock hardness measurements were made on the diorite to granodiorite in the Fourbay Lake pluton area. In 66 instances (96%) it exhibited a very strong (R5) character, in the remaining three instances (4%), it exhibited an extremely strong (R6) character.

A total of 66 magnetic susceptibility measurements of the diorite to granodiorite typically yielded very high readings with similar results for both the dioritic and granodioritic end members (Figure 5.2.4E). Diorite measurements range from 3.17 $x10^{-3}$ SI to 54.98 $x10^{-3}$ SI, with an average value of 18.10 $x10^{-3}$ SI, and a standard deviation of 13.04 $x10^{-3}$ SI. Granodiorite measurements range from 5.00 $x10^{-3}$ SI to 34.86 $x10^{-3}$ SI, with an average value of 19.87 $x10^{-3}$ SI, and a standard deviation of 8.14 $x10^{-3}$ SI.

A total of 66 gamma-ray spectrometry measurements were taken from diorite to granodiorite in the Fourbay Lake pluton area (Figure 5.2.4F). The measurements yielded the following results for diorite:

- Total Count (Range: 87 – 200 Average: 144 Std. Dev: 31)
- Potassium (%) (Range 1.9 – 4.5 Average: 2.7 Std. Dev: 0.6)
- Uranium (ppm) (Range 0 – 2.2 Average: 1.1 Std. Dev: 0.7)
- Thorium (ppm) (Range 3.5 – 14.3 Average: 7.6 Std. Dev: 3.3)

The measurements yielded the following results for granodiorite:

- Total Count (Range: 96 – 210 Average: 144 Std. Dev: 25)
- Potassium (%) (Range 2.0 – 3.5 Average: 2.7 Std. Dev: 0.3)
- Uranium (ppm) (Range 0 – 3.8 Average: 1.2 Std. Dev: 0.8)
- Thorium (ppm) (Range 1.9 – 16.5 Average: 7.6 Std. Dev: 3.5)

5.2.3.2 Minor Lithological Units

Two minor lithological units were observed in the Fourbay Lake pluton area and include isolated occurrences of intrusive granite and an occurrence of tonalite of the Black-Pic batholith (Figure 5.2.5).

Granite

Granite was observed in 15 of the 76 bedrock outcrops investigated (20%) in the Fourbay Lake pluton area (Figure 5.2.5). In 12 of these occurrences, the percentage of exposed bedrock underlain by granite was less than 10% by area, and no occurrence accounted for more than 60%.

Granite primarily occurs as a range of centimetre to half-metre wide linear to curvilinear dykes intruding the diorite to granodiorite in multiple orientations throughout the Fourbay Lake pluton area (Figures 5.2.6A-B). In one instance (Station 16BH0151), granite of similar composition and texture to the dykes was observed to comprise half of the outcrop and was interpreted as a minor intrusion (Figures 5.2.6C-D).

Granite is characterized by multiple crystal forms (porphyritic, equigranular, inequigranular, vari-texture), medium to very coarse grain size (1 to 50 millimetre crystals), and massive in texture. Granite is pink on both fresh and weathered surfaces.

A total of 13 rock hardness measurements were made on the granite in the Fourbay Lake pluton area. In 11 instances (85) it exhibited a very strong (R5) character. It exhibited a strong (R4) character, and an extremely strong (R6) character, in one each of the two other instances.

A total of 9 magnetic susceptibility measurements were made on the granite and these yielded an average value of 21.45 $x10^{-3}$ SI. A total of 3 gamma-ray spectrometry measurements were taken from granite in the Quetico area with the following average results: K = 3.9%; U = 2.1 ppm; and Th = 7.2 ppm.

Tonalite

Tonalite was observed in a single occurrence in the northwest corner of the study area beyond the margin of the Fourbay Lake pluton (Figure 5.2.5). Tonalite is characterized by an equigranular, medium-grained crystal form (0.5 to 5 millimetre crystals) and foliated texture (Figure 5.2.6E). Tonalite is light-grey on both fresh and weathered surfaces.

One rock hardness measurement on the tonalite yielded a very strong (R5) character, one magnetic susceptibility value was measured in tonalite with a result of 7.24 $x10^{-3}$ SI, and one gamma-ray spectrometry measurement was taken from tonalite in the Quetico area with the following result: Total Count = 57, K = 1.1%, U = 0.0 ppm, and Th = 3.1 ppm.

5.2.4 Structure

Ductile and brittle structures observed throughout the Fourbay Lake pluton area are discussed below and presented in Figures 5.2.7 to 5.2.20. Ductile structures include foliation, shear zones and associated mineral lineations. Brittle structures include joints, veins, faults, and associated lineations (i.e., slickenlines). Fracture infilling minerals, alteration and the orientation of the hosting fracture sets are also discussed.

5.2.4.1 Ductile Structure

Ductile structures observed in the Fourbay Lake pluton area include limited foliation, and a very limited number of ductile shear zones and mineral lineations. While many of these features can be described qualitatively, statistically many of them represent uniform distributions, or there is too little data to provide meaningful average values. A summary of ductile structures is presented in Table 5.2.2.

Table 5.2.2: Summary of Ductile Structures in the Fourbay Lake Pluton Area

Structure Type	Orientation Family	Peak (°)	Frequency (%)	Range (°)	Confidence
Tectonic Foliation	N-NNE	355	20.5	20	High
		015	19.9	18	High
	NE	038	12.7	12	Medium
Shear Zones	WNW	297	50	5	Medium-high
	NNW	330	50	5	Medium-high

Tectonic Foliation

A total of 22 tectonic foliation measurements (21 with a measured dip) were recorded in the diorite to granodiorite (Figures 5.2.7 and 5.2.8), dominantly within the central-eastern portion of the Fourbay Lake pluton area. In the remainder of the pluton, ductile fabrics are absent and the diorite to granodiorite exhibits a homogeneous massive texture.

The only type of tectonic foliation recognized in the Four Bay Lake pluton area is a mineral foliation. This mineral foliation is defined by a weak to moderate, linear to anastomosing alignment of hornblende, and locally biotite and feldspar (Figure 5.2.11). Locally the mineral foliation wraps

around xenoliths. The style, intensity, aligned mineralogy and overall geometry of the mineral foliation and lineation observations suggested that these structures may in part be magmatic in origin (i.e., igneous flow textures). However, a north-trending domain of increased foliation intensity is coincident to flattened, aligned mafic xenoliths, suggesting a tectonic component to the fabric development. Lithological observations indicated a gradational change in mafic content to the east of this domain. Variations in gamma-ray spectrometry readings and elevated magnetic susceptibility measurements along this trend, along with the alignment of this trend with the eastern margin of the pluton also suggest that this area may represent the margin of separate magmatic domain within the Fourbay Lake pluton

The tectonic foliation measurements typically trend north to north-northeast and dip steeply to both the east and west (Figure 5.2.8A). The total foliation population includes two main orientation peaks, at 355° and 015°, within a range between 341° and 026°. One additional orientation peak is evident at 038° (Figure 5.2.8B).

Two south- and north-trending horizontal weak mineral lineations, without associated measureable tectonic foliation (Figure 5.2.8C), were observed in the eastern portion of the study area, proximal to the aforementioned foliation observations. These lineations are characterized by the weak alignment of hornblende in otherwise massive granodiorite.

Ductile Shear Zones

Ductile shear zones were rarely observed in the Fourbay Lake pluton area. A total of two ductile shear zones were observed in the study area, both along strike with a previously mapped fault (Figure 5.2.9 and 5.2.10). These shear zones strike northwest, at 297° and 330°, and dip steeply to the northeast (Figures 5.2.10A and 5.2.10B).

The ductile shear zones are both less than 2 centimetres wide and are focused within narrow felsic dykes. The shear zones are characterized by strong foliation that was rotated into parallelism along the shear zone indicating a sinistral movement sense (Figure 5.2.11D).

5.2.4.2 Brittle Structure

Brittle structures observed in the Fourbay Lake pluton area include extensive joints, faults and associated slickenlines, and occasional veins. A summary of brittle structures observed in the area is provided in Table 5.2.3 and details are shown in Figures 5.2.12 to 5.2.20.

Joints

A total of 249 joint measurements were recorded in the Fourbay Lake pluton area (Figures 5.2.12 and 5.2.13). Most joint sets are found across the entire area but not necessarily at the same outcrop.

Several steeply dipping joint sets, and one shallowly dipping joint set, are evident in the total joint dataset (Figure 5.2.13A). The total joint population includes a west-northwest-trending, joint set ranges between 292° and 312°, and includes one orientation peak at 300°. A second broad north-trending joint set ranges between 347° and 013°, and includes orientation peaks at 350° and 005°. It also includes a broad northeast-trending joint set that ranges between 022° and 064°, and which includes orientation peaks at 033°, 042°, and 056° (Figure 5.2.13B).

Out of the total joint population, 29 joints (12%) dip between 0° and 30° and are classified as subhorizontal, 17 joints (7%) dip between 31° and 60° and are classified at intermediate, and 203 joints (81%) dip greater than 60° and are classified as subvertical. The subhorizontal joints show a strong cluster with strike/dip at 225/10 and a secondary concentration at 040/09 on the stereonet (Figure 5.2.13A), and on a rose diagram exhibit a west-trending set with a peak orientation at 270°, a

north-northwest and north-northeast-trending set with orientation peaks at 350° and 008°, and a broad northeast-trending set that ranges between 019° and 069° with a peak orientation at 043° (Figure 5.2.13C). The intermediate joints have a large number of peaks on the rose diagram (Figure 5.2.13D), but the small number of data (n=17) in this range suggests none of them are significant. The subvertical joints include a west-northwest-trending joint set ranges between 292° and 312°, and includes one orientation peak at 300°. They also include a broad north-trending joint set that ranges between 347° and 014°, and which includes orientation peaks at 350° and 003°. Finally, the subvertical set also includes a broad northeast-trending joint set that ranges between 022° and 064°, and which includes orientation peaks at 030°, 043° and 057° (Figure 5.2.13E).

Table 5.2.3: Summary of Brittle Structures in the Fourbay Lake Pluton Area

Structure Type	Orientation Family	Peak (°)	Peak Frequency (%)	Range (°)	Confidence
Joints - All	WNW	300	7.9	20	Medium-High
	N	350	6.4	10	Medium-Low
		005	6.2	16	Medium-Low
		033	7.9	13	Medium-High
	NE	042	9.0	16	Medium-High
		056	6.9	13	Medium-Low
Joints - Subhorizontal	W	270	12.7	7	Medium
	NNW	350	10.3	8	Medium
	NNE	008	6.3	5	Medium-Low
	NE	043	16.7	48	Medium-High
Joints - Intermediate	W	280	22.1	8	Medium-High
	NW	313	12.4	21	Medium
	NNW	342	11.7	8	Medium
	NNE	017	5.6	3	Medium-Low
		031	10.7	8	Medium
	NE	049	6.4	13	Medium-Low
	ENE	075	6.0	14	Medium-Low
Joints - Subvertical	WNW	300	8.8	22	Medium-High
	N	350	6.3	8	Medium-Low
		003	7.0	19	Medium-Low
		030	7.2	10	Medium
	NE	043	8.2	17	Medium
		057	7.1	13	Medium-Low
	E	080	5.9	3	Medium-Low
Faults - All	WNW	297	11.8	27	Medium-High
	NNW	329	6.3	5	Medium-Low
	NNE	012	8.5	17	Medium
		033	9.5	13	Medium
	ENE	060	8.0	14	Medium-Low
	E	085	6.4	7	Medium-Low
Veins	WNW	282	16.5	6	Medium
		300	16.6	10	Medium
	N	360	22.6	15	Medium
	NE	042	16.5	7	Medium
	E	080	16.1	8	Medium
Secondary Mineral Infill	WNW	302	13.1	32	High
	N	350	5.6	16	Medium-Low
	NE	034	9.0	23	Medium
	ENE	058	7.4	13	Medium-Low

Joints with 30 to 100 and 100 to 500 centimetre-spacing are the most common overall in the Fourbay Lake pluton area (Figure 5.2.14). Tighter spaced joint sets (10 to 30 centimetres and 30 to 100 centimetres) are more common in the northeast and west-northwest sets. The north-trending joint set has slighter wider spacing on average, although the small number of 3 to 10 centimetre spaced joints are most commonly north-trending (Figure 5.2.14). Figure 5.2.15 illustrates the range of joint spacing and the nature of some of the joint sets.

The majority of joints in the Fourbay Lake pluton area did not contain any fill. However, locally throughout the pluton, and in particular proximal to faults, abundant hematite and minor epidote, quartz and chlorite were observed. A small number of hematite stained joints were observed away from faults throughout the area. Epidote and quartz were only observed in limited instances, both present as fill within joints. Epidote and quartz filled veins were always associated with hematite staining, and typically located along or proximal to faults. Chlorite filled joints were observed in limited outcrop in the southeast corner of the study area, both proximal and distal to faults. A discussion of secondary mineral infilling and alteration observed in association with joints is included below in Section 5.2.4.3.

Faults

A total of 39 faults were measured throughout the Fourbay Lake pluton area (Figures 5.2.16 and 5.2.17). All faults are hosted within the diorite to granodiorite unit of the Fourbay Lake pluton.

Faults occur as discrete millimetre to centimetre wide slip surfaces. Locally, single discrete slip surfaces were observed, and in other instances, multiple closely spaced consecutive discrete slip surfaces were present (Figure 5.2.18). Where multiple discrete faults were present, a series of sub-parallel joints were also commonly observed. Offsets along faults are typically minor (less than 10 centimetres). Faults commonly exhibit hematite staining, and in rare instances, also contain epidote fill, as discussed below in Section 5.2.4.3.

Faults dip steeply and trend in two dominant orientations, west-northwest and north-northeast (Figure 5.2.17A). The total fault population includes several peak trends consistent with these dominant orientations, as well as other less prominent orientations (Figure 5.2.17B). The west-northwest-oriented faults exhibit a broad range between 283° and 310°, and include one orientation peak at 297°. The north-northeast-oriented faults exhibit a broad range between 008° and 038°, and include orientation peaks at 012° and 033°. Lesser orientation peaks are evident at 060°, 085° and 329°.

West-northwest-trending faults are most common, and exhibit both sinistral and dextral senses of movement (Figures 5.2.17C and 5.2.17D). North-northeast-trending faults are less common and no sense of movement was evident along most of these faults. The north-northeast-trending faults have rare sinistral kinematic indicators preserved. Several observed faults also had unclear movement history (Figure 5.2.17E). Rare slickenlines with steps that are developed along certain north-northeast- and northwest-trending brittle faults all plunge shallowly to subhorizontally, suggesting strike-slip movement is common (Figure 5.2.17F).

Veins

A total of 6 veins were measured dominantly in the diorite to granodiorite of the Fourbay Lake pluton area, and are distributed throughout the southeast portion of the study area (Figures 5.2.19 and 5.2.20).

Veins were observed to be less than 10 centimetres wide, typically exhibited extensional textures, and were filled with quartz feldspar and biotite (i.e., granitic veins). Often, veins are oriented sub-parallel to the dominant orientation of joints and faults. Other veins are distributed in a range of orientations. A single granitic vein was observed to be offset by a fault.

Measured veins trend north and northeast to northwest and are moderately to steeply dipping (Figure 5.2.20A). The total vein population exhibits orientation peaks at 360°, 042°, 080°, 282° and 300° (Figure 5.2.20B).

5.2.4.3 Secondary Minerals/Alteration

Secondary minerals were observed in association with numerous brittle structures throughout the Fourbay Lake pluton area (Figure 5.2.21). Structures with secondary minerals and alteration are described below and summarized in Table 5.2.4 to Table 5.2.7 below, for all fractures in the Four Bay Lake pluton area (N = 294), including 249 joints, 39 faults and 6 veins. Secondary mineral orientation information is summarized in Figure 5.2.22 and some representative field examples are illustrated in Figure 5.2.23.

Overall, 183 out of 294 total fractures (62%) observed exhibited no secondary mineral infill or alteration (Table 5.2.4), leaving 111 fractures (38%) with some evidence of secondary mineral infill or alteration. The majority of secondary mineral infillings and alteration were observed on sub-vertical structures, dipping greater than 60° (Figure 5.2.22A).

The total secondary mineral and alteration fracture population includes a north-trending orientation peak at 350°, a northeast-trending orientation peak at 034°, an east-northeast-trending orientation peak at 058°, and a west-northwest-trending orientation peak at 302° (Figure 5.2.22B).

The most common secondary mineral and alteration types identified within all fractures in the Fourbay Lake pluton area are: hematite identified in 96 fractures (33%), epidote in 25 fractures (9%), quartz in 20 fractures (7%), and chlorite in 14 fractures (5%). In some instances, more than one infilling mineral was identified within a single fracture. An additional four fractures (1%) hosted the assemblage of plagioclase+K-feldspar+biotite.

Table 5.2.4: All Fractures - Secondary Minerals and Alteration in the Four Bay Lake Pluton Area

Mineral Phase/Alteration	All Occurrences	% of Total
Hematite	96	33
Epidote	25	9
Quartz	20	7
Chlorite	14	5
Plag+KF+Bt	4	1
None	183	62
Total # of Fractures	**294**	

Hematite was observed mainly as an iron staining within joints and faults, most commonly in northwest-trending structures (Figure 5.2.22C). Epidote was observed filling joints, faults, and a single vein, most commonly in northeast-oriented structures (Figure 5.2.22D). Quartz was observed filling a limited number of faults, joints and along dyke contacts, most commonly with a west-northwest orientation (Figure 5.2.22E). Certain veins contained quartz, but typically in conjunction with feldspar (i.e., granitic veins) and not as secondary quartz. Quartz was observed primarily in the central-eastern portion of the study area, often proximal to interpreted faults. Chlorite was observed

as a coating along faults and associated veinlets, joint surfaces, and within a single vein, most commonly with a west-northwest orientation (Figure 5.2.22F). Chlorite was also observed in limited outcrop in the southeast corner of the study area, both within and away from interpreted faults.

Secondary mineral infilling and alteration was identified on 86 out of 249 (35%) total documented joints, leaving the remaining 163 occurrences (65%) unfilled (Table 5.2.5). Filled joints include occurrences of hematite (33%), epidote (6%), Quartz (3%) and chlorite (2%). The majority of secondary minerals and alteration were identified on subvertical joints, however several occurrences of hematite were also observed on intermediate and subhorizontal joints.

Table 5.2.5: Joints -Secondary Minerals and Alteration in the Four Bay Lake Pluton Area

Mineral Phase/Alteration	All Occurrences	% of Total	Subvertical Dip (61-90°)	Intermediate Dip (31-60°)	Subhorizontal Dip (0-30°)
Hematite	81	33	68	10	3
Epidote	16	6	16	0	0
Quartz	7	3	6	1	0
Chlorite	5	2	5	0	0
None	163	65	130	7	26
Total # of Joints	**249**				

Secondary mineral infilling and alteration was identified on 20 out of 39 (51%) total documented faults, leaving the remaining 19 occurrences (49%) unfilled (Table 5.2.6). Filled faults include occurrences of hematite (38%), epidote (21%), quartz (21%) and chlorite (21%). Secondary minerals and alteration were identified primarily on sub-vertical faults.

Table 5.2.6: Faults - Secondary Minerals and Alteration in the Four Bay Lake Pluton Area

Mineral Phase/Alteration	All Occurrences	% of Total	Subvertical Dip (61-90°)	Intermediate Dip (31-60°)	Subhorizontal Dip (0-30°)
Hematite	15	38	14	1	0
Epidote	8	21	7	1	0
Quartz	8	21	8	0	0
Chlorite	8	21	8	0	0
None	19	49	17	2	0
Total # of Joints	**39**				

Secondary mineral infilling and alteration for the six observed veins is shown in Table 5.2.7 below. The most common fill was quartz with five occurrences (83%), which was associated with four occurrences of plagioclase + K-feldspar + biotite (67%). Chlorite and epidote each occurred in one vein (17%). The majority of observed veins were subvertical in orientation.

Table 5.2.7: Veins - Secondary Minerals and Alteration in the Four Bay Lake Pluton Area

Mineral Phase/Alteration	All Occurrences	% of Total	Subvertical Dip (61-90°)	Intermediate Dip (31-60°)	Subhorizontal Dip (0-30°)
Chlorite	1	17	1	0	0
Epidote	1	17	1	0	0
Quartz	5	83	4	1	0
Plag+KF+Bt	4	67	3	1	0
Total # of Veins	**6**				

5.3 Black-Pic Batholith Area - West

5.3.1 Accessibility and Surface Constraints

The Black-Pic batholith area - west overlaps with the south part of the Township of Manitouwadge and is located directly south-southeast of the town site. The area can be accessed from primary and secondary roads, and from a network of logging roads and trails originating from these roads (Figure 5.3.1). Highway 614 originates from Highway 17 (Trans-Canada Highway), and passes through the northwestern portion of the study area before arriving at Manitouwadge. This highway is a paved and maintained primary road (Figure 5.3.2A). A series of maintained, informally maintained and unmaintained tertiary roads originating from Highway 614 provide access to western portion of the study area, including to boat access points on Agonzon Lake and the northern portion of the Black River. The west-trending Camp 70 road connects to the Twist Lake road, and these roads provide access to the southwest-trending Camp 60, Agonzon Lake, and Lampson Lake roads that traverse most of the Black-Pic batholith area - west. The Camp 60 and Lampson Lake roads can also be accessed from Highway 614, south of the study area. These roads, except the Camp 60 road, are all maintained, double track, secondary gravel roads. A series of informally maintained and non-maintained tertiary roads, as well as active logging roads originate from these secondary roads and provide access to the eastern portion of the study area.

Certain tertiary and former logging roads, particularly in the eastern portion of the Black-Pic batholith area - west, have degraded into overgrown trails that were partially passable by ATV. Once trails degraded to an unpassable level, extensive foot traverses were required. Collectively, the road and trail network, boat access along Agonzon Lake and the Black River, and foot traverses, provided access to the majority of the study area. Helicopter assistance proved beneficial in accessing the far southeastern and southwestern portions of the Black-Pic batholith area - west (Figure 5.3.2B). Limited forestry operations were active in the southern part of the Lampson Lake road in areas of extensive recent logging during mapping.

5.3.2 Bedrock Exposure and Overburden Thickness

The Black-Pic batholith area - west is located in an area previously mapped as bedrock terrain with limited surficial cover (AECOM, 2014). Previously mapped surficial cover is restricted to a relatively narrow (approximately 200-500 metre wide) and linear northeast-trending zone of alluvial terrain, following the southern portion of the Black River and a northern tributary. The alluvial terrain near the river is haloed by a wider zone of glaciolacustrine and morainal material extending up to 5.5 kilometres on either side of the river.

Remotely predicted outcrop for the Black-Pic batholith area - west were identified throughout the study area, and typically occurred as large northeast-oriented zones of predicted bedrock and clusters of smaller, multiple, northeast-oriented outcrops. The orientation of outcrop and outcrop clusters is a result of the dominant northeast-oriented glacial trends. Less predicted outcrop was identified in the northeast-oriented zone previously mapped as overburden.

Of the 242 predicted outcrops visited, 217 were confirmed to be bedrock, while 25 were overburden. Field investigations confirm that predicted outcrop in areas previously mapped as bedrock terrain were consistently exposed bedrock. The best exposures occurred as large northeast-oriented outcrop lacking vegetation (Figures 5.3.2C and 5.3.2D). Within the northeast-trending zone previously mapped as overburden, many remotely predicted outcrops were identified as overburden that are

typically covered by light coloured moss (Figure 5.3.2E). Areas of overburden are characterized by extensive thick cover (minimum greater than 1 metre) and forest regrowth (Figure 5.3.2F).

5.3.3 Lithology and Physical Character

The descriptions below provide an overview of the main and minor bedrock lithological units observed in the Black-Pic batholith area - west, including their main physical characteristics. Lithological units described below as main units tend to occur as the predominant rock type covering at least 60% of the exposed bedrock, by area, at any individual bedrock station, and are observed at a high frequency of bedrock stations overall. Minor lithological units described below may occasionally occur as the main rock type at individual bedrock stations, but in general they occur infrequently, and represent only a small portion overall of the bedrock in the Black-Pic batholith area - west.

The Black-Pic batholith area - west consisted predominantly of foliated to gneissic tonalite of the Black-Pic batholith, which represented the only main lithology identified in the study area (Figure 5.3.3). Minor lithological units identified in the Black-Pic batholith area - west included a suite of foliated to gneissic mafic rocks interlayered with the tonalite, granite and diorite to granodiorite which intrude the tonalite, and gabbro preserved as inclusions and dykes within the tonalite (Figure 5.3.5).

A summary of characteristics of the lithological units encountered in the Black-Pic batholith area - west is included in Table 5.3.1 below.

Table 5.3.1: Summary of Bedrock Characteristics by Lithological Unit for the Black-Pic Batholith Area - West

Lithological Unit	# of Occurrences (% of bedrock stations)	Fabric	Magnetic Susceptibility (average S.I.)	Gamma Spectrometry (average)	Strength (range)
Tonalite	202 (93%)	Foliated to Gneissic	3.898 x10^{-3}	K = 1.2% U = 0.6 ppm Th = 2.5 ppm	R4-R6
Foliated to Gneissic Mafic Rocks	6 (3%)	Foliated to Gneissic	6.671 x10^{-3}	K = 0.8% U = 0.1 ppm Th = 1.4 ppm	R4-R5
Diorite to Granodiorite	36 (17%)	Massive to Weakly Foliated	4.865 x10^{-3}	K = 1.9% U = 0.8 ppm Th = 4.6 ppm	R4-R5
Gabbro	20 (9%)	Massive to Foliated	1.649 x10^{-3}	K = 2.1% U = 1.6 ppm Th = 4.3 ppm	R3-R5
Granite	47 (22%)	Massive	3.944 x10^{-3}	K = 2.8% U = 1.6 ppm Th = 6.2 ppm	R4-R6

Note: Percentages in the second column exceed 100% because more than one rock type can be found at a single station.

5.3.3.1 Tonalite

The Black-Pic batholith area - west is located entirely within a large tonalite complex of the Black-Pic batholith. Tonalite was observed at 202 of the 217 bedrock outcrop stations (84%) investigated. Tonalite most commonly represents greater than 90% of any bedrock outcrop by area (Figure 5.3.4A), and is interpreted to represent greater than 90 percent of the underlying bedrock of

the entire Black-Pic batholith area - west. A total of 137 representative samples of tonalite were collected during the field investigations.

The tonalite is grey to off white both when fresh and when weathered. It is characterized by equigranular, fine- to medium-grained crystal form (0.5 to 5 millimetre crystals) (Figure 5.3.4B). Accessory minerals typically included biotite, occasionally hornblende, and magnetite. The tonalite is typically very heterogeneous; frequently intruded by felsic dykes and diorite to granodiorite to granite intrusions, and locally contained mafic gabbroic dykes, enclaves and panels (Figures 5.3.4B and 5.3.4C). Ductile features are pervasive and well-developed throughout the tonalite, including weak to intense foliation, gneissosity, and brittle-ductile shear zones (e.g., Figure 5.3.4D). One area east of Morley Lake (Figure 5.3.3), is dominated by a more homogeneous foliated tonalite that may represent a subdomain within the Black-Pic batholith that is able to be mapped.

A total of 201 rock hardness measurements were made on the tonalite in the Black-Pic batholith area - west. In 197 instances (98%) it exhibited a very strong (R5) character, and in the remaining four instances, it exhibited 2 instances (1%) of strong (R4) character, and two instances (1%) of extremely strong (R6) character.

A total of 188 magnetic susceptibility measurements were taken on the tonalite, typically yielding low values (Figure 5.3.4E). The results ranged from 0.09 to 16.20 $x10^{-3}$ SI, with an average value of 3.90 $x10^{-3}$ SI, and a standard deviation of 3.21 $x10^{-3}$ SI.

A total of 184 gamma-ray spectrometry measurements were taken from tonalite in the Black-Pic batholith area - west (Figure 5.2.4F). The measurements yielded the following values for tonalite:

- Total Count (Range: 43-184 Average: 73 Std. Dev: 20)
- Potassium (%) (Range 0.4-3.2 Average: 1.2 Std. Dev: 0.4)
- Uranium (ppm) (Range 0-7.6 Average: 0.6 Std. Dev: 0.9)
- Thorium (ppm) (Range 0-9.9 Average: 2.5 Std. Dev: 1.5)

5.3.3.2 Minor Lithological Units

Four groups of minor lithological units were observed in the Black-Pic batholith area - west, including foliated panels/relicts of fine-grained foliated to gneissic mafic rocks, intrusions and irregular xenoliths of diorite to granodiorite, intrusions of granite, and mafic gabbroic dykes and inclusions (Figure 5.3.5). A single outcrop of a magmatic breccia composed predominantly of gneissic tonalite clasts (Figure 5.3.6F) was identified but it does not represent a significant component of the minor lithological units and will not be discussed further below.

Foliated to Gneissic Mafic Rocks

Panels of foliated to gneissic mafic rocks were observed at 6 of the 217 bedrock outcrop stations (3%) investigated. Foliated to gneissic mafic rocks occur in a domain in the southeast part of the area, coincident with a stronger and more steeply dipping gneissosity. These panels represent phases of the tonalite complex, potentially either strongly deformed mafic phases, or relict panels of mafic metavolcanic rocks. They are strongly foliated in an orientation sub-parallel to the main fabric (Figure 5.3.6A), suggesting they represent portions of the main Black-Pic batholith that have experienced strong ductile deformation. In addition to the strongly foliated panels of mafic rocks, a common component of the foliated to gneissic tonalite complex are irregularly shaped xenoliths or early phases of foliated diorite interlayered with tonalite are common (Figures 5.3.6B and 5.3.6C).

Foliated to gneissic mafic rocks are characteristically dark green to black when fresh and when weathered. They are heterogeneous, equigranular to variable textured fine- to coarse-grained crystal form (0.5 to 10 millimetre crystals), and exhibit a foliated to gneissic texture.

A total of 6 rock hardness measurements were made on the foliated to gneissic mafic rocks. In 2 instances they exhibited a strong rock hardness (R4), and in 4 instances they exhibited a very strong rock hardness (R5).

A total of 5 magnetic susceptibility measurements were made on the foliated to gneissic mafic rocks and these yielded an average value of 6.67 $x10^{-3}$ SI. A total of 5 gamma-ray spectrometry measurements were taken from foliated to gneissic mafic rocks with the following average results: K = 0.8%; U = 0.1 ppm; and Th = 4.6 ppm.

Diorite to Granodiorite

Occurrences of diorite to granodiorite were observed throughout the Black-Pic Batholith area - west, predominantly in the northern half, and along the western margin, of the study area. Diorite to granodiorite was identified at 36 out of 217 bedrock outcrop stations (17%) in the Black-Pic batholith area - west (Figure 5.3.5). These units tend to be the main lithology covering the majority of one or a small group of closely spaced outcrops. Overall the diorite to granodiorite occurrences are interpreted to represent relatively small and discontinuous intrusions.

The diorite component is generally black to dark green when fresh and when weathered, while the granodiorite component is pink, off-white or light grey when fresh and when weathered. These intrusions are characterized by homogenous, equigranular fine- to coarse-grained crystal form (0.5 to 10 millimetre crystals), with a massive to weakly foliated texture. The degree of foliation development in these units is variable and suggests their intrusive history may span a considerable time interval. The outcrop scale dykes and xenoliths of similar composition are described below, but may be equivalent to these larger intrusions.

A total of 36 rock hardness measurements were made on the diorite to granodiorite unit in the Black-Pic batholith area - west. In 33 instances (92%) it exhibited a very strong (R5) character and in the other three instances (8%) it exhibited a strong (R4) character.

A total of 29 magnetic susceptibility measurements were made on the diorite to granodiorite and these yielded an average value of 4.87 $x10^{-3}$ SI. A total of 30 gamma-ray spectrometry measurements were taken from diorite to granodiorite with the following average results: K = 1.9%; U = 0.8 ppm; and Th = 4.6 ppm.

Gabbro

Gabbro was identified at 20 out of 217 bedrock outcrop stations (9%) in the Black-Pic batholith area - west (Figure 5.3.5). Gabbro was observed to dominantly occur as narrow foliated dykes (less than 2 metres wide) intruding tonalite (Figure 5.3.6E), and was also less commonly observed as enclaves of various sizes and shapes. In the majority of these occurrences it occupied less than 10% of the outcrop by area. In two instances, entire outcrops of gabbro were documented. The gabbro dykes are strongly concentrated in a north-trending corridor parallel to the Barehead Lake fault (discussed below) along the west edge of the in the Black-Pic batholith area - west.

Gabbro is dark green to black when fresh and when weathered. It is characterized by equigranular, very fine- to fine-grained crystal form (0.1 to 1 millimetre crystals) and a foliated texture.

A total of 18 rock hardness measurements were made on the gabbro in the Black-Pic batholith area - west. In 14 instances (78%) it exhibited a very strong (R5) character, in 3 (17%) of the remaining instances it exhibited a strong (R4) character, and in 1 (6%) instance it exhibited a medium strong (R3) character.

A total of 14 magnetic susceptibility measurements were made on the gabbro and these yielded an average value of 1.65 $x10^{-3}$ SI. A total of 9 gamma-ray spectrometry measurements were taken from gabbro with the following average results: K = 2.1%; U = 1.6 ppm; and Th = 4.3 ppm.

Granite

Granite occurrences were recorded at 47 out of 217 bedrock outcrop stations (21.6%) in the Black-Pic batholith area - west (Figure 5.3.6), where they usually accounted for less than 10% of the outcrop, by area. Granite typically occurs as centimetre to half-metre wide linear to curvilinear felsic dykes intruding the tonalite in multiple orientations. The number of occurrences may slightly underestimate the total distribution of the granite dykes as they were a very common occurrence throughout the entire area underlain by tonalite.

The felsic dykes are pink to off-white when fresh and when weathered (Figure 5.3.6D). They are characterized by multiple crystal forms (porphyritic, equigranular, inequigranular, vari-texture), fine to coarse grain size (0.5 to 10 millimetre crystals), and massive texture. They consistently exhibit competent contacts with the surrounding tonalite without evidence of localized brittle deformation.

On individual outcrops, the felsic dykes often show clear cross-cutting relationships. These suggest that early white, strongly deformed granite dykes are cut by straight, weakly deformed granite dykes, which may in turn be cut by pink to white aplitic to pegmatitic dykes.

A total of 43 rock hardness measurements were made on the granite in the Black-Pic batholith area - west. In 36 instances (84%) it exhibited a very strong (R5) character, and of the remaining instances in 3 instances (7%) it exhibited a strong (R4) character, and in 4 instances (9%) it exhibited an extremely strong (R6) character.

A total of 32 magnetic susceptibility measurements were made on the granite and these yielded an average value of 3.94 $x10^{-3}$ SI. A total of 29 gamma-ray spectrometry measurements were taken from granite with the following average results: K = 2.8%; U = 1.6 ppm; and Th = 6.2 ppm.

5.3.4 Structure

Ductile and brittle structures observed throughout the Black-Pic batholith area - west are discussed below and presented in Figures 5.3.7 – 5.3.20. Ductile structures include foliation, gneissosity, shear zones and associated mineral lineations, fold axes and axial planes, and brittle-ductile shear zones. Brittle structures include joints, veins, faults, and associated lineations (i.e., slickenlines). Fracture infilling minerals, alteration and the orientation of the fracture sets are also discussed.

5.3.4.1 Ductile Structure

Ductile structures observed in the Black-Pic batholith area - west include extensive foliation and gneissosity, ductile and brittle-ductile shear zones and associated mineral lineations, fold axes and axial planes (Figures 5.3.7 to 5.3.11). A summary of ductile structures is presented in Table 5.3.2.

Table 5.3.2: Summary of Ductile Structures in the Black-Pic Batholith Area

Structure Type	Orientation Family	Peak (°)	Frequency (%)	Range (°)	Confidence
Tectonic Foliation	NW	327	7.2	16	Medium
	NNE-ENE	015	8.5	20	Medium
		045	8.4	30	Medium
		078	8.0	29	Medium
Gneissic Layering	W	275	7.1	16	Medium-Low
	WNW	295	6.3	6	Medium-Low
	NNW	335	7.3	13	Medium-Low
	NNE	012	10.8	32	Medium-High
	ENE	054	7.1	15	Medium-Low
		062	7.4	25	Medium-Low
Mineral Foliation	NW	325	9.0	16	Medium
	NNE-NE	020	7.6	15	Medium-Low
		042	11.1	29	Medium-High
	ENE	075	9.8	24	Medium
Shear Zones	WNW	293	5.8	2	Medium-Low
	NW	307	11.0	9	Medium
	NNW	328	5.8	2	Medium-Low
	NNE	010	10.8	10	Medium-Low
	NE	046	17.3	16	Medium-High
	E	083	19.7	22	Medium-High
		095	11.9	9	Medium

Foliation and Gneissosity

Within the Black-Pic batholith area - west, a mineral foliation and a gneissosity represent a spectrum of planar fabrics resulting from the alignment and segregation of mineral grains due to progressive deformation. These planar fabrics often exhibit similar orientations and minor variations in texture (i.e., reside on the boundary between foliated and gneissic), and are interpreted to represent components of a composite tectonic foliation that developed during a series of progressive deformation events; these fabrics are therefore discussed together.

A total of 93 mineral foliation and 97 gneissosity measurements were recorded in the Black-Pic batholith area - west, dominantly within tonalite (e.g., Figure 5.3.11A), and locally also within mafic gabbroic dykes, diorite and granodiorite (Figures 5.3.7 and 5.3.8). Penetrative planar fabrics are typically not developed within the numerous late felsic dykes that cross-cut the tonalite suite, although a set of early, commonly folded and foliated felsic dykes are observed in the tonalite suite (Figure 5.3.11D).

Foliation varies from weak to strong and is defined by the alignment of biotite and locally hornblende. Gneissosity is moderate to intense and defined by the segregation and alignment of felsic and mafic minerals (Figure 5.3.11B). Weak to moderate foliation and gneissosity anastomosed around mafic xenoliths and exhibited planar to curvi-planar geometries, whereas strong to intense foliation and gneissosity developed a strong, consistent planar geometry.

Mineral foliation and gneissosity are predominantly shallowly dipping, but also exhibit a broad range in both orientation and dip magnitude (Figure 5.3.8A). The total tectonic foliation population (N = 190) exhibits one broad north-northeast to east-northeast trend that ranges between 010° and 089° and which includes peak orientations at 015°, 045° and 075°. It also exhibits one northwest trend with a peak orientation at 327° (Figure 5.3.8B).

The gneissic layering population (N = 97) exhibits one broad trend to the north-northeast that ranges between 358° and 030° and which includes an orientation peak at 012°, and another broad trend to the east-northeast that ranges between 042° and 082° and which includes orientation peaks at 054° and 062°. Lesser peak orientations are evident at 275°, 295° and 335° (Figure 5.3.8C).

The mineral foliation population (N = 93) exhibits one broad north-northeast to northeast trend that ranges between 014° and 058° and which includes peak orientations at 020° and 042°. It also exhibits a broad east-northeast trend that ranges between 065° to 089°, and which includes an orientation peak at 075°. One additional northwest trend exhibits an orientation peak at 325° (Figure 5.3.8D).

A total of five mineral lineations were measured in foliated units. Where observed, lineations are well-defined by the alignment of biotite, and plunge moderately to the east or west-northwest (Figure 5.3.8E).

Mineral foliation and gneissosity form a complex pattern indicative of a protracted history of ductile deformation that can be classified into four distinct domains described below:

1. **Moderate to steep dipping, moderate to intense foliation and gneissosity associated with the edges of intrusive tonalite domes.** These structures were observed along the northwestern boundary of the study area where a tonalite dome progressively steepened towards the greenstone belt north of the study area; and in the southeast of the study area where two tonalite domes are interpreted to abut one another. In particular, an arcuate array of foliation and gneissosity measurements in the central-southern portion of the study area progressively steepen and are interpreted to define the curvilinear boundary of a tonalite dome.

2. **Shallow dipping, strong to intense gneissosity and foliation define a broad northeast-trending high-strain corridor originating from the western boundary of the study area and trending through Agonzon Lake up to the northeast corner of the mapping block.** The southern portion of the zone is dominated by strong to intense strained gneissic tonalite dipping shallow to the northwest. Progressing towards the northeast, the zone transitions from gneissic to foliated and may intersect the progressively steeping foliation associated with the northern boundary of a tonalite dome. This zone appears to separate two distinctive phases of the tonalite suite. To the northwest, the tonalite exhibits relative higher total counts, increased potassium and thorium concentration, an elevated magnetic signature (total field) and contains a greater proportion of granodiorite intrusions, relative to the tonalite to the southeast. One potential interpretation of this domain may be that it represents the high strain base of a sheeted tonalite intrusion, overlying a separate distinctive tonalite intrusion.

3. **Limited, shallowly northeast-dipping gneissosity and foliation, located mainly within the central-western portion of the study area.** This set of structures were only observed in limited instances, are orthogonal to the main northeast-trending high strain domain, and are locally aligned along magnetic lows and adjacent to the surface expression of northwest-trending Proterozoic mafic dykes. (Note that despite being coincident with the dykes at surface, these ductile structures were shallow dipping and are not sub-parallel with the sub-vertical mafic dykes). These structures may represent a later stage of spaced relatively narrow ductile shear zones.

4. **Shallow to flat-lying, weak to strong foliation and gneissosity associated with the core of tonalite domes.** This set of structures was best observed away from aforementioned structural zones, in particular in the northeastern portion of the study area.

Folds (Folds Axes, Fold Axial Planes)

A total of five fold axes and three axial planes were measured in the Black-Pic batholith area - west, all within gneissic tonalite (Figures 5.3.7 and 5.3.8F). The folds are minor structures, occurring on the centimetre to metre scale, and are characterized by open, tight, and isoclinal U-, S- and Z-shaped geometries with no common orientation. Folds are either coeval with the development of the tectonic foliation or post-date it and are minor folds of the foliation.

In the first case, the folds are best developed in early felsic intrusions that have axial planes subparallel to the main planar fabric (Figures 5.3.11C and 5.3.11D). In the second case, folding of the foliation suggested that folding occurred at a late stage during a progressive ductile deformation event or during a separate later deformation event. It is likely that any early stage folding would have been transposed planar to the main tectonic fabric during ongoing ductile deformation.

Neither the axial planes nor the fold axes have a consistent orientation. Early folds are axial planar to the surrounding main tectonic fabric with typically shallow-plunging fold axes of varying trends. The later folds tend to be upright, with northwest-trending axial planes and shallow to moderate, northwest- or southeast-plunging fold axes (5.3.8F).

Ductile and Brittle-Ductile Shear Zones

A total of 17 shear zones, including 12 ductile and 5 brittle-ductile shear zones, were identified in the Black Pic Batholith area - west (Figures 5.3.9 and 5.3.10). The majority of shear zone occurrences were identified in the western, northwestern and southeastern parts of the area.

The total shear zone population dips steeply in multiple directions and shallowly towards the north (Figure 5.3.10A). The total shear zone population is characterized by several discrete trends, with orientation peaks at 010°, 046°, 293°, 307° and 328°. One slightly broader east trend includes orientation peaks at 083° and 095° (Figure 5.3.10B).

A total of 12 discrete ductile shear zones were measured in the Black-Pic batholith area - west, dominantly within tonalite, and in two instances within mafic gabbroic dykes (Figures 5.3.9 and 5.3.10). Observed discrete ductile shear zones were typically less than 1 metre wide, characterized by strong to intense foliation, and extensional shear bands commonly exhibiting dextral kinematics (Figures 5.3.11E and 5.3.11F).

Ductile shear zones are located along the edges of tonalite domes and within the central-western portion of the study area. When located along the boundaries of intrusive domes, the ductile shear zones are oriented sub-parallel to the general trend of the dome and dip steeply, similar to the orientation of the tectonic foliation in these areas. Ductile shear zones in the central-western portion of the study area formed an east-west trend and dip shallowly to moderately to the north.

These measured structures represent discrete ductile shear zones that could be observed in individual outcrops, but do not provide a complete representation of large scale high strain zones. Examining the strain intensity of ductile features across the study area, reveals area scale high strain zones, including the southwest-striking, shallow northwest-dipping broad shear zone of strong to intense foliation and gneissosity that bisects Agonzon Lake and divides the mapping block into distinct phases of tonalite (described in above sections), and ductile shear zones along the edges of tonalite domes in the southeast of the study area.

A total of nine lineations (mineral and stretching) were measured, either associated with ductile shear zones or in areas of high strain tonalite (i.e., associated with regional rather than discrete shear zones), but do not have a common orientation. Lineations varied from weak to intense, are characterized by alignment and/or stretching of biotite and locally hornblende, and are typically shallow- to steep-plunging to the east and northwest.

A total of five brittle-ductile shear zones were measured in the Black-Pic batholith area - west (Figure 5.3.9). Three of these structures are less than 1 metre wide, and represent minor foliation and discrete partings along or oblique to mafic dykes. These structures are considered minor.

The remaining two structures define a significant northeast-striking, steeply dipping, multi-metre wide brittle-ductile shear zone that parallels the part of the Black River to the northwest of Agonzon Lake. Limited exposure of this fault (the core of the fault lies under the river) is characterized by the following progression from the fault boundaries to the fault core: slight hematite alteration and fractured gneissic tonalite along the fault boundaries, strong hematite alteration and spaced brittle-ductile cleavage moving towards the core of the fault, and complete transposition of the gneissic tonalite by a brittle-ductile schistose foliation and extensive hematite alteration approaching the core of the fault. The geometrical arrangement of composite fabrics (C-S fabric) from within the shear zone indicate dextral kinematics. This brittle-ductile shear zone was also clearly defined as a linear northeast-trending magnetic low in the high-resolution aeromagnetic survey. Furthermore, this structure is located in the core of the high ductile strain gneissic tonalite corridor, suggesting that this structural domain was reactivated in the brittle-ductile regime.

5.3.4.2 Brittle Structure

Brittle structures observed in the Black-Pic batholith area - west include extensive joints, faults and associated slickenlines, and occasional veins. A summary of brittle structures is presented in Table 5.3.3 and details are shown in Figures 5.3.12 to 5.3.20.

Joints

A total of 908 joint measurements were recorded in the Black-Pic Batholith area - west (Figures 5.3.12 and 5.3.13). Most joint sets are found across the entire area but not necessarily at the same outcrop. The well-represented, shallowly dipping set is partly due to the good vertical exposure of road cuts along Highway 614.

Steeply dipping joints in a number of orientations, and one shallowly dipping joint set, are evident in the total joint dataset (Figure 5.3.13A). Significant overlap and dispersion in the data result in a high background and subdued peaks in the rose diagram (Figure 5.3.13B). The total joint population exhibits multiple subdued northeast trends, including weak orientation peaks to the north-northeast at 024°, to the northeast at 050° and to the east-northeast at 066°. A broad west-northwest trend ranges between 280° and 306°, and includes an orientation peak at 290°. A broad northwest trend ranges between 317° and 345°, and includes orientation peaks at 320° and 338°. The north-northwest and west-northwest sets are the most common.

Out of the total joint population, 80 joints (9%) dip between 0° and 30° and are classified as subhorizontal, 60 joints (7%) dip between 31° and 60° and are classified at intermediate, and 768 joints (84%) dip greater than 60° and are classified as subvertical. The subhorizontal joints are strongly clustered about a peak orientation of 270/07, whereas the rose diagram exhibits a north-northwest-trending set with a peak orientation at 295°, a north-northeast-trending set with one orientation peak at 013°, and a broad northeast-trending set that ranges between 032° and 076° and which includes peak orientations at 037°, 050° and 065° (Figure 5.3.13C). The intermediate joints

are too sparse to have any significant concentrations (Figure 5.3.13A), but the two largest peaks occur at 335° and 038° (Figure 5.3.13D). The subvertical joints include a broad west-northwest trend that ranges between 277° and 307°, and with orientation peaks at 290° and 304°, a broad north-west to north-northwest trend that ranges between 317° and 347°, and which includes orientation peaks at 320° and 338°, and subdued northeast trends with orientation peaks at 025°, 050°and 078° (Figure 5.3.13E).

Table 5.3.3: Summary of Brittle Structures in the Black-Pic Batholith Area - West

Structure Type	Orientation Family	Peak (°)	Peak Frequency (%)	Range (°)	Confidence
Joints - All	WNW	290	7.9	26	High
	NW-NNW	320	5.9	8	Medium-Low
		338	7.5	20	Medium-High
	NNE	024	5.7	4	Medium-Low
	NE	050	6.4	9	Medium-High
	ENE	066	5.6	3	Medium-Low
Joints - Subhorizontal	NNW	295	10.6	19	Medium-High
	NW	320	6.2	9	Medium-Low
	N	358	6.5	6	Medium-Low
	NNE	013	6.2	6	Medium-Low
		037	6.8	8	Medium-Low
	NE-ENE	050	13.1	20	High
		065	9.6	16	Medium
Joints - Intermediate	WNW-NW	288	7.5	17	Medium-Low
		297	6.9	13	Medium-Low
		312	5.9	8	Medium-Low
	NNW	335	9.7	16	Medium
	N	000	5.7	3	Medium-Low
	NNE	018	8.0	13	Medium-Low
	NE	038	9.0	19	Medium
	ENE	068	5.8	3	Medium-Low
Joints - Subvertical	WNW-NW	290	7.8	22	Medium-High
		304	5.9	8	Medium-Low
	NW-NNW	320	6.0	8	Medium-Low
		338	7.9	22	Medium-High
	NNE	025	6.0	8	Medium-Low
	NE	050	5.8	4	Medium-Low
	ENE	078	5.6	1	Medium-Low
Faults - All	WNW	290	9.9	18	Medium-High
	NNW	338	13.3	23	High
	NNE	024	8.0	18	Medium
Veins	W-WNW	273	10.2	10	Medium-Low
		287	13.8	18	Medium
		300	13.8	17	Medium
	NW	317	10	10	Medium-Low
	NNE	020	9.7	9	Medium-Low
		035	10.4	9	Medium-Low
	NE	044	10.4	11	Medium-Low
		056	9.9	10	Medium-Low
Secondary Mineral Infill	WNW	290	9.2	17	High
	NNW	355	10.5	23	High
	NNE	023	5.7	5	Medium-Low
	NE	045	6.0	7	Medium-Low

Joints with 30 to 100 centimetre spacing are the most common overall in the Black-Pic batholith area - west (Figure 5.3.14), and this narrower average spacing is the most distinct of all the withdrawal areas. The prevalence of narrow joint spacing (1 to 3 and 3 to 10 centimetre spacing) in the north-northwest-trending joint set is the most distinctive feature of the joint spacing analysis (Figure 5.3.14). This correlates with the corridor of strong brittle deformation observed on the west margin of the area subparallel to the Barehead Lake fault (Figure 5.3.12). Otherwise most joint sets have a similar distribution of joint spacing. Figure 5.3.15 illustrates the range of joint spacing and the nature of some of the joint sets.

Select joints throughout the Black-Pic batholith area - west contained secondary minerals (i.e., joint fill), including significant hematite staining, considerable epidote-fill, and minor quartz- and chlorite-fill. Hematite is widely distributed across most of the area and in most rock types, whereas chlorite is typically present in joints developed within mafic dykes. A discussion of secondary mineral infilling and alteration observed in association with joints is included below in Section 5.3.4.3.

Faults

A total of 155 faults were measured throughout the Black-Pic batholith area - west (Figures 5.3.16 and 5.3.17). Faults were observed dominantly within the tonalite, but also within the diorite, granodiorite, granite, and felsic and mafic dykes.

The majority of measured faults occur as discrete millimetre- to centimetre-wide slip surfaces. Locally, single discrete slip surfaces were observed, and in other instances multiple, closely spaced parallel, discrete slip surfaces were present. Where multiple, closely spaced, discrete faults were observed the associated fault zones vary from a few centimetres to greater than 10 metres wide, and commonly form series of scarps and sub-parallel joints (Figure 5.3.18). In these instances, faults often exhibit hematite staining and epidote-fill. Offsets along individual, discrete faults are typically minor (less than 10 centimetres). Fault zones are often partially buried by overburden and located in topographic lows, including rivers, valleys, and swamps.

Faults are typically very steep, to sub-vertical and trend in three dominant orientations, west-northwest, north-northwest and north-northeast (Figure 5.3.17A). The total fault population includes several peak trends consistent with these dominant orientations. The north-northeast-oriented faults exhibit an orientation peak at 024°, the west-northwest-oriented faults exhibit an orientation peak at 290° and the north-northwest-oriented faults exhibit an orientation peak at 335° (Figure 5.3.17B).

Dextral faults exhibit a prominent north-northwest trend with an orientation peak at 338° and lesser orientation peaks at 290° and 063° (Figure 5.3.17C). Sinistral faults exhibit prominent west-northwest and north-northwest trends with orientation peaks at 290° and 335, respectively, along with a lesser orientation peak at 024° (Figure 5.3.17D). Broadly northeast and northwest trends are also evident in the fault data set with unknown movement history (Figure 5.3.17E).

Slickenlines and steps are locally developed along faults, and characterized by polished and striated surfaces with secondary, fibrous mineral growth (typically either epidote or quartz). Slickenlines have very shallow plunges, indicating predominantly strike-slip movement (Figure 5.3.17F). A discussion of secondary mineral infilling and alteration observed in association with faults is included below in Section 5.3.4.3.

The distribution and orientations of stronger faulting in the Black-Pic batholith area - west can be roughly divided into four domains (Figure 5.3.16):

1. **A north-trending domain of north-northwest- and occasional northeast-trending faults located along the central part of the western boundary of the study area.** These faults are directly east of and associated with the major north-trending fault that passes through Barehead Lake and offsets the greenstone belt with a sinistral strike-separation north of the mapping block. Associated slickenlines plunge shallowly to the north-northwest and south-southeast. Well-defined, dextral kinematic indicators are most common in the north-northwest-trending discrete faults, whereas the northeast-trending structures more commonly have a sinistral movement sense. The northeast and north-northwest orientations of observed faults in this domain suggest they may represent conjugate secondary or reactivated structures located in the margin of the main north-trending fault.

2. **A northeast-trending domain of northeast- and occasional northwest-trending faults originating from the southwestern boundary of the mapping block and extending northeast through Agonzon Lake and up to Kaginu Lake.** The location of this structural zone is coincident with the previously described major northeast-trending ductile high strain zone, the mapped major brittle-ductile shear zone, and numerous northeast-trending regional magnetic lows and surficial features (rivers, lakes, valleys). This domain represents a significant northeast-trending brittle deformation zone. Associated slickenlines plunge shallowly to the northeast, north, and south. Kinematic indicators suggest a dominantly dextral sense of movement, but rare indicators of sinistral movement were also observed.

3. **A northwest-trending domain of northwest- and occasional northeast-trending faults located along the central-eastern boundary of the study area.** These structures are associated and coincident with a northwest-trending structural zone observed in the regional magnetics, and interpreted from ductile structures to represent the edge of a tonalite dome. Only one shallowly southeast-plunging slickenline was observed in this domain. Kinematic indicators are also limited, and suggest a roughly equal distribution of dextral and sinistral strike-separation faults.

4. **A minor domain along the west half of the northern boundary of the mapping block comprising limited east-northeast and west-northwest-trending faults.** These structures are also associated and coincident with an east-trending structural zone observed in the regional magnetics, and interpreted from ductile structures to represent the edge of a tonalite dome. Limited slickenlines plunge shallowly to the northwest and west-southwest, and kinematics suggest a dominantly dextral sense of motion.

Limited additional faults and associated slickenlines were also observed beyond these four zones and interpreted to represent discrete brittle structures distributed throughout the Black-Pic batholith.

Veins

A total of 10 veins were measured in the Black-Pic batholith area - west, distributed throughout the study area (Figures 5.1.19 and 5.1.20). Observed veins were typically located within tonalite and gabbro, and are not a significant structural feature throughout the mapping area.

Veins are typically less than 3 centimetres wide, exhibit extensional textures, and are filled with either quartz, or quartz-feldspar-biotite (i.e., granitic veins). Veins are generally northwest- and northeast-trending and steeply dipping.

Measured veins exhibit intermediate to subvertical dips and trend northwest and northeast (Figure 5.3.20A). The total vein population exhibits a broad west-northwest trend that ranges between 267° and 312° and which includes orientation peaks at 273°, 287° and 300°, and a broad northeast trend that ranges between 030° and 060° and which includes orientation peaks at 035°, 044° and 056°. Less prominent, narrow, orientation peaks are evident at 020°and 317° (Figure 5.3.20B).

5.3.4.3 Secondary Minerals/Alteration

Secondary minerals were observed along numerous brittle structures throughout the Black-Pic batholith area - west (Figure 5.3.21). Structures with secondary minerals and alteration are described below and summarized in Tables 5.3.3 to 5.3.7 below, for all fractures in the Black-Pic batholith area - west (N = 1073), including 908 joints, 155 faults and 10 veins. Secondary mineral orientation information is summarized in 5.3.22 and some representative field examples are illustrated in Figure 5.3.23.

Overall, 704 out of 1073 total fractures (66%) observed exhibited no secondary mineral infill or alteration (Table 5.3.4), leaving 369 fractures (34%) with some evidence of secondary mineral infill or alteration. The majority of secondary mineral infillings and alteration were observed on sub-vertical structures, dipping greater than 60° (Figure 5.3.22A).

The total secondary mineral and alteration fracture population includes subdued north-northeast to northeast trends, with orientation peaks at 023° and 045°, a west-northwest trend with orientation peak at 290° and a north-northwest trend with orientation peak at 335° (Figure 5.3.22B).

In general, fractures commonly exhibited extensive hematite staining, locally significant epidote fill, limited quartz fill, and minor chlorite fill. In some instances, more than one infilling mineral was identified within a single fracture. The number of secondary mineral and alteration types identified within all fractures in the Black-Pic batholith area - west are: hematite identified in 326 fractures (30%), epidote in 139 fractures (13%), quartz in 32 fractures (3%), and chlorite in 11 fractures (1%). Less prominent secondary minerals observed, classified below in Table 5.3.4 as ‘other’, include three occurrences of plagioclase+K-feldspar+biotite, within veins, and one occurrence each of magnetite and carbonate, both within faults. In total these other occurrences fill 0.5% of all fractures.

Table 5.3.4: All Fractures - Secondary Minerals and Alteration in the Black-Pic Batholith Area - West

Mineral Phase/Alteration	All Occurrences	% of Total
Hematite	326	30
Epidote	139	13
Quartz	32	3
Chlorite	11	1
Other	5	0.5
None	704	66
Total # of Fractures	**1073**	

Hematite was observed as iron staining in all types of brittle structures and is present throughout the area. Hematite is strongly associated with north-northwest-, west-northwest- and to a lesser extent northeast-trending structures (Figure 5.3.22C). It is strongly associated with the north-trending corridor parallel to the Barehead Lake fault and the northeast-trending brittle deformation zone along Agonzon and Kaginu lakes. Hematite is also present in north, southeast, central-west, and central-east portions of study area, corresponding to zones of brittle deformation near steep edges of tonalite

domes, and northwest-trending brittle structures. Hematite alteration occurs in association with all other secondary minerals.

Epidote was observed as filling in all types of brittle structures and has the same distribution throughout the area as hematite, but is less abundant. Epidote is preferentially associated with north-northwest and to a lesser degree, northeast-trending structures (Figure 5.3.22D). Epidote is typically associated with hematite, and locally with quartz and chlorite.

Quartz is observed filling all brittle structure types and along Proterozoic mafic dyke contacts. Quartz is preferentially found in west-northwest-, and to a lesser extent north-northwest- and northeast-trending structures (Figure 5.3.22E). It is most abundant in the centre of the northeast-trending brittle deformation zone near Agonzon Lake, and also located in southeast part of the mapping block near the interpreted steep edge of a tonalite dome. Limited other occurrences are dispersed throughout the northern portion of the study area. Quartz occurs in isolation and in association with all other secondary minerals.

Chlorite is observed as a coating along all types of brittle structures. It occurs primarily in west-southwest to north-northwest trending fractures (Figure 5.3.22F). Chlorite was observed in limited outcrops throughout the study area, both within and away from interpreted brittle fault zones. Chlorite has a particularly strong association with the Barehead Lake fault corridor. Chlorite is often associated with other secondary minerals.

Secondary mineral infilling and alteration was identified on 297 out of 908 (33%) total documented joints, leaving the remaining 611 occurrences (67%) unfilled (Table 5.3.5). Filled joints include occurrences of hematite (29%), epidote (10%), quartz (2%) and chlorite (<1%). The majority of secondary minerals and alteration were identified on subvertical joints, however several occurrences of hematite and epidote were also observed on intermediate and subhorizontal joints.

Table 5.3.5: Joints - Secondary Minerals and Alteration in the Black-Pic Batholith Area - West

Mineral Phase/Alteration	All Occurrences	% of Total	Subvertical Dip (61-90°)	Intermediate Dip (31-60°)	Subhorizontal Dip (0-30°)
Hematite	267	29	237	19	11
Epidote	92	10	83	4	5
Quartz	19	2	18	1	0
Chlorite	5	<1	5	0	0
None	611	67			
Total # of Joints	**908**				

Secondary mineral infilling and alteration was identified on 62 out of 155 (40%) total documented faults, leaving the remaining 93 occurrences (60%) unfilled (Table 5.3.6). Filled faults include occurrences of hematite (35%), epidote (26%), chlorite (3%), quartz (3%), and limited magnetite and carbonate (1% each). Secondary minerals and alteration were identified primarily on sub-vertical faults, though few intermediate dip faults also exhibited secondary mineralization.

Table 5.3.6: Faults - Secondary Minerals and Alteration in the Black-Pic Batholith Area - West

Mineral Phase/Alteration	All Occurrences	% of Total	Subvertical Dip (61-90°)	Intermediate Dip (31-60°)	Subhorizontal Dip (0-30°)
Hematite	55	35	49	6	0
Epidote	41	26	37	4	0
Chlorite	5	3	3	2	0
Quartz	4	3	4	0	0
Magnetite	1	1	0	1	0
Carbonate	1	1	1	0	0
None	93	60			
Total # of Joints	**155**				

Secondary mineral infilling and alteration for the 10 observed veins is shown in Table 5.3.7 below. The most common fill was quartz with eight occurrences (80%), followed by epidote with four occurrences (40%), three occurrences of plagioclase + K-feldspar + biotite (30%), and one occurrence of chlorite (10%). Both subvertical and intermediate dip veins exhibited secondary mineral infill.

Table 5.3.7: Veins - Secondary Minerals and Alteration in the Black-Pic Batholith Area - West

Mineral Phase/Alteration	All Occurrences	% of Total	Subvertical Dip (61-90°)	Intermediate Dip (31-60°)	Subhorizontal Dip (0-30°)
Quartz	8	80	4	4	0
Epidote	4	40	2	2	0
Plag+KF+Bt	3	30	0	3	0
Chlorite	1	10	1	0	0
Total # of Veins	**10**				

5.4 Black-Pic Batholith Area - East

The Black-Pic batholith area - east consists predominantly of foliated tonalite of the Black-Pic batholith, typically intruded by felsic dykes and several small intrusions of leucocratic granite. The Black-Pic batholith area - east is located approximately 30 kilometres east-southeast of Manitouwadge.

5.4.1 Accessibility and Surface Constraints

The Black-Pic batholith area - east can be accessed from a network of primary, secondary and tertiary logging roads and trails (Figure 5.4.1). A single north-south primary road (the 400 logging road) bisects the mapping area from north to south and provides access to multiple secondary and tertiary roads (Figure 5.4.2). This road can be accessed by travelling east from Manitouwadge along the Camp 70, Twist Lake and Ice Lake roads. Alternatively, it can be accessed via a road system originating from the Township of White River. The 400 road is a maintained, primary, double track gravel road that is actively being used for logging.

Numerous secondary and tertiary logging roads and trails originate from this road and are single track gravel and mud roads that are currently being used for logging. Maintenance of these roads will persist for the duration of logging activities. Additional logging roads were continually being built throughout the mapping campaign. Active logging was observed along all maintained roads, and

considerable caution should be taken when travelling in this area. Trails in the area comprise abandoned logging roads that were partly traversable by ATV.

Collectively, the secondary road network provided access to the north-central and northeastern portions of the mapping area. The 400 logging road provided limited access to the southeast portion of the study area. The remainder of the study area was only accessible by helicopter and extensive foot traverses.

5.4.2 Bedrock Exposure and Overburden Thickness

The Black-Pic batholith area - east is located in an area previously mapped as bedrock terrain with limited surficial cover (AECOM, 2014). Previously mapped surficial cover is restricted to a zone of north- and northeast-trending glaciofluvial terrain along the east margin and in the southeast portion of the study area, and isolated zones of organic and glaciofluvial terrain throughout the remainder of the mapping area. Mapping revealed that these areas of overburden can be significantly thick (<10 metres).

Remotely predicted outcrop for the Black-Pic batholith area - east were identified throughout the study area, and typically occurred as clusters of relatively small predicted bedrock outcrops extending in northwest, north, and northeast orientations. The orientation of outcrop clusters is a result of the dominant glacial and structural trends. Limited predicted outcrop was identified in the areas previously mapped as overburden.

Field investigations confirm that predicted outcrop in areas previously mapped as bedrock terrain are consistently exposed bedrock. The best exposures occurred along or adjacent to north- and northeast-trending physiographic features (lakes, ridges, valleys) and are particularly well-exposed in areas of recent logging (Figures 5.4.2B-D). Areas of overburden are characterized by extensive thick cover (minimum greater than 1 metre), that can be significantly thicker (<10 metres) along eskers and where exposed in gravel pits (Figure 5.4.2E). Predicted outcrops identified during mapping as overburden are typically located in or near areas previously mapped as glaciofluvial terrain (Figure 5.4.2F). Of the 124 predicted outcrops visited, 123 were confirmed to be bedrock, whereas only one was confirmed as overburden, with three additional overburden stations added to document other areas of known overburden.

5.4.3 Lithology and Physical Character

The descriptions below provide an overview of the main and minor bedrock lithological units observed in the Black-Pic batholith area - east, including their main physical characteristics. Lithological units described below as main units tend to occur as the predominant rock type covering at least 60% of the exposed bedrock, by area, at any individual bedrock station, and are observed at a high frequency of bedrock stations overall. Minor lithological units described below may occasionally occur as the main rock type at individual bedrock stations, but in general they occur infrequently, and represent only a small portion overall of the bedrock in the Black-Pic batholith area - east.

The Black-Pic batholith area - east consists predominantly of foliated to massive tonalite to granodiorite which represents the only main lithological unit in this portion of the Black-Pic batholith (Figure 5.4.3). Five minor lithological units are recognized in the Black Pic Batholith area - east (Figure 5.4.5). Irregular xenoliths of diorite and tonalite gneiss are hosted by the foliated to massive tonalite to granodiorite unit and represent early components of it. The foliated tonalite to

granodiorite unit is also intruded by mafic gabbroic dykes, a diorite to granodiorite unit, and granite. In addition, migmatitic metasedimentary rock was identified in one occurrence.

A summary of characteristics of the lithological units encountered in the Black-Pic batholith area - east is included in Table 5.4.1 below.

Table 5.4.1: Summary of Bedrock Characteristics by Lithological Unit for the Black-Pic Batholith Area - East

Lithological Unit	# of Occurrences (% of bedrock stations)	Fabric	Magnetic Susceptibility (average S.I.)	Gamma Spectrometry (average)	Strength (range)
Tonalite to Granodiorite	110 (89%)	Foliated to Gneissic	Tonalite: 4.565×10^{-3} Granodiorite: 4.207×10^{-3}	Tonalite: K = 1.1% U = 0.6 ppm Th = 2.0 ppm Granodiorite: K = 1.3% U = 0.5 ppm Th = 2.8 ppm	R5-R6
Diorite to Granodiorite	7 (6%)	Massive to weakly foliated	2.839×10^{-3}	K = 1.5% U = 0.8 ppm Th = 4.1 ppm	R5-R6
Gabbro	3 (2%)	Foliated	1.635×10^{-3}	K = 2.4% U = 0.1 ppm Th = 2.4 ppm	R5
Granite	22 (18%)	Massive	1.939×10^{-3}	K = 2.6% U = 0.9 ppm Th = 6.8 ppm	R4-R5
Migmatitic Metasedimentary Rock	1 (<1%)	Strongly foliated	12.534×10^{-3}	K = 0.8% U = 0.4 ppm Th = 2.5 ppm	R4

Note: Percentages in the second column exceed 100% because more than one rock type can be found at a single station.

Tonalite to Granodiorite

The Black-Pic batholith area - east is located dominantly within a tonalite to granodiorite suite of the Black-Pic batholith. Tonalite and granodiorite were observed in 110 of the 123 bedrock outcrops visited (89%). In the majority of occurrences, the tonalite to granodiorite suite represents more than 90% of the exposed bedrock, by area (e.g., Figures 5.4.4A and 5.4.4B). Overall, this unit is interpreted to represent greater than 90 percent of the underlying bedrock of the entire area. A total of 85 representative samples of tonalite and granodiorite were collected during the field investigations.

Tonalite and granodiorite have similar mineral compositions with slight differences in feldspar content, and were interpreted to be a single intrusive phase straddling the tonalite-granodiorite composition ranges and are reported here as a single intrusive suite. Granodiorite was observed more commonly in the centre, while tonalite was observed in the eastern and western portions of the Black-Pic batholith area - east. The tonalite to granodiorite varies from homogenous to moderately heterogeneous, locally contains irregular xenoliths of diorite and rarely tonalite gneiss, and is intruded by several minor phases, which are described separately below. In general, the granodiorite phase is more homogenous than the tonalite, with fewer observations of secondary rock types recorded in the granodiorite.

The tonalite to granodiorite is characterized by an equigranular, fine- to medium-grained crystal form (0.5 to 5 millimetre crystals), with a pink to grey to white weathered and fresh colour (Figures 5.4.4C and 5.4.4D). Accessory minerals typically include biotite, occasionally hornblende, and magnetite. A weak to strong, typically shallowly dipping foliation is developed throughout the majority of the tonalite to granodiorite. Locally, however, no ductile fabric is clearly present and the tonalite to granodiorite exhibited a massive texture. In particular, massive textures were observed more frequently within outcrops forming a northeast-oriented cluster in the central portion of the mapping area, south of a previously mapped unnamed northeast-trending granite to granodiorite pluton (Figure 5.4.7). Additional ductile features (i.e., shear zones) were rarely observed.

A total of 118 rock hardness measurements were made on the tonalite to granodiorite in the Black-Pic batholith area - east. In 115 instances (97%) it exhibited a very strong (R5) character, and in the remaining 3 instances (3%), it exhibited an extremely strong (R6) character.

A total of 110 magnetic susceptibility measurements were taken of the tonalite to granodiorite in the Black-Pic batholith area - east and the results suggest a typically low intensity magnetic character (Figure 5.4.4E). The tonalite ranged from 0.16 to 12.48 $x10^{-3}$ SI, and yielding an average value of 4.57 $x10^{-3}$ SI, and a standard deviation of 2.77 $x10^{-3}$ SI. The granodiorite ranged from 1.01 to 9.61 $x10^{-3}$ SI, and yielding an average value of 4.21 $x10^{-3}$ SI, and a standard deviation of 2.24 $x10^{-3}$ SI.

A total of 104 gamma-ray spectrometry measurements were taken of the tonalite to granodiorite in the Black-Pic batholith area - east (Figure 5.4.4F). The measurements yielded the following results for tonalite:

- Total Count (Range: 41 – 116 Average: 67 Std. Dev: 16)
- Potassium (%) (Range 0.6 – 2.1 Average: 1.1 Std. Dev: 0.3)
- Uranium (ppm) (Range 0 – 5.0 Average: 0.6 Std. Dev: 0.9)
- Thorium (ppm) (Range 0 – 5.9 Average: 2.0 Std. Dev: 1.2)

The measurements yielded the following results for granodiorite:

- Total Count (Range: 30 – 200 Average: 71 Std. Dev: 37)
- Potassium (%) (Range 0.6 – 3.5 Average: 1.3 Std. Dev: 0.8)
- Uranium (ppm) (Range 0 – 3.1 Average: 0.5 Std. Dev: 0.7)
- Thorium (ppm) (Range 0.6 – 18.3 Average: 2.8 Std. Dev: 3.2)

Minor Lithological Units

Four groups of minor lithological units were observed in the Black-Pic batholith area - east, including minor intrusions of diorite to granodiorite, mafic gabbroic dykes, granite, and a single occurrence of migmatitic metasedimentary rock (Figures 5.4.5 and 5.4.6).

Diorite to Granodiorite

Diorite to granodiorite was observed in 7 of the 123 bedrock outcrops visited (6%). Occurrences of diorite to granodiorite to granite were dominantly observed in the northern portion of the Black-Pic batholith area - east. Diorite to granodiorite to granite typically form minor intrusions within the foliated tonalite to granodiorite main unit. The geometry and size of the diorite to granodiorite intrusions could not be determined, however based upon the distance to adjacent outcrops of tonalite they are interpreted to be relatively small (e.g., sub-kilometre scale diameter) and discontinuous.

The diorite to granodiorite unit is characterized by a homogeneous, equigranular fine- to medium-grained crystal form (0.5 to 5 millimetre crystals), with a massive to weakly foliated texture. The diorite component is grey to dark green when fresh and when weathered. The granodiorite component is pink to off white when fresh and when weathered.

A total of seven rock hardness measurements were made on the diorite to granodiorite in the Black-Pic batholith area - east. In six instances (86%) it exhibited a very strong (R5) character, and in the remaining instance (14%), it exhibited an extremely strong (R6) character.

A total of six magnetic susceptibility measurements were made on the diorite to granodiorite and these yielded an average value of 2.84 $x10^{-3}$ SI. A total of five gamma-ray spectrometry measurements were taken from diorite to granodiorite with the following average results: K = 1.5%; U = 0.8 ppm; and Th = 4.1 ppm.

Gabbro

Rare occurrences of gabbro were documented at 3 of the 123 bedrock outcrops visited (2%). Gabbro is distributed throughout the Black-Pic batholith area - east, primarily as narrow foliated dykes (less than 1 metre wide) intruding tonalite and granodiorite. No clear systematic distribution of gabbro dykes could be discerned. Contacts between gabbro and the surrounding bedrock are generally intact and exhibit no evidence of localized brittle deformation.

Gabbro occurrences are characterized by an equigranular, very fine- to fine-grained crystal form (0.1 to 1 millimetre crystals), and foliated texture. They are dark green to green when fresh and when weathered.

A total of three rock hardness measurements were made on the gabbro in the Black-Pic batholith area - east. In all instances (100%) it exhibited a very strong (R5) character.

A total of two magnetic susceptibility measurements were made on the gabbro and these yielded an average value of 1.63 $x10^{-3}$ SI. One gamma-ray spectrometry measurements was taken from gabbro with the following results: K = 2.4%; U = 0.1 ppm; and Th = 2.4 ppm.

Granite

Granite was identified at 22 of the 123 bedrock outcrops visited (18%). Granite occurs as intrusive bodies of significant sizes (up to 1 kilometre wide), such as the granite units mapped west of Longnega Lake (Figure 5.4.5). Granite also occurs as a range of centimetre to half-metre wide, linear to curvilinear and variably-oriented aplitic or pegmatitic felsic dykes. Granite intrudes the tonalite to granodiorite throughout the entirety of the Black-Pic batholith area - east, however homogenous granite is more abundant in the north-central part of the area. A greater abundance of felsic dykes was typically observed in the tonalite relative to the granodiorite. Larger occurrences of granite may represent a phase of the main foliated to massive tonalite to granodiorite unit. The contact between granite intrusions and the surrounding tonalite to granodiorite is consistently intact, with no evidence of brittle re-activation.

Granite is pink to red to off white when fresh and when weathered. It exhibits multiple crystal forms (porphyritic, equigranular, inequigranular, vari-texture, graphic), a fine to coarse grain size (0.5 to 10 millimetre crystals), and a massive texture.

A total of 22 rock hardness measurements were made on the granite. In 21 instances (95%) it exhibited a very strong (R5) character, and in the remaining instance (5%), it exhibited a strong (R4) character.

A total of 18 magnetic susceptibility measurements were made on the granite and these yielded an average value of 1.94 $x10^{-3}$ SI. A total of 15 gamma-ray spectrometry measurements were taken from granite with the following average results: K = 2.6%; U = 0.9 ppm; and Th = 6.8 ppm.

Migmatitic Metasedimentary Rocks

A single occurrence of migmatitic metasedimentary rock consisting of metatexite, and representing less than one percent of all bedrock outcrops visited, was documented in the central northern portion of the Black-Pic batholith area - east. This lithology is characterized by a strongly foliated, fine-grained, variable-textured multi-metre wide raft of biotite-garnet pelite bound between diorite and granite intrusions.

In one rock hardness measurement, the migmatitic metasedimentary rock exhibited a strong (R4) character. One magnetic susceptibility measurement was made on the migmatitic metasedimentary rock and these yielded an average value of 12.53 $x10^{-3}$ SI. One gamma-ray spectrometry measurements was taken from migmatitic metasedimentary rock with the following results: K = 0.8%; U = 0.4 ppm; and Th = 2.5 ppm.

5.4.4 Structure

Ductile and brittle structures observed throughout the Black-Pic batholith area - east are discussed below and presented in Figures 5.4.7 – 5.4.20. Ductile structures include foliation and limited gneissosity, ductile and brittle-ductile shear zones, and associated mineral lineations. Brittle structures include joints, veins, faults, and associated lineations (i.e., slickenlines). Fracture infilling minerals, alteration, and the orientation of the fracture sets are also discussed.

5.4.4.1 Ductile Structure

Ductile structures observed in the Black-Pic batholith area include abundant foliations, and limited gneissosity, ductile and brittle-ductile shear zones, and associated mineral lineations. While many of these features can be described qualitatively, many of them represent statistically uniform distributions, or there is too little data to provide meaningful average values. A summary of ductile structures is presented in Table 5.4.2.

Table 5.4.2: Summary of Ductile Structures in the Black-Pic Batholith Area - East

Structure Type	Orientation Family	Peak (°)	Frequency (%)	Range (°)	Confidence
Tectonic Foliation	W	270	6.8	12	Medium-Low
	WNW	290	11.4	31	Medium-High
	NE	038	10.7	23	Medium
	ENE	066	6.9	19	Medium-Low
Gneissic Layering	NW	302	49.6	17	Medium-High
	NNW	337	49.6	17	Medium-High
Mineral Foliation	W	270	7.0	14	Medium-Low
	WNW	290	11.7	30	Medium-High
	NE	038	11.0	24	Medium-High
	ENE	066	7.1	22	Medium-Low
Shear Zones	NNE	023	49.6	17	Medium-High
	NW	304	49.6	17	Medium-High

Foliation and Gneissosity

Within the Black-Pic batholith area - east, a mineral foliation and a gneissosity represent a spectrum of planar fabrics resulting from the alignment and segregation of mineral grains due to progressive deformation. These planar fabrics often exhibit similar orientations and have only minor variations in texture (i.e., are transitional between foliated and gneissic), and are interpreted to represent components of composite tectonic foliation that developed during a series of progressive deformation events; these fabrics are therefore discussed together.

A total of 72 foliation and two gneissosity measurements were recorded in the Black-Pic batholith area - east, dominantly within tonalite and granodiorite, and locally also within granite and diorite intrusions (Figures 5.4.7 and 5.4.8). Penetrative planar fabrics are typically not developed within the felsic dykes that cross-cut the tonalite to granodiorite suite.

Foliation within the Black-Pic batholith area - east is typically weak to moderate, with the exception of a single domain of moderate to strong foliation, and is defined by the alignment of biotite and locally hornblende (Figure 5.4.11A-C). Gneissic layering was only observed in a single station in what was interpreted to be xenolithic panels of gneiss. The gneissic layering is defined by the segregation and alignment of felsic and mafic minerals and a moderate intensity planar fabric. In general, ductile structures are much weaker in the Black-Pic batholith area - east relative to the Black-Pic batholith area - west.

Foliation is dominated by sub-horizontal to shallowly dipping measurements (Figure 5.4.8A and 5.4.11C) suggesting that the area is largely at a structural culmination or series of culminations. The structural pattern is not as clear on the map view due to the shallowly dipping foliation having strong swings in strike (Figure 5.4.7).

The total tectonic foliation population (N = 74) exhibits a broad west to west-northwest trend that ranges 265° and 308° and with one prominent peak orientation at 290° and a lesser peak at 270°, a broad northeast trend that ranges between 024° and 047° and with a peak orientation at 038°, and a broad east-northeast trend that ranges between 059° and 078° and with a peak orientation at 066° (Figure 5.4.8B).

The two gneissic layering measurements west-northwest and north-northwest and are oriented at 302° and 337°, respectively (Figure 5.4.8C). The mineral foliation population (N = 72) exhibits trends that are virtually identical to the total tectonic foliation population described above (Figure 5.4.8D).

In addition to the foliation measured, a single shallow southeast-plunging mineral lineation was measured on a south-dipping foliation surface in the central northern portion of the mapping area (Figures 5.4.7 and 5.4.8E). Typically, rocks in the Black-Pic batholith area - east do not contain a measurable mineral lineation.

The distribution of foliation throughout the mapping area, as shown in Figure 5.4.7, can be classified into four separate structural domains described from north to south below:

1. **Shallowly dipping and roughly east- to northeast-trending, weak to strong foliation located along the northern boundary of the mapping area**.

2. **Northeast-striking weak to strong foliation forming a curving, northeast-trending corridor from the central-western boundary up to the central-northern boundary of the study area**. This domain is steeply dipping in the central portion of the study area, and

shallowly southwest-dipping in the northern portion. It separates the generally flat-lying domain to the north from the southwest-dipping domain to the southeast, and is subparallel to the trend of the granitic intrusions, but it is not clear what tectonic event this structural domain is associated with.

3. **Shallowly southwest-dipping and roughly southeast-striking domain of weak to strong foliation forming a northwest-trending domain in the eastern-central portion of the map area**. Limited shallow dipping northeast-striking foliation measurements were also located within this area. This domain is approximately coincident with a cluster of tightly spaced northwest-trending Matachewan dykes, and may represent a pre-existing structural domain that was later exploited during dyke emplacement.

4. **Very shallowly dipping, southeast-striking, weak to moderate foliation located in the southern portion of the mapping area**. This area represents a domain of weakly deformed, shallowly dipping tonalite to granodiorite, potentially located at the core of a structural basin in the tonalite. Domains 2 to 4 potentially form one side of this poorly defined southwest plunging structural basin.

In the south-central part of the mapping area, a significant number of outcrops have very weak to absent foliation. This area has no road cuts nor has it been logged so exposure is not as clean as elsewhere in the map area, which may have hampered identification of the flat-lying foliation. Alternatively, this zone may represent either a later phase of the intrusion that did not experience the same degree of ductile deformation, a portion of the tonalite-granodiorite suite that was sheltered from ductile deformation.

Ductile and Brittle-Ductile Shear Zones

A total of two shear zones, including one ductile shear zone and one brittle-ductile shear zones, were identified in the Black Pic Batholith area - east (Figure 5.4.9). The single steeply dipping north-northeast-striking ductile shear zone, trending 023°, was measured in tonalite in the central northern portion of the Black-Pic batholith area - east (Figures 5.4.9 and 5.4.10). This shear zone is less than 10 centimetres wide, displays sinistral kinematic indicators (Figure 5.4.11D), and is located within, and is likely related to, the northeast-trending ductile structural domain located in the north-central part of the area. It is also adjacent to a north-northeast-trending Marathon dyke.

The single moderate-dipping, southeast-striking brittle-ductile shear zone, trending 304° was measured in the central northern portion of the study area (at the same station as the aforementioned ductile shear zone). The observed brittle-ductile shear zone were less than 3 centimetres wide, did not possess any kinematic indicators, and were oriented parallel to, and located adjacent to a major northwest-trending lineament. The brittle-ductile shear zone and the major northwest-trending lineament are also coincident with a northwest-trending cluster of tightly spaced Matachewan dykes.

5.4.4.2 Brittle Structure

Brittle structures observed in the Black-Pic batholith area - east include extensive joints, brittle faults and associated slickenlines, and rare veins. A summary of brittle structures observed in the Black-Pic batholith area - east is provided in Table 5.4.3 and details are shown in Figures 5.4.12 to 5.4.20.

Table 5.4.3: Summary of Brittle Structures in the Black-Pic Batholith Area - East

Structure Type	Orientation Family	Peak (°)	Peak Frequency (%)	Range (°)	Confidence
Joints - All	NW	310	8.1	21	Medium-High
		325	7.2	14	Medium
	NNE	018	7.2	14	Medium
	NE	038	5.8	8	Medium-Low
		054	7.8	32	Medium-High
Joints - Subhorizontal	WNW	276	8.8	15	Medium-Low
	NW	310	9.5	17	Medium
		323	10.6	13	Medium
	NNW	350	15.8	19	Medium-High
	NE	048	8.1	10	Medium-Low
Joints - Intermediate	WNW	282	5.7	3	Medium-Low
		300	10	8	Medium
	NNW	340	9.7	12	Medium
	N	000	6.5	4	Medium-Low
	NNE	025	15.6	15	Medium-High
	NE - ENE	055	11.3	14	Medium
		078	11.1	21	Medium
Joints - Subvertical	NW	310	8.6	19	Medium-High
		325	7.2	14	Medium
	NNE	018	7.6	14	Medium
	NE	038	8.2	10	Medium-Low
		054	7.8	30	Medium-High
Faults - All	WNW	292	7.9	8	Medium-Low
	NW	325	10.8	15	Medium
	NNW - NNE	346	9.7	19	Medium
		003	7.2	11	Medium-Low
		013	6.7	8	Medium-Low
	NNE	026	6.6	7	Medium-Low
	NE	053	6.9	7	Medium-Low
	ENE	066	10.2	13	Medium
Veins	NE	045	100	6	High
Secondary Mineral Infill	NW	307	7.0	11	Medium-Low
		325	8.1	21	Medium
	NNW	344	6.8	13	Medium-Low
	NNE	019	7.5	13	Medium
	NE - ENE	052	7.2	15	Medium
		068	8.0	18	Medium

Joints

A total of 496 joint measurements were recorded in the Black-Pic batholith area - east (Figures 5.4.12 and 5.4.13). Most joint sets are found across the entire area but not necessarily at the same outcrop.

Steeply dipping joints in a number of orientations, and one shallowly dipping joint set, are evident in the total joint dataset (Figure 5.4.13A). The shallowly dipping set has fewer observations than in the Black-Pic batholith area - west but this is inferred to be a result of exposure not the development of this set. Identifying a shallowly dipping joint set requires good exposure and sufficient outcrop

topography. Shallowly dipping joint sets were more commonly measured in the more rugged parts of the area and in logged areas.

The total joint population exhibits several main trends, including a broad northwest trend that ranges between 299° and 334° with orientation peaks at 310° and 325°, a north-northeast trend with an orientation peak at 018°, and a broad northeast trend that ranges between 034° and 074° with one main orientation peak at 054° and an adjacent subdued peak at 038° (Figure 5.4.13B).

Out of the total joint population, 35 joints (7%) dip between 0° and 30° and are classified as subhorizontal, 30 joints (6%) dip between 31° and 60° and are classified at intermediate, and 431 joints (87%) dip greater than 60° and are classified as subvertical. The subhorizontal joints exhibit a single moderate cluster with a peak at 333/15, and smaller concentrations at 128/21 and 223/09 on the stereonet (Figure 5.4.13A), whereas the rose diagram has peaks at 276°, 310°, 323°, 350°, and 048° (Figure 5.4.13C). The intermediate joints are too sparse to have any significant concentrations (Figure 5.4.13A), but the largest peaks on the rose diagram occur at 300°, 340°, 025°, 055°, and 078° (Figure 5.4.13D). The subvertical joints exhibit similar trends and ranges, and identical orientation peaks, to those of the total joint set (Figure 5.4.13E).

Joints with 30 to 100 centimetre spacing are the most common overall in the Black-Pic batholith area - east (Figure 5.4.14), and this average spacing is smaller than the Quetico and Fourbay Lake pluton areas, but comparable to the Black-Pic batholith area - west. In the Black-Pic batholith area - east tighter spaced sets (3 to 10 centimetres and 10 to 30 centimetres) are more common in the northwest, northeast, and north-northeast joint sets, but the average spacing is larger (100 to 500 centimetres) for the east and shallowly dipping joint sets. Figure 5.4.15 illustrates the range of joint spacing and the nature of some of the joint sets.

Select joints throughout the Black-Pic batholith area - east contain secondary minerals (i.e., joint fill), including significant hematite staining, considerable epidote fill, and minor quartz and chlorite. A discussion of secondary mineral infilling and alteration observed in association with joints is included below in Section 5.4.4.3.

Faults

A total of 65 faults were measured throughout the Black-Pic batholith area - east. Faults were observed dominantly within the tonalite to granodiorite, but also within granite, and felsic and mafic dykes (Figures 5.4.16 and 5.4.17)

The majority of measured faults occurred as discrete millimetre to centimetre wide slip surfaces (Figure 5.4.18B). However, in multiple other instances, multiple closely spaced consecutive discrete slip surfaces are present, forming fault zones up to 10 metres wide, and often manifested as a series of scarps and sub-parallel joints, and incised valleys (e.g., Figures 5.4.18A and 5.4.18C). Fault zones are often partially buried by overburden and located in topographic lows, including rivers, valleys and swamps. Significant faults (those greater than 10 centimetres wide) are often located adjacent to northwest-trending Matachewan dykes. In particular, the most significant of these faults (those greater than 1 metre wide) are often located adjacent and oriented sub-parallel to clusters of tightly spaced Matachewan dykes.

Faults primarily dip sub-vertically (Figure 5.4.17A). The total fault population exhibits multiple trends, including, a west-northwest trend with one orientation peak at 292°, a northwest trend with one orientation peak at 325°, a broad north-northwest to north-northeast trend that ranges between 338° and 016°, and includes one main orientation peak at 346° and adjacent subdued peaks at 003° and 013°, another north-northeast trend with one orientation peak at 026°, a northeast trend with one

orientation peak at 053°, and an east-northeast trend with one orientation peak at 066° (Figure 5.4.17B).

The distribution and orientation of faults throughout the Black-Pic batholith area - east can be roughly classified into three categories.

1. North-northeast to north-northwest-trending faults located in the central northern portion of the study area, south of Longnega Lake, and adjacent, and often subparallel to a north-northeast-trending Marathon dyke. The north-trending Longnega Lake likely forms the northern continuation of this group of brittle faults.
2. Northeast-trending brittle faults located adjacent to the northeast-trending Biscotasing dyke that bisects the centre of the study area.
3. Northwest-trending brittle faults are located adjacent, and often sub-parallel, to Matachewan dykes. These faults occur most commonly within clusters of tightly spaced Matachewan dykes, and were also observed adjacent to isolated Matachewan dykes.

Offsets along faults were observed in only 14 out of 65 faults, and each total offset was typically minor (less than 10 centimetres). Dextral strike-separation or slip is observed in eight brittle faults with north-northwest and east-northeast trends (Figure 5.4.17C), and sinistral strike-separation or slip is defined in six brittle faults with north to north-northwest and northeast trends (Figure 5.4.17D). The remaining faults with unknown offset exhibit a broad range of orientations similar to that of the total fault population (Figure 5.4.17E). The spatial distribution of dextral and sinistral faults often overlap and do not clearly define distinct fault zones with clear movement senses. Rather, these data suggest a complex brittle deformation history, potentially with multiple stages of fault movement.

Limited weak to moderate slickenlines and steps are locally developed along fault surfaces and are characterized by polished surfaces with secondary mineral growth (typically quartz, epidote). Slickenlines exhibited shallow plunges, also indicating predominant strike-slip movement, and primarily on north to north-northwest trending fault planes (Figure 5.4.17F).

Numerous faults, both narrow and wide, exhibit hematite staining (Figure 5.4.18E), whereas only a limited number of faults contain epidote, chlorite, and quartz fill. A discussion of secondary mineral infilling and alteration observed in association with faults is included below in Section 5.4.4.3.

Veins

One northeast-striking vein was identified in the Black-Pic batholith area - east (Figures 5.4.19 and 5.4.20). The measured vein is located in the southeast portion of the study area within foliated tonalite, and is not a significant structural feature throughout the mapping area. The vein is less than 3 centimetres wide, steeply dipping, exhibits extensional textures, and is filled with quartz (Figure 5.4.20C).

5.4.4.3 Secondary Minerals/Alteration

Secondary minerals were observed along numerous brittle structures throughout the Black-Pic batholith area - east (Figure 5.4.21). Structures with secondary minerals and alteration are described below and summarized in Tables 5.4.3 to 5.4.5 below, for all fractures in the Black-Pic batholith area - east (N = 562), including 496 joints, 65 faults and 1 vein. Secondary mineral orientation information is summarized in Figure 5.4.22 and some representative field examples are illustrated in Figure 5.4.23.

Overall, 366 out of 562 total fractures (65%) observed exhibited no secondary mineral infill or alteration (Table 5.4.3), leaving 196 fractures (35%) with some evidence of secondary mineral infill or alteration. The majority of secondary mineral infillings and alteration were observed on sub-vertical structures, dipping greater than 60° (Figure 5.4.22A).

The total secondary mineral and alteration fracture population includes a broad northwest trend ranging between 302° and 334° and with orientation peaks at 307° and 323°, and a north-northwest trend with an orientation peak at 344° a north-northeast trend with an orientation peak at 019°, a broad northeast trend ranging between 042° and 075° and with orientation peaks at 052° and 068° (Figure 5.3.22B).

In general, fractures commonly exhibit extensive hematite staining, local epidote fill, and limited quartz and chlorite fill. The number of secondary mineral and alteration types identified within all fractures in the Black-Pic batholith area - east are: hematite identified in 184 fractures (33%), epidote in 36 fractures (6%), chlorite in 10 fractures (2%), and quartz in 6 fractures (1%) (Table 5.4.4). In some instances, more than one infilling mineral was identified within a single fracture.

Table 5.4.4: All Fractures - Secondary Minerals and Alteration in the Black-Pic Batholith Area - East

Mineral Phase/Alteration	All Occurrences	% of Total
Hematite	184	33
Epidote	36	6
Chlorite	10	2
Quartz	6	1
None	366	65
Total # of Fractures	**562**	

Hematite was observed as iron staining in faults and joints, present throughout area in all the common structure trends (Figure 5.4.22C). Hematite was observed in association with all other identified secondary minerals. The distribution of hematite in fractures, predominantly joints, defines multiple northwest- and northeast-trending domains throughout the mapping area, include significant domains along the northeast-trending Biscotasing dyke that bisects the centre of the study area, and along a cluster of tightly spaced northwest-trending Matachewan dykes in the northeast portion of the study area. These observations, and similar ones below for epidote, quartz and chlorite, indicate that secondary minerals were best developed along fractures proximal to Proterozoic dykes.

Epidote was observed as filling in faults and joints. Epidote was relatively more common along northwest-trending structures parallel to the Matachewan dyke trend and north-northeast-trending structures (Figure 5.4.22D). Epidote was typically associated with hematite, and locally with quartz and chlorite.

Quartz was observed filling faults, joints and the single vein occurrence. Quartz was most commonly observed in north-trending structures (Figure 5.4.22E). It is most abundant in the northern portion of mapping area, and typically located proximal to northwest-trending Matachewan dykes. Limited other quartz occurrences are dispersed throughout the northern portion of the study area. Quartz typically occurs in association with hematite and epidote, and locally chlorite.

Chlorite was observed as a coating along faults and joints and, similar to quartz, was most commonly observed in north-trending structures (Figure 5.4.22F). Chlorite is observed in the northern portion of

the mapping area, and typically located proximal to northwest-trending Matachewan dykes. Chlorite occurred in isolation and in association with all other secondary minerals.

Secondary mineral infilling and alteration was identified on 175 out of 496 (35%) total documented joints, leaving the remaining 321 occurrences (65%) unfilled (Table 5.4.5). Filled joints include occurrences of hematite (33%), epidote (6%), quartz (1%) and chlorite (1%). The majority of secondary minerals and alteration were identified on subvertical joints, however several occurrences of hematite were also observed on intermediate and subhorizontal joints.

Table 5.4.5: Joints - Secondary Minerals and Alteration in the Black-Pic Batholith Area - East

Mineral Phase/Alteration	All Occurrences	% of Total	Subvertical Dip (61-90°)	Intermediate Dip (31-60°)	Subhorizontal Dip (0-30°)
Hematite	164	33	154	5	5
Epidote	31	6	30	1	0
Quartz	4	1	4	0	0
Chlorite	5	1	5	0	0
None	321	65			
Total # of Joints	**496**				

Secondary mineral infilling and alteration was identified on 20 out of 65 (31%) total documented faults, leaving the remaining 45 occurrences (69%) unfilled (Table 5.4.6). Filled faults include occurrences of hematite (31%), epidote (8%), chlorite (8%), and quartz (1%). Secondary minerals and alteration were identified primarily on sub-vertical faults, though few intermediate dip faults also exhibited secondary hematite mineralization.

Table 5.4.6: Faults - Secondary Minerals and Alteration in the Black-Pic Batholith Area - East

Mineral Phase/Alteration	All Occurrences	% of Total	Subvertical Dip (61-90°)	Intermediate Dip (31-60°)	Subhorizontal Dip (0-30°)
Hematite	20	31	18	2	0
Epidote	5	8	5	0	0
Chlorite	5	8	5	0	0
Quartz	1	2	1	0	0
None	45	69	39	6	0
Total # of Faults	**65**				

As noted above, only one, quartz-filled, sub-vertical, vein was observed in the Black-Pic batholith area - east.

5.5 Dykes in the Township of Manitouwadge Area

Multiple generations of dykes were observed throughout the Manitouwadge area, including Proterozoic diabase dykes (Figure 5.5.1) and older mafic to felsic dykes (Figure 5.5.2). Proterozoic dykes are the most abundant, and could be separated into three generations based on their trend direction, including northwest-trending Matachewan dykes (Section 5.5.1), north- to north-northeast-trending Marathon dykes (Section 5.5.2), and northeast-trending Biscotasing dykes (Section 5.5.3). Section 5.5.4 provides an overview of additional information on the older, Archean-aged, mafic to felsic dykes. This information supplements what was presented on these features in the area-specific descriptions above.

A summary of lithological and physical properties for each of the Proterozoic mafic dyke sets is included in Table 5.5.1. The maximum database dyke width division is >1000 centimetres and does not adequately characterize the width of the Proterozoic dykes. The width for Matachewan, Marathon and Biscotasing dykes in Table 5.5.1 and Figures 5.5.1.1D, 5.5.2.1D, and 5.5.3.1D are based on a manual compilation of widths found in comment notes, and measurements between tracked mapped contacts and well defined contacts visible on high resolution aerial photographs.

Table 5.5.1: Summary of Proterozoic Mafic Dyke Characteristics

Mafic Dyke Swarm	Number of Bedrock Station Occurrences	Width (m)	Orientation	Peaks (°)	Magnetic Susceptibility (average SI)	Gamma (average K, U, Th)	Strength (range)
Matachewan	31	1.0 – 36.9	NW	300 315	37.6 $x10^{-3}$	K = 0.64% U = 0.67 ppm Th = 2.78 ppm	R4-R6
Marathon	29	<1.0 - 19	N-NNE	000 027	29.76 $x10^{-3}$	K = 0.97% U = 0.62 ppm Th = 4.92 ppm	R4-R6
Biscotasing	12	<1.0 - 59	NE	032 045	30.04 x 10^{-3}	K = 0.62% U = 0.20 ppm Th = 2.89 ppm	R5-R6

5.5.1 Matachewan Dykes

Numerous Matachewan dykes were observed throughout the Manitouwadge area and were distinguished based on their consistent northwest trend. These dykes are Proterozoic in age (circa 2.473 Ga; Buchan and Ernst, 2004), and cross-cut all Archean bedrock units.

5.5.1.1 Lithology and Physical Characteristics

Matachewan dykes were observed in 31 outcrops and represent the most abundant generation of Proterozoic dykes observed within the Manitouwadge area (Figure 5.5.1). A total of 24 representative samples of Matachewan dykes were collected during the field investigations.

Matachewan dykes occur as continuous linear dykes, and were observed in multiple outcrops in all mapping areas except the Fourbay Lake pluton area. Dykes occur as individual features (Figure 5.5.1.1A), and also as series of closely spaced, sub-parallel dykes. Clusters of Matachewan dykes are most common in the Black-Pic batholith area - east.

Matachewan dykes exhibit an equigranular, diabase, and porphyritic texture characterized by a very fine- to medium-grained groundmass (0.1 to 5 millimetre crystals) of mafic minerals (pyroxene, plagioclase, hornblende, +/- magnetite, olivine and biotite) (Figure 5.5.1.1B), that commonly includes characteristic fine- to very coarse-grained elongate plagioclase phenocrysts (0.5 to 50 millimetre crystals) (Figure 5.5.1.1C). These dykes are dark green to dark grey when fresh and brown to green when weathered.

A total of 31 rock hardness measurements were made on the Matachewan dykes. In 26 instances (84%) it exhibited a very strong (R5) character, and in the remaining five instances, it exhibited one instance (3%) of strong (R4) character, and four instances (13%) of extremely strong (R6) character.

A histogram of Matachewan mafic dyke width measurements, based on a manual compilation of widths found in comment notes, and measurements between tracked mapped contacts and well defined contacts visible on high resolution aerial photographs, is presented in Figure 5.5.1.1D. Contacts on both edges of dykes were rarely observed, making it difficult to assess true dyke width

and so in some cases only a minimum width was assigned. More than half (8/15; 53%) of the measurements yielded dyke widths of at least 20 metres. Where both bounding contacts were observed, dykes were measured up to a maximum width of 36.9 metres (station 16BH0036).

A total of 27 magnetic susceptibility measurements were taken for the Matachewan dykes (Figure 5.5.5.1E). The measurements range from 15.6 to 55.5 $x10^{-3}$ SI, yielding an average value of 37.6 $x10^{-3}$ SI, and a standard deviation of 8.63 $x10^{-3}$ SI. Overall, the measured values are slightly higher than the other Proterozoic dykes but the histogram has the same peak as the other dyke sets. The distribution of magnetic susceptibility measurements for the Matachewan dykes throughout the Manitouwadge area is relatively consistent, but does exhibit zones of minor variability, including elevated magnetism in Matachewan dykes in the Quetico area, and lower magnetism along the southernmost dyke in the Black-Pic Batholith area - west.

A total of 25 gamma-ray spectrometry measurements were taken for the Matachewan dykes (Figure 5.5.5.1F). The measurements yielded the following results:

- Total Count (Range: 40 – 80 Average: 60.2 Std. Dev: 9.74)
- Potassium (%) (Range 0.3 – 1.2 Average: 0.64 Std. Dev: 0.264)
- Uranium (ppm) (Range 0 – 3.0 Average: 0.67 Std. Dev: 0.621)
- Thorium (ppm) (Range 1.6 – 4.5 Average: 2.78 Std. Dev: 0.809)

All gamma-ray spectrometry measurements for the Proterozoic dykes are relatively consistent. Generally the Matachewan dykes cluster tightly near the thorium apex on a thorium-uranium-potassium ternary diagram but show a higher spread toward the uranium apex compared to the other dyke sets. The Matachewan dykes in particular exhibit relatively uniform and average to slightly below average total count, potassium, uranium and thorium values (relative to other Proterozoic dykes). Two elevated uranium readings were recorded in the Quetico and Black-Pic batholith - east areas and do not correlate with any significant known geological feature.

5.5.1.2 Structure

Matachewan dykes and dyke contacts were observed in all mapping areas except in the Fourbay Lake Pluton area (Figure 5.5.1). Dykes are typically hosted in tonalite within the Black-Pic Batholith areas or migmatitic metasedimentary rocks within the Quetico area. Where contacts were observed, Matachewan dykes consistently dip steeply, with a tendency towards a northeasterly dip (Figure 5.5.1.2A). Matachewan dykes consistently strike northwest, with a main orientation peak at 315°, a lesser peak at 300°, and a total range in orientation of between 293° and 333° (Figure 5.5.1.2B).

Dyke contacts are characterized by distinctive glassy/aphanitic chilled margins between 0.5 – 1 centimetres that transition into fine-grained crystalline texture moving into the dyke away from the margins for up to 30 centimetres. Dykes and dyke contacts were observed to be linear on a regional scale, but exhibit minor variability on the outcrop scale, including narrow dyke splays (Figure 5.5.1.3A).

Jointing within Matachewan dykes is typically pervasive (Figure 5.5.1.3). A summary of joint orientations is provided in Figures 5.5.1.2C and 5.5.1.2D. The majority of measured joints dip steeply and multiple orientation peaks, at 020°, 040°, 080°, 282°, 304° and 342°, are evident. In individual dykes the systematic orientations of measured joints relative to the dyke margin, and the pervasive nature of these joints, suggests they may have resulted from cooling of dykes within a rigid host rock.

Joint spacing measurements are summarized for dyke-hosted joints (Figure 5.5.1.2E) and joints within the adjacent bedrock (Figure 5.5.1.2F). Within-dyke joints are spaced from 3 to 10 centimetres to 500 to1000 centimetres peaking in the 30 to 100 centimetre range. Generally, joint spacing adjacent to the dyke contact is tighter in the dyke compared to the host rock, but the cores of thicker dykes often have similar spacing as the host rock. Joint spacing within Matachewan dykes locally decreases adjacent (approximately 1 to 5 metres) to the dyke contact, with rare instances of tighter spacing at the contact. Locally, joints are also more closely spaced in the host rock up to 1 metre beyond the dyke contact, but in most instances no increased jointing in the host rock was observed directly adjacent to Matachewan dykes. Beyond this distance, joint spacing in the host rock reflects the joint spacing characteristic of the regional structural domain in which the station resides.

In many cases, limited bedrock exposure prevents making the very detailed observations required to assess variability in joints and joint spacing within dykes, along the dyke contacts and within the surrounding rock. For a detailed description of the variability of jointing across Matachewan dykes, refer to the following section describing the Matachewan dyke scanline exercise.

Joints within the dyke are typically clean and do not exhibit any fill or alteration (Figure 5.5.1.3A). In rare instances, hematite and epidote were observed along joint surfaces within the dyke (Figures 5.5.1.3B and 5.5.1.3C). Considering the limited joint fill observed, no observations could be made regarding increases or decreases in the abundance of these secondary minerals relative to the cores versus the edges of the Matachewan dykes.

Abundant hematite, occasional epidote, and rare quartz and chlorite were observed within joints in the host rock surrounding Matachewan dykes at some stations (including stations where the dyke was directly observed, and stations located proximal to predicted dykes but where no dykes are exposed). Two additional observations suggest that that the dykes can, but do not necessarily, act as fluid conduits:

- Alteration is not limited to adjacent to the dykes, and where it continues away from the dyke, nearby brittle faults are a likely pathway for the alteration fluids (e.g., the majority of Matachewan dykes in the Black-Pic batholith area - west).
- Alteration within the host rock adjacent to individual dykes is only present at certain places along a single dyke, and is not present in all adjacent stations adjacent to the dyke (e.g., host rock alteration adjacent to Matachewan dykes in the Quetico area).

Considering these observations, dykes locally, but not universally, are interpreted to have acted as conduits for later fluids, and that the evaluation of a dyke as a conduit for groundwater must be assessed on a case by case basis.

Multiple brittle faults are located proximal to, and along Matachewan dykes, including brittle faults cross-cutting dykes at high angles, low angles, and brittle faults located parallel and along or adjacent to dykes (Figure 5.5.1.3D). Brittle faults at a high angle to Matachewan dykes were best observed in the southern portion of the Black River / Agonzon Lake northeast-trending brittle fault zone, where series of discrete, steeply dipping, northeast-trending brittle faults are located within and directly south of a Matachewan dyke (stations 16JK0251, 0253, 0254).

Multiple brittle faults oriented sub-parallel and located adjacent to northwest-trending Matachewan dykes were observed, however relatively few brittle faults located directly along or within dykes were observed in outcrop. Examples of brittle structures located along dyke contacts include a brittle fault defined by a 5 metre scarp and rare slickenlines along the chilled margin of a dyke at station 16BH0264. This structure indicates that certain northwest-trending brittle faults exploited pre-existing Matachewan dykes. Directly adjacent to Matachewan dykes, numerous brittle faults were

observed, typically as a series of discrete faults locally forming scarps (stations 16BH0023, 0189, 250, 225, 226, 238, 248, 262; 16JK0176, 208; and Figure 5.5.1.3). These features represent discrete brittle structures localized proximal to northwest-trending Matachewan dykes, and indicate that brittle structures exploited and were developed adjacent to pre-existing northwest-trending Matachewan dykes. However, most of the actual contacts of field-verified Matachewan dykes are intact and show no evidence of faulting at the contact, indicating that the presence and intensity of brittle faulting along Matachewan dykes must be, like alteration, evaluated on a case by case basis.

5.5.1.3 Matachewan Dyke Scanline Fracture Mapping Exercise

The scanline fracture mapping exercise was undertaken along a transect at a trend of 227° oriented nearly perpendicular to a northwest-trending Matachewan dyke located on the western shore of Agonzon Lake, within the Black-Pic batholith area - west (Station 16BH0195). The results are summarized in Figure 5.5.1.4 and below.

Observations were made on an inclined plane along the sloping shoreline outcrop. Most of the dyke and the southern contact is well exposed, but several metres of overburden cover the northern contact (Figure 5.5.1.1A). The selected dyke intrudes foliated tonalite, exhibits a well-defined aeromagnetic signature, and trends northwest across the entirety of the Black-Pic batholith area - west. The dyke is characterized by typical physical properties of a Matachewan mafic dyke (see previous section) and is estimated to a minimum of 19 and a maximum of 28 metres wide. This dyke is located within the northeast-trending ductile and brittle deformation zones defining the northern portion of the Black River and Agonzon Lake. Representative field photographs of the dyke transect are included in Figure 5.5.1.5, with photograph locations noted in Figure 5.5.1.4A.

The scanline exercise was completed over a single continuous transect of outcrop across a Matachewan dyke from the centre of the exposed dyke to 5 metres beyond the dyke contact into the adjacent tonalite (Figure 5.5.1.5). An analysis of joint orientation within the host rocks and dyke (Figure 5.5.1.4B) reveal that the joint orientations are quite similar between the dyke and adjacent host rock, with a west-northwest-trending joint set prominent in both of these domains. Shallowly dipping joints are slightly stronger in the dyke, which also has a weak northeast-trending joint set, whereas the host rock has a weak north-northwest-trending, moderately dipping joint set not evident in the dyke.

An analysis of fracture frequency along the scanline transect (Figure 5.5.1.4C) reveals several trends. The core of the dyke has a lower joint frequency compared to the outer 5 metres of the dyke. In the 70 centimetres closest to the host rock contact, a distinct set of joints approximately perpendicular to the contact is prominent. The high fracture frequency in the dyke extends across the contact and continues in the host rock for approximately 80 centimetres before abruptly decreasing to values similar to the core of the dyke. This suggests that the contact between the dyke and the host rock was a locus of increased fracturing and that, at least in this instance, the dyke-host rock contact is not intact.

An analysis of alteration and fracture infilling of brittle structures along the scanline transect (Figure 5.5.1.4D) reveals that hematite alteration is concentrated in the dyke near the dyke contact, but continues in the host rock to the end of the transect. Chlorite alteration is focused at the contact in both the dyke and host rock. Epidote alteration is weak but locally evident along the entire transect.

An analysis of magnetic susceptibility values across the scanline (Figure 5.5.1.4E) reveals the dyke has relatively high and consistent values in the Matachewan dyke, ranging from 30.5 to 70.9 $x10^{-3}$ SI with an average value of 43.9 $x10^{-3}$ SI. The magnetic susceptibility drop at the contact and the host

foliated tonalite has much lower values ranging from 1.13 to 3.39 $x10^{-3}$ SI, with an average value of 2.29 $x10^{-3}$ SI.

In summary, these results reveal that the strongest joint set in both dyke and host rock is oriented essentially parallel to the dyke margin. The frequency of joints increases inside the dyke towards the contact, and continues for the first metre of host rock before dropping to background levels. The major north-northeast-trending lineament that follows Agonzon Lake appears to have little effect on the dyke or its contact.

5.5.2 Marathon Dykes

Numerous Marathon dykes were observed throughout the Manitouwadge area and were distinguished based upon their relatively consistent north to north-northeast trends. These dykes are Proterozoic in age (circa 2.121 Ga; Buchan et al., 1996; Hamilton et al., 2002), and cross-cut all Archean bedrock units.

5.5.2.1 Lithology and Physical Characteristics

Marathon dykes were observed in 29 outcrops investigated and represent the second most abundant generation of Proterozoic dykes observed in the Manitouwadge area (Figure 5.5.1). A total of 20 representative samples of Marathon dykes were collected during the field investigations. Lithological and physical characteristics of the Marathon dykes are locally very similar to the Matachewan dykes.

Marathon dykes occur as continuous linear dykes (Figures 5.5.2.1A and 5.5.2.1B), and were observed in outcrops dominantly in the Black-Pic batholith area - east, and less so in the other mapping areas. Dykes typically occur as parallel sets of one to three north- to north-northeast-trending dykes. Locally, Marathon dykes are segmented and step to the left and right (Figure 5.5.2.3A). This phenomenon is typically attributed to intrusive offsets during dyke emplacement and not to post-emplacement faulting.

Marathon dykes are dark green to dark grey when fresh and brown to green when weathered. They typically exhibit an equigranular texture characterized by a very fine- to medium-grained groundmass (0.1 to 5 millimetre crystals) of dominantly mafic minerals (pyroxene, plagioclase, hornblende, +/- magnetite, olivine and biotite) (Figure 5.5.2.1C).

A total of 29 rock hardness measurements were made on the Marathon dykes. In 25 instances (87%) it exhibited a very strong (R5) character, and in the remaining four instances, it exhibited one instance (3%) of strong (R4) character, and 3 instances (10%) of extremely strong (R6) character.

A histogram of Marathon mafic dyke width measurements, based on a manual compilation of widths found in comment notes, and measurements between tracked mapped contacts and well defined contacts visible on high resolution aerial photographs, is presented in Figure 5.5.2.1D. Contacts on both edges of dykes were rarely observed, making it difficult to assess dyke width. Where both bounding contacts were observed, dykes varied from less than a metre up 19 metres (station 16BH0126). Overall, there is a broad range in measured widths for Marathon dykes, with examples in the 20 - 40 metre width bin only slightly more frequent than any other width bin (6/22; 27%).

A total of 21 magnetic susceptibility measurements of the Marathon dykes, presented in Figure 5.5.2.1E, suggest that their magnetic character is generally similar to the other Proterozoic dykes. The measurements range from 1.83 to 54.20 $x10^{-3}$ SI, yielding an average value of 29.76 $x10^{-3}$ SI, and a standard deviation of 11.57 $x10^{-3}$ SI. However, these dykes also return a range of anomalously high and low values, including an elevated measurement in the northwest of the Black-Pic batholith

area - west, and a very depressed measurement in the southeast of the Quetico area. These and other slightly anomalous measurements do not appear to consistently correlate with any geological feature.

A total of 21 gamma-ray spectrometry measurements were taken for the Marathon dykes (Figure 5.5.5.1F). The measurements yielded the following results:

- Total Count (Range: 45 – 193 Average: 77.38 Std. Dev: 32.04)
- Potassium (%) (Range 0.2 – 3.0 Average: 0.97 Std. Dev: 0.643)
- Uranium (ppm) (Range 0 – 3.4 Average: 0.62 Std. Dev: 0.837)
- Thorium (ppm) (Range 2.0 – 16.8 Average: 4.92 Std. Dev: 3.22)

All gamma-ray spectrometry measurements for the Proterozoic dykes are relatively consistent. Generally the Marathon dykes cluster tightly near the thorium apex on a thorium-uranium-potassium ternary diagram with less spread than the Matachewan dykes. The Marathon dykes in particular exhibit slightly variable and above average total count, potassium, uranium and thorium values (relative to other Proterozoic dykes), including several dykes that are slightly elevated in all gamma-ray readings within the Quetico and Black-Pic batholith areas. For unknown reasons, a single dyke located in the northwest of the Black-Pic batholith area - east yielded anomalously high gamma-ray measurements. The station yielding these anomalous measurements is located adjacent to the Marathon dyke identified from the aeromagnetic survey.

5.5.2.2 Structure

Marathon dykes and dyke contacts were observed in all mapping areas, but are most abundant in the Black-Pic batholith area - east. Dykes are typically hosted in tonalite within the Black-Pic batholith areas, diorite in the Fourbay Lake Pluton area, or metasedimentary rocks within the Quetico area. Where contacts were observed, Marathon dykes consistently dip steeply, with a tendency towards an easterly dip (Figure 5.5.2.2A). Marathon dykes typically strike north to north-northeast and dip steeply, with peak orientations evident at 000° and 027°, and a total range in orientation of between 354° and 051° (Figure 5.5.2.2B).

Dykes and dyke contacts exhibit variability on a regional and outcrop scale, including deviations between north and north-northeast trends, step-overs to the east and west (Figure 5.5.2.3A), and interfingering of dyke segments. Similar to other Proterozoic dykes, dyke contacts are characterized by distinctive glassy/aphanitic chilled margins between 0.5 to 1 centimetre that transition into fine-grained crystalline texture moving into the dyke away from the margins for up to 30 centimetres (Figures 5.5.2.3A and 5.5.2.3B).

Jointing within Marathon dykes is typically pervasive and there are joint sets oriented sub-parallel and at high angles to the trend of the dykes, but the strongest set in the dykes are north-northwest trending, subparallel to brittle faults throughout the Manitouwadge area, including the Barehead Lake fault zone. The majority of measured joints dip sub-vertically, however intermediate to sub-horizontally dipping joints are also evident (Figure 5.5.2.2C). One prominent joint orientation peak is evident at 340°, with additional lesser peaks at 026°, 072° and 285° (Figure 5.5.2.2D). Similar to other Proterozoic mafic dykes, the systematic orientations and pervasive nature of these joints suggests they resulted from cooling of Marathon dykes within a rigid host rock.

Joint spacing measurements are summarized for dyke-hosted joints (Figure 5.5.2.2E) and joints within the adjacent bedrock (Figure 5.5.2.2F). Spacing of both joint types varies from 3 to 10 centimetres to 500 to 1000 centimetres, with the most common range being 30 to 100 centimetres. Two domains containing Marathon dykes, one in the Barehead Lake fault zone and one on the east

side of the Black-Pic batholith area - west, have relatively tight joint spacing (less than 30 centimetres) in the dykes.

Generally, joint spacing adjacent to the dyke contact is tighter in the dyke compared to the host rock, but the cores of thicker dykes often have similar spacing as the host rock. Joint spacing in Marathon dykes locally decreases within 1 to 5 metres of the dyke contact. Locally, joints are also more closely spaced in the host rock of up to 1 metre beyond the dyke contact. Beyond this distance, joint spacing in the host rock reflects the joint spacing characteristic of the regional structural domain in which the station resides. In some instances, no increased jointing in the host rock was observed directly adjacent to Marathon dykes.

In many cases, limited bedrock exposure inhibits the very detailed observations required to assess variability in joints and joint spacing within dykes, along the dyke contacts and within the surrounding rock. For a detailed description of the variability of jointing across Marathon dykes, refer to the following section describing the Marathon dyke scanline exercise.

Joints within Marathon dykes are dominantly clean and exhibit minimal fill or alteration (Figure 5.5.2.3), with the exception of certain areas. These areas include a Marathon dyke along the western boundary of the Black-Pic batholith area - west and adjacent to the Barehead Lake brittle fault zone, where joints contain extensive hematite and epidote alteration. The distribution of secondary minerals throughout this dyke does not indicate any systematic changes in abundance across its width, although parts of the dyke including the core have less alteration. A second area exhibiting considerable secondary minerals includes a Marathon dyke along the western boundary of the Quetico area, where joints contain considerable hematite, epidote, and chlorite alteration. Minor epidote, hematite, and chlorite alteration were also observed in isolated joints within Marathon dykes throughout the Black-Pic batholith.

Considerable hematite and moderate epidote were observed within joints in the host rock surrounding some Marathon dykes (including stations where the dyke was directly observed, and stations located proximal to predicted dykes but where no dykes are exposed). Two additional observations suggest that that the dykes can, but do not necessarily, act as fluid conduits:

- Alteration is not limited to adjacent to the dykes, and where it continues away from the dyke, nearby brittle faults are a likely source of the alteration.
- Alteration within the host rock adjacent to individual dykes is only present at certain instances along a single dyke, and is not present in all adjacent stations adjacent to the dyke.

Numerous brittle faults are located proximal to, and along, Marathon dykes, including brittle faults cross-cutting dykes at low and high angles, and brittle faults located parallel and along or adjacent to dykes. Brittle faults at a high angle to Marathon dykes were best observed in the cluster of dykes bisecting the centre of Black-Pic batholith area - west (e.g., station 16BH0040; 16BH0254, 16JK0135). These structures typically occur as individual faults and zones of discrete faults.

Multiple brittle faults located adjacent and oriented at low angles and sub-parallel to north-trending Marathon dykes were also observed. Similar to the Matachewan dykes, relatively few brittle faults located directly along dyke contacts or within dykes were observed in outcrop. In general, there are fewer brittle faults associated with Marathon dykes relative to Matachewan dykes, however the brittle faults associated with Marathon dykes tend to be more significant. These faults include:

1. **The Barehead Lake fault zone**. This brittle fault zone is described in detail in Section 5.3.4 and comprises a broad zone of pervasively jointed, brittle faulted and altered rock along the western boundary of Black-Pic batholith area - west. This brittle fault zone is coincident

with and spans beyond the extent of a north-trending Marathon dyke (Figure 5.5.2.3). Brittle faults within this zone trend north-northwest at a low angle to the Marathon dyke, and may represent secondary structures associated with a major north-trending fault located directly west of the mapping area. The exact location of the Barehead Lake fault relative to the Marathon dyke is unclear, however this fault clearly occurs proximal to the dyke, and both may have exploited the same zone of structural weakness.

2. **The northern portion of the Black River brittle-ductile fault**. This fault is described in detail in Section 5.3.4 and comprises a multi-metre wide fault characterized by the complete transposition of gneissic layering into brittle-ductile fabric, and surrounded by sub-parallel brittle faults. This fault trends northeast along the northern part of the Black River and changes to a more north-northeast geometry near the junction of this fault and a north-trending Marathon dyke (best observed in the aeromagnetic data). Discrete brittle fault surfaces parallel to the fault and dyke were observed at this junction (Stations 16JK0190 and 192). In this case, the geometry and location of the pre-existing Marathon dyke appear to have been in part responsible for the re-orientation of the fault into a more northerly trend.

3. **Brittle faults located along the southeastern lakeshore of Agonzon Lake and approximately 700 metres west of the lakeshore**. These brittle faults are characterized by pronounced greater than 10 metre tall cliffs and valleys that form adjacent to north-trending Marathon dykes (Stations 16JK0132, 134, 135). Other brittle faults sub-parallel to Marathon dykes are also present throughout the Black-Pic batholith, and occur as scarps and discrete fault planes (e.g., 16BH0092, 274).

These observations suggest that major and minor north-trending, and occasionally northeast-trending brittle faults exploited domains with pre-existing north-trending Marathon dykes. However, similar to the Matachewan dykes, many field-verified Marathon dyke contacts are not deformed, indicating that the presence and intensity of brittle faulting along individual Marathon dykes should be evaluated on a case by case basis.

5.5.2.3 Marathon Dyke Scanline Fracture Mapping Exercise

The scanline fracture mapping exercise was completed along a transect at a trend of 168° oriented obliquely to a north-northeast-trending Marathon dyke located on the western boundary of Black-Pic batholith area - west (Station 16BH0193). Results of the exercise are summarized in Figure 5.5.2.4 and below.

The entire dyke transect, including the southeast contact is well exposed along Highway 614, but the northwest dyke contact is covered (Figure 5.5.2.4A). Observations were made on a sectional view along the highway road cut. The selected dyke intrudes into foliated tonalite to granodiorite, exhibits a well-defined aeromagnetic signature, and trends north-northeast down the entire west boundary of Black-Pic batholith area - west. The dyke is characterized by typical physical properties of a Marathon mafic dyke (see previous section) and is from a minimum of 18 to a maximum of 24 metres wide. Of particular importance is that this dyke is emplaced within the Barehead Lake brittle fault zone and is strongly jointed and locally faulted. Representative field photographs of the dyke transect are included in Figure 5.5.2.5, with photograph locations noted in Figure 5.5.2.4A.

The scanline exercise was completed over a single continuous transect of outcrop with narrow covered intervals from the core of a Marathon dyke into its host rock. Images of these outcrops are stitched together and visible in Figure 5.5.2.5A.

An analysis of joint orientation within the host rocks and dyke (Figure 5.5.2.4B) reveal that three strong joint sets exist in this dyke; one oriented parallel to the contact, one perpendicular to the

contact, and a third east-trending set. Due to the orientation of the dyke transect, few north-northwest-trending joints and faults were measured. The dominant joint set in the host rock is oriented slightly clockwise from the peak of the same set in the dyke.

An analysis of fracture frequency along the scanline transect (Figure 5.5.2.4C) reveals that the frequency of joints varies significantly along the transect. Frequencies of 12 to 14 joints/metre are common for the first 12 metres from the core of the dyke, but decrease for the following 10 metres, before increasing significantly at the contact of the dyke. There is a zone approximately 1 metre wide that has significantly higher fracture frequency (30 joints/metre) in the dyke at its contact with the tonalite, with the most proximal 10 to 20 centimetres having the highest frequency. The fracture frequency decreases sharply to 9 to 10 joints/metre in the host tonalite.

Discrete faults, typically with epidote fill and hematite alteration, are present along most of the transect except for the core of the dyke. The north-northwest orientation of the scanline is parallel to the Barehead Lake fault zone, reducing the probability of intersecting structures of that same orientation, resulting in most of the measured faults trending west-northwest. The faults observed contain well-developed slickenlines and steps that indicate they are predominantly strike-slip faults with both dextral and sinistral senses of movement on the west-northwest-trending faults and dextral movement on the less common north-northwest-trending faults.

An analysis of alteration and fracture infilling of brittle structures along the scanline transect (Figure 5.5.2.4D) shows the dyke and surrounding host rock are strongly altered. Hematite and epidote are ubiquitous along the entire transect, with strong chlorite alteration within some sections of the dyke centred away from both the core and the margin of the dyke. Minor localized carbonate alteration was also noted.

An analysis of magnetic susceptibility values across the scanline (Figure 5.5.2.4E) shows a bimodal population of high values in the Marathon dyke and low values in the host foliated tonalite to granodiorite. In the dyke the values range from 15.5 to 50.9 $x10^{-3}$ SI, both of which represent anomalous values, with most values between 20.4 and 44.1 $x10^{-3}$ SI with an average value of 33.1 $x10^{-3}$ SI. The host foliated granodiorite has values between 8.3 and 10.4 $x10^{-3}$ SI, with an average value of 9.6 $x10^{-3}$ SI. There are no systematic changes within either the dyke or the host rock, and the change in values between the two is abrupt and coincident with the contact.

In summary, these results reveal that the fracture frequency away from the dyke contact is similar to the Matachewan and Biscotasing dykes, but increased jointing has clearly been focussed at the contact of the dyke. This observation plus the large number of faults and strong hematite and epidote alteration observed along this scanline transect are all interpreted to be the result of post-dyke emplacement fault movement associated with the Barehead Lake fault zone. In a situation where a post-dyke fault cuts subparallel to the dyke, localization of deformation at the dyke-host contact, as observed in this transect, is a likely result.

5.5.3 Biscotasing Dykes

A limited number of Biscotasing dykes were observed in the Manitouwadge area and were distinguished based upon their consistent northeast trends. Marathon dykes have also been documented to locally trend northeast, in which case they cannot be differentiated from Biscotasing dykes. Considering this, all northeast-trending dykes were interpreted as Biscotasing. These dykes are Proterozoic in age (circa 2.167 Ga; Hamilton et al., 2002), and cross-cut all Archean bedrock units.

5.5.3.1 Lithology and Physical Characteristics

Biscotasing dykes were observed in 12 outcrops investigated and represent the least abundant generation of Proterozoic dykes observed in the Manitouwadge area (Figure 5.5.1). A total of 10 representative samples of Biscotasing dykes were collected during the field investigations. Lithological and physical characteristics of the Biscotasing dykes are similar to the Matachewan and Marathon dykes.

Biscotasing dykes occur as single, continuous, linear dykes and as networks of interweaving 30 centimetre to multi-metre wide dykes. Biscotasing dyke field observations are based primarily on investigation of a single continuous linear northeast-trending dyke with a prominent aeromagnetic signature that bisected the core of the Black-Pic batholith area - east, and a second discontinuous lower magnetic signature Biscotasing dyke located subparallel and southeast of the aforementioned dyke. Both contacts of the continuous Biscotasing dyke were observed at station 16BH0212, revealing a 59 metre thick, linear dyke. Both contacts of the discontinuous Biscotasing dyke were observed at station 16CN0117, revealing a network of interweaving 30 centimetre to multi-metre wide dykes. Additional Biscotasing dyke observations are from occurrences located in the northwest corner of the Black-Pic batholith area - west. Several Biscotasing dyke observations are from occurrences located in the northwest corner of the Fourbay Lake pluton area.

Biscotasing dykes are dark green to dark grey when fresh and light brown to green when weathered (Figure 5.5.3.1). Biscotasing dykes typically exhibit equigranular texture characterized by a very fine to medium-grained groundmass (0.1 to 5 millimetre crystals), composed of dominantly mafic minerals (pyroxene, plagioclase, hornblende, +/- magnetite, olivine and biotite). Locally, these dykes also exhibit diabase texture characterized by medium-grained acicular plagioclase phenocrysts (1 to 5 millimetres) within the groundmass. In coarse-grained dykes, the margins of the dyke are typically fine-grained and the core of the dyke is coarse-grained.

A total of 12 rock hardness measurements were made on the Biscotasing dykes. In 11 instances (92%) it exhibited a very strong (R5) character, and in the remaining one instance (8%), it exhibited extremely strong (R6) character.

A histogram of Biscotasing mafic dyke width measurements (N = 8), based on a manual compilation of widths found in comment notes, and measurements between tracked mapped contacts and well defined contacts visible on high resolution aerial photographs, is presented in Figure 5.5.3.1D. Contacts on both edges of the dyke were rarely observed, making it difficult to assess true dyke width and so in some cases only a minimum width was assigned. Biscotasing dykes were measured up to a maximum width of 59 metres, with half of the width measurements in the 40 to 80 metre wide bin.

A total of 10 magnetic susceptibility measurements were taken for the Biscotasing dykes (Figure 5.5.3.1E), with results generally similar to the other Proterozoic dykes. The measurements range from 15.74 to 59.75 $x10^{-3}$ SI, yielding an average value of 30.04 $x10^{-3}$ SI, and a standard deviation of 11.96 $x10^{-3}$ SI. Locally, along the Biscotasing dykes located in the Black-Pic batholith - east and Fourbay Lake pluton areas, magnetic values are depressed. A single elevated magnetic value was recorded in the northwest corner of the Black-Pic batholith area - west.

A total of nine gamma-ray spectrometry measurements were taken for the Biscotasing dykes (Figure 5.5.3.1F). The measurements yielded the following results:

- Total Count (Range: 32 – 95 Average: 56.56 Std. Dev: 25.43)
- Potassium (%) (Range 0.2 – 1.5 Average: 0.62 Std. Dev: 0.471)

- Uranium (ppm) (Range 0 – 0.6 Average: 0.20 Std. Dev: 0.226)
- Thorium (ppm) (Range 1.1 – 5.8 Average: 2.89 Std. Dev: 1.62)

Generally the Biscotasing dykes cluster most tightly near the thorium apex on a thorium-uranium-potassium ternary diagram. The Biscotasing dykes in particular exhibit two populations of total count, potassium and thorium values, including average to below average values along the well-defined Biscotasing dykes within the Black-Pic batholith area - east, and average to above average values in the dykes recorded in the northwest corner of the Fourbay Lake pluton area. Overall the average values are lower than the Marathon dykes but similar to the Matachewan dykes.

5.5.3.2 Structure

Biscotasing dykes and dyke contacts were observed dominantly within the Black-Pic batholith area - east, and in rare instances in the Black-Pic batholith - west and Fourbay Lake pluton areas. Dykes are typically hosted in tonalite within the Black-Pic batholith areas and diorite in the Fourbay Lake pluton area. Where contacts were observed, Biscotasing dykes are consistently steeply dipping with a slight tendency towards a northwesterly dip direction (Figure 5.5.3.2A). Biscotasing dykes trend northeast with a range in orientation between 022° and 069°, with two main orientation peaks at 032° and 045°, and two lesser peaks at 062° and 082°, and (Figure 5.5.3.2B).

Similar to other Proterozoic dykes, dyke contacts are characterized by distinctive glassy/aphanitic chilled margins between 0.5 to 1 centimetres that transition into fine-grained crystalline texture moving into the dyke away from the margins for up to 30 centimetres (Figure 5.5.3.3). Well-defined dykes and dyke contacts (i.e., those in the Black-Pic batholith area - east) are typically straight on individual outcrops (Figure 5.5.3.3A), and exhibit limited variability in trend on a regional scale.

A summary of joint orientations, for joints within Biscotasing dykes, is provided in Figures 5.5.3.2C and 5.5.3.2D. The majority of measured joints dip steeply and multiple orientation peaks, at 026°, 075°, 280° and 298°, are evident. Similar to other Proterozoic dykes, the systematic orientations and pervasive nature of these joints suggests they result from the cooling of dykes within a rigid host rock.

Joint spacing measurements are summarized for dyke-hosted joints (Figure 5.5.3.2E) and joints within adjacent bedrock (Figure 5.5.3.2F). Spacing of joints varies from 3 to 10 centimetres to 500 to 1000 centimetres in the dykes and greater than 1000 centimetres in the host rock. The most common range is 30 to 100 centimetres in the dyke and 100 to 500 centimetres in adjacent host rock. No observations were made, including along the scanline traverse described further below, of decreased jointing within the dyke adjacent to the contact. In rare instances, joints are more closely spaced in the host rock in a 1 to 5 metre domain adjacent to the dyke contact. Beyond this distance, joint spacing in the host rock reflects the joint spacing characteristic of the regional structural domain in which the station resides. In most instances, no increased jointing in the host rock was observed directly adjacent to Biscotasing dykes.

The best exposure of the Biscotasing dyke and dyke contacts, located in an area of recent logging, was analyzed during the dyke scanline exercise and is reported in the following section. In most other dyke outcrops, limited exposure inhibited very detailed observations required to assess variability in joints and joint spacing across the dyke and host rock.

With the exception of two joint sets containing hematite alteration, joints observed within Biscotasing dykes are clean and exhibit no fill or alteration (Figure 5.5.3.3E). The two joint sets containing hematite are located at opposite ends of a single, continuous Biscotasing dyke in Black-Pic batholith area - east. A subtle coating of iron oxide/hematite was observed during the scanline

mapping on a higher percentage of the joint faces than was recognized during mapping, as discussed below.

Considerable hematite and occasional epidote were observed within joints in the host rock surrounding Biscotasing dykes (including stations where the dyke was directly observed, and stations located proximal to predicted dykes but where no dykes were exposed), but this is not unique to outcrops proximal to the Biscotasing dykes. It is challenging to assess how alteration varied in the host rock distal to Biscotasing dykes as the majority of outcrops investigated in the areas surrounding the dominant Biscotasing dykes (located within the Black-Pic batholith area - east) are either proximal to other dykes or to interpreted lineaments. Both these features may also have contributed to the presence of secondary minerals along joint surfaces.

Biscotasing dykes are the least abundant set of Proterozoic dykes in the Manitouwadge area, and as a result, were observed in outcrop less frequently than Matachewan and Marathon dykes. The majority of information regarding brittle structures related to Biscotasing dykes were observed in a series of outcrops distributed across several Biscotasing dykes in the Black-Pic batholith area - east.

A limited number of brittle faults cross-cutting the Biscotasing dykes were observed in the field (e.g., 16JK0082, 0176), and exhibit similar attributes to brittle faults cross-cutting other Proterozoic dykes (i.e., discrete brittle faults expressed as a series of closely spaced joints; Figure 5.5.3.3D).

A series of brittle faults located adjacent and oriented at low angles and sub-parallel to northeast-trending Biscotasing dykes were also observed (stations 16JK0172, 0173, 0174). In addition, rare brittle faults were observed within Biscotasing dykes (stations 16JK0082, 0231). These structures are typically characterized by single to multiple discrete brittle faults, and in rare cases, fault scarps and cliffs (Figure 5.5.3.3D). None of these structures produce significant offset, damage zones or physiographic expression, suggesting these brittle faults may only have a relatively minor significance. No brittle faults were observed directly along Biscotasing dyke contacts. In general, the brittle faults associated with the Biscotasing dykes are fewer and less significant than brittle faults associated with the Matachewan and Marathon dykes.

5.5.3.3 Biscotasing Dyke Scanline Fracture Mapping Exercise

The scanline fracture mapping exercise was undertaken along a Biscotasing dyke located in the northeast of Black-Pic batholith area - east in a recently logged area just east of the 400 logging road (Station 16BH0288). This particular Biscotasing dyke exhibits a prominent aeromagnetic signature that can be followed across the entire Black-Pic batholith area - east. The dyke is hosted by foliated granodiorite, and is characterized by typical physical properties of a Biscotasing mafic dyke (see previous section). It is 56 metres wide and based on the high-resolution aeromagnetic data, is not cut by any faults in the area of the transect. However, two northwest-trending breaks in the aeromagnetic lineaments suggest the dyke is cut by faults located approximately 300 metres to the northeast and 1000 metres to the southwest along strike of the dyke. Results of the Biscotasing scanline exercise are summarized in Figure 5.5.3.4 and below.

The scanline exercise was completed along a transect at a trend of 305° oriented nearly perpendicular to the Biscotasing dyke. Observations were made on horizontal or shallowly dipping outcrop surfaces. The dyke is not continuously exposed from one contact to the other. However, four separate segments of outcrop exposed along strike less than 10 metres away from each other were used in the exercise, and form a near continuous transect across one half of the dyke (Figure 5.5.3.4A). Representative field photographs of the dyke transect can be seen in Figure 5.5.3.5, with photograph locations noted in Figure 5.5.3.4A.

An analysis of joint orientation within the host rocks and dyke (Figure 5.5.3.4B) reveal that three joint sets are common in the dyke and its host rock. The first is common in both and trends east-northeast, slightly clockwise to the trend of the dyke. The second is nearly perpendicular to the dyke contact and is more common inside the dyke compared to the host rock, and the weakest of the three trends north-northwest and is dominantly found in the dyke.

An analysis of fracture frequency along the scanline transect (Figure 5.5.3.4C) reveals that the fracture density varies significantly within the dyke. One of the highest frequencies occurs at the dyke margin, but other high fracture frequency zones are found within the dyke, and do not have an obvious cause. The fracture frequency decreases in the host rock and continues to decline away from the dyke contact.

An analysis of alteration and fracture infilling of brittle structures along the scanline transect (Figure 5.5.3.4D) shows that hematite or related iron oxide staining is common on the joint surfaces. In the dyke this is a very subtle coating on the joints and is not considered strong alteration. More prominent hematite staining accompanies epidote fill in narrow joints in the host rock. Chlorite was rarely observed in the joint sets, and only within the dyke.

An analysis of magnetic susceptibility values across the scanline (Figure 5.5.3.4E) shows a bimodal population of high values in the Biscotasing dyke and low values in the host foliated tonalite to granodiorite. In the dyke, the values range from 21.9 to 62.8 $x10^{-3}$ SI, with the maximum representing an anomalously high value, and the average value is 31.5 $x10^{-3}$ SI. The host foliated granodiorite has uniformly low values between 6.7 to 7.8 $x10^{-3}$ SI, with an average value of 7.4 $x10^{-3}$ SI. There are no systematic changes within either the dyke or the host rock, and the change in values between the two is abrupt and coincident with the contact.

In summary, these results reveal a similar pattern to the other dykes. The frequency of joints is generally slightly higher in the dyke compared to its host rock, but in this case very little increase in frequency as observed at the contact in either the dyke or host rock. Joints perpendicular and slightly oblique to the dyke contact are common, but the strong north-northeast-trending joint set that was prominent in the mapping data was not measured as frequently along the scanline traverse because that joint set is subparallel to the transect orientation.

5.5.4 Felsic and Mafic Dykes

Multiple sets of older felsic and mafic dykes were observed throughout the Manitouwadge area. This includes felsic dykes (including aplitic and pegmatitic examples with the composition of granite, granodiorite or tonalite), and a set of foliated mafic gabbroic dykes. The felsic dykes were observed within migmatitic metasedimentary rocks of the Quetico Subprovince, the Fourbay Lake pluton, and the Black-Pic batholith areas whereas the mafic gabbroic dykes were only commonly observed in the Black-Pic batholith areas. As both types are observed as both dykes and larger intrusion, additional description can be found in sections 5.1, 5.2, 5.3 and 5.4. The felsic dykes and the mafic gabbroic dykes often exhibit a component of ductile deformation, and are locally cross-cut by non-foliated Proterozoic mafic dykes. These observations indicate that these felsic and mafic dykes are older than the Proterozoic dykes, however their absolute ages are not known and may include both Archean and Proterozoic ages. An overview of the physical and structural properties of these dykes is presented below.

5.5.4.1 Lithology and Physical Characteristics

Felsic dykes (which include all non-mafic dykes) were recorded in the database in 138 outcrops, and mafic gabbroic dykes were recorded in the database in 18 outcrops. The vast majority of outcrops

within the Black-Pic batholith, and abundant outcrops within the Fourbay Lake pluton contain felsic dykes, but lithology data points are only created if they represent greater than 30 percent of the volume of the outcrop. Therefore the distribution of felsic dykes and mafic gabbroic dykes as seen in Figure 5.5.2 is not representative of the overall distribution of these dykes throughout the Manitouwadge area. A total of 22 representative samples of felsic dykes and nine representative samples of mafic gabbroic dykes were collected during the field investigations.

The felsic dykes are pink to red to off white on both fresh and weathered surfaces. These dykes typically exhibit a variety of textures (porphyritic, equigranular, inequigranular, vari-texture, graphic), and are typically fine to coarse grain size (0.5 to 10 millimetre crystals) and are typically not foliated (Figure 5.5.4.1A). Certain characteristics are more common with certain subsets of felsic dykes (i.e., aplitic dykes are fine-grained, while pegmatitic dykes are coarse-grained). Felsic dykes typically occur as centimetre to half-metre wide continuous and discontinuous linear, curvilinear and irregular dykes intruding the host rock in multiple orientations (Figure 5.5.4.1a). It is not uncommon for a single outcrop of tonalite within the Black-Pic batholith to exhibit five or more sets of felsic dykes in different orientations. Within the Fourbay Lake pluton, felsic dykes appear to be more abundant proximal to interpreted brittle faults, whereas in the Black-Pic batholith, felsic dykes are typically ubiquitous. Within the Black-Pic batholith area - east, felsic dykes are more abundant in the tonalite relative to the granodiorite.

A total of 75 rock hardness measurements were made on the felsic dykes in the Manitouwadge area. In 73 instances (98%) felsic dykes exhibited a very strong (R5) character, and in the remaining two instances, they exhibited one instance (1%) of strong (R4) character, and one instances (1%) of extremely strong (R6) character.

A total of 63 magnetic susceptibility measurements were taken of the felsic dykes in the Manitouwadge area (Figure 5.5.4.1E). The felsic dykes ranged from 0.004 to 18.04 $x10^{-3}$ SI, and yielding an average value of 2.87 $x10^{-3}$ SI, and a standard deviation of 2.93 $x10^{-3}$ SI. Felsic dykes are typically narrow and not volumetrically significant, and as a result are not apparent in the high-resolution aeromagnetic survey.

A total of 36 gamma-ray spectrometry measurements were taken of the felsic dykes in the Manitouwadge area (Figure 5.5.4.1E). The measurements yielded the following results:

- Total Count (Range: 57 – 410 Average: 138 Std. Dev: 80)
- Potassium (%) (Range 0.6 – 6.8 Average: 2.8 Std. Dev: 1.1)
- Uranium (ppm) (Range 0.0 – 17.1 Average: 1.7 Std. Dev: 3.1)
- Thorium (ppm) (Range 0.6 – 39.4 Average: 6.4 Std. Dev: 7.8)

Several occurrences of mafic gabbroic dykes were observed throughout the Black-Pic batholith, but they are primarily concentrated along the western boundary of the Black-Pic batholith area -west in the Barehead Lake fault domain. Mafic gabbroic dykes are dark green to green on both weathered and fresh surfaces. They are typically characterized by equigranular very fine- to fine-grained crystal form (0.1 to 1 millimetre crystals) and a foliated texture (Figure 5.5.4.1b). Mafic gabbroic dykes occur as narrow foliated dykes (less than 1 metre wide) intruding tonalite and granodiorite, and in rare instances within metasedimentary rocks.

A total of 15 rock hardness measurements were made on the mafic gabbroic dykes in the Manitouwadge area. In 13 instances (86%) they exhibited a very strong (R5) character, and in the remaining two instances, exhibited one instance (7%) of medium strong (R3) character, and one instance (7%) of strong (R4) character.

A total of 12 magnetic susceptibility measurements were taken of the mafic gabbroic dykes and the results suggest a typically low intensity magnetic character (Figure 5.5.4.2E). The tonalite ranged from 0.36 to 2.75 $x10^{-3}$ SI, and yielding an average value of 1.37 $x10^{-3}$ SI, and a standard deviation of 0.81 $x10^{-3}$ SI. Mafic gabbroic dykes are typically narrow and not volumetrically significant, and as a result are not apparent in the high-resolution aeromagnetic survey.

A total of 6 gamma-ray spectrometry measurements were taken of the mafic gabbroic dykes in the Manitouwadge area (Figure 5.4.4F). The measurements yielded the following results:

- Total Count (Range: 72 – 159 Average: 105 Std. Dev: 30)
- Potassium (%) (Range 1.4 – 2.9 Average: 2.1 Std. Dev: 0.6)
- Uranium (ppm) (Range 0.1 – 2.8 Average: 1.2 Std. Dev: 0.9)
- Thorium (ppm) (Range 2.4 – 12.6 Average: 5.5 Std. Dev: 3.7)

5.5.4.2 Structure

Felsic dykes were observed within all mapping areas. In particular, felsic dykes were observed in almost all outcrops within the Black-Pic batholith. Contacts of felsic dykes and the host rock are typically sharp and intact but not chilled (Figure 5.5.4.3). The geometry of these dykes from linear to irregular and trend in multiple different orientations in all outcrops. Often, three or more different dyke orientations are present in a single outcrop (Figure 5.5.4.3). A total of 50 granitic dyke contacts were measured, however, due to the variability in geometries and the relatively minor number of contacts measured, the mean orientation calculated from these contacts did not provide a statistically meaningful mean contact orientation.

Furthermore, unless these dykes comprised greater than 30 percent of the outcrop or interacted with a geologically meaningful feature (i.e., lineament, fault, Proterozoic dyke, etc.), joints and associated alteration were not recorded separately. A total of only 13 joints were measured specifically and exclusively within felsic dykes. Empirical observations indicated that in general, felsic dykes exhibit the same jointing as the dominant lithology defining the outcrop, with the exception of rare felsic dykes that exhibit more tightly spaced joints relative to the host rock (Figure 5.5.4.3). More closely spaced joints in dykes occasionally exhibit increased hematite and rarely epidote alteration. Jointing within the host rock is typically unaffected by the presence of felsic dykes. Due to the relatively few number of joints measured within felsic dykes, and the variability within these joints due to the large variability within the orientations of the felsic dykes, the analysis of joints and associated alteration within these dykes and the surrounding rock did not yield meaningful results. Rather, these joint measurements should be analyzed in conjunction with other joint data.

Locally, faults were observed offsetting felsic dykes (Figure 5.5.4.3). Although certain faults did exploit felsic dykes, there did not appear to be a consistent relationship between faulting and felsic dykes throughout the Black-Pic batholith. In contrast, faulting within the Fourbay Lake pluton typically correlated with increased abundance of felsic dykes (additional detail in Section 5.2). Brittle faults occur along, adjacent to and offset felsic dykes in multiple stations (e.g., 16BH0105, 0107, 0110, 0185; 16JK0150, 0212). In particular, at station 16BH0178, granitic veins (i.e., minor felsic dykes) follow the orientation of fractures (associated with brittle faults). These brittle faults occur as single to multiple discrete slip surfaces, locally forming multi-metre scarps, cliffs and incised valleys.

Mafic gabbroic dykes were observed primarily in the Black-Pic Batholith. Contacts of mafic gabbroic dykes and the host rock are typically sharp and foliated (Figure 5.5.4.2). Often, the entire mafic gabbroic dyke is also strongly foliated. The geometry of these mafic dykes are typically linear

to irregular. Locally, mafic gabbroic dykes are deformed and pulled apart. It is probable that other gabbroic enclaves and panels observed throughout the Manitouwadge area are genetically related to the mafic gabbroic dykes described here. A total of 19 mafic gabbroic dyke contacts were measured, yielding a peak orientation of 259/74.

A total of eight joints were measured within mafic gabbroic dykes. Empirical observations indicated that in general, mafic gabbroic dykes exhibited the same jointing pattern and spacing as the dominant lithology defining the outcrop (Figure 5.5.4.2). Jointing within the host rock is typically unaffected by the presence of mafic gabbroic dykes. Due to the few number of joints measured within mafic gabbroic dykes, the analysis of joints and associated alteration within these dykes and the surrounding rock did not yield meaningful results. Rather, these joint measurements should be analyzed in conjunction with other joint data.

Locally, minor brittle faults were observed offsetting mafic gabbroic dykes (stations 16JK0054, 0238), however there does not appear to be a consistent or genetic relationship between brittle faulting and the presence of mafic gabbroic dykes. These brittle faults occur as minor discrete slip surfaces.

6 Summary of Findings

This report presents the results of the Phase 2 Geological Mapping conducted in the Manitouwadge area in 2016. Observations were made at outcrops within and around the Quetico area, the Fourbay Lake pluton area, and western and eastern portions of the Black-Pic batholith area. The geological mapping was conducted using a consistent approach to confirm and field verify the presence and nature of key geological features within these two areas, including, bedrock lithology and structural character, fracture character and spacing, and bedrock exposure and surface constraints.

The following sections summarize the key findings of the results presented in Section 5, and discusses how the newly collected geological information builds upon our historical understanding of the bedrock geology of the area (Section 3).

6.1 Quetico Area

The Quetico area is located approximately 40 kilometres north of Manitouwadge, Ontario and is accessed via a network of logging roads originating from the Caramat Industrial Road. These logging roads provide partial access to the perimeter of the mapping area but are locally obstructed, limiting access. Much of the central portion of the block was accessible only by helicopter at the time of the Phase 2 Geological Mapping.

The Quetico area is in an area previously mapped as bedrock terrain with considerable surficial cover (AECOM, 2014) and generally low relief. Previously mapped surficial cover consisted of large areas of roughly northeast-trending morainal terrain, and limited areas of organic terrain. Mapping has confirmed that areas of no predicted outcrop are indeed characterized by extensive thick overburden (generally greater than 1 metre depth). A total of 106 predicted outcrops were visited, including 88 (83%) that were confirmed to be bedrock, and 18 (17%) that were determined to be overburden. Overall, the bedrock outcrop prediction provided a useful update to the understanding of the distribution of exposed bedrock in the Quetico area.

6.1.1 Lithology

Three lithological units were identified in the Quetico area including migmatitic metasedimentary rock and granite, which underlie most of the area in varying relative amounts, and, to a much lesser extent magnetite-rich granite. Previous geological mapping (Coates, 1967) throughout the Quetico area characterized much of the area as migmatitic metasedimentary rocks intruded by granite lobate plutons. The field observations reported here are generally consistent with this previous mapping but suggest a higher percentage of moderate sized granitic intrusions are present in the area, and indicate that the current boundary of the large mapped granite intrusion to the north of the block should be moved further to the southeast. In addition, the magnetite-rich composition of a sub-set of the granite intrusions, is a new observation. The abundance of leucosome and cross-cutting peraluminous or S-type granites (i.e., granites derived from the partial melting of metasedimentary rocks) suggests that significant anatexis (i.e., partial melting) of the metasedimentary rocks has taken place. This suggests the area has reached a peak metamorphic grade of upper amphibolite to granulite facies.

On an area-wide scale, granite intrusions form resistant units that are commonly exposed, while migmatitic metasedimentary rocks were interpreted to be preferentially eroded and often covered by thick overburden. As a result, available outcrop, particularly in areas of low relief (e.g., eastern portion of the Quetico area), are commonly granitic intrusions.

Mafic dykes of all three main Proterozoic mafic dyke swarms (Matachewan, Biscotasing, and Marathon) were identified in the Quetico area. Their overall density, orientation, and character are consistent with the mapped distributions and features of these mafic dyke swarms regionally. The northwest- trending Matachewan dyke swarm are the most numerous. Felsic dykes are distributed through the centre of the Quetico area, and in increasing density towards the southwest and northeast.

Overall, the results from the Phase 2 Geological Mapping are generally consistent with previous mapping while providing an updated understanding of the Quetico area.

6.1.2 Structure

Information on the structure of the Manitouwadge area is based primarily on structural investigations of the Manitouwadge and Dayohessarah greenstone belts, with little previous detailed information available on the structural history of the Quetico area. Most of the structural information presented above represents a new structural dataset for the Quetico area. The orientation information for all observed structures is summarized above in Tables 5.1.2 (ductile structures) and 5.1.3 (brittle structures).

The migmatitic metasedimentary units that underlie most of the Quetico area exhibit a strong tectonic foliation, including mineral foliation and gneissosity, that typically strikes west to west-southwest, and dips steeply to the north. Folding of that tectonic foliation locally produced a second almost co-planar mineral foliation. Numerous shear zones were identified in the area, including examples of a purely ductile and brittle-ductile character. Overall, sinistral shear zones tend to trend northeast and dextral shear zones tend to trend north-northwest.

Joints are the predominant fracture type observed at the outcrop scale throughout the Quetico area. The three main joint orientations observed trend broadly west, west-northwest, and east-northeast, and predominantly dip at greater than 60°. A less prominent subhorizontal set of joints was also identified. Joint spacing throughout the Quetico area is mostly within the 30 to 100 and 100 to 500 centimetre range.

Faults have north-northwest, east, and northeast trends and are typically steeply dipping, whereas the few veins present typically trend northeast and northwest, and are moderately to steeply dipping. Faults are characterized by discrete slip surfaces typically less than 5 centimetres wide, with minor (centimetre-scale) sinistral offsets, and most of these faults are interpreted as minor structural features. However, certain faults are associated with series of sub-parallel joints, and are located adjacent to linear lakes and minor valleys indicating the influence of these faults beyond their immediate area. Only about 11% of all fractures (joints, faults and veins) are infilled with secondary minerals or exhibit some evidence of alteration.

A total of seven veins were measured in the Quetico area, with three veins located in the migmatitic metasedimentary rocks, a single vein located within granite, and the remaining three veins located within a northeast-trending Proterozoic mafic dyke of the Biscotasing diabase dyke swarm. Observed veins are typically less than 3 centimetres wide and are filled with quartz, quartz-feldspar, biotite and/or chlorite.

The most common secondary minerals/alteration observed include hematite staining, epidote, chlorite and quartz, with a few occurrences of the assemblage of plagioclase+k-feldspar+biotite. Faults are mostly associated with epidote veins, quartz veins, and hematite staining.

6.2 Fourbay Lake Pluton Area

The Fourbay Lake pluton area is located approximately 25 kilometres southwest of Manitouwadge and can be accessed via a network of logging roads and trails originating from two, well-maintained, secondary roads. At the time of the Phase 2 Geological Mapping, these trails in conjunction with foot traverses provided access to most of the study area, and boat or helicopter access was not required.

The Fourbay Lake pluton area is in an area previously mapped as bedrock terrain with very limited surficial cover (AECOM, 2014, Figure 2.3). Remotely predicted outcrop for this area identified a series of elongated northeast-trending clusters of relatively small outcrops (Figure 5.2.1). Of the 76 predicted outcrops visited, 68 (89%) were confirmed to be bedrock, while eight (11%) were overburden. Mapping has confirmed that areas of no predicted outcrop are indeed characterized by extensive thick overburden (generally greater than 1 metre depth). These areas of surficial cover were often observed to occur in broad northeast-oriented valleys.

6.2.1 Lithology

Three lithological units were identified in the Fourbay Lake pluton area including diorite to granodiorite, and minor granite and tonalite. Previous geological mapping characterized the entire Fourbay Lake pluton area as granite-granodiorite of the Fourbay Lake pluton (Milne, 1967), except for the northeast and southwest corners, where the pluton was mapped in contact with tonalite of the encompassing Black-Pic batholith (Figure 5.2.3). The current geological mapping confirmed that the Fourbay Lake pluton occupies almost the entire area, as well as the presence of the previously mapped contact with the tonalite in the northeastern corner of the study area. The mapping did define clear sub-domains of diorite and granodiorite that were not previously distinguished. This is a new lithological observation.

Mafic dykes of all three main Proterozoic mafic dyke swarms (Matachewan, Biscotasing, and Marathon) were identified in the Fourbay Lake pluton area. Their overall density, orientation, and character are consistent with the mapped distributions and features of these mafic dyke swarms regionally. The northwest-trending Matachewan dyke swarm are the most numerous. Felsic dykes are distributed through the centre of the Fourbay Lake pluton area, and in increasing density towards the southwest and northeast.

Overall, the results from the Phase 2 Geological Mapping have provided an updated understanding of the lithology of the Fourbay Lake pluton area.

6.2.2 Structure

Information on the structure of the Manitouwadge area is based primarily on structural investigations of the Manitouwadge and Dayohessarah greenstone belts, with little previous detailed information available on the structure of the Fourbay Lake pluton area. Most of the structural information presented above represents a new structural dataset for the Fourbay Lake pluton area.

The structural features observed in the Fourbay Lake pluton area indicate a deformation history characterized by limited ductile deformation followed by significant brittle deformation. A series of north-northeast-trending foliations were observed in the eastern portion of the pluton. The orientation of these foliations is subparallel to the pluton contact and nearly perpendicular to the regional foliation in the surrounding country rock, suggesting that it may comprise a combination of magmatic and tectonic foliation components. Only two ductile or brittle-ductile shear zones were observed in the area, both of which were sinistral, northwest-striking features.

Extensive evidence of brittle deformation was observed throughout the Fourbay Lake pluton, including widespread joints and brittle faults. The major joint sets are subparallel to the dominant fault orientations, with west-northwest-, north-, and northeast-trending sets being the most common. A moderately developed set of subhorizontal joints are also present. Joint spacing throughout the Fourbay Lake pluton area is mostly within the 30 to 100 and 100 to 500 centimetre range.

Faults exhibit dominant west-northwest and north-northeast orientations, and dip steeply. Faults occur as discrete millimetre- to centimetre- wide slip surfaces, with typically minor offsets (less than 10 centimetres). Where multiple discrete faults were present, a series of sub-parallel joints were also commonly observed. Insufficient cross-cutting relationships were observed in outcrop to determine the relative timing relationship between these structures. However, truncation relationships seen in the regional magnetic data suggest that north- and northeast-trending brittle faults are truncated by through going northwest-trending faults. These relative age relationships indicate that northwest-trending brittle faults are younger than north- and northeast-trending, and that a minimum of two stages of brittle deformation affected the area. Furthermore, the three dominant brittle fault and joint orientations are parallel to the orientation of the Proterozoic diabase dyke swarms, suggesting that brittle deformation may have been in part related to dyke emplacement, or influenced by the pre-existing orientation of the dykes themselves.

The few veins observed were consistently less than 10 centimetres wide, typically exhibited extensional textures, and were filled with quartz feldspar and biotite (i.e., granitic veins). Often, veins were observed to be oriented sub-parallel to the dominant orientation of joints and faults.

About 38% of all fractures (joints, faults, and veins) are infilled with secondary minerals or exhibit some evidence of alteration. The most common secondary minerals/alteration observed include hematite, epidote, quartz, and chlorite, in both joints and faults.

6.3 Black-Pic Batholith Area - West

The Black-Pic batholith area - west is accessed from primary and secondary roads south of the town of Manitouwadge, and from a network of logging roads and trails originating from these roads (Figure 5.3.1). A series of informally maintained and non-maintained tertiary roads, as well as active logging roads originate from these secondary roads and provide access to the northern, western, and eastern portion of the study area. Helicopter assistance proved beneficial in accessing the far southeastern and southwestern portions of the Black-Pic batholith area - west during the Phase 2 Geological Mapping.

The Black-Pic batholith area - west is in an area previously mapped as bedrock terrain with limited surficial cover (AECOM, 2014). Previously mapped surficial cover is restricted to a relatively narrow (approximately 200 to 500 metres wide) and linear northeast-trending zone of alluvial terrain, following the southern portion of the Black River and a northern tributary.

Remotely predicted outcrop for the Black-Pic batholith area - west were identified throughout the study area, and typically occurred as large northeast-oriented zones of predicted bedrock and clusters of smaller, multiple, northeast-oriented outcrops. The orientation of outcrop and outcrop clusters is a result of the dominant northeast-oriented glacial trends. Less predicted outcrop was identified in the northeast-oriented zone previously mapped as overburden.

Of the 242 predicted outcrops visited, 217 were confirmed to be bedrock, while 25 were overburden. Overall, field investigations confirm that predicted outcrop in areas previously mapped as bedrock terrain were consistently exposed bedrock. Within the northeast-trending zone previously mapped as overburden, many remotely predicted outcrops were identified as overburden that are typically covered by light coloured moss. Areas of overburden are characterized by extensive thick cover (minimum greater than 1 metre) and forest regrowth.

6.3.1 Lithology

Five lithological units are identified in the Black-Pic batholith area - west, including tonalite, which underlies most of the area, and several minor units including foliated mafic rocks, and diorite to granodiorite, granite and gabbro intrusions. Previous geological mapping characterized the entire Black-Pic batholith area - west as a gneissic tonalite suite of the Black-Pic batholith, but this is a simplification of the range of foliated to gneissic tonalite to granodiorite identified in the original mapping (Milne, 1968).

The current mapping work confirms this, and also suggests that the tonalite in this study area may potentially be differentiated into two separate phases. One phase, located in the northwest portion of the study area to the west of Agonzon Lake and Agonzon Lake road, exhibited slightly elevated gamma-ray spectrometry values and an increased proportion of diorite to granodiorite intrusions, and the second phase comprises the remainder of the tonalite in the southeast portion of the study area. In addition, the more homogeneous foliated tonalite that outcrops east of Morley Lake (Figure 5.3.3) may represent a mappable subdomain within the Black-Pic batholith. Overall, it is evident that the mapping observations documented herein add a significant amount of detail regarding the variation in type and spatial distribution of minor lithological units that are characteristic of the batholith.

Mafic dykes of all three main Proterozoic mafic dyke swarms (Matachewan, Biscotasing, and Marathon) were identified in the Black-Pic batholith area - west. Their overall density, orientation and character are consistent with the mapped distributions and features of these mafic dyke swarms regionally. The northwest-trending Matachewan dyke swarms are the most numerous. Felsic dykes are distributed through the centre of the Black-Pic batholith area - west, and in increasing density towards the southwest and northeast.

Overall, the results from the Phase 2 Geological Mapping are generally consistent with previous mapping while providing an updated understanding of the Black-Pic batholith area - west.

6.3.2 Structure

Within the Black-Pic batholith area - west, a mineral foliation and a gneissosity represent a spectrum of tectonic foliations resulting from the alignment and segregation of mineral grains due to progressive deformation. The mineral foliation and gneissosity are predominantly shallowly dipping, but also exhibit a broad range in both orientation and dip magnitude. The total tectonic foliation population predominantly has a general north-northeast to east-northeast trend. Minor folds of early felsic dykes synchronous with development of the main tectonic foliation and later folds that deform the tectonic foliation were both observed.

A significant number of shear zones were identified in the area, including examples of a purely ductile, and brittle-ductile shear zones. Although individual shear zones exhibit a wide range of orientations, the distribution and character of ductile features across the study area define distinct high strain zones. This includes a southwest-striking, shallowly, northwest-dipping broad high strain zone that bisects Agonzon Lake and divides the mapping block into distinct phases of tonalite, and

moderately to steeply dipping high strain zones evident along the edges of tonalite domes in the southeast of the study area.

Joints are the predominant fracture type observed at the outcrop scale throughout the Black-Pic batholith area - east. Steeply dipping joints in several orientations, and one shallowly dipping joint set, are evident in the total joint dataset. The well-represented, shallowly dipping set is partly due to the good vertical exposure of road cuts along Highway 614. Significant overlap and dispersion in the data result in a high background and subdued peaks in the rose diagram(Figure 5.3.13). The total joint population exhibits multiple subdued northeast trends, a broad west-northwest trend, and a broad northwest trend. Joint spacing throughout the Black-Pic batholith area - east is mostly within the 30- to 100-centimetre range.

Faults are typically very steep, to sub-vertical and trend in three dominant orientations, west-northwest, north-northwest, and north-northeast. Most measured faults occur as discrete millimetre- to centimetre-wide slip surfaces. Locally, single discrete slip surfaces were observed, and in other instances multiple, closely spaced parallel, discrete slip surfaces were present. Where multiple, closely spaced, discrete faults were observed, the associated fault zones vary from a few centimetres to greater than 10 metres wide, and commonly form series of scarps and sub-parallel joints.

Veins are typically less than 3 centimetres wide, exhibit extensional textures, and are filled with either quartz, or quartz-feldspar-biotite (i.e., granitic veins). Veins are generally northwest- and northeast-trending and steeply dipping. Veins are not considered to be a significant structural feature throughout the Black-Pic batholith area - west.

About 34% of all fractures (joints, faults and veins) are infilled with secondary minerals or exhibit some evidence of alteration. In general, fractures commonly exhibited extensive hematite staining, locally significant epidote fill, limited quartz fill, and minor chlorite fill. Faults are most strongly associated with hematite staining and epidote veinlets.

6.4 Black-Pic Batholith Area - East

The Black-Pic batholith area - east was accessed from a single north-south primary road that bisects the mapping area from north to south and provides further access to multiple secondary and tertiary roads. Collectively, the secondary road network provided access to the north-central and northeastern portions of the mapping area. The remainder of the study area was only accessible by helicopter and extensive foot traverses. Active logging was observed along all maintained roads, and considerable caution should be taken when travelling in this area. Trails in the area comprise abandoned logging roads that were partly traversable by ATV.

The Black-Pic batholith area - east is in an area previously mapped as bedrock terrain with limited surficial cover (AECOM, 2014). Previously mapped surficial cover is restricted to a zone of north- and northeast-trending glaciofluvial terrain along the east margin and in the southeast portion of the study area, and isolated zones of organic and glaciofluvial terrain throughout the remainder of the mapping area. Mapping revealed that these areas of overburden can be significantly thick (<10 metres). Remotely predicted outcrop for the Black-Pic batholith area - east were identified throughout the study area, and typically occur as clusters of relatively small predicted bedrock outcrops extending in northwest, north, and northeast orientations. The orientation of outcrop clusters is a result of the dominant glacial and structural trends. Limited predicted outcrop was identified in the areas previously mapped as overburden.

Field investigations confirm that predicted outcrop in areas previously mapped as bedrock terrain are consistently exposed bedrock. Of the 124 predicted outcrops visited, 123 were confirmed to be bedrock, whereas only one was confirmed as overburden. Three additional overburden stations were also added in areas predicted to be overburden. Areas of overburden are characterized by extensive thick cover (minimum greater than 1 metre), that can be significantly thicker (<10 metres) along eskers and where exposed in gravel pits. Predicted outcrops identified during mapping as overburden are typically located in or near areas previously mapped as glaciofluvial terrain.

6.4.1 Lithology

Five lithological units were identified in the Black-Pic batholith area - east, including tonalite to granodiorite, which underlies most of the area, and diorite to granodiorite, granite, and gabbro intrusions. In addition, one occurrence of migmatitic metasedimentary rock was mapped. The compilation of previous geological mapping depicts the Black-Pic batholith area - east as a gneissic tonalite suite of the Black-Pic batholith intruded by an up-to-15-kilometre-long and up-to-6-kilometre-wide northeast-trending elliptical granite to granodiorite intrusion (Figure 5.4.3).

The current mapping suggests that except for two relatively minor domains of granite mapped in the central and central-north portions of the study area (discussed below), the entire mapping area dominantly consists of foliated tonalite to granodiorite, likely of the Black-Pic batholith. The historical geological map of the area (Giguere, 1972), upon which the compilation was based, identifies several separated massive granite outcrops in the area between the Foch River and Longnega, Upper Foch, and Macutagon lakes (Giguere, 1972). It appears that the boundaries of the larger northeast-trending intrusion portrayed on the compilation map are enlarged and extended to the east from these outcrops into overburden covered areas (Figure 5.4.4; Johns and McIlraith, 2003).

In contrast, new lithological observations from the current mapping suggests that these intrusions of massive granite are limited in size, and do not form a large northeast-trending intrusion, but rather a series of discrete plutons surrounded by foliated tonalite country rock. Overall, the tonalite to granodiorite of the Black-Pic batholith area - east is more homogenous and has a weaker foliation than the tonalite of the Black-Pic batholith area - west.

Mafic dykes of all three main Proterozoic mafic dyke swarms (Matachewan, Biscotasing, and Marathon) were identified in the Black-Pic batholith area - east. Their overall density, orientation, and character are consistent with the mapped distributions and features of these mafic dyke swarms regionally. The northwest-trending Matachewan dyke swarms are the most numerous. Felsic dykes are distributed through the centre of the Black-Pic batholith area - east, and in increasing density towards the southwest and northeast.

Overall, the results from the Phase 2 Geological Mapping have provided an updated understanding of the Black-Pic batholith area - east.

6.4.2 Structure

The Black-Pic batholith area - east has preserved a very similar structural history as the Black-Pic area -west, the most significant difference being the dominance of moderately foliated granodiorite to tonalite phases of the Black-Pic batholith in the east compared to a high percentage of gneissic to foliated tonalite phases of the batholith in the west.

Foliation within the Black-Pic batholith area - east is typically weak to moderate, except for a single domain of moderate to strong foliation, with gneissic layering only observed in a single station in what was interpreted to be xenolithic panels of gneiss. Foliation is dominated by sub-horizontal to shallowly dipping measurements suggesting that the area is largely at a structural culmination or series of culminations. Only two shear zones were identified in the area, including a northeast-striking, sinistral ductile shear zone, and a moderate-dipping, southeast-striking brittle-ductile shear zone with unknown kinematics.

Joints are the predominant fracture type observed at the outcrop scale throughout the Black-Pic batholith area - east. The total joint population exhibits several main trends, including a broad northwest trend, a north-northeast trend, and a broad northeast trend, all of which predominantly dip at greater than 60°. A less prominent subhorizontal set of joints was also identified. Joint spacing throughout the Black-Pic batholith area - east is most commonly within the 30- to 100-centimetre range. Northeast-southwest and northwest-southeast orientations were also identified in faults and veins with similar steep to subvertical dips.

Faults primarily dip sub-vertically but exhibit many preferred orientations, with the most common trending northwest to north-northwest. Most measured faults occur as discrete millimetre- to centimetre-wide slip surfaces. However, in multiple other instances, multiple closely spaced consecutive discrete slip surfaces are present, forming fault zones up to 10 metres wide, and often manifested as a series of scarps and sub-parallel joints, and incised valleys. The most significant of these faults (those greater than 1 metre wide) are often located adjacent, and oriented sub-parallel, to clusters of tightly spaced Matachewan dykes.

One northeast-striking vein was identified in the southeast portion of the Black-Pic batholith area - east. The vein is less than 3 centimetres wide, steeply dipping, exhibits extensional textures, and is filled with quartz. Veins are not considered to be a significant structural feature throughout the Black-Pic batholith area - east.

About 35% of all fractures (joints, faults, and veins) are infilled with secondary minerals or exhibit some evidence of alteration. The most common secondary minerals/alteration observed include hematite staining, epidote, chlorite, and quartz. Both joint and faults have similar alteration types.

6.5 Geological History of the Manitouwadge Area

A brief summary of the geological history of the Manitouwadge area, integrated with the regional geological history of this part of the Superior Province outlined in Section 3.3 and Table 3.3.1, is described below. The Manitouwadge area straddles a structurally complex boundary between the metasedimentary-migmatitic Quetico Subprovince and the volcano-plutonic Wawa Subprovince within the Archean Superior Province, and the structural style and recorded structural history in the Quetico area is quite distinct from the remaining three areas. Overall, the observations made during the geological mapping in the Manitouwadge area integrate well with the regional geological history as it is currently understood.

6.5.1 Quetico Structural Summary

The Quetico sedimentary rocks are interpreted to be deposited in an accretionary prism (Percival and Williams, 1989) between circa 2.700 to 2.688 Ga (Percival, 1989; Zaleski et al., 1999). The structural features observed in the Quetico area indicate a protracted ductile and brittle deformation history, with a minimum of three deformation events. The initial ductile deformation event was

responsible for the formation of the main penetrative ductile fabric (i.e., east-west-oriented foliation and gneissosity). A second ductile deformation resulted in the folding of the foliated migmatitic sedimentary rocks into upright, moderately plunging folds and the development of an associated weak axial planar foliation. A third brittle deformation event resulted in limited brittle faults and associated veins and joints.

The Quetico area is located at least 20 kilometres from the Quetico-Wawa Subprovince boundary and therefore the increased transposition and deformation strain recorded at the boundary (Zaleski et al., 1999) is not observed in the mapping area.

Numerous joint sets were observed throughout the Quetico area, and were ultimately interpreted to represent a single protracted brittle deformation event, as insufficient cross-cutting relationships were observed to segregate brittle structures into separate events. Many of these joint sets are also parallel to the orientation of Proterozoic diabase dykes, suggesting that brittle deformation may have been in part related to dyke emplacement, or influenced by the pre-existing orientation of the dykes themselves.

6.5.2 Black-Pic Batholith and Fourbay Lake Pluton Structural Summary

The structural features observed in the Black-Pic batholith area indicate a protracted deformation history characterized by extensive ductile and brittle deformation.

The age of emplacement of the Black-Pic batholith has been constrained by U-Pb (zircon) dating of the oldest recognized phase of the tonalite at circa 2.720 Ga (Jackson et al., 1998). After emplacement, the intrusion underwent multiple phases of ductile deformation. Field observations reveal several distinct sets of ductile features associated with what could be interpreted as up to three separate phases of ductile deformation, although some phases may be parts of a progressive ductile deformation event.

The first phase of ductile deformation is characterized by the development of pervasive foliation, gneissosity and local sub-parallel shear zones. The second stage of ductile deformation is characterized by the formation of tonalite domes caused by continuing compression, resulting in progressive foliation and gneissosity development, folding and the steepening of ductile fabrics along the margins of the domes (i.e., northern border and southeast portion of study area). Consistent with the second phase of deformation, a broad southwest-striking, shallow, northwest-dipping high strain zone was developed across the area and separated two distinct phases of tonalite occupying the northwest and southeast portions of the mapping area. The final phase of ductile deformation is characterized by the formation of narrow, northwest-striking, shallowly dipping high strain zones.

The Fourbay Lake pluton intruded the Black-Pic batholith at approximately 2.678 Ga (Beakhouse, 2001), and postdated most of the tectonic activity affecting the Manitouwadge area. As a result, ductile features are generally not well developed within the pluton. However, a series of north-northeast-trending foliations were observed in the eastern portion of the pluton. The orientation of these foliations is subparallel to the pluton contact and nearly perpendicular to the regional foliation in the surrounding country rock and are often defined by magmatic minerals. Based on those observations, this is interpreted to represent at least partly a magmatic foliation related to the emplacement of the pluton rather than entirely a tectonic fabric related to regional tectonic stresses.

Following the ductile deformation, the Black-Pic batholith experienced extensive brittle deformation. Brittle structures (joints, faults, veins) define two major fault zones including the north-trending Barehead Lake fault zone on the western border of the study area, and a northeast-trending fault zone trending through Agonzon Lake. The northeast-trending fault zone is parallel with a major brittle-

ductile shear zone. Additional brittle deformation zones were observed along the northwestern boundary and in the central-western portion of the study area, and may represent brittle deformation along boundaries of tonalite domes. The timing relationship between these brittle to brittle-ductile structural domains is unclear from field observations and may be the result of a single progressive brittle-ductile to brittle deformation event, or multiple deformation events. However, it is clear that brittle structures exploited the pre-existing ductile structural framework.

Extensive evidence of brittle deformation was also observed throughout the Fourbay Lake pluton, including widespread joints and faults. The major joint sets are subparallel to the dominant fault orientations, with west-northwest- and northeast-trending sets being the most common. Formation of the joint sets are interpreted to be related to the same tectonic events that generated the brittle faults. Mapped faults in the Fourbay Lake pluton exhibit dominant northwest and north-northeast to northeast orientations, and a minor east-northeast orientation. Insufficient cross-cutting relationships were observed in outcrop to determine the relative timing relationship between these structures. However, truncation relationships seen in the regional magnetic data suggest that north- and northeast-trending brittle faults are truncated by thoroughgoing northwest-trending faults. These relative age relationships indicate that northwest-trending faults are younger than those trending north and northeast, and that a minimum of two stages of brittle deformation affected the area.

Regional-scale crustal extension related to incipient Proterozoic breakup of the craton (Buchan and Ernst 2004) began circa 2.5 Ga, with subsequent emplacement of the northwest-trending Matachewan dyke swarm at circa 2.473 Ga. Later intrusion of the circa 2.167 Ga Biscotasing dykes and the circa 2.121 Ga Marathon dykes occurred towards the end of this period of extension. Dominant fault and joint orientations are sub-parallel to the orientation of Proterozoic diabase dykes, suggesting that brittle deformation may have been in part related to dyke emplacement, or influenced by the pre-existing orientation of the dykes themselves. Few age constraints are available on the timing of the brittle deformation events. However, Matachewan dykes are locally faulted along their contacts, and Marathon mafic dykes appear to follow pre-existing faulted zones implying that some brittle deformation may have occurred between circa 2.473 to 2.121 Ga.

Significant internal deformation of the Superior craton including rotation of the older Proterozoic dyke swarms occurred during the 1.9 Ga Kapuskasing uplift of the central Superior Province (Percival et al., 2006), as well as during the circa 1.9 to 1.7 Penokean Orogeny on the south margin of the Superior craton. A third disruption of the stable Superior craton occurred at circa 1.11 to 1.09 Ga during the development of the failed arcuate midcontinent rift, representing an approximately 20-kilometre wide rift filled with basalt and clastic sedimentary rocks (Percival et al., 2006). The effects of these three younger deformation events are not strongly expressed in the Manitouwadge area.

7 References

AECOM, 2014. Phase 1 Geoscientific Desktop Preliminary Assessment of Potential Suitability for Siting a Deep Geological Repository for Canada's Used Nuclear Fuel, Township of Manitouwadge, Ontario. Prepared for Nuclear Waste Management Organization (NWMO). NWMO Report Number: APM-REP-06144-0075. 86p. plus appendices and figures.

Barnett, P.J. 1992. Quaternary Geology of Ontario. *In* Geology of Ontario. Ontario Geological Survey, Special Volume 4, Part 2, p. 1010–1088.

Beakhouse, G.P., 2001. Nature, timing and significance of intermediate to felsic intrusive rocks associated with the Hemlo greenstone belt and implications for the regional geological setting of the Hemlo gold deposit. Ontario Geological Survey, Open File Report 6020, 248p.

Buchan, K.L. and Ernst, R.E. 2004. Diabase dyke swarms and related units in Canada and adjacent regions. Geological Survey of Canada, Map 2022A, scale 1:5,000,000.

Buchan, K.L., Halls, H.C. and Mortensen, J.K. 1996. Paleomagnetism, U-Pb geochronology, and geochemistry of Marathon dykes, Superior Province, and comparison with the Fort Frances swarm. Canadian Journal of Earth Sciences, v. 33, p. 1583-1595.

Chown, E.H.M. 1957. The geology of the Wilroy property, Manitouwadge Lake, Ontario. MSc thesis, University of British Columbia.

Coates, M.E. 1967. Stevens sheet, Thunder Bay District. Ontario Department of Mines, Map 2141, scale 1:63,360 or 1 inch to 1 mile.

Coates, M.E. 1970. Geology of the Killala-Vein Lake area. Ontario Department of Mines, Geological Report 81, 35p.

Corfu, F., Stott, G.M. and Breaks, F.W. 1995. U-Pb geochronology and evolution of the English River subprovince, an Archean low P – high T metasedimentary belt in the Superior Province. Tectonics, v. 14, p. 1220-1233

Corrigan, D., Galley, A.G. and Pehrsson, S. 2007. Tectonic evolution and metallogeny of the southwestern Trans-Hudson Orogen. *In* Goodfellow, W.D., ed., Mineral Deposits of Canada: A Synthesis of Major Deposit-Types, District Metallogeny, the Evolution of Geological Provinces, and Exploration Methods. Geological Association of Canada, Mineral Deposits Division, Special Publication No. 5, p. 881-902.

Fraser, J.A. and Heywood, W.W. (editors) 1978. Metamorphism in the Canadian Shield. Geological Survey of Canada, Paper 78-10, 367p.

Gartner. J.F. and McQuay. D.F. 1980a. Obakamiga Lake Area (NTS 42F/SW). Districts of Algoma and Thunder Bay. Ontario Geological Survey, Northern Ontario Engineering Geology Terrain Study 45, 16p. Accompanied by Map 5084, scale 1:100,000.

Geddes, R.S. and Kristjansson, F.J. 1984. Quaternary geology of the Hemlo area; constraints on mineral exploration. Paper presented at 8th District 4 Meeting, Canadian Institute of Mining and Metallurgy, Thunder Bay, October, 1984.

Geddes. R.S., Bajc, A.F. and Kristjansson, F.J. 1985. Quaternary geology of the Hemlo region, District of Thunder Bay. *In* Summary of Field Work, 1985. Ontario Geological Survey, Ontario Geological Survey, Miscellaneous Paper 126, p. 151-154.

Geofirma Engineering Ltd. 2013. Initial Screening for Siting a Deep Geological Repository for Canada's Used Nuclear Fuel, Township of Manitouwadge, Ontario. Prepared for Nuclear Waste Management Organization. 37p plus figures.

Giguere, J.F. 1972. Granitehill Lake area, Thunder Bay and Algoma districts. Ontario Department of Mines and Northern Affairs, Map 2219; scale 1:63 360 or 1 inch to 1 mile.

Halls, H.C., Stott, G.M., Ernst, R.E. and Davis, D.W., 2006. A Paleoproterozoic mantle plume beneath the Lake Superior region. *In* Institute on Lake Superior Geology, 52nd Annual Meeting, Sault Ste. Marie, Ontario, Part 1, Program and Abstracts, p. 23-24.

Hamilton, M.A., David, D.W., Buchan, K.L. and Halls H.C. 2002. Precise U-Pb dating of reversely magnetized Marathon diabase dykes and implications for emplacement of giant dyke swarms along the southern margin of the Superior Province, Ontario. Geological Survey of Canada, Current Research 2002-F6, 10p.

Jackson, S.L. 1998. Stratigraphy, structure and metamorphism; part 1. *In* Jackson, S.L., Beakhouse, G.P., and Davis, D.W., eds., Geological Setting of the Hemlo Gold Deposit; an Interim Progress Report. Ontario Geological Survey, Open File Report 5977, p.1-58.

Johns, G.W., and McIlraith, S. 2003. Precambrian geology compilation series – Hornepayne sheet. Ontario Geological Survey, Map 2668, scale 1:250,000.

Kettles, I.M. and Way Nee, V. 1998. Surficial geology, Vein Lake, Ontario. Geological Survey of Canada, Map 1921A, scale 1:50,000.

Kristjansson. F.J., and Geddes, R.S. 1986. Quaternary geology of the Manitouwadge area, District of Thunder Bay. Ontario Geological Survey, Map P.3055, Geological Series-Preliminary Map, scale 1:50,000.

Lin, S. 2001. Stratigraphic and structural setting of the Hemlo gold deposit, Ontario, Canada. Economic Geology, v. 96, p. 477–507.

Lin, S. and Beakhouse, G.P. 2013. Synchronous vertical and horizontal tectonism at late stages of Archean cratonization and genesis of Hemlo gold deposit, Superior craton, Ontario, Canada. Geology, v. 41, p. 359–362.

Miles, W.F. 1998. An Interpretation of high resolution aeromagnetic data over the Manitouwadge greenstone belt, Ontario, Canada. MSc thesis, Ottawa-Carleton Geoscience Centre and University of Ottawa, Ottawa, Canada, 250p.

Milne, V.G. 1967. Barehead Lake sheet, Thunder Bay District. Ontario Department of Mines, Map 2143, scale 1:31,680 or 1 inch to 1/2 mile.

Milne, V.G., 1968. Geology of the Black River Area-District of Thunder Bay. Ontario Department of Mines, Geological Report 72, 68p.

Milne, V.G., 1969. Progress report on a field study of the Manitouwadge area ore deposits [abs.]: Canadian Institute of Mining and Metallurgy, Annual Meeting, Montreal.

Muir, T.L. 2003. Structural evolution of the Hemlo greenstone belt in the vicinity of the world-class Hemlo gold deposit. Canadian Journal of Earth Sciences, v. 40, p. 395-430.

Osmani, I.A. 1991. Proterozoic mafic dyke swarms in the Superior Province of Ontario. *In* Geology of Ontario. Ontario Geological Survey, Special Volume 4, Part 1, p. 661-681.

Pan, Z. and Fleet, H.M. 1992. Calc-silicate alteration in the Hemlo Gold deposit, Ontario: mineral assemblages, P-T-X constraints, and significance. Economic Geology, v. 87, p. 1104-1120.

Pan, Y., Fleet, M.E., Williams, H.R., 1994. Granulite–facies metamorphism in the Quetico Subprovince, north of Manitouwadge, Ontario. Canadian Journal of Earth Sciences, v. 31, p. 1427–1439.

Pan, Y., Fleet, M.E. and Heaman, L.M. 1998. Thermo-tectonic evolution of an Archean accretionary complex: U-Pb geochronological constraints on granulites from the Quetico Subprovince, Ontario, Canada. Precambrian Research, v. 92, p. 117-128.

Pease, V., Percival, J., Smithies, H., Stevens, G. and Van Kranendonk, M. 2008. When did plate tectonics begin? Evidence from the orogenic record. *In* Condie, K.C. and Pease, V., eds., When Did Plate Tectonics Begin on Earth? Geological Society of America Special Paper 440, p. 199-228.

Percival, J.A. and Williams, H.R. 1989. Late Archean Quetico accretionary complex, Superior Province, Canada. Geology, v. 17, p. 23-25.

Percival, J.A., Sanborn-Barrie, M., Skulski, T., Stott, G.M., Helmstaedt, H. and White, D.J. 2006. Tectonic evolution of the western Superior Province from NATMAP and Lithoprobe studies. Canadian Journal of Earth Sciences, v. 43, p. 1085-1117.

Percival, J.A. 1989. A regional perspective of the Quetico metasedimentary belt, Superior Province, Canada; Canadian Journal of Earth Sciences, v. 26, p. 677-693.

Peterson, V.L., and Zaleski, E. 1999. Structural history of the Manitouwadge greenstone belt and its volcanogenic Cu-Zn massive sulphide deposits, Wawa Subprovince, south-central Superior Province. Canadian Journal of Earth Sciences, v. 36, p. 605-625.

Polat, A. 1998. Geodynamics of the Late Archean Wawa Subprovince greenstone belts, Superior Province, Canada. PhD thesis, Department of Geological Sciences, University of Saskatchewan, Saskatoon, 249p.

Powell, W.G., Carmichael, D.M. and Hodgson, C.J. 1993. Thermobarometry in a subgreenschist to greenschist transition in metabasites of the Abitibi greenstone belt, Superior Province, Canada; Journal of Metamorphic Geology, v. 11, p.165-178.

Prest, V.K. 1970. Quaternary geology of Canada. *In* Geology and Economic Minerals of Canada. Geological Survey of Canada, Economic Geology Report no.1, Fifth Edition, p.675-764.

PGW (Paterson, Grant and Watson Ltd.). 2014. Phase 1 Geoscientific Desktop Preliminary Assessment, Processing and Interpretation of Geophysical Data, Township of

Manitouwadge, Ontario. Prepared for Nuclear Waste Management Organization (NWMO). NWMO Report Number: APM-REP-06144-0077.

Santaguida, F. 2001. Precambrian geology compilation series – Schreiber sheet. Ontario Geological Survey, Map 2665 -Revised, scale 1:250,000.

SGL (Sander Geophysics Ltd.). 2017. Phase 2 Geoscientific Preliminary Assessment, Acquisition, Processing and Interpretation of High-Resolution Airborne Geophysical Data, Township of Manitouwadge and Area, Ontario. Prepared for Nuclear Waste Management Organization (NWMO). NWMO Report Number: APM-REP-01332-0213.

SRK Consulting (Canada) Inc. 2014. Phase 1 Geoscientific Desktop Preliminary Assessment, Lineament Interpretation, Township of Manitouwadge, Ontario. Prepared for Nuclear Waste Management Organization (NWMO). NWMO Report Number: APM-REP-06144-0078.

SRK Consulting (Canada) Inc. 2016. Data Collection System for Outcrop Mapping: Overview, Procedures and Guidance. Prepared for Nuclear Waste Management Organization (NWMO). 29p.

SRK Consulting (Canada) Inc. 2017. Phase 2 Geoscientific Preliminary Assessment, Lineament Interpretation, Township of Manitouwadge and Area, Ontario. Prepared for Nuclear Waste Management Organization (NWMO). NWMO Report Number: APM-REP-01332-0214.

Sutcliffe, R.H. 1991. Proterozoic geology of the Lake Superior area. *In* Geology of Ontario. Ontario Geological Survey, Special Volume 4, Part 1, p. 627-658.

Williams, H.R. and F.W. Breaks, 1996. Geology of the Manitouwadge-Hornepayne region, Ontario. Ontario Geological Survey, Open File Report 5953, 138p.

Williams, H. R., G.M. Stott, K.B. Heather, T.L. Muir and R.P. Sage. 1991. Wawa Subprovince. *In* Geology of Ontario, Ontario Geological Survey, Special Volume 4, Part 1, p. 485-525.

Williams, H.R. and Breaks, F.W. 1989. Geological studies in the Manitouwadge-Hornepayne area; Ontario Geological Survey, Miscellaneous Paper 146, p. 79-91.

Zaleski E. and V.L. Peterson, 1995. Depositional setting and deformation of massive sulfide deposits, iron-formation, and associated alteration in the Manitouwadge greenstone belt, Superior Province, Ontario. Economic Geology, v. 90, p. 2244-2261.

Zaleski, E. and Peterson, V.L. 1993. Lithotectonic setting of mineralization in the Manitouwadge greenstone belt, Ontario; preliminary results. *In* Current Research, Part C, Geological Survey of Canada, Paper 93-1C, p.307-317.

Zaleski, E., Peterson, V.L., and van Breemen, O., 1995. Geological and age relationships of the margins of the Manitouwadge greenstone belt and the Wawa-Quetico subprovince boundary, northwestern Ontario. *In* Current Research 1995-C; Geological Survey of Canada, p.35-44.

Zaleski, E., van Breemen, O. and Peterson, V.L. 1999. Geological evolution of the Manitouwadge greenstone belt and the Wawa-Quetico subprovince boundary, Superior Province, Ontario, constrained by U-Pb zircon dates of supracrustal and plutonic rocks. Canadian Journal of Earth Sciences, v. 36, p. 945-966.

APPENDIX A

Methodology Section: Supporting Tables

Table A.1: Source Data Descriptions

Source Data	File Name	Format
Water bodies	Manitouwadge_Water.gdb Manitouwadge_National_Waterbodies Manitouwadge_Waterbody Manitouwadge_Watercourse	.gdb
Roads network	Manitouwadge_FMURoadsPicandBigPic_r0.shp White_River_FMURoadsMagpieandWhiteRiver_r0.shp	.shp
	Manitouwadge_Base_Map.gdb Manitouwadge_Regional_Roads Manitouwadge_Road_AECOM Manitouwadge_Roads	.gdb
Other base map data	Manitouwadge_Base_Map.gdb Manitouwadge_Community Manitouwadge_Municipal_Boundary Manitouwadge_Railway Manitouwadge_Townships Manitouwadge_Utility_Lines Manitouwadge_Wooded_Areas	.gdb
Overburden	Manitouwadge_Quaternary_Geology.gdb Manitouwadge_Eskers Manitouwadge_GSC_1921a_Surficial_Geology Manitouwadge_M2683_Surficial_Geology Manitouwadge_M2684_Surficial_Geology Manitouwadge_Quaternary_Surficial_Geology Manitouwadge_Sand_Dunes	.gdb
Forest Resources Inventory (FRI) Imagery	Manitouwadge_TileIndexFRI_r0.shp	.shp
	HP_West_RGB.tif MAN_S_RGB.tif ManE_RGB.tif ManN_RGB.tif	.tif
Topography	Manitouwadge_Topography.gdb Manitouwadge_DEM_Elevation Manitouwadge_DEM_Hillshade Manitouwadge_DEM_Relief_20km_departure Manitouwadge_DEM_Relief_250m_departure Manitouwadge_DEM_Relief_2km_departure Manitouwadge_DEM_Slope Manitouwadge_Slope_Density	.gdb
	MN_DEM.grd	.grd
Geophysics	Manitouwadge_Gravity_Anomalies.shp Manitouwadge_Gravity_Polylines.shp Manitouwadge_Gravity_Polylines.shp Manitouwadge_Magnetic_Polylines.shp	.shp
	MN_1VDRTP.grd MN_2VDRTP.grd MN_MAG_RTP.grd MN_TILT.grd	.grd
Bedrock Geology	Manitouwadge_Bedrock_Geology_v2.gdb Manitouwadge_Geologic_Provinces Manitouwadge_Local_Bedrock_Geology Manitouwadge_Regional_Bedrock_Geology Manitouwadge_Terrane_Subdivision Manitouwadge_Available_Geology_Coverage Manitouwadge_Quetico_Wawa_Subprovince_Boundary	.gdb
Predicted outcrop locations	Manitouwadge_OutcropInterpreted_r1.shp MAN_Mapping_Outcrops_CN_rev01.shp	.shp

Table A1: Continued

Source Data	File Name	Format
Faults	Manitouwadge_Bedrock_Geology_v2.gdb Manitouwadge_Local_Bedrock_Geology Manitouwadge_Local_Faults Manitouwadge_Regional_Bedrock_Geology Manitouwadge_Regional_Faults	.gdb
Historical geological maps	Manitouwadge_Bedrock_Geology_v2.gdb Manitouwadge_Available_Geology_Coverage	.gdb
Lineaments	Manitouwadge_Phs2Ext_MAG_Lins_Final_20160602_r1.shp Manitouwadge_Phs2Ext_SURFICIAL_Lins_Final_20160602_r1.shp	.shp
NWMO Mapping Areas	Manitouwadge_CandidateAreas_r1.shp Manitouwadge_WithdrawalAreas_r1.shp	.shp

Table A.2: Equipment Requirements

Equipment	Calibration Required
Compass (Brunton Pocket Transit or similar)	Y – Check magnetic declination setting daily
iOS or Android Fieldmove Clino	Y – Daily check against Compass measurement at reference location
Handheld GPS	Y – Check against fixed calibration location
Handheld field data collector w/GPS (Trimble T41/5 or equivalent)	Y – Check against hand held GPS
Customized ArcPad software	Y – Daily check of uploaded data against hard copy maps
Magnetic Susceptibility Meter (KT-10 or equivalent)	Y – Calibrated by supplier before rental and upon return from rental period. Daily check of reading at a reference rock outcrop. Certificate of Calibration to be provided by supplier and provided to NWMO.
Gamma Ray Spectrometer (RS-125 or equivalent)	Y – Calibrated by supplier before rental and upon return from rental period. Daily check of reading at a reference rock outcrop. Certificate of Calibration to be provided by supplier and provided to NWMO.
Digital Camera	N
Notebook and Pen	N
Geological Hammer	N
Sample Bags	N
Personal Protective Equipment	N

Table A.3: Task Allocation

Task	Responsibility
Daily safety briefing	Project Manager
Daily equipment calibration	Lead Structural Geologist, Geotechnical Engineer
Host rock lithology characterization	Lead Structural Geologist
Host rock structural characterization	Lead Structural Geologist
Digital photographs	Lead Structural Geologist
Fracture characterization	Geotechnical Engineer
Lineament observation/assessment	Project Manager, Lead Structural Geologist
Data input into ArcPad	Lead Structural Geologist
Manual (pencil and paper) note transcription	Geotechnical Engineer
Magnetic susceptibility measurements	Lead Structural Geologist
Rock strength assessment - Hammer test	Geotechnical Engineer
Bedrock overburden assessment	Lead Structural Geologist
Sample collection (if necessary)	Lead Structural Geologist
Surface constraint assessment	Lead Structural Geologist
Identification of potential detailed mapping areas	Project Manager, Lead Structural Geologist
Daily QC verification of notebook with digital entry for two locations for each team	Geotechnical Engineer
Daily QC verification of instrument readings (KT-20, RS-125) with entries in notebook and digital database	Lead Structural Geologist/ Geotechnical Engineer
Daily log write-up and transmittal	Lead Structural Geologist
Daily data back-up (and back-up for the back-up)	Lead Structural Geologist
Planning the next day traverse	Project Manager, Lead Structural Geologist

Table A.4: Key General and Geological Attributes Characterized During Observing General Geological Features and Detailed Geological Mapping

General Attributes		Characterization Method(s)
	Outcrop Location	Geo-locate exposed bedrock observation locations using GPS Take representative digital photograph of outcrop area.
	Bedrock exposure and overburden thickness	Visually inspect the distribution and thickness of overburden vs. exposed bedrock during the daily traverse (in comparison to existing understanding).
	Surface Constraints	Visually identify and geo-locate any surface constraints that would create challenges for further geological characterization activities (e.g., bridge wash-outs, poorly or unmaintained logging roads, beaver dams, steep and deep (impassable) valleys, etc.). Visually identify access issues in areas without mapped roads or navigable waterways.
Geological Attributes		
Bedrock Characteristics	Lithology	Visually inspect weathered and fresh rock surfaces for identification of major and minor lithological units and their constituent colour, primary minerals (e.g., granitic rocks have varying proportions of quartz, K-feldspar and plagioclase plus other minerals including micas, hornblende, etc.), grain size, texture, etc. Name the lithological unit(s) in terms of relative abundance at the outcrop scale. Collect a representative sample(s) of the dominant lithological unit(s) at each outcrop (will require use of hammer and chisel only; collect fist-sized piece with both weathered and fresh surface). Take digital photographs of representative lithological unit(s) across the area of interest (documentation will include, at a minimum, file name, scale, GPS coordinates, direction of view and description of the photo).
	Primary and Ductile Structure	Observe and document the bedrock structural features (e.g., bedding, foliations, lineations, folds and shear zones). Take digital photographs/make field sketches of representative key structural features. Measure and document (by hand with compass-clinometer and subsequent digital and manual entry): - Strike and dip of planar structures. - Trend and plunge of linear structures. - Orientations of fold hinge lines and axial surfaces.
	Geophysical and Geomechanical Character	Record 5 magnetic susceptibility measurements for each identified lithological unit using a magnetic susceptibility metre (e.g. KT10 or KT20). Undertake gamma ray readings for each identified lithological unit using a gamma ray spectrometer (e.g. RS-125 or equivalent) measuring total counts, Th (ppm), U (ppm),%K. Undertake field rock strength test on representative rock types at each station and in spatial relation to identified structural features (i.e. lineaments, fracture zones, dykes).

Notes:

Samples will be stored in bags numbered in accordance with the sample number generated in the database.

Effort will be made to characterize fractures of all dip magnitudes (including horizontal to shallow dipping features).

Strike and dip measurements follow Canadian right-hand-rule notation.

All observations will be recorded in digital format with manual (pen and paper) backup for most pertinent field observations only, unless required due to digital device failure.

Table A.4: Continued

Geological Attributes		Characterization Method(s)
Fracture Characteristics		Visually inspect the rock surface for identification of systematic fracture sets. Characterize fracture sets by type (joints, faults, veins, altered wallrock around fractures). Measure and document (by hand with compass-clinometer and subsequent digital and manual entry): - Strike and dip of planar structures - Trend and plunge of linear structures on fracture planes Document: - Fracture mineral filling. - Abutting, cross-cutting and intersection (relative age) relationships between fracture sets. - Displacement (strike separations and dip separations if visible) - Fracture surface ornamentation. - Fracture set spacing. Take representative digital photograph(s) as needed to show key fracture characteristics, for example cross-cutting relationships, damage zone width, alteration, mineral infill.
Dyke Characteristics		Visually inspect dyke for characteristic features (e.g., mineralogy, colour). Collect a representative sample of each dyke type. Take representative digital photograph of dyke, including contact relationship with bedrock, if exposed. Document: - Internal structure (fractures) - Width - Orientation (strike and dip along bedrock contact). - Nature of bedrock contact (e.g., welded, fractured, sheared, - altered, extent of damage, etc.).
	Geophysical and Geomechanical Character	Record 5 magnetic susceptibility measurements for each identified dyke. Undertake gamma ray readings for each identified dyke. Undertake field rock strength test on each dyke.

Notes:

Samples will be stored in bags numbered in accordance with the sample number generated in the database.

Effort will be made to characterize fractures of all dip magnitudes (including horizontal to shallow dipping features).

Strike and dip measurements follow Canadian right-hand-rule notation.

All observations will be recorded in digital format with manual (pen and paper) backup for most pertinent field observations only, unless required due to digital device failure.

Table A.5: Field Estimates of Intact Rock Strength

Grade	Description	Field Identification
R6	Extremely strong	Specimen can only be chipped with a geological hammer
R5	Very strong	Specimen requires many blows of a geological hammer to fracture it
R4	Strong	Specimen requires more than one blow of a geological hammer to fracture it
R3	Medium strong	Cannot be scraped or peeled with a pocket knife, specimen can be fractured with a single blow from a geological hammer
R2	Weak	Can be peeled with a pocket knife with difficulty, shallow indentation made by firm blow with point of a geological hammer
R1	Very weak	Crumbles under firm blows with a geological hammer, can be peeled by a pocket knife
R0	Extremely weak	Indented by thumbnail

Note: From Barton (1978)

APPENDIX B

Remote Predictive Bedrock Analysis

Potential outcrop locations were identified through an automated object based image analysis (OBIA), filtered, and prioritized for use in planning and implementing the Phase 2 Geological Mapping in the Manitouwadge area of Ontario. This work involved 2 main tasks: 1) automated OBIA and 2) manual filtering of OBIA results to produce an output of potential outcrop locations.

Object Based Image Analysis using eCognition

Automated OBIA was conducted using Trimble's eCognition 9.1 software for the two withdrawal areas identified for detailed mapping in the White River area. Forest Resource Inventory (FRI) orthoimagery of the White River area, from 2009, was the primary dataset used in the analysis. FRI imagery is 4-band (red, green, blue, near infra-red) multi-resolution, 40 cm airborne imagery collected and used for forest resource purposes by the Ministry of Natural Resources.

A ruleset was developed in eCognition which initially employed multi-resolution segmentation to develop small image objects of almost pixel size. Through a series of iterative steps, the ruleset was refined and the small image objects were merged into larger more identifiable objects of distinct classes. Areas of water were classified first, followed by those areas that are spatially and spectrally similar to exposed bedrock, such as unpaved road surfaces, sand covered areas and brightly reflecting bogs. The remaining image objects were considered to most likely represent exposed outcrop and output as a distinct data set. This raw eCognition output provided a framework for remotely interpreting the location of probable bedrock outcrops in the four potentially suitable areas.

Filtering of OBIA results

It is understood that similarities in spectral response of areas of ground cover versus areas of exposed bedrock in the Manitouwadge area results in instances of false positive exposed bedrock classification when classifying by means of OBIA. In order to use the remotely predicted outcrop data set in a meaningful way for detailed outcrop mapping an additional step of manually comparing the raw output, against the FRI imagery, was required.

The process to undertake this filtering was straightforward and involved examining the FRI imagery in areas where the eCognition output showed clusters of pixels locating possible exposed bedrock. The cluster area was visually evaluated in the FRI imagery and a determination by consensus of two or more individual interpreters was made as to whether the location in question did or did not likely represent actual exposed bedrock. If it was determined likely, then the location was outlined and defined as a unique polygon. This analysis produced a set of shapefiles of polygons representing interpreted priority outcrop locations, for both withdrawal areas in the Manitouwadge area (see Figure 1.2 from main report). The planning for the Phase 2 Geological Mapping activity in Manitouwadge is based upon these interpreted priority outcrop locations.

FIGURES

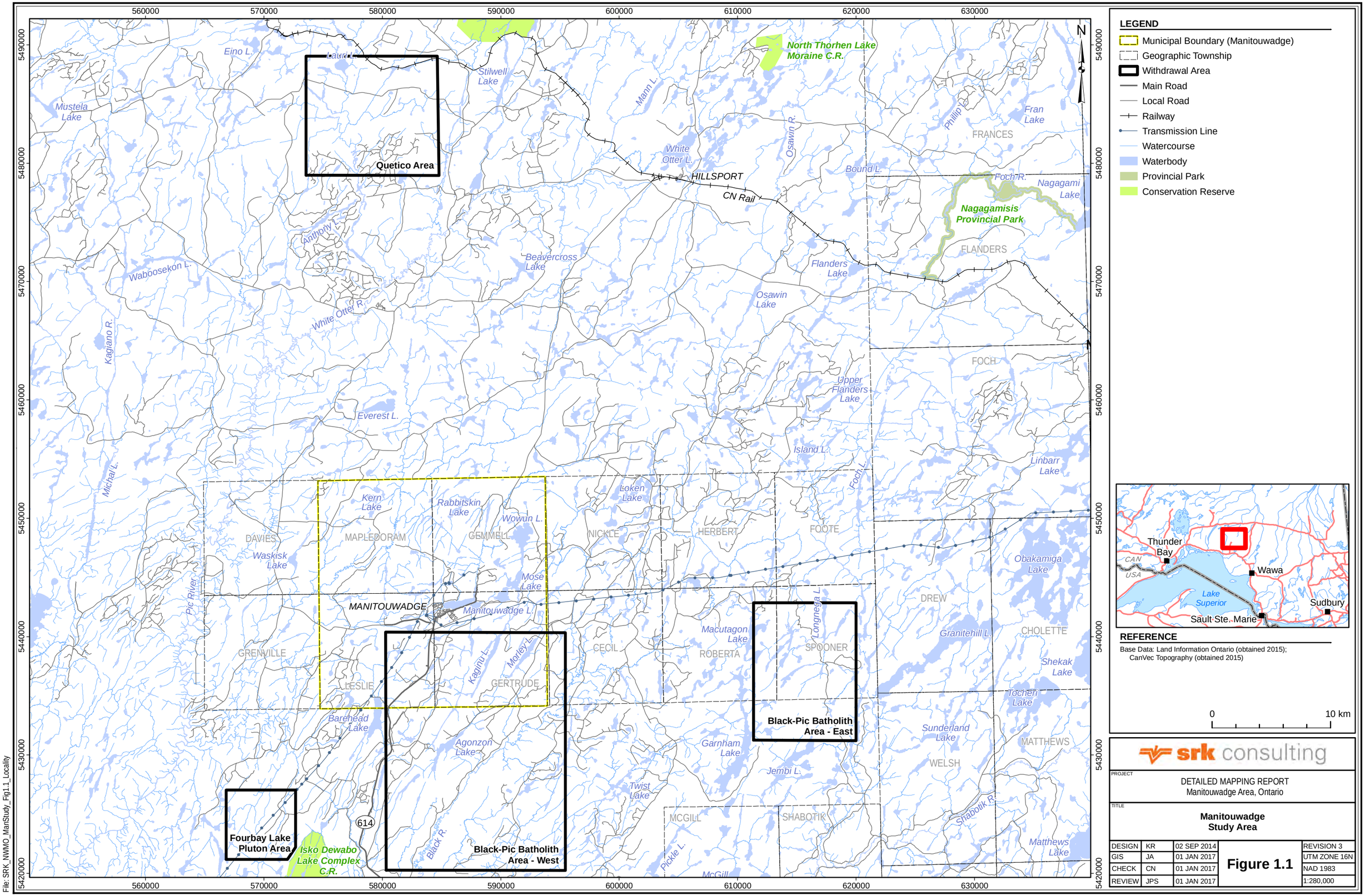
560000
570000
580000
590000
600000
610000
620000
630000
5490000
5480000
5470000
5460000
5450000
5440000
5430000
5420000
N
Quetico Area
Eino L.
Laurie L.
Stilwell Lake
Mann L.
North Thorhen Lake Moraine C.R.
Mustela Lake
Phillip L.
Fran Lake
FRANCES
White Otter L.
Osawin R.
HILLSPORT
CN Rail
Bound L.
Foch R.
Nagagami Lake
Nagagamisis Provincial Park
FLANDERS
Anthony L.
Beavercross Lake
Flanders Lake
Waboosekon L.
Osawin Lake
White Otter R.
Kagiano R.
FOCH
Upper Flanders Lake
Everest L.
Island L.
Linbarr Lake
Michal L.
Kern Lake
Rabbitskin Lake
Wowun L
Loken Lake
Foch L.
DAVIES
MAPLEDORAM
GEMMELL
NICKLE
HERBERT
FOOTE
Waskisk Lake
Obakamiga Lake
Pic River
Mose Lake
MANITOUWADGE
Manitouwadge L.
DREW
Longnega L.
Macutagon Lake
Granitehill L.
CHOLETTE
GRENVILLE
CECIL
ROBERTA
SPOONER
Kagintu L.
Money L.
Shekak Lake
LESLIE
GERTRUDE
Tocheri Lake
Barehead Lake
Black-Pic Batholith Area - East
Sunderland Lake
MATTHEWS
Agonzon Lake
Garnham Lake
WELSH
Jembi L.
Twist Lake
Fourbay Lake Pluton Area
614
Isko Dewabo Lake Complex C.R.
Black R.
Black-Pic Batholith Area - West
MCGILL
SHABOTIK
Shabotik R.
Pickle L.
Matthews Lake
McGill
LEGEND
Municipal Boundary (Manitouwadge)
Geographic Township
Withdrawal Area
Main Road
Local Road
Railway
Transmission Line
Watercourse
Waterbody
Provincial Park
Conservation Reserve
Thunder Bay
CAN
USA
Wawa
Lake Superior
Sudbury
Sault Ste. Marie
REFERENCE
Base Data: Land Information Ontario (obtained 2015);
CanVec Topography (obtained 2015)
0
10 km
srk consulting
PROJECT
DETAILED MAPPING REPORT
Manitouwadge Area, Ontario
TITLE
Manitouwadge
Study Area
DESIGN KR 02 SEP 2014
GIS JA 01 JAN 2017
CHECK CN 01 JAN 2017
REVIEW JPS 01 JAN 2017
Figure 1.1
REVISION 3
UTM ZONE 16N
NAD 1983
1:280,000
File: SRK_NWMO_ManStudy_Fig1.1_Locality

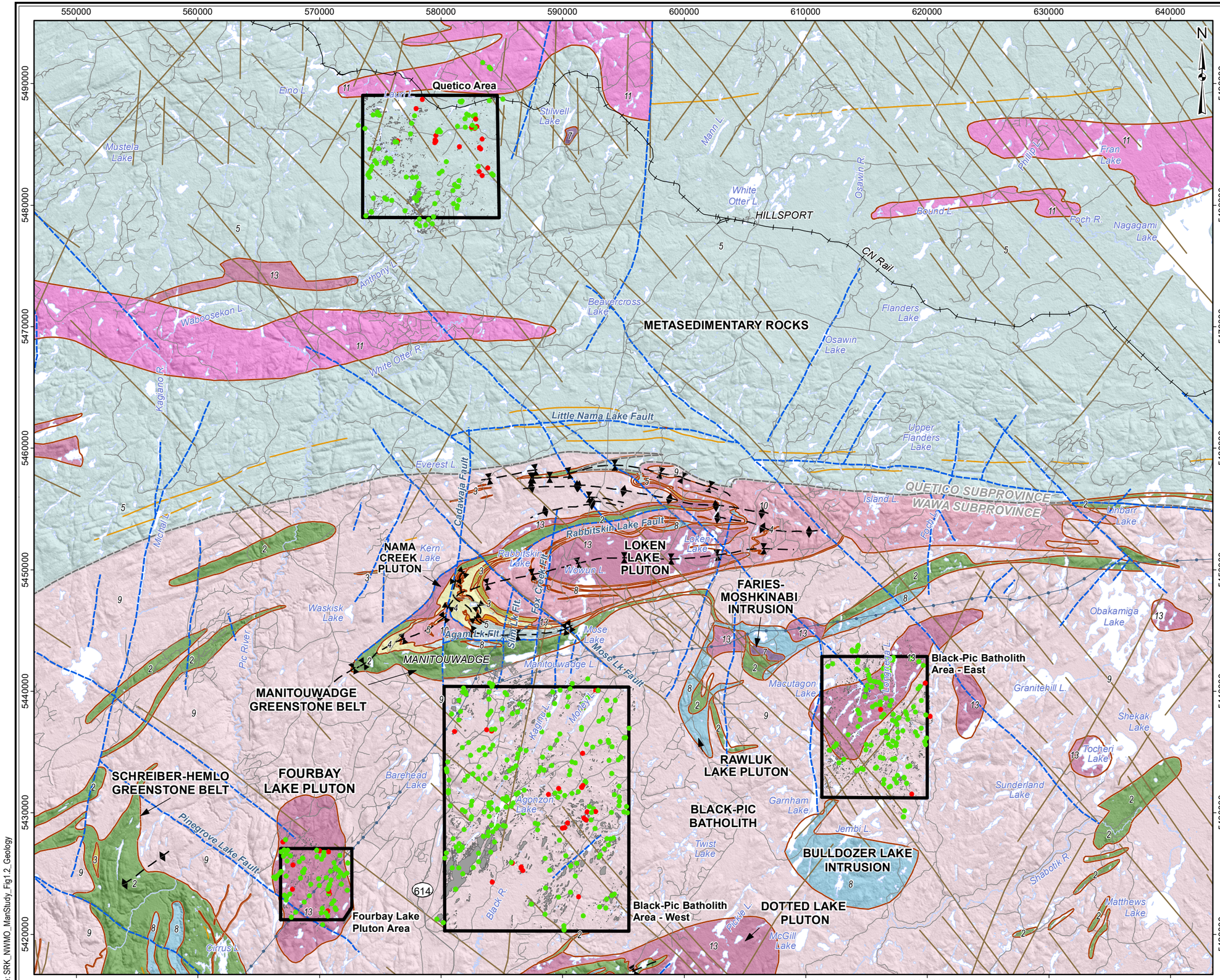

LEGEND

- Withdrawal Area
- Main Road
- Local Road
- Railway
- Transmission Line
- Waterbody
- Observation - Outcrop (496)
- Observation - Overburden (55)
- Predicted Outcrop

Bedrock Geology

- Geological Boundary
- Subprovince Boundary
- Fault
- Dyke
- Fold (syncline)
- Fold (anticline)
- 13: Granite-granodiorite
- 11: Granite-granodiorite
- 10: Foliated tonalite suite
- 9: Gneissic tonalite suite
- 8: Gabbro
- 7: Ultramafic plutonic rocks
- 5: Metasedimentary rocks
- 4: Felsic volcanic rocks
- 3: Felsic and intermediate metavolcanic rocks
- 2: Mafic metavolcanic Rocks
- Iron Formation

REFERENCE

Base Data: Land Information Ontario (obtained 2015); CanVec Topography (obtained 2015)

Bedrock Geology: MRD 126-REV1 (Ontario Geological Survey, 2011); Ontario Geological Survey Map 2665 (Santaguida, 2001); Map 2666 (Santaguida, 2001); Map 2667 (Johns, McIlraith and Stott, 2003); Map 2668 (Johns and McIlraith, 2003)

0 10 km

srk consulting

PROJECT
DETAILED MAPPING REPORT
Manitouwadge Area, Ontario

TITLE
Manitouwadge Mapping Observation Locations

DESIGN	KR	02 SEP 2014	**Figure 1.2**	REVISION 6
GIS	JA	02 OCT 2017		UTM ZONE 16N
CHECK	CN	02 OCT 2017		NAD 1983
REVIEW	JPS	02 OCT 2017		1:303,009

File: SRK_NWMO_ManStudy_Fig1.2_Geology

570000
580000
590000
5490000
5480000
N
5
11
7
3
Eino L.
Lauri L.
Stilwell Lake
Bishop Lake
Anthony L.
White Otter R.
HARKNESS ROAD
BISHOP LAKE ROAD
CARAMAT INDUSTRIAL RD
16BH0286
16JK0095
16JK0094
16JK0093
16JK0092
16JK0052
16JK0050
16JK0051
16BH0281
16BH0282
16BH0283
16BH0284
16BH0285
16BH0051
16BH0052
16JK0223
16JK0222
16JK0221
16JK0220
16BH0142
16BH0141
16BH0140
16BH0144
16BH0143
16BH0146
16BH0145
16JK0114
16JK0109
16JK0111
16JK0110
16JK0113
16JK0115
16JK0112
16CN0027
16CN0029
16CN0028
16BH0280
16CN0030
16BH0277
16BH0279
16BH0278
16JK0108
16BH0220
16BH0222
16BH0221
16JK0226
16JK0224
16JK0225
16BH0084
16BH0087
16BH0162
16BH0085
16BH0163
16BH0164
16JK0141
16BH0161
16BH0086
16JK0140
16JK0138
16JK0139
16JK0137
16BH0219
16CN0132
16CN0131
16CN0133
16CN0130
16CN0134
16CN0135
16BH0218
16BH0217
16CN0051
16CN0053
16CN0052
16CN0041
16CN0042
16CN0039
16CN0040
16CN0054
16CN0050
16BH0130
16CN0038
16BH0098
16BH0270
16JK0106
16BH0132
16BH0131
16BH0269
16JK0105
16JK0104
16BH0133
16CN0018
16CN0021
16CN0019
16BH0100
16CN0020
16BH0268
16BH0267
16JK0103
16BH0266
16BH0101
16CN0108
16CN0107
16CN0109
16BH0102
16CN0110
16CN0111

LEGEND

- Withdrawal Area
- Main Road
- Local Road
- Railway
- Waterbody
- Observation - Outcrop (88)
- Observation - Overburden (18)
- Predicted Outcrop

Bedrock Geology

- Geological Boundary
- Mapped Fault
- 13: Granite-granodiorite
- 11: Granite-granodiorite
- 7: Ultramafic plutonic rocks
- 5: Metasedimentary rocks

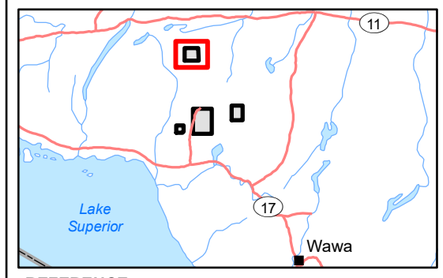

REFERENCE

Base Data: Land Information Ontario (obtained 2015); CanVec Topography (obtained 2015)

Bedrock Geology: MRD 126-REV1 (Ontario Geological Survey, 2011); Ontario Geological Survey Map 2665 (Santaguida, 2001); Map 2666 (Santaguida, 2001); Map 2667 (Johns, McIlraith and Stott, 2003); Map 2668 (Johns and McIlraith, 2003)

0 2 km

srk consulting

PROJECT
DETAILED MAPPING REPORT
Manitouwadge Area, Ontario

TITLE
Quetico Area
Mapping Observation Locations

DESIGN	KR	02 SEP 2014	**Figure 5.1.1**	REVISION 5
GIS	JA	20 AUG 2017		UTM ZONE 16N
CHECK	CN	20 AUG 2017		NAD 1983
REVIEW	JPS	20 AUG 2017		1:80,000

File: SRK_NWMO_ManStudy_AreaA_Fig5.1.1

Figure 5.1.2: Quetico Area – Field Examples of Accessibility and Bedrock Exposure

A: New logging road access (Stn 16BH0281, looking N, person for scale).
B: Aerial view of low lying topography (Stn 16BH0221, looking E, no scale).
C: Typical migmatitic metasedimentary rock outcrop exposure along ATV trail (Stn 16CN0040, looking E, person for scale).
D: Typical, low rounded outcrop of granite (Stn 16CN0028, looking N, person for scale).
E: Aerial view of light coloured, moss covered overburden resembling outcrop (Stn 16BH0222, looking N, no scale).
F: Light coloured moss on low relief, overburden covered, open areas (Stn 16BH0146, looking N, person for scale).

570000
580000
590000
5490000
5480000
N
Eino L.
Lauri L.
Stilwell Lake
Bishop Lake
Anthony L.
White Otter R.
11
7
3
CARAMAT INDUSTRIAL RD
HARKNESS ROAD
BISHOP LAKE ROAD

LEGEND

- Withdrawal Area
- Main Road
- Local Road
- Railway
- Waterbody
- Outcrop

Bedrock Geology

- Geological Boundary
- Mapped Fault
- 13: Granite-granodiorite
- 11: Granite-granodiorite
- 7: Ultramafic plutonic rocks
- 5: Metasedimentary rocks
- Outcrop

Main Lithology

- Migmatitic Metasedimentary Rock (70)
- Granite (67)
- Granodiorite (6)

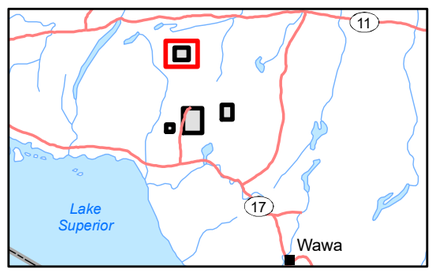

REFERENCE

Base Data: Land Information Ontario (obtained 2015); CanVec Topography (obtained 2015)

Bedrock Geology: MRD 126-REV1 (Ontario Geological Survey, 2011); Ontario Geological Survey Map 2665 (Santaguida, 2001); Map 2666 (Santaguida, 2001); Map 2667 (Johns, McIlraith and Stott, 2003); Map 2668 (Johns and McIlraith, 2003)

0 2 km

srk consulting

PROJECT
DETAILED MAPPING REPORT
Manitouwadge Area, Ontario

TITLE
Quetico Area
Main Lithological Units

DESIGN	KR	02 SEP 2014	**Figure 5.1.3a**	REVISION 5
GIS	JA	15 NOV 2017		UTM ZONE 16N
CHECK	BH	15 NOV 2017		NAD 1983
REVIEW	JPS	15 NOV 2017		1:80,000

File: SRK_NWMO_ManStudy_AreaA_Fig5.1.3

570000
580000
590000
5490000
5480000
N
5
11
13
7
Eino L.
Lauri L.
Stilwell Lake
Bishop Lake
Anthony L.
White Otter R.
CARAMAT INDUSTRIAL RD
HARKNESS ROAD
BISHOP LAKE ROAD

LEGEND

- Withdrawal Area
- Main Road
- Local Road
- Railway
- Waterbody
- Outcrop

Bedrock Geology

- Geological Boundary
- Mapped Fault
- 13: Granite-granodiorite
- 11: Granite-granodiorite
- 7: Ultramafic plutonic rocks
- 5: Metasedimentary rocks
- Metatexite (62)
- Diatexite (8)

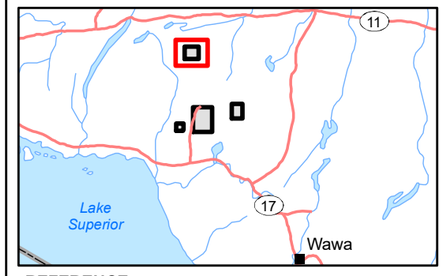

REFERENCE

Base Data: Land Information Ontario (obtained 2015); CanVec Topography (obtained 2015)

Bedrock Geology: MRD 126-REV1 (Ontario Geological Survey, 2011); Ontario Geological Survey Map 2665 (Santaguida, 2001); Map 2666 (Santaguida, 2001); Map 2667 (Johns, McIlraith and Stott, 2003); Map 2668 (Johns and McIlraith, 2003)

0 2 km

srk consulting

PROJECT
DETAILED MAPPING REPORT
Manitouwadge Area, Ontario

TITLE
Quetico Area
Migmatite Classification

DESIGN	KR	02 SEP 2014	**Figure 5.1.3b**	REVISION 6
GIS	JA	15 NOV 2017		UTM ZONE 16N
CHECK	BH	15 NOV 2017		NAD 1983
REVIEW	JPS	15 NOV 2017		1:80,000

File: SRK_NWMO_ManStudy_AreaA_Fig5.1.3b

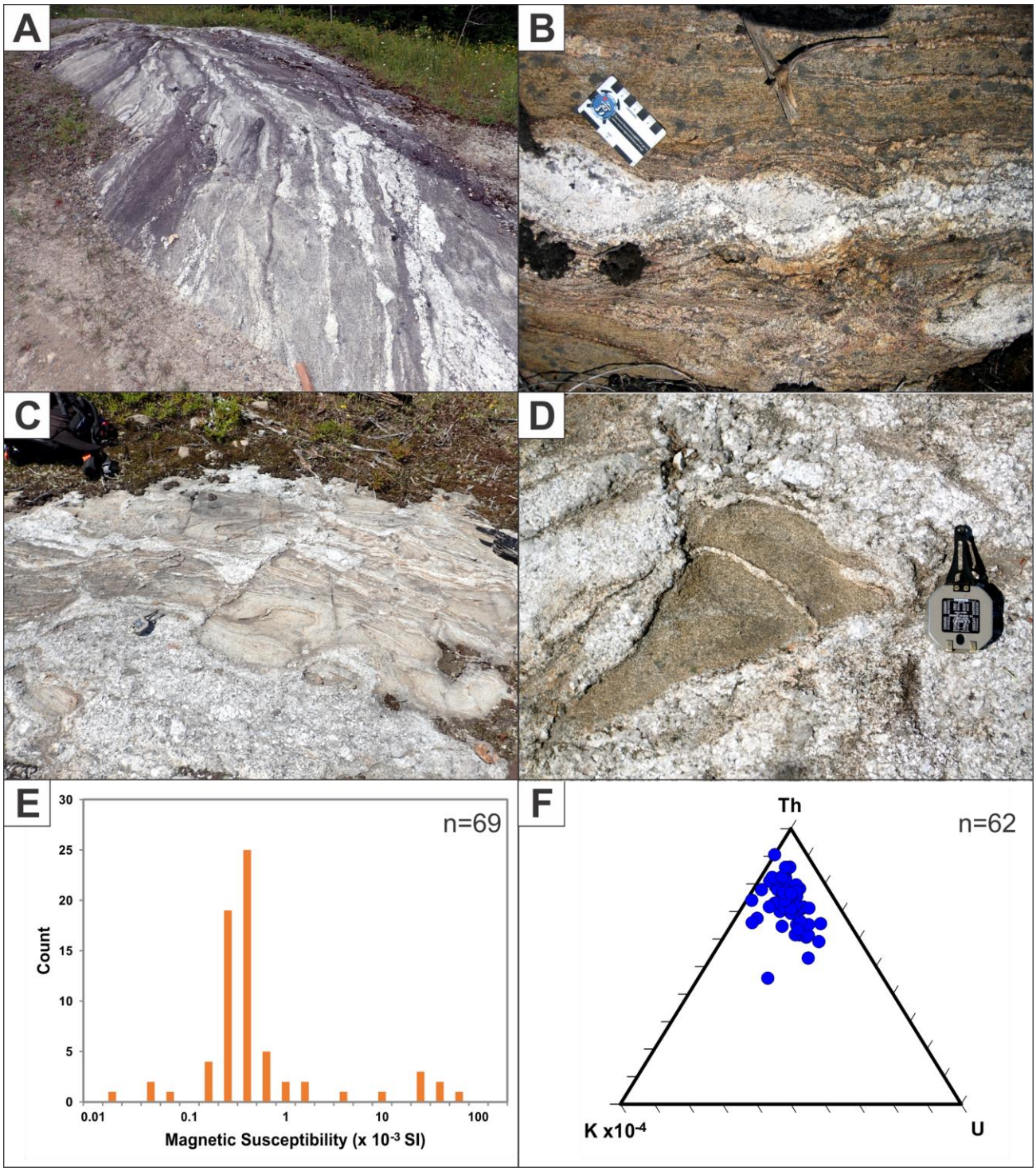

Figure 5.1.4a: Quetico Area – Field Examples of Main Lithology – Migmatitic Metasedimentary Rocks

A: Migmatitic metasedimentary rock (metatexite) at outcrop scale (Stn 16BH0051, looking SW, hammer handle for scale).
B: Close-up of metasedimentary rock (metatexite) showing mineral composition and texture (Stn 16JK0137, looking N, card for scale).
C: Two mica granite intruding metasedimentary rocks (Stn 16BH0086, looking NW, compass for scale).
D: Remnant metasedimentary xenolith in granite (Stn 16BH0086, looking N, compass for scale).
E: Logarithmic histogram plot of magnetic susceptibility for migmatitic metasedimentary rocks.
F: Ternary plot of gamma ray spectrometer data for migmatitic metasedimentary rocks.

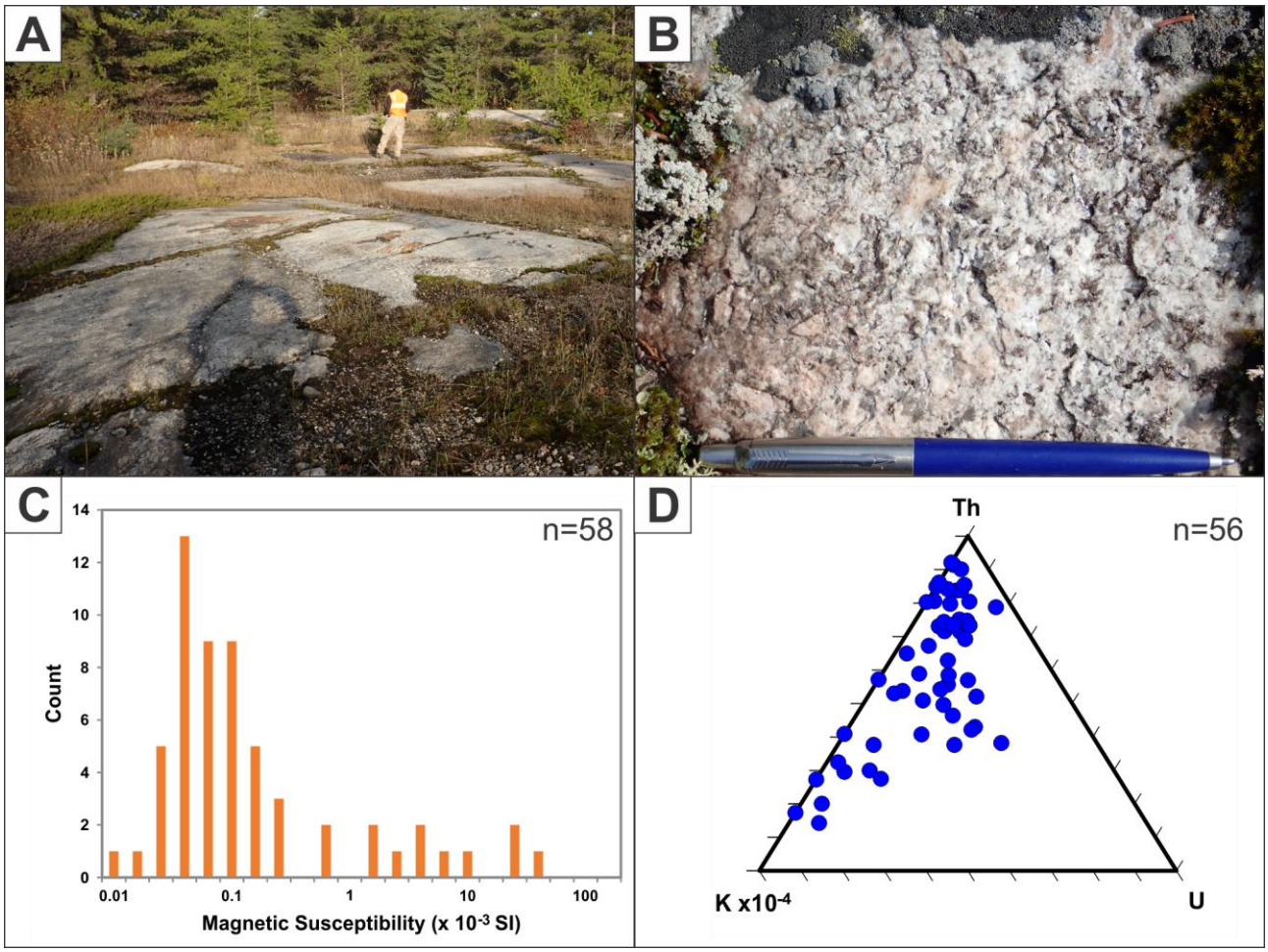

Figure 5.1.4b: Quetico Area – Field Examples of Main Lithology – Granite

A: Granite at outcrop scale (Stn 16BH0286, looking E, person for scale).
B: Close-up of granite showing characteristic two-mica mineral composition and texture (Stn 16BH0140, looking northeast, pen for scale).
C: Logarithmic histogram plot of magnetic susceptibility for granite.
D: Ternary plot of gamma ray spectrometer data for granite.

570000
580000
590000
5490000
5480000
N
5
11
13
7
Eino L.
Lauri L.
Stilwell Lake
Bishop Lake
Anthony L.
White Otter R.
CARAMAT INDUSTRIAL RD
HARKNESS ROAD
BISHOP LAKE ROAD

LEGEND

- Withdrawal Area
- Main Road
- Local Road
- Railway
- Waterbody

Bedrock Geology

- Geological Boundary
- Mapped Fault
- 13: Granite-granodiorite
- 11: Granite-granodiorite
- 7: Ultramafic plutonic rocks
- 5: Metasedimentary rocks
- Observation - Outcrop

Minor Lithology

- Magnetite-rich Granite (3)

REFERENCE

Base Data: Land Information Ontario (obtained 2015); CanVec Topography (obtained 2015)

Bedrock Geology: MRD 126-REV1 (Ontario Geological Survey, 2011); Ontario Geological Survey Map 2665 (Santaguida, 2001); Map 2666 (Santaguida, 2001); Map 2667 (Johns, McIlraith and Stott, 2003); Map 2668 (Johns and McIlraith, 2003)

0 2 km

srk consulting

PROJECT
DETAILED MAPPING REPORT
Manitouwadge Area, Ontario

TITLE
Quetico Area
Minor Lithological Units

DESIGN	KR	02 SEP 2014	**Figure 5.1.5**	REVISION 3
GIS	JA	02 AUG 2017		UTM ZONE 16N
CHECK	CN	02 AUG 2017		NAD 1983
REVIEW	JPS	02 AUG 2017		1:80,000

File: SRK_NWMO_ManStudy_AreaA_Fig5.1.5v2

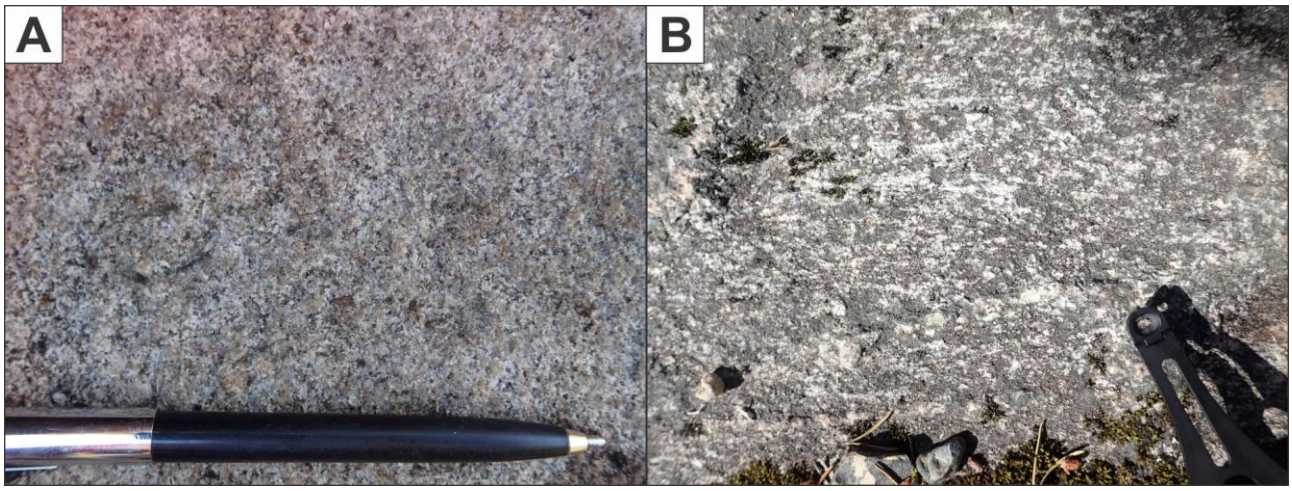

Figure 5.1.6: Quetico Area – Field Examples of Minor Lithological Units

A: Massive, magnetite bearing granite whose contact (not shown) is oblique to regional foliation (Stn16BH0219, looking S, pen for scale).

B: Foliated, magnetite bearing granitoid or completely recrystallized metasedimentary rock units aligned parallel to dominant foliation (Stn16BH0087, looking N, compass for scale).

570000
580000
590000
5490000
5480000

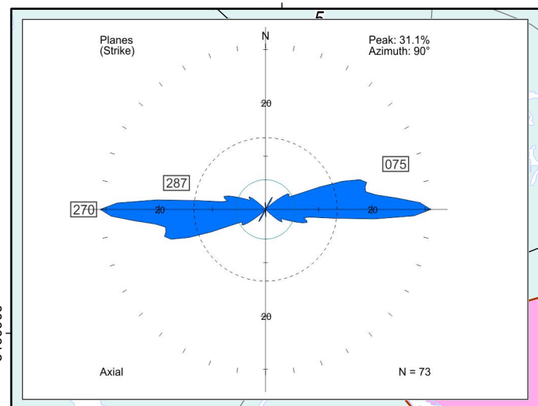

11

CARAMAT INDUSTRIAL RD

Lauri L.

HARKNESS ROAD

Stilwell Lake

7

Bishop Lake

BISHOP LAKE ROAD

Anthony L.

White Otter R.

13

N

LEGEND

- Withdrawal Area
- Main Road
- Local Road
- Railway
- Waterbody
- Observation - Outcrop (24)
- Observation - Overburden (17)
- Foliation (53)
- Gneissic Layering (20)
- Fold Axial Plane (4)
- Fold Axis (10)
- Mineral Lineation (4)

Bedrock Geology

- Geological Boundary
- Mapped Fault
- 13: Granite-granodiorite
- 11: Granite-granodiorite
- 7: Ultramafic plutonic rocks
- 5: Metasedimentary rocks

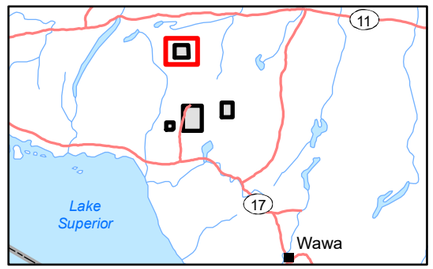

REFERENCE

Base Data: Land Information Ontario (obtained 2015);
CanVec Topography (obtained 2015)

Bedrock Geology: MRD 126-REV1 (Ontario Geological Survey, 2011);
Ontario Geological Survey Map 2665 (Santaguida, 2001);
Map 2666 (Santaguida, 2001);
Map 2667 (Johns, McIlraith and Stott, 2003);
Map 2668 (Johns and McIlraith, 2003)

0 2 km

srk consulting

PROJECT
DETAILED MAPPING REPORT
Manitouwadge Area, Ontario

TITLE
Quetico Area
Tectonic Foliation

DESIGN	KR	02 SEP 2014	**Figure 5.1.7**	REVISION 5
GIS	JA	02 AUG 2017		UTM ZONE 16N
CHECK	CN	02 AUG 2017		NAD 1983
REVIEW	JPS	02 AUG 2017		1:80,000

File: SRK_NWMO_ManStudy_AreaA_Fig5.1.7

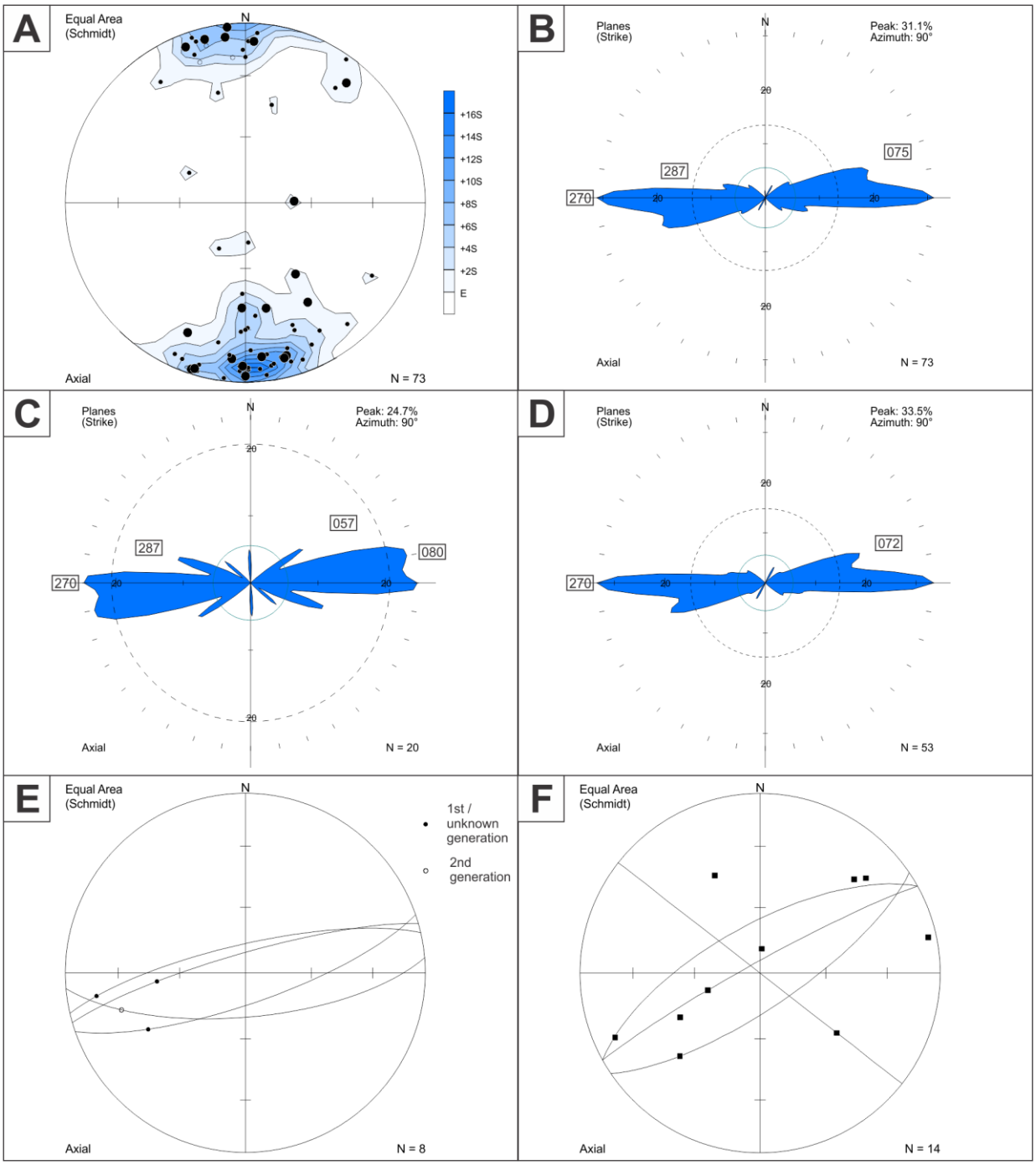

Figure 5.1.8: Quetico Area – Tectonic Foliation Orientation Data

A: All main gneissic layering and tectonic foliation displayed as equal area lower hemisphere stereonet plot of poles to planes. Gneissic layering: large circles (n=20). Mineral foliation: First/unknown generation - small circles (n=50); Second generation – open circles (n=3).

B: All main gneissic layering and tectonic foliation displayed as rose diagram of trends of planes with orientation of all peaks greater than the expected value E (n=73).

C: Gneissic layering displayed as rose diagram of trends of planes (n=20).

D: Mineral foliation displayed as rose diagram of trends of planes (n=53).

E: Mineral lineation data displayed as equal area lower hemisphere stereonet plot of lineation points and great circles of respective foliation planes in the same outcrops. Lineation plotted as rake calculated from measured trend and plunge.

F: Fold axis and axial plane data displayed as equal area lower hemisphere stereonet plot of fold axis points and great circles of axial planes.

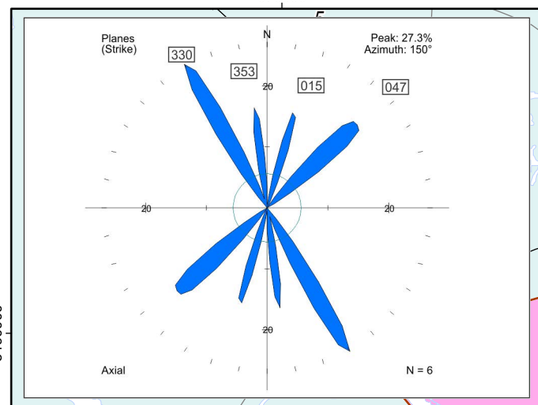

570000 580000 590000

5490000

5480000

N

11

CARAMAT INDUSTRIAL RD

Lauri L.

Stilwell Lake

7

HARKNESS ROAD

67

66

84

72

64

88

Bishop Lake

BISHOP LAKE ROAD

Anthony L.

White Otter R.

13

LEGEND

- Withdrawal Area
- Main Road
- Local Road
- Railway
- Waterbody
- Observation - Outcrop (72)
- Observation - Overburden (18)
- Brittle-Ductile Shear Zone (1)
- Ductile Shear Zone - Sinistral (2)
- Ductile Shear Zone - Dextral (2)
- Ductile Shear Zone - Strike (1)

Bedrock Geology

- Geological Boundary
- Mapped Fault
- 13: Granite-granodiorite
- 11: Granite-granodiorite
- 7: Ultramafic plutonic rocks
- 5: Metasedimentary rocks

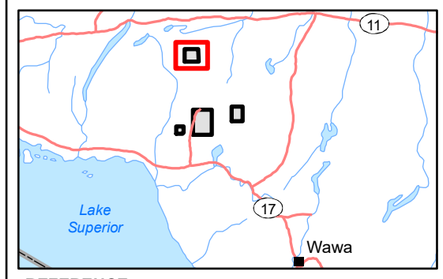

REFERENCE

Base Data: Land Information Ontario (obtained 2015); CanVec Topography (obtained 2015)

Bedrock Geology: MRD 126-REV1 (Ontario Geological Survey, 2011); Ontario Geological Survey Map 2665 (Santaguida, 2001); Map 2666 (Santaquida, 2001); Map 2667 (Johns, McIlraith and Stott, 2003); Map 2668 (Johns and McIlraith, 2003)

0 2 km

srk consulting

PROJECT
DETAILED MAPPING REPORT
Manitouwadge Area, Ontario

TITLE
Quetico Area
Ductile and Brittle-Ductile Shear Zones

DESIGN	KR	02 SEP 2014	**Figure 5.1.9**	REVISION 6
GIS	JA	02 AUG 2017		UTM ZONE 16N
CHECK	CN	02 AUG 2017		NAD 1983
REVIEW	JPS	02 AUG 2017		1:80,000

File: SRK_NWMO_ManStudy_AreaA_Fig5.1.9

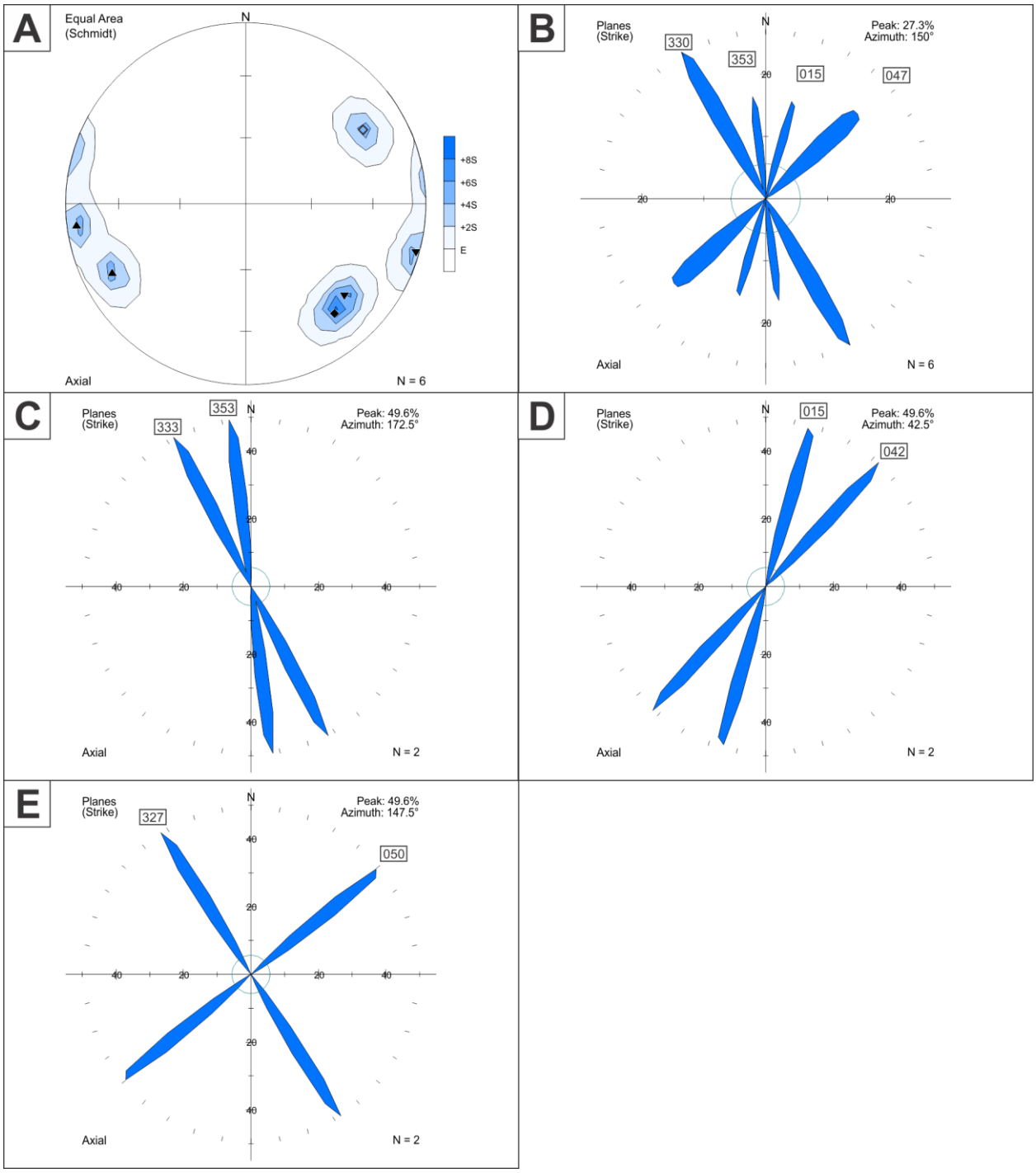

Figure 5.1.10: Quetico Area – Ductile and Brittle-Ductile Shear Zone Orientation Data

A: All ductile and brittle-ductile shear zones displayed as equal area lower hemisphere stereonet plot of poles to planes. Dextral shear zones: filled upright triangles (n=2). Sinistral shear zones: filled inverted triangles (n=2). Other or unknown movement sense shear zones: filled diamond (n=1). Other or unknown movement sense brittle-ductile shear zone: open diamond (n=1).

B: All ductile and brittle-ductile shear zones displayed as rose diagram of trends of planes with orientation of all peaks greater than the expected value E (n=6).

C: Dextral shear zones displayed as rose diagram of trends of planes (n=2).

D: Sinistral shear zones displayed as rose diagram of trends of planes (n=2).

E: Unknown movement sense shear zones displayed as rose diagram of trends of planes (n=2).

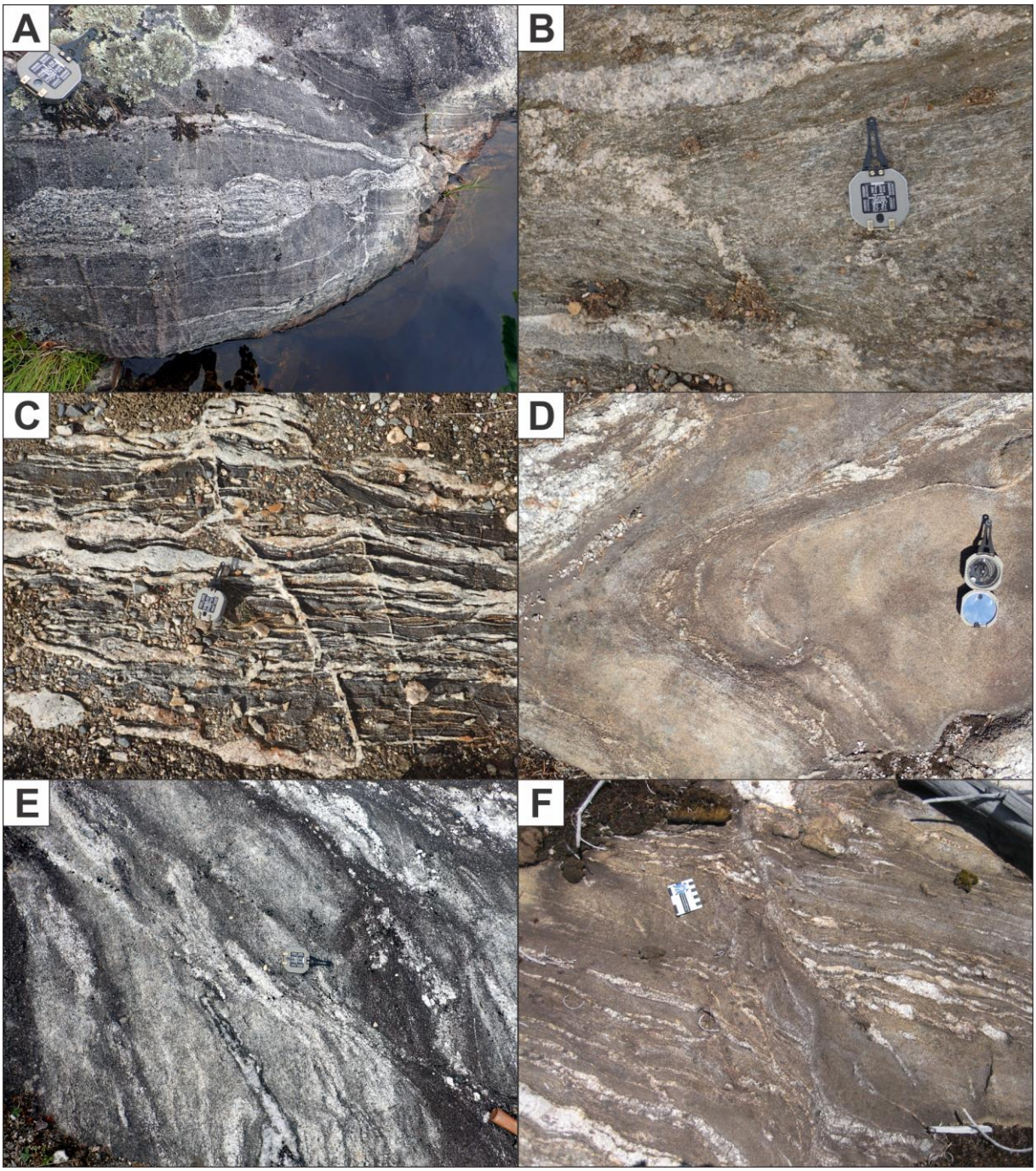

Figure 5.1.11: Quetico Area – Field Examples of Ductile Structures

A: Gneissic layering in migmatitic metasedimentary rock with boudinaged intrusive leucosome (Stn 16BH0052, looking NW, compass for scale).
B: Main foliation and early intrusive leucosome folded about moderately SW-plunging fold (Stn 16BH0266, looking N, compass for scale).
C: Transposed main foliation and early intrusive leucosome (Stn 16BH0269, looking N, compass for scale).
D: Fold of compositional layers/main foliation with weak E-trending axial planar foliation in nose of fold (Stn 16BH0161, looking N, compass for scale).
E: NE-trending, sinistral strike -separation ductile shear zone cutting migmatitic metasedimentary rock (Stn 16BH0051, looking W, compass for scale).
F: NNW-trending, dextral strike-separation ductile shear zone cutting migmatitic metasedimentary rock (Stn 16JK0137, looking N, card for scale).

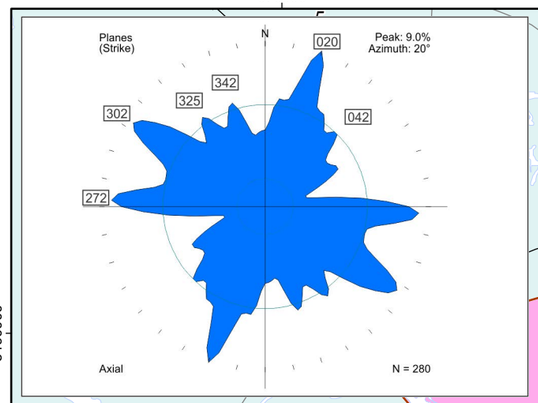

570000
580000
590000
5490000
5480000

11
CARAMAT INDUSTRIAL RD
Lauri L.
Stilwell Lake
7
HARKNESS ROAD
Bishop Lake
BISHOP LAKE ROAD
Anthony L.
White Otter R.
13

N

LEGEND

- Withdrawal Area
- Main Road
- Local Road
- Railway
- Waterbody
- Observation - Outcrop (7)
- Observation - Overburden (17)
- Sub horizontal joint: 0-30° (23)
- Intermediate joint: 31-60° (20)
- Sub vertical joint: 61-90° (237)

Bedrock Geology

- Geological Boundary
- Mapped Fault
- 13: Granite-granodiorite
- 11: Granite-granodiorite
- 7: Ultramafic plutonic rocks
- 5: Metasedimentary rocks

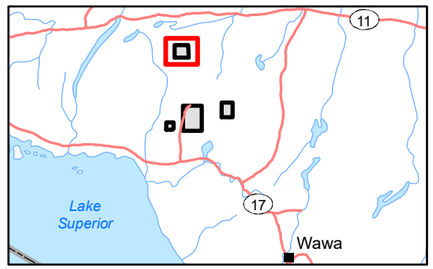

REFERENCE

Base Data: Land Information Ontario (obtained 2015);
CanVec Topography (obtained 2015)

Bedrock Geology: MRD 126-REV1 (Ontario Geological Survey, 2011);
Ontario Geological Survey Map 2665 (Santaguida, 2001);
Map 2666 (Santaguida, 2001);
Map 2667 (Johns, McIlraith and Stott, 2003);
Map 2668 (Johns and McIlraith, 2003)

0 2 km

srk consulting

PROJECT
DETAILED MAPPING REPORT
Manitouwadge Area, Ontario

TITLE
Quetico Area
Joints

DESIGN	KR	02 SEP 2014	**Figure 5.1.12**	REVISION 5
GIS	JA	02 AUG 2017		UTM ZONE 16N
CHECK	CN	02 AUG 2017		NAD 1983
REVIEW	JPS	02 AUG 2017		1:80,000

File: SRK_NWMO_ManStudy_AreaA_Fig5.1.12

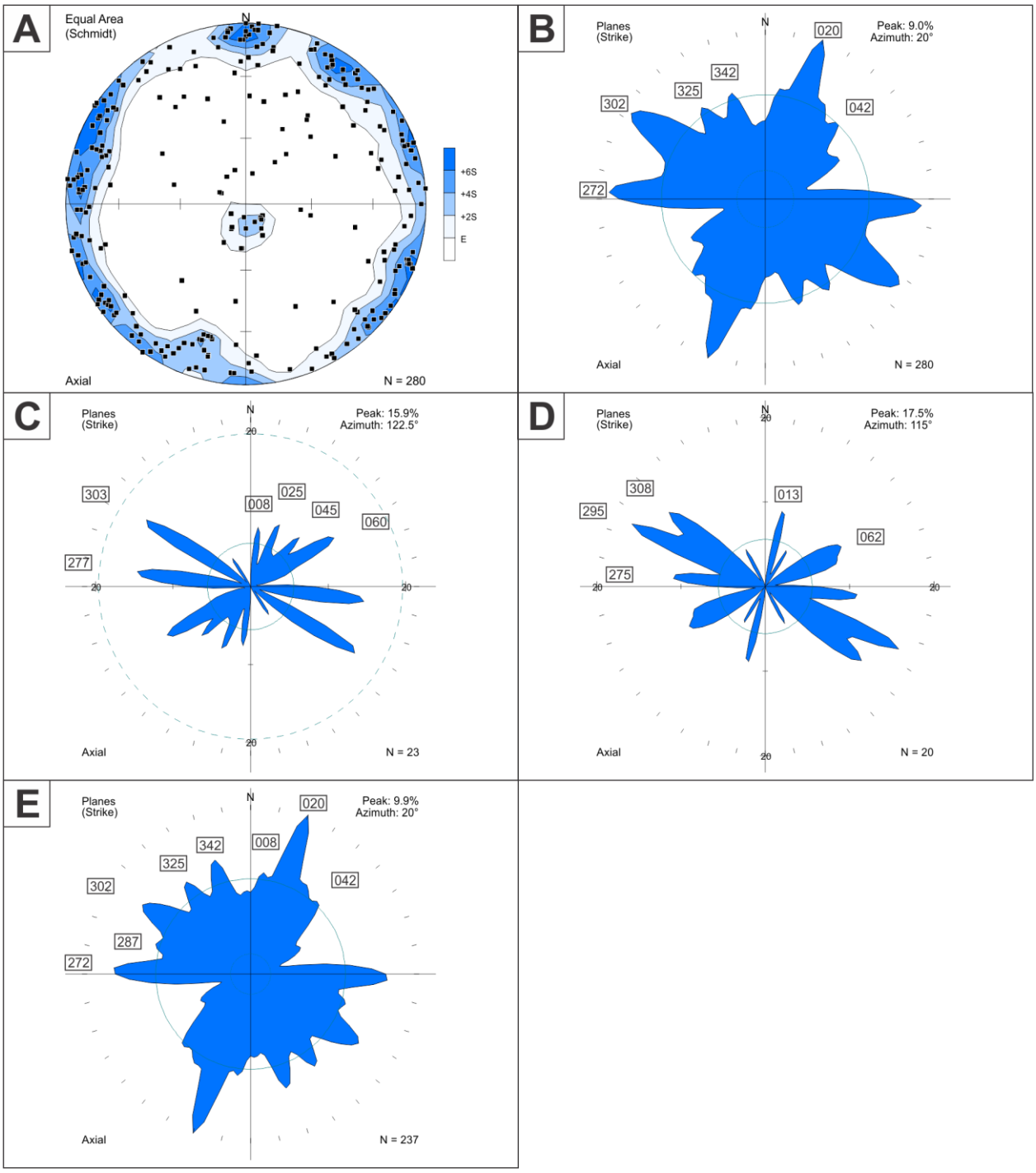

Figure 5.1.13: Quetico Area – Joint Orientation Data

A: All joints displayed as equal area lower hemisphere stereonet plot of poles to planes. (n=280).
B: All joints displayed as rose diagram of trends of planes with orientation of all peaks greater than the expected value E (n=280).
C: All joints with a dip ≤ 30 degrees displayed as rose diagram of trends of planes (n=23).
D: All joints with a dip between 31 - 60 degrees displayed as rose diagram of trends of planes (n=20).
E: All joints with a dip > 60 degrees displayed as rose diagram of trends of planes (n=237).

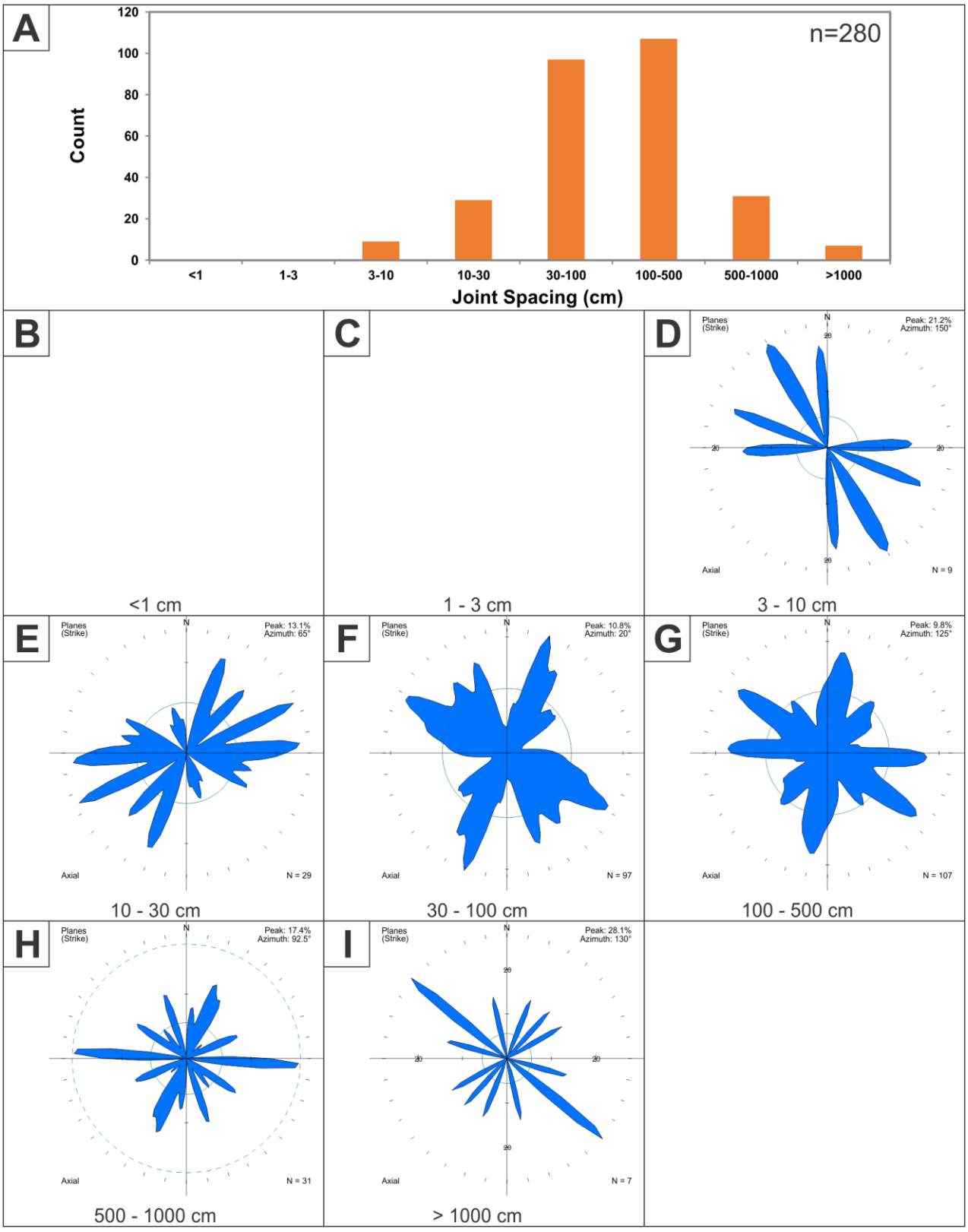

Figure 5.1.14: Quetico Area – Joint Spacing Summary

A: Histogram showing frequency distribution of joint spacing for all orientations and rock types (n=280).
B – I: Joints with the given joint spacing displayed as rose diagram of trends of planes. Any missing figures indicate no joints with that spacing were measured in this area.

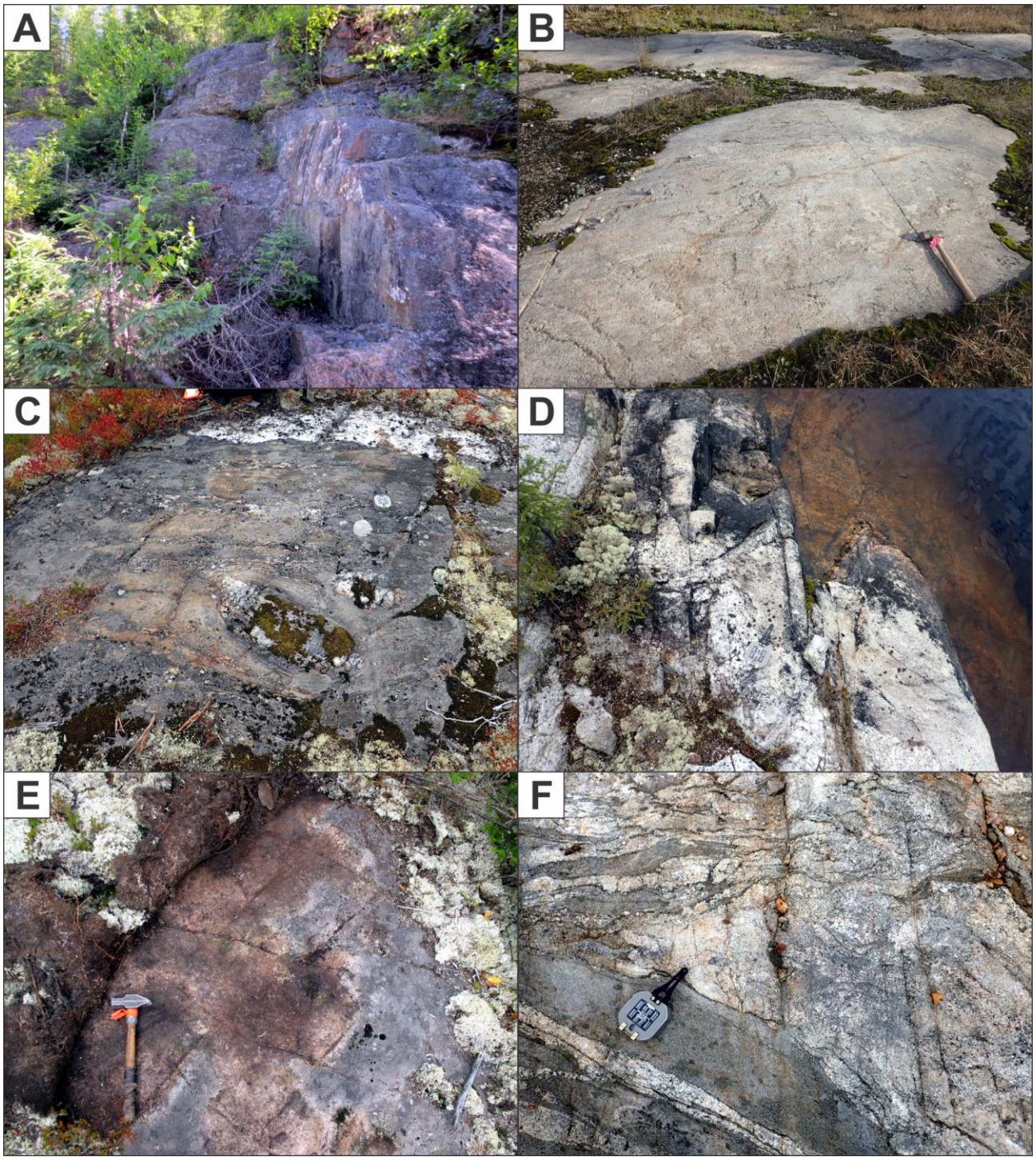

Figure 5.1.15: Quetico Area – Field Examples of Joints

A: Example of sub horizontal joint set with wide spacing cutting granite (Stn 16JK0093, looking S, no scale).
B: Example of wide joint spacing in granite (Stn 16BH0286, looking SE, hammer for scale).
C: Example of moderate joint spacing in migmatitic metasedimentary rock (Stn 16BH0131, looking N, compass for scale).
D: Example of tight joint spacing in granite (Stn 16BH0052, looking NW, compass for scale).
E: Example of multiple joint sets cutting granite (Stn 16CN0041, looking N, hammer for scale).
F: Preferential development of joints in intrusive leucosome compared to host migmatitic metasedimentary rock (Stn 16BH0266, looking NW, compass for scale).

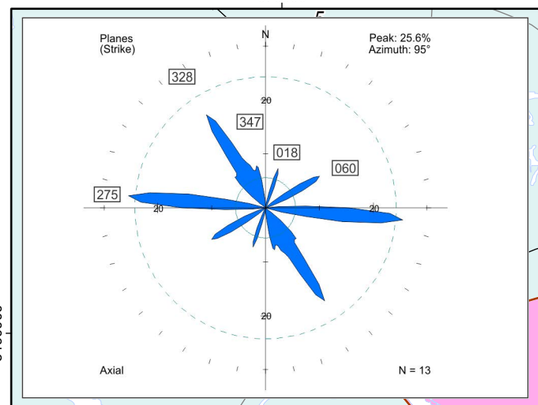

570000 580000 590000

5490000

5480000

N

11

CARAMAT INDUSTRIAL RD

Lauri L.

Stilwell Lake

7

HARKNESS ROAD

BISHOP LAKE ROAD

Bishop Lake

Anthony L.

White Otter R.

13

84 78 76 88 82 4 70 58 76 84 27 81 86 21 86

LEGEND

- Withdrawal Area
- Main Road
- Local Road
- Railway
- Waterbody
- Observation - Outcrop (76)
- Observation - Overburden (18)
- Fault - Sinistral (6)
- Fault - Strike (1)
- Fault - Unknown (7)
- Slickenline (3)

Bedrock Geology

- Geological Boundary
- Mapped Fault
- 13: Granite-granodiorite
- 11: Granite-granodiorite
- 7: Ultramafic plutonic rocks
- 5: Metasedimentary rocks

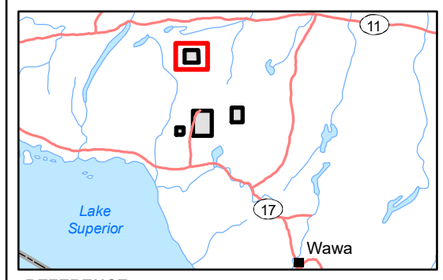

REFERENCE

Base Data: Land Information Ontario (obtained 2015); CanVec Topography (obtained 2015)

Bedrock Geology: MRD 126-REV1 (Ontario Geological Survey, 2011); Ontario Geological Survey Map 2665 (Santaguida, 2001); Map 2666 (Santaquida, 2001); Map 2667 (Johns, McIlraith and Stott, 2003); Map 2668 (Johns and McIlraith, 2003)

0 2 km

srk consulting

PROJECT
DETAILED MAPPING REPORT
Manitouwadge Area, Ontario

TITLE
Quetico Area Faults

DESIGN	KR	02 SEP 2014	**Figure 5.1.16**	REVISION 4
GIS	JA	02 AUG 2017		UTM ZONE 16N
CHECK	CN	02 AUG 2017		NAD 1983
REVIEW	JPS	02 AUG 2017		1:80,000

File: SRK_NWMO_ManStudy_AreaA_Fig5.1.16

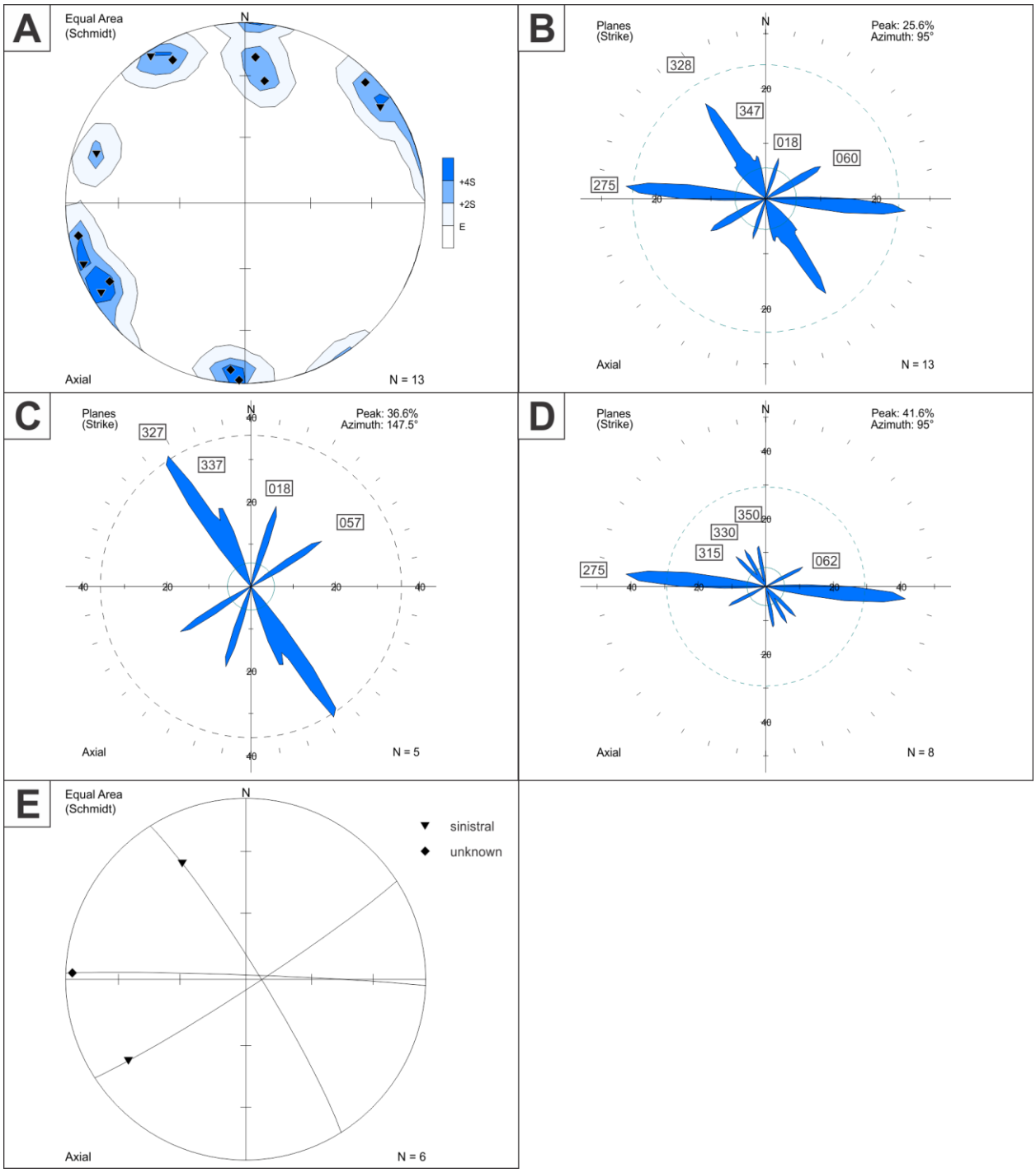

Figure 5.1.17: Quetico Area – Fault Orientation Data

A: All faults with measured dips displayed as equal area lower hemisphere stereonet plot of poles to planes. Sinistral faults: filled inverted triangles (n=5). Other or unknown movement sense faults: filled diamond (n=8).

B: All faults with measured dips displayed as rose diagram of trends of planes with orientation of all peaks greater than the expected value E (n=13).

C: Sinistral faults with measured dips displayed as rose diagram of trends of planes (n=5).

D: Other or unknown movement sense faults displayed as rose diagram of trends of planes (n=8).

E: Slickenline data displayed as equal area lower hemisphere stereonet plot of lineation points and great circles of the respective faults on which they were measured. Lineation plotted as rake calculated from measured trend and plunge.

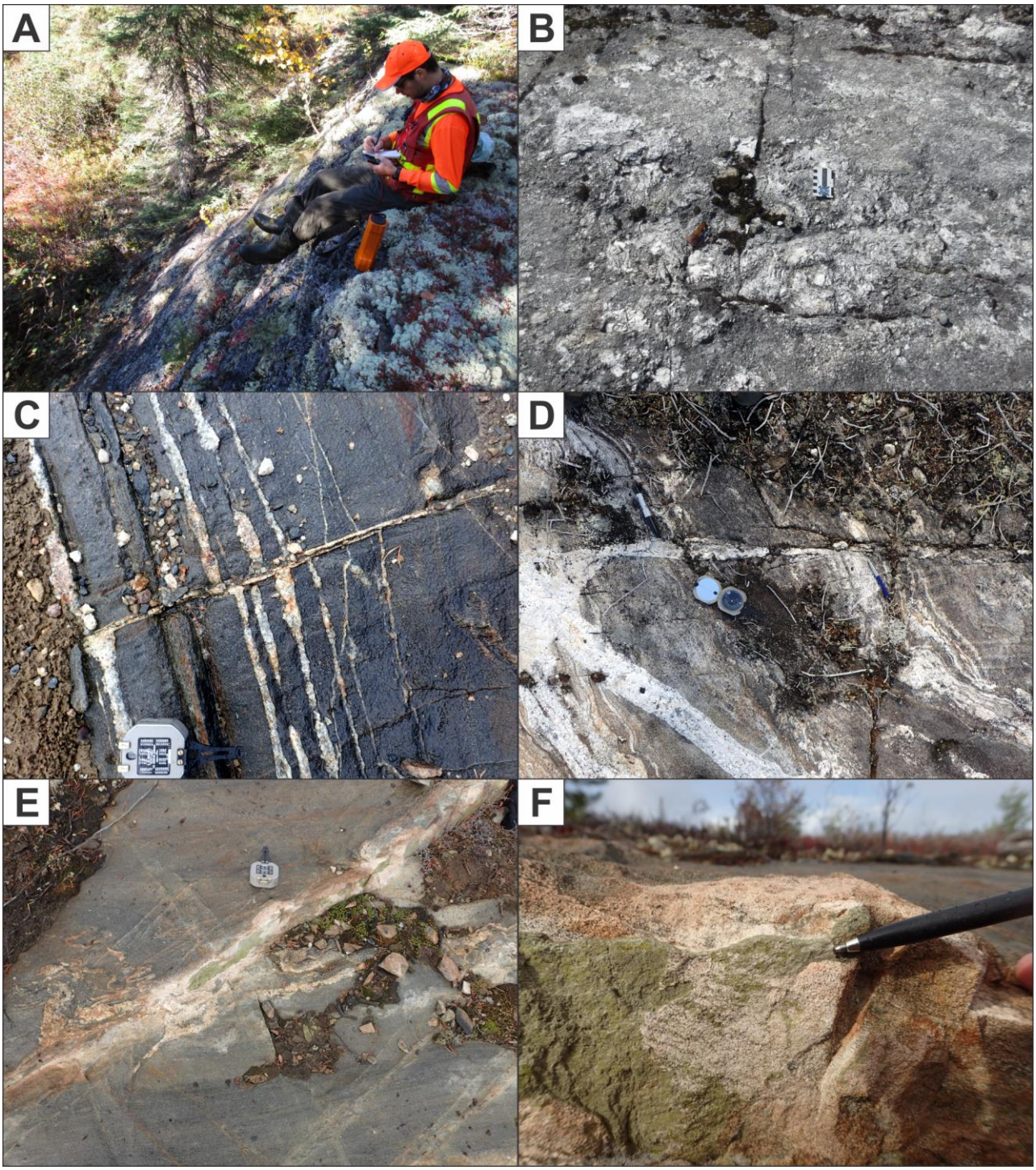

Figure 5.1.18: Quetico Area – Field Examples of Faults

A: E-striking, moderately S-dipping fault scarp coincident with surficial lineament (Stn 16JK0221, looking W, person for scale).
B: Discrete, NW-trending, right stepping, en echelon fault (Stn 16JK0094, looking NW, card for scale).
C: Discrete, NNW-trending, sinistral strike-separation fault (Stn 16BH0269, looking W, compass for scale).
D: Discrete, NW-trending, sinistral strike-separation fault filled by quartz vein (Stn 16BH0474, looking NW, compass for scale).
E: Epidote, hematite and bleaching alteration along oblique dominantly sinistral fault (Stn 16BH0268, looking N, compass for scale).
F: Slickenlines and steps indicate sinistral-oblique slip on fault (Stn 16BH0268, looking NW, pen for scale).

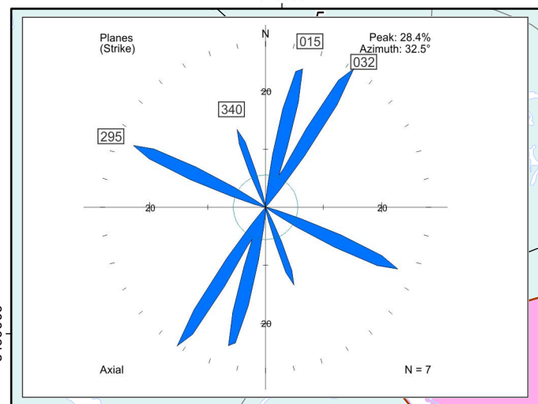

570000 580000 590000

5490000

5480000

11

CARAMAT INDUSTRIAL RD

Lauri L.

Stilwell Lake

7

HARKNESS ROAD

72

53 70 85 77 59

67

Bishop Lake

BISHOP LAKE ROAD

Anthony L.

White Otter R.

13

N

LEGEND

- Withdrawal Area
- Main Road
- Local Road
- Railway
- Waterbody
- Observation - Outcrop (81)
- Observation - Overburden (18)
- Extension Vein (5)
- Shear Vein (2)

Bedrock Geology

- Geological Boundary
- Mapped Fault
- 13: Granite-granodiorite
- 11: Granite-granodiorite
- 7: Ultramafic plutonic rocks
- 5: Metasedimentary rocks

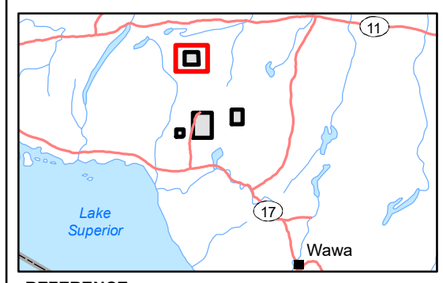

REFERENCE

Base Data: Land Information Ontario (obtained 2015); CanVec Topography (obtained 2015)

Bedrock Geology: MRD 126-REV1 (Ontario Geological Survey, 2011); Ontario Geological Survey Map 2665 (Santaguida, 2001); Map 2666 (Santaguida, 2001); Map 2667 (Johns, McIlraith and Stott, 2003); Map 2668 (Johns and McIlraith, 2003)

0 2 km

srk consulting

PROJECT
DETAILED MAPPING REPORT
Manitouwadge Area, Ontario

TITLE
Quetico Area Veins

DESIGN	KR	02 SEP 2014	**Figure 5.1.19**	REVISION 4
GIS	JA	31 JAN 2017		UTM ZONE 16N
CHECK	CN	31 JAN 2017		NAD 1983
REVIEW	JPS	31 JAN 2017		1:80,000

File: SRK_NWMO_ManStudy_AreaA_Fig5.1.19

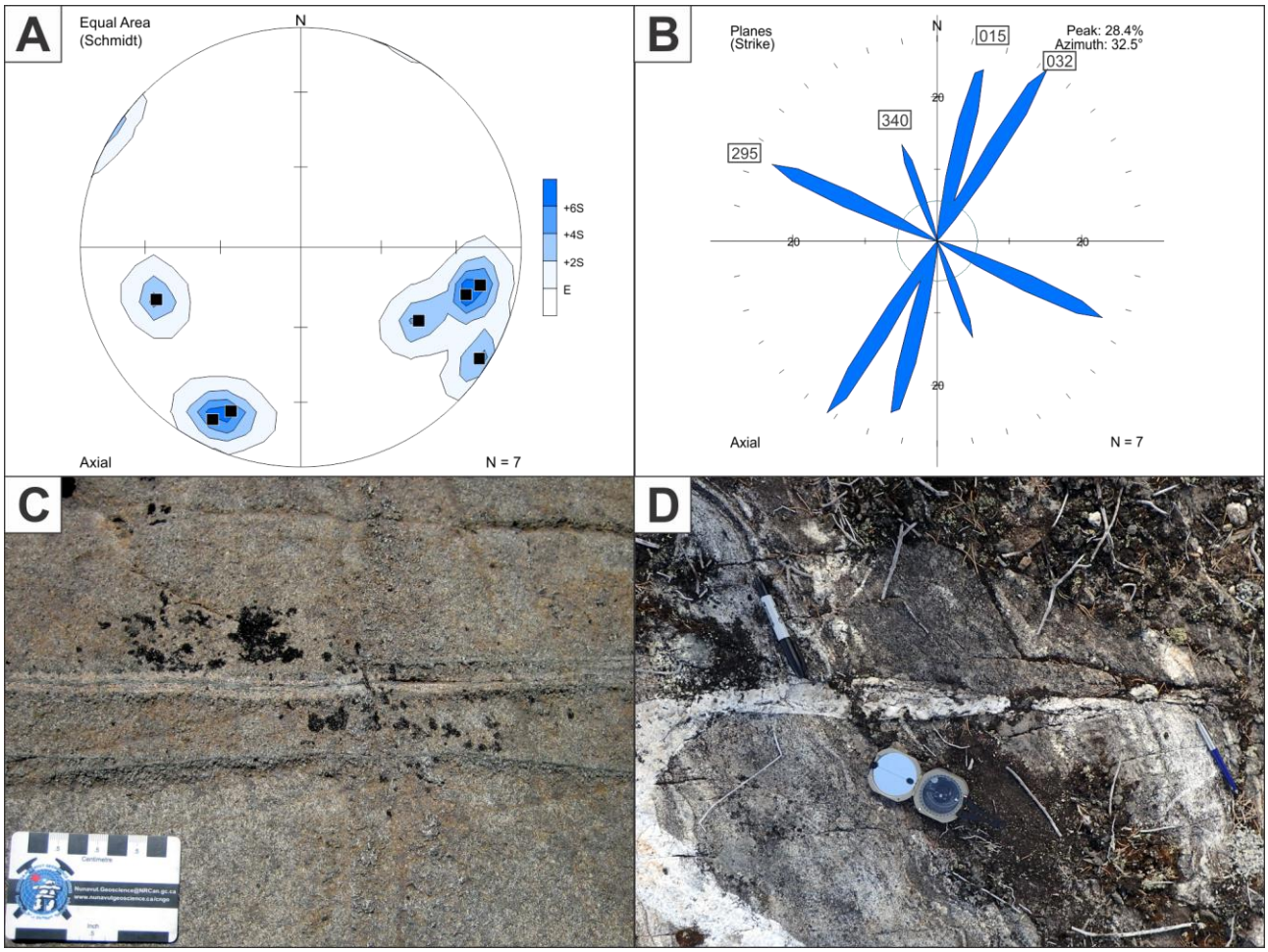

Figure 5.1.20: Quetico Area – Vein Orientation Data and Field Examples

A: All veins displayed as equal area lower hemisphere stereonet plot of poles to planes. (n=7).
B: All veins displayed as rose diagram of trends of planes with orientation of all peaks greater than the expected value E (n=7).
C: Narrow, NNW-trending chlorite veinlet (Stn 16JK0138, looking SW, card for scale).
D: NW-trending quartz vein filling discrete fault (Stn 16BH0474, looking NW, compass for scale).

570000
580000
590000
5490000
5480000
N
5
11
13
7
Eino L.
Lauri L.
Stilwell Lake
Bishop Lake
Anthony L.
White Otter R.
CARAMAT INDUSTRIAL RD
HARKNESS ROAD
BISHOP LAKE ROAD

LEGEND

- Withdrawal Area
- Main Road
- Local Road
- Railway
- Waterbody
- Observation - Outcrop (88)
- Observation - Overburden (18)
- Alteration - Hematite
- Alteration - Quartz
- Alteration - Epidote
- Alteration - Chlorite

Bedrock Geology

- Geological Boundary
- Mapped Fault
- 13: Granite-granodiorite
- 11: Granite-granodiorite
- 7: Ultramafic plutonic rocks
- 5: Metasedimentary rocks

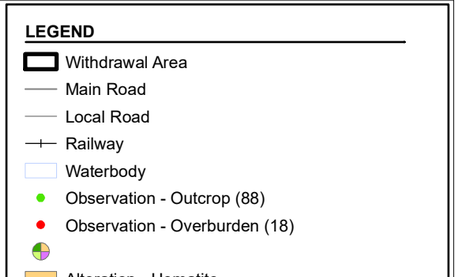

REFERENCE

Base Data: Land Information Ontario (obtained 2015);
CanVec Topography (obtained 2015)

Bedrock Geology: MRD 126-REV1 (Ontario Geological Survey, 2011);
Ontario Geological Survey Map 2665 (Santaguida, 2001);
Map 2666 (Santaguida, 2001);
Map 2667 (Johns, McIlraith and Stott, 2003);
Map 2668 (Johns and McIlraith, 2003)

0 2 km

srk consulting

PROJECT
DETAILED MAPPING REPORT
Manitouwadge Area, Ontario

TITLE
Quetico Area
Secondary Minerals and Alteration

DESIGN	KR	02 SEP 2014	**Figure 5.1.21**	REVISION 3
GIS	JA	31 JAN 2017		UTM ZONE 16N
CHECK	CN	31 JAN 2017		NAD 1983
REVIEW	JPS	31 JAN 2017		1:80,000

File: SRK_NWMO_ManStudy_AreaA_Fig5.1.21

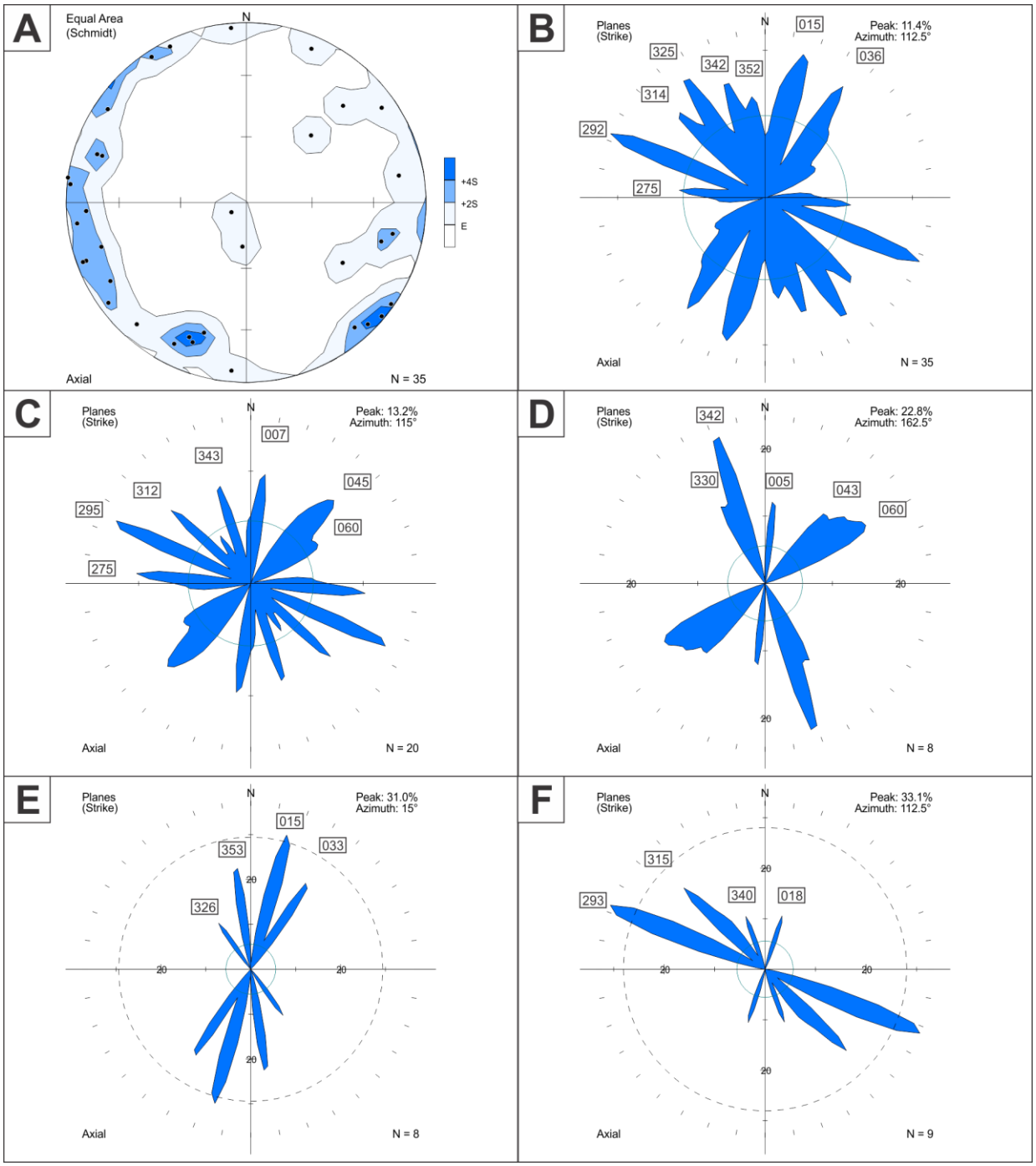

Figure 5.1.22: Quetico Area – Secondary Minerals and Alteration Orientation Data

A: All structures with visible alteration displayed as equal area lower hemisphere stereonet plot of poles to planes. (n=35).

B: All structures with visible alteration displayed as rose diagram of trends of planes with orientation of all peaks greater than the expected value E (n=35).

C: All structures with visible hematite alteration displayed as rose diagram of trends of planes with orientation of all peaks greater than the expected value E (n=20).

D: All structures with visible epidote alteration displayed as rose diagram of trends of planes with orientation of all peaks greater than the expected value E (n=8).

E: All structures with visible quartz alteration displayed as rose diagram of trends of planes with orientation of all peaks greater than the expected value E (n=8).

F: All structures with visible chlorite alteration displayed as rose diagram of trends of planes with orientation of all peaks greater than the expected value E (n=9).

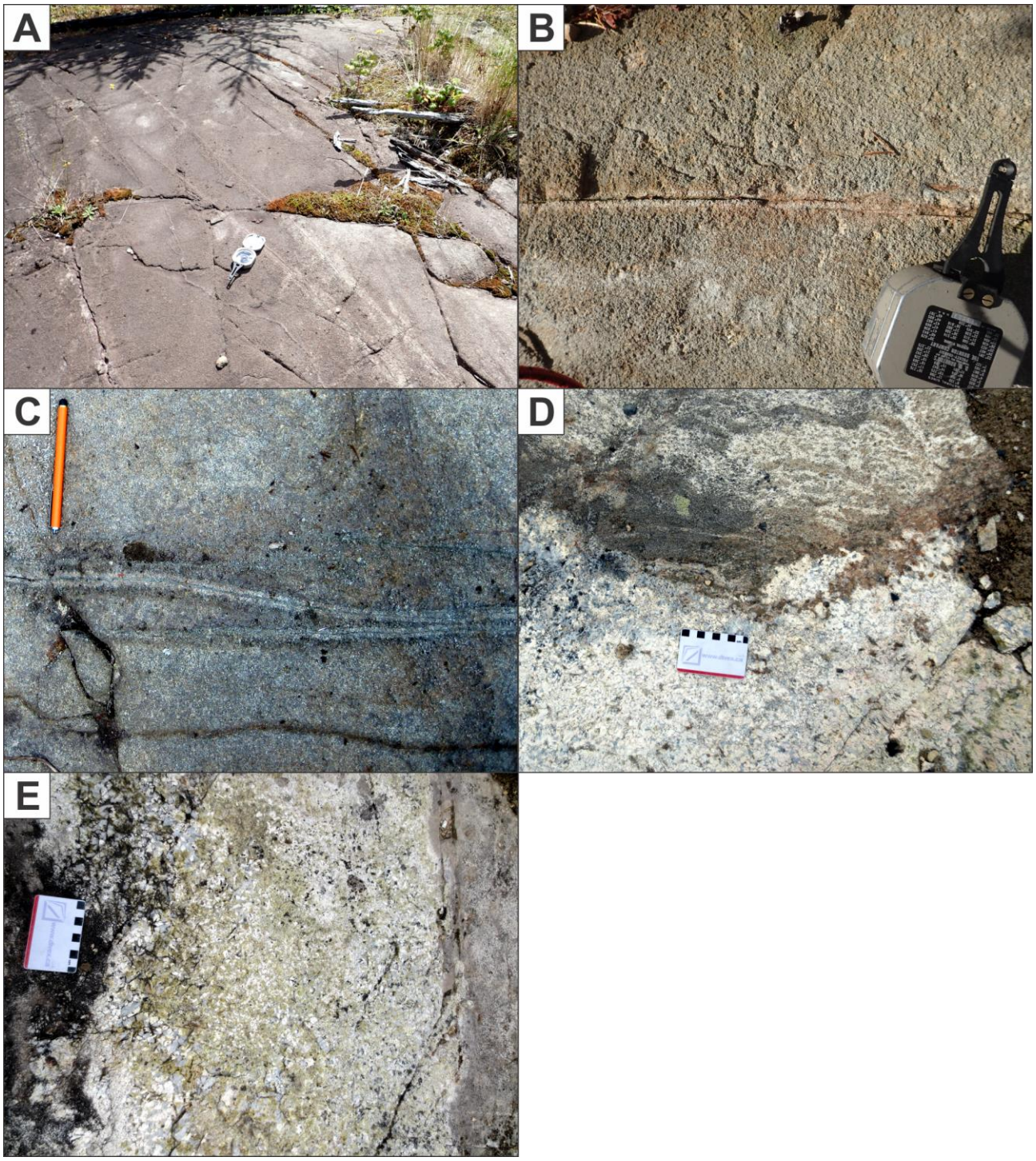

Figure 5.1.23: Quetico Area – Field Examples of Secondary Minerals and Alteration

A: Narrow, NW-trending chlorite-epidote veinlets with bleached margins cutting a Marathon dyke (Stn 16BH0270, looking SE, compass for scale).
B: Narrow, NE-trending epidote-hematite veinlets with bleached margins cutting a Matachewan dyke (Stn 16BH0270, looking NW, compass for scale).
C: Narrow, NNW-trending chlorite-hematite veinlet and bleached margins (Stn 16JK0138, looking NE, pen for scale).
D: Hematite and epidote alteration focussed at contact between granite and migmatitic metasedimentary rock (Stn 16JK0106, looking S, card for scale).
E: Pervasive epidote alteration in granite (Stn 16JK0106, looking E, card for scale).

560000
570000
580000
5430000
5420000
N
FOURBAY LAKE PLUTON
GAFFHOOK LAKE ROAD
BAREHEAD ROAD
Barehead L.
Fourbay Lake
Cirrus L.
Lake Superior
614
11
17
Wawa
16CN0105
16CN0104
16JK0126
16CN0033
16CN0032
16BH0006
16JK0130
16JK0127
16JK0128
16BH0005
16JK0129
16CN0065
16CN0063
16CN0034
16JK0214
16CN0036
16CN0066
16CN0062
16BH0004
16CN0061
16CN0035
16JK0005
16CN0064
16BH0057
16CN0002
16CN0103
16CN0059
16JK0008
16JK0007
16CN0057
16BH0210
16JK0002
16CN0102
16CN0058
16JK0017
16CN0101
16BH0107
16BH0110
16JK0006
16BH0056
16BH0104
16BH0209
16JK0018
16CN0056
16BH0178
16BH0105
16BH0208
16BH0179
16JK0022
16JK0143
16BH0111
16BH0186
16JK0019
16BH0185
16BH0184
16JK0213
16JK0147
16JK0144
16BH0183
16BH0182
16BH0151
16JK0145
16JK0020
16JK0146
16BH0150
16JK0021
16JK0152
16JK0211
16JK0212
16BH0149
16JK0149
16JK0151
16JK0150
16BH0148
16JK0153
16JK0154
8
9
13
g

LEGEND

- Withdrawal Area
- Main Road
- Local Road
- Waterbody
- Observation - Outcrop (68)
- Observation - Overburden (8)
- Predicted Outcrop

Bedrock Geology

- Geological Boundary
- Mapped Fault
- Fold (syncline)
- Fold (anticline)
- 13: Granite-granodiorite
- 9: Gneissic tonalite suite
- 8: Gabbro
- 3: Felsic and intermediate metavolcanic rocks
- 2: Mafic metavolcanic Rocks
- Iron Formation

REFERENCE

Base Data: Land Information Ontario (obtained 2015);
CanVec Topography (obtained 2015)

Bedrock Geology: MRD 126-REV1 (Ontario Geological Survey, 2011);
Ontario Geological Survey Map 2665 (Santaguida, 2001);
Map 2666 (Santaguida, 2001);
Map 2667 (Johns, McIlraith and Stott, 2003);
Map 2668 (Johns and McIlraith, 2003)

0 2 km

srk consulting

PROJECT
DETAILED MAPPING REPORT
Manitouwadge Area, Ontario

TITLE
Fourbay Lake Pluton Area
Mapping Observation Locations

DESIGN	KR	02 SEP 2014	**Figure 5.2.1**	REVISION 2
GIS	JA	02 AUG 2017		UTM ZONE 16N
CHECK	CN	02 AUG 2017		NAD 1983
REVIEW	JPS	02 AUG 2017		1:80,000

File: SRK_NWMO_ManStudy_AreaB_Fig5.2.1

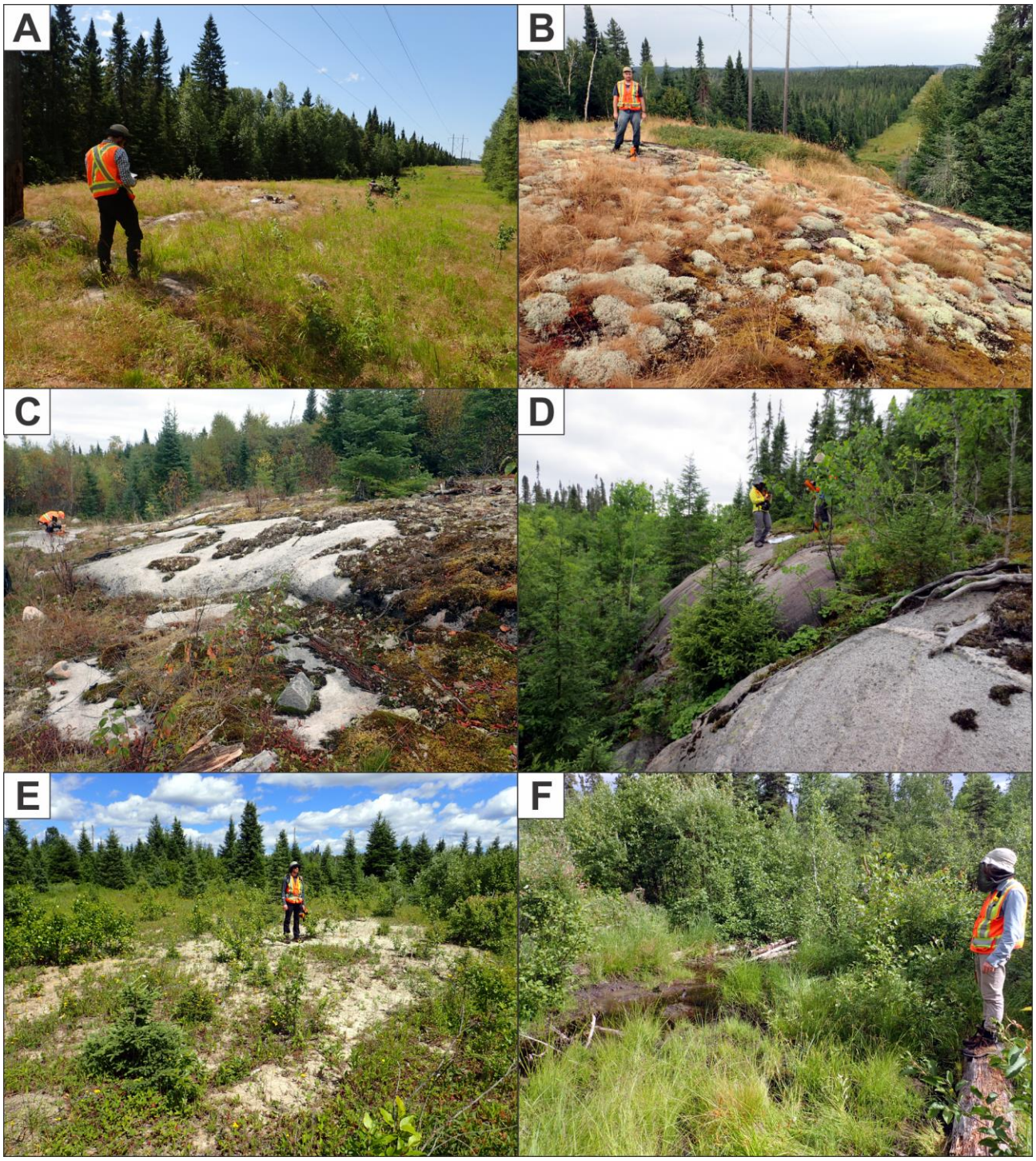

Figure 5.2.2: Fourbay Lake Pluton Area – Field Examples of Accessibility and Bedrock Exposure

A: ATV trail along powerline provides access across area (Stn 16BH0111, looking S, person for scale).
B: Rugged topography adjacent to well-defined lineaments (Stn 16BH0151, looking N, person for scale).
C: Well-exposed, clean outcrop of granodiorite (Stn 16BH0209, looking N, person for scale).
D: Representative, high rounded outcrop of diorite (Stn 16JK0002, looking S, person for scale).
E: Light coloured, exposed clay resembles outcrop on aerial photographs (16BH0005, looking NE, person for scale).
F: Streams in topographic lows cutting clay overburden inhibit access (Stn 16BH0106, looking SE, person for scale).

560000
570000
580000
5430000
5420000
N
FOURBAY LAKE PLUTON
GAFFHOOK LAKE ROAD
BAREHEAD ROAD
BAREHEAD ROAD
Barehead L.
614
Fourbay Lake
Cirrus L.
8
9
13
9
Lake Superior
11
17
Wawa

LEGEND

- Withdrawal Area
- Main Road
- Local Road
- Waterbody
- Observation - Outcrop

Bedrock Geology

- Geological Boundary
- Mapped Fault
- Fold (syncline)
- Fold (anticline)
- 13: Granite-granodiorite
- 9: Gneissic tonalite suite
- 8: Gabbro
- 3: Felsic and intermediate metavolcanic rocks
- 2: Mafic metavolcanic Rocks

Main Lithology

- Diorite (26)
- Granodiorite (41)

REFERENCE

Base Data: Land Information Ontario (obtained 2015);
CanVec Topography (obtained 2015)

Bedrock Geology: MRD 126-REV1 (Ontario Geological Survey, 2011);
Ontario Geological Survey Map 2665 (Santaguida, 2001);
Map 2666 (Santaguida, 2001);
Map 2667 (Johns, McIlraith and Stott, 2003);
Map 2668 (Johns and McIlraith, 2003)

0 2 km

srk consulting

PROJECT
DETAILED MAPPING REPORT
Manitouwadge Area, Ontario

TITLE
Fourbay Lake Pluton Area
Main Lithological Units

DESIGN	KR	02 SEP 2014	**Figure 5.2.3**	REVISION 2
GIS	JA	02 AUG 2017		UTM ZONE 16N
CHECK	CN	02 AUG 2017		NAD 1983
REVIEW	JPS	02 AUG 2017		1:80,000

File: SRK_NWMO_ManStudy_AreaB_Fig5.2.3

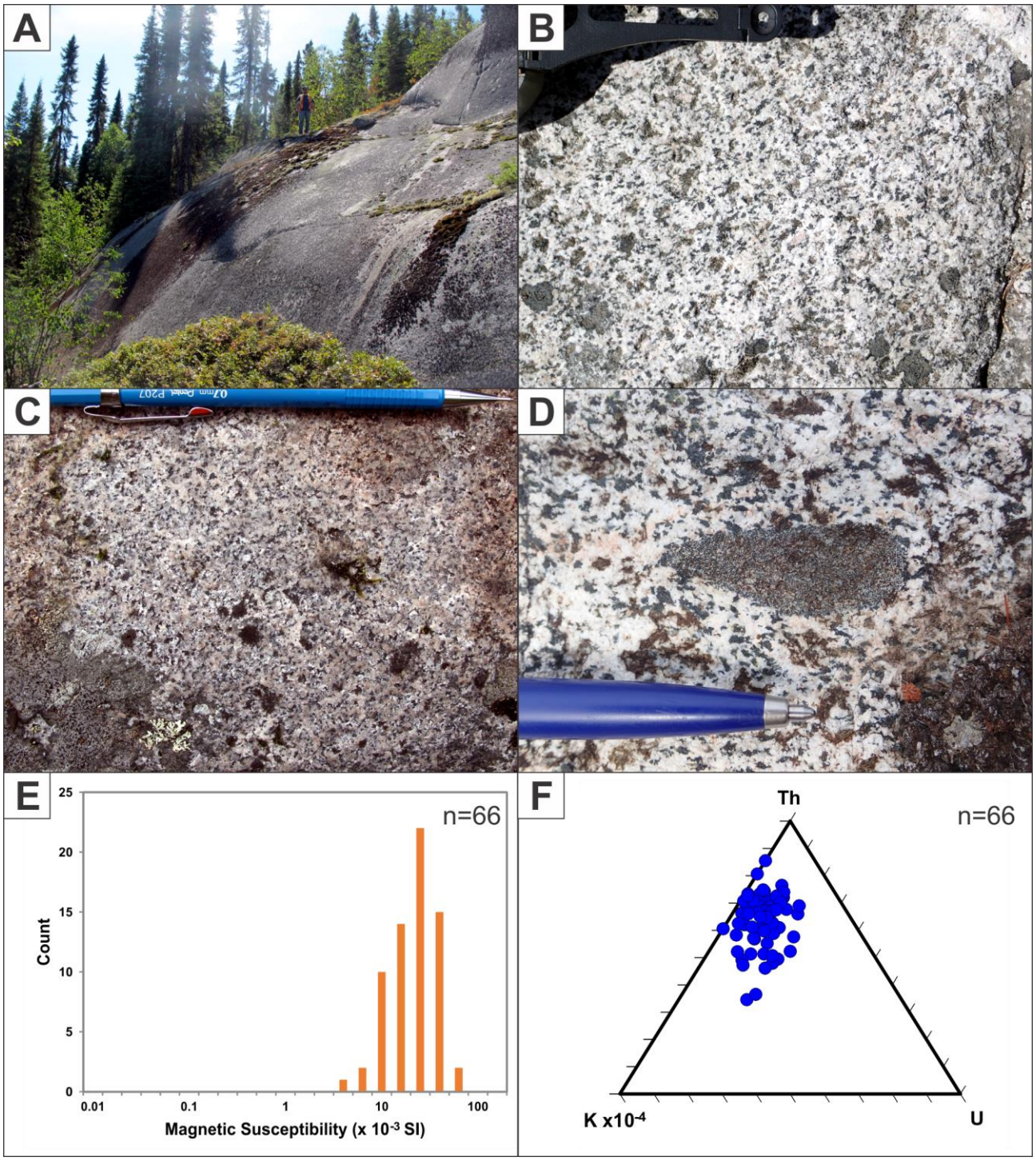

Figure 5.2.4: Fourbay Lake Pluton Area Field Examples of Main Lithology: Granodiorite to Diorite

A: Fourbay Pluton granodiorite to diorite at outcrop scale (Stn 16CN0059, looking SW, person for scale).
B: Close-up of granodiorite showing mineral composition and texture (Stn 16BH0004, looking W, compass for scale).
C: Close-up of diorite showing mineral composition and texture (Stn 16CN0035, looking NW, compass for scale).
D: Centimetre scale mafic xenolith in diorite (Stn 16BH0056, looking W, compass for scale).
E: Logarithmic histogram plot of magnetic susceptibility for granodiorite to diorite.
F: Ternary plot of gamma ray spectrometer data for granodiorite to diorite.

560000
570000
580000
5430000
5420000
N
FOURBAY LAKE PLUTON
GAFFHOOK LAKE ROAD
BAREHEAD ROAD
BAREHEAD ROAD
Barehead L.
614
Fourbay Lake
Cirrus L.
8
9
13
9

LEGEND

- Withdrawal Area
- Main Road
- Local Road
- Waterbody
- Observation - Outcrop

Bedrock Geology

- Geological Boundary
- Mapped Fault
- Fold (syncline)
- Fold (anticline)
- 13: Granite-granodiorite
- 9: Gneissic tonalite suite
- 8: Gabbro
- 3: Felsic and intermediate metavolcanic rocks
- 2: Mafic metavolcanic Rocks
- Iron Formation

Minor Lithology

- Granite (5)
- Tonalite (1)

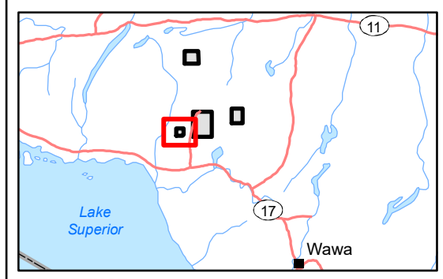

REFERENCE

Base Data: Land Information Ontario (obtained 2015); CanVec Topography (obtained 2015)

Bedrock Geology: MRD 126-REV1 (Ontario Geological Survey, 2011); Ontario Geological Survey Map 2665 (Santaguida, 2001); Map 2666 (Santaguida, 2001); Map 2667 (Johns, McIlraith and Stott, 2003); Map 2668 (Johns and McIlraith, 2003)

0 2 km

srk consulting

PROJECT
DETAILED MAPPING REPORT
Manitouwadge Area, Ontario

TITLE
Fourbay Lake Pluton Area
Minor Lithological Units

DESIGN	KR	02 SEP 2014	**Figure 5.2.5**	REVISION 2
GIS	JA	02 AUG 2017		UTM ZONE 16N
CHECK	CN	02 AUG 2017		NAD 1983
REVIEW	JPS	02 AUG 2017		1:80,000

File: SRK_NWMO_ManStudy_AreaB_Fig5.2.5

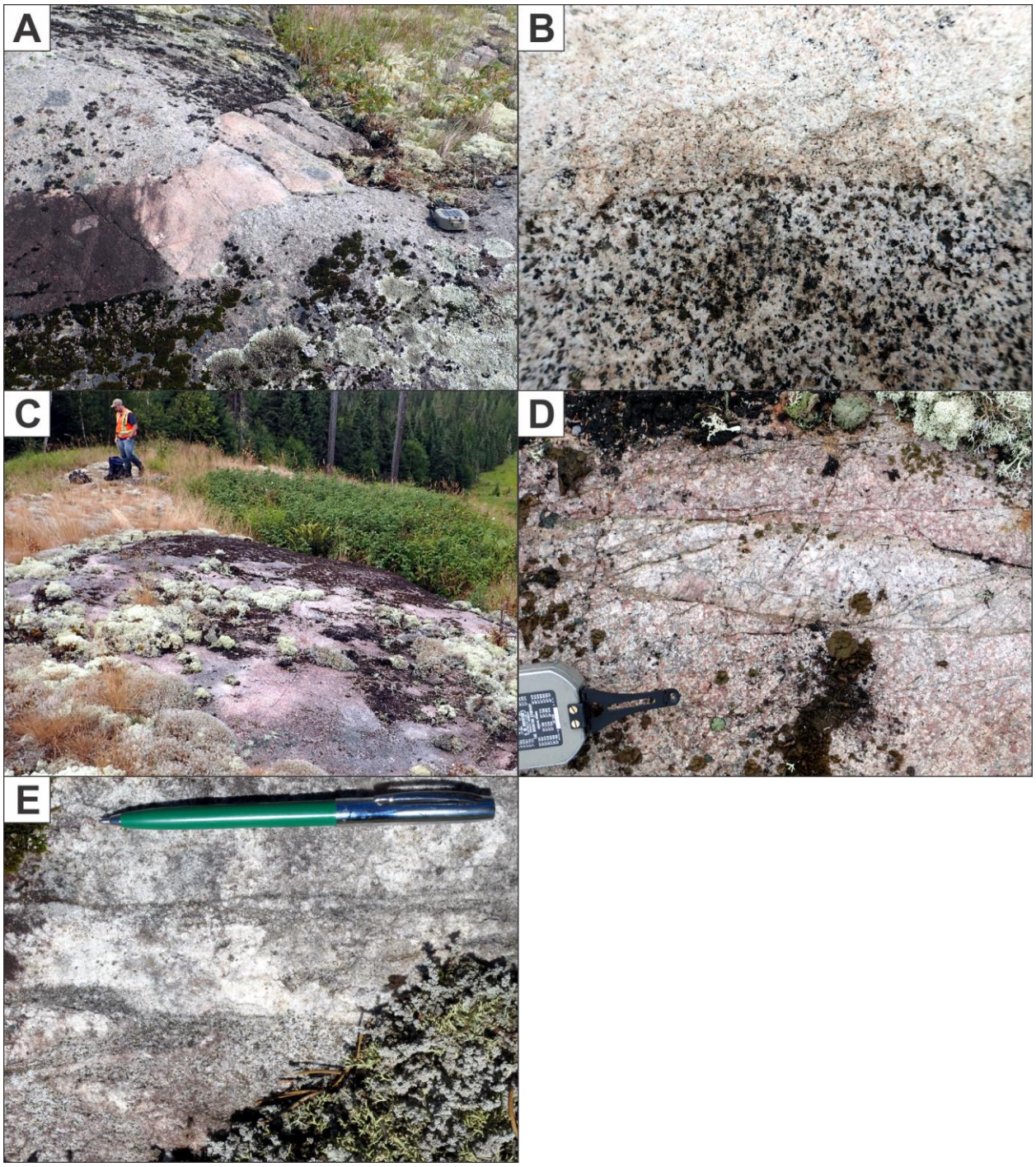

Figure 5.2.6: Fourbay Lake Pluton Area – Field Examples of Minor Lithological Units

A: Felsic dyke intruding Fourbay Pluton granodiorite (Stn 16BH0057, looking N, compass for scale).
B: Close-up of felsic dyke (upper part of photo) showing mineral composition and texture (Stn 16BH0105, looking NW, no scale, field of view is ~10cm across).
C: Rare, wider (>10m) intrusion of leucocratic, pink, coarse-grained to pegmatitic granite in foreground adjacent to typical granodiorite in small outcrop in background (Stn 16BH0151, looking N, person for scale).
D: Close-up of leucocratic, pink, coarse-grained to pegmatitic granite intrusion showing mineral composition and texture (Stn 16BH0151, looking W, compass for scale).
E: Foliated tonalite of Black-Pic batholith on eastern margin of the Fourbay Lake pluton (Stn 16JK0005, looking NW, pen for scale).

560000 570000 580000

5430000 5420000

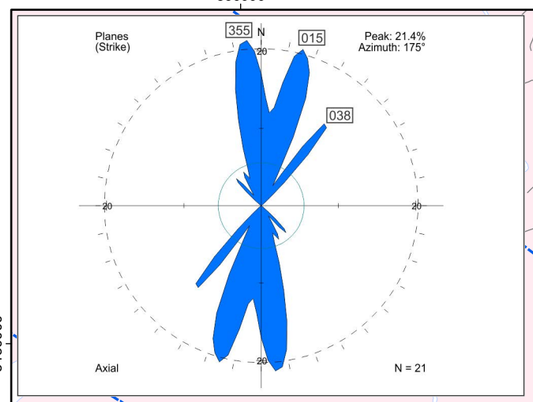

FOURBAY LAKE PLUTON

GAFFHOOK LAKE ROAD

BAREHEAD ROAD

BAREHEAD ROAD

Barehead L.

614

Fourbay Lake

Cirrus L.

8

9

13

9

N

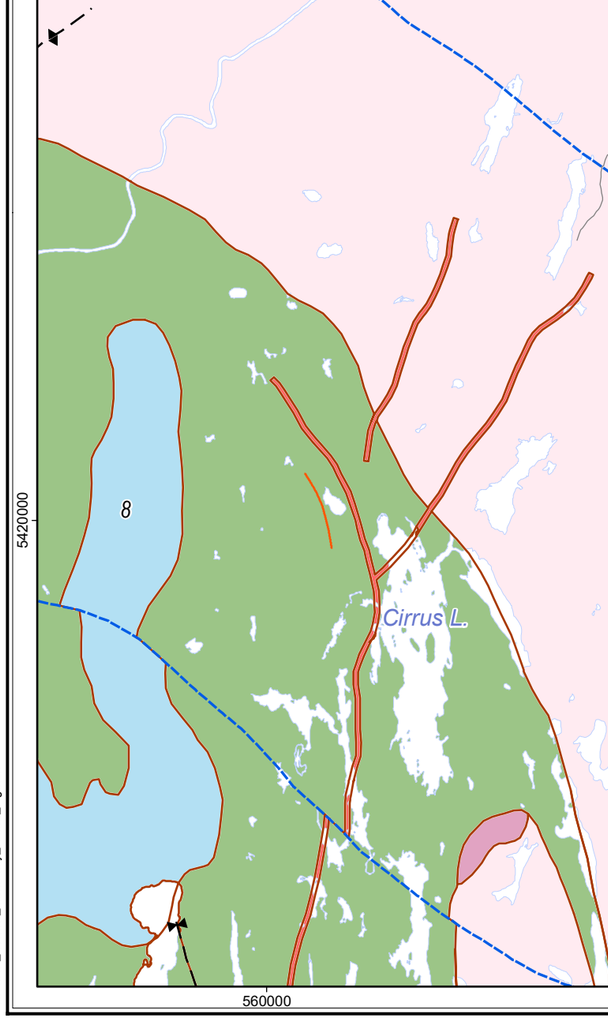

LEGEND

- Withdrawal Area
- Main Road
- Local Road
- Waterbody
- Observation - Outcrop (45)
- Observation - Overburden (8)
- Foliation (22)
- Mineral Lineation (2)

Bedrock Geology

- Geological Boundary
- Mapped Fault
- Fold (syncline)
- Fold (anticline)
- 13: Granite-granodiorite
- 9: Gneissic tonalite suite
- 8: Gabbro
- 3: Felsic and intermediate metavolcanic rocks
- 2: Mafic metavolcanic Rocks
- Iron Formation

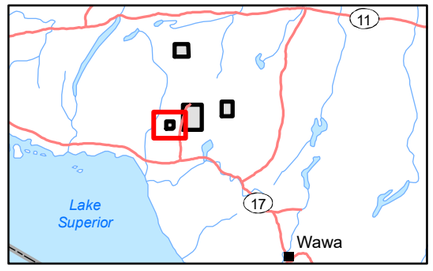

REFERENCE

Base Data: Land Information Ontario (obtained 2015);
CanVec Topography (obtained 2015)

Bedrock Geology: MRD 126-REV1 (Ontario Geological Survey, 2011);
Ontario Geological Survey Map 2665 (Santaguida, 2001);
Map 2666 (Santaguida, 2001);
Map 2667 (Johns, McIlraith and Stott, 2003);
Map 2668 (Johns and McIlraith, 2003)

0 2 km

srk consulting

PROJECT
DETAILED MAPPING REPORT
Manitouwadge Area, Ontario

TITLE
Fourbay Lake Pluton Area
Tectonic Foliation

DESIGN	KR	02 SEP 2014	**Figure 5.2.7**	REVISION 2
GIS	JA	02 AUG 2017		UTM ZONE 16N
CHECK	CN	02 AUG 2017		NAD 1983
REVIEW	JPS	02 AUG 2017		1:80,000

File: SRK_NWMO_ManStudy_AreaB_Fig5.2.7

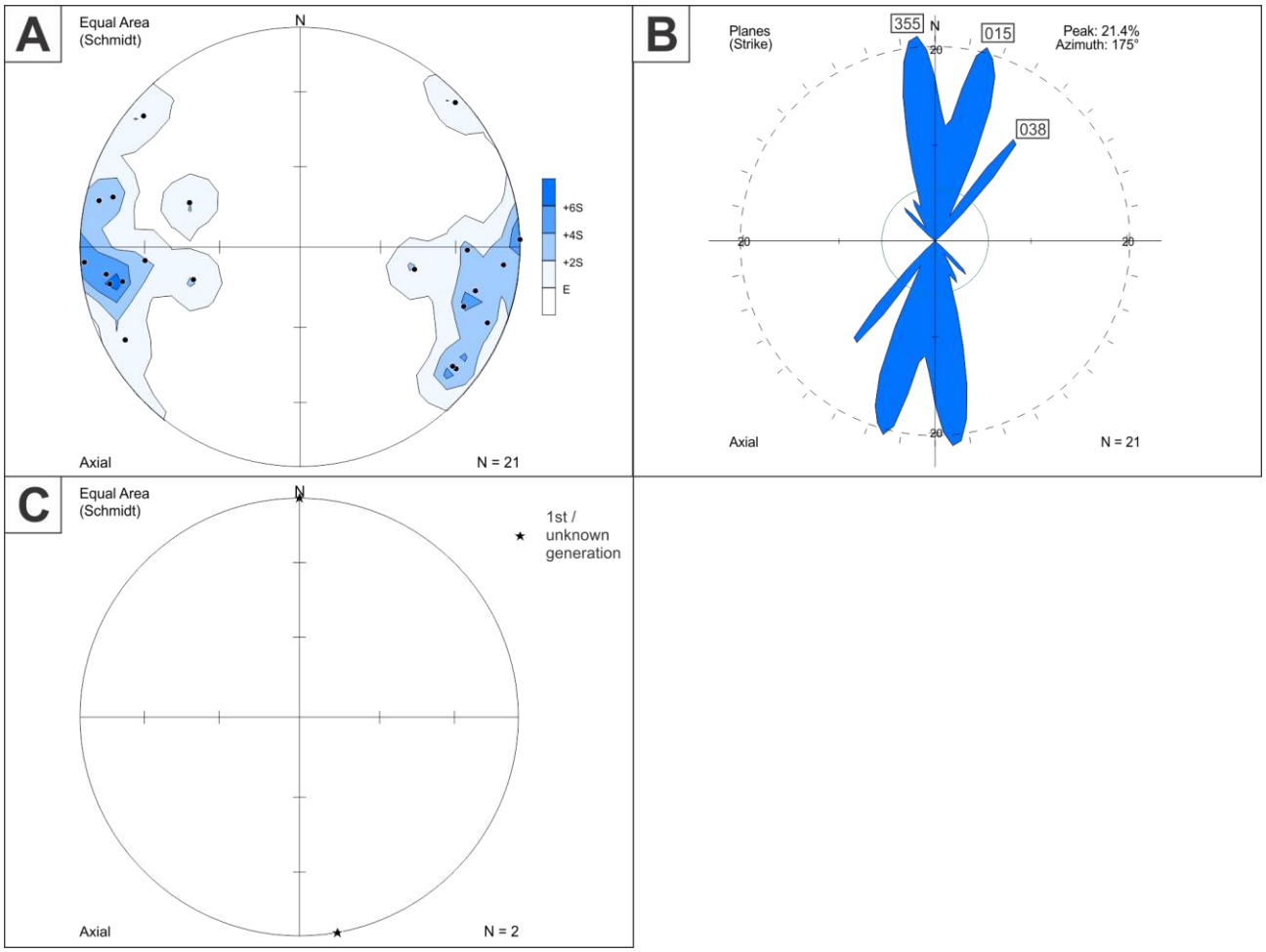

Figure 5.2.8: Fourbay Lake Pluton Area – Tectonic Foliation Orientation Data

A: All tectonic foliation displayed as equal area lower hemisphere stereonet plot of poles to planes (n=24).
B: All foliation displayed as rose diagram of trends of planes with orientation of all peaks greater than the expected value E (n=24).
C: All lineations displayed as equal area lower hemisphere stereonet plot (n=2). No foliation was evident at these stations.

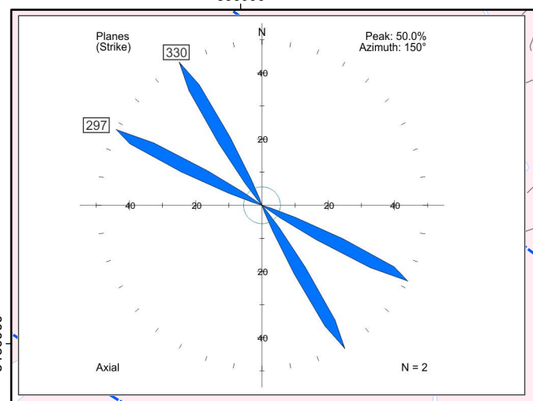

560000
570000
580000
5430000
5420000

FOURBAY LAKE PLUTON
GAFFHOOK LAKE ROAD
BAREHEAD ROAD
BAREHEAD ROAD
Barehead L.
614
Fourbay Lake
Cirrus L.
8
9
13
9
68
85

N

LEGEND

- Withdrawal Area
- Main Road
- Local Road
- Waterbody
- Observation - Outcrop (65)
- Observation - Overburden (8)
- Ductile Shear Zone - Sinistral (2)

Bedrock Geology

- Geological Boundary
- Fold (anticline)
- Fold (syncline)
- Mapped Fault
- 13: Granite-granodiorite
- 9: Gneissic tonalite suite
- 8: Gabbro
- 3: Felsic and intermediate metavolcanic rocks
- 2: Mafic metavolcanic Rocks
- Iron Formation

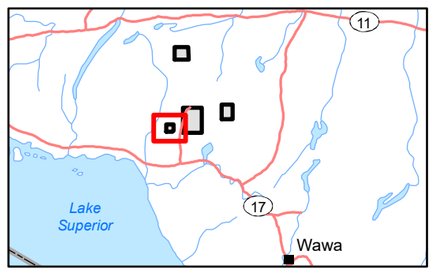

REFERENCE

Base Data: Land Information Ontario (obtained 2015);
CanVec Topography (obtained 2015)

Bedrock Geology: MRD 126-REV1 (Ontario Geological Survey, 2011);
Ontario Geological Survey Map 2665 (Santaguida, 2001);
Map 2666 (Santaguida, 2001);
Map 2667 (Johns, McIlraith and Stott, 2003);
Map 2668 (Johns and McIlraith, 2003)

0 2 km

srk consulting

PROJECT
DETAILED MAPPING REPORT
Manitouwadge Area, Ontario

TITLE
Fourbay Lake Pluton Area
Ductile and Brittle-Ductile Shear Zones

DESIGN	KR	02 SEP 2014	**Figure 5.2.9**	REVISION 2
GIS	JA	02 AUG 2017		UTM ZONE 16N
CHECK	CN	02 AUG 2017		NAD 1983
REVIEW	JPS	02 AUG 2017		1:80,000

File: SRK_NWMO_ManStudy_AreaB_Fig5.2.9

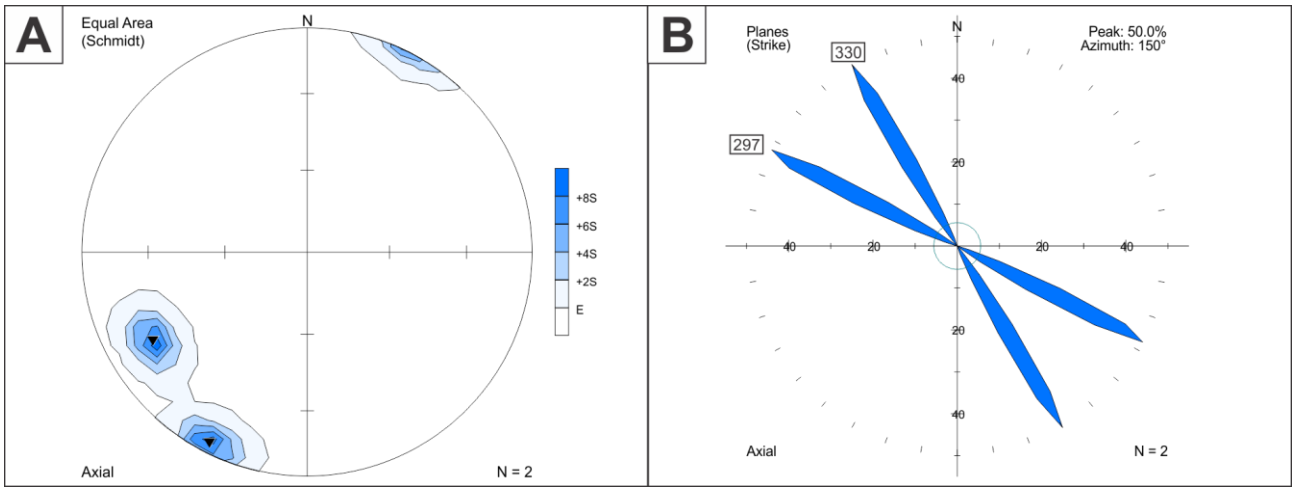

Figure 5.2.10: Fourbay Lake Pluton Area – Ductile and Brittle-Ductile Shear Zone Orientation Data

A: All ductile and brittle-ductile shear zones displayed as equal area lower hemisphere stereonet plot of poles to planes. Sinistral shear zones: filled inverted triangles (n=2).

B: All shear zones displayed as rose diagram of trends of planes with orientation of all peaks greater than the expected value E (n=2). Both mapped features are sinistral shear zones.

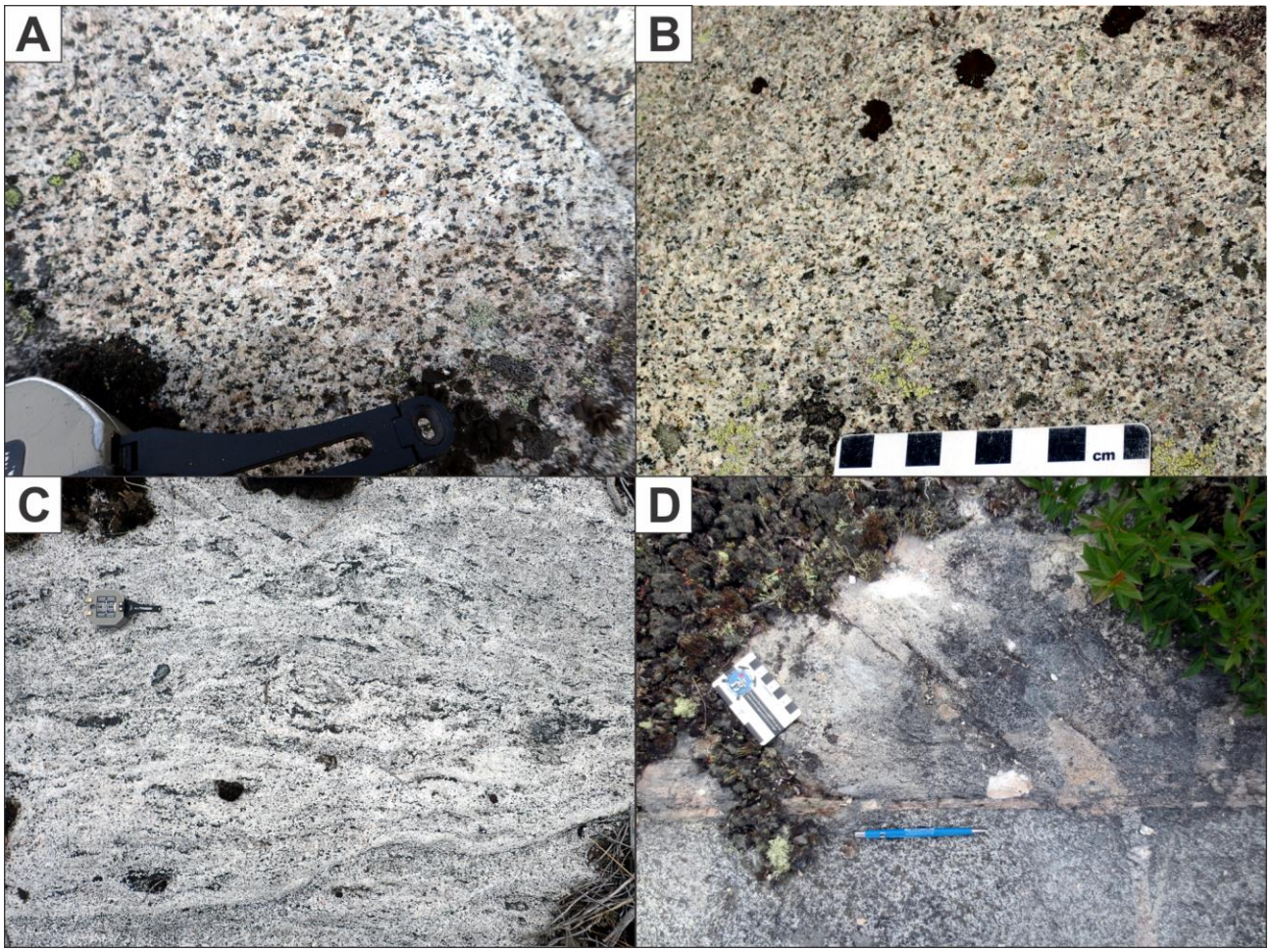

Figure 5.2.11: Fourbay Lake Pluton Area – Field Examples of Ductile Structures

A: Weak foliation developed in granodiorite defined by flattening of quartz grains and alignment of hornblende and biotite (Stn 16BH0057A, looking W, compass for scale).

B: Weak lineation in granodiorite defined by alignment of hornblende grains (Stn 16JK0020, looking W, card for scale).

C: Outcrop in domain of stronger foliation development and xenolith occurrence (Stn 16BH0179, looking W, compass for scale).

D: Foliation rotated counter clockwise into narrow sinistral ductile shear zone just above pencil (Stn 16JK0008, looking SW, card for scale).

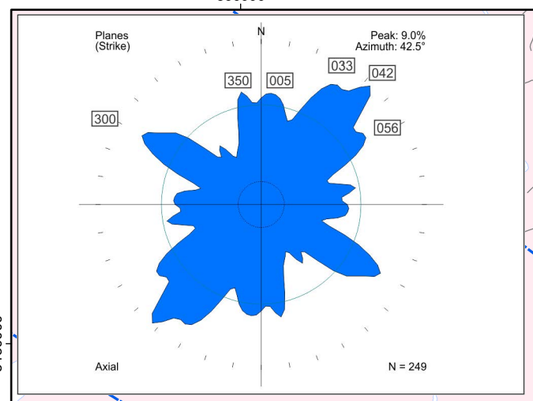

560000
570000
580000
5430000
5420000

FOURBAY LAKE PLUTON

GAFFHOOK LAKE ROAD
BAREHEAD ROAD
BAREHEAD ROAD
Barehead L.
614
Fourbay Lake
Cirrus L.
Lake Superior
Wawa
11
17
8
9
13

N

LEGEND

- Withdrawal Area
- Main Road
- Local Road
- Waterbody
- Observation - Overburden (8)
- Sub horizontal joint: 0-30° (29)
- Intermediate joint: 31-60° (17)
- Sub vertical joint: 61-90° (203)

Bedrock Geology

- Geological Boundary
- Mapped Fault
- Fold (syncline)
- Fold (anticline)
- 13: Granite-granodiorite
- 9: Gneissic tonalite suite
- 8: Gabbro
- 3: Felsic and intermediate metavolcanic rocks
- 2: Mafic metavolcanic Rocks
- Iron Formation

REFERENCE

Base Data: Land Information Ontario (obtained 2015);
CanVec Topography (obtained 2015)

Bedrock Geology: MRD 126-REV1 (Ontario Geological Survey, 2011);
Ontario Geological Survey Map 2665 (Santaguida, 2001);
Map 2666 (Santaguida, 2001);
Map 2667 (Johns, McIlraith and Stott, 2003);
Map 2668 (Johns and McIlraith, 2003)

0 2 km

srk consulting

PROJECT
DETAILED MAPPING REPORT
Manitouwadge Area, Ontario

TITLE
Fourbay Lake Pluton Area
Joints

DESIGN	KR	02 SEP 2014	**Figure 5.2.12**	REVISION 2
GIS	JA	02 AUG 2017		UTM ZONE 16N
CHECK	CN	02 AUG 2017		NAD 1983
REVIEW	JPS	02 AUG 2017		1:80,000

File: SRK_NWMO_ManStudy_AreaB_Fig5.2.12

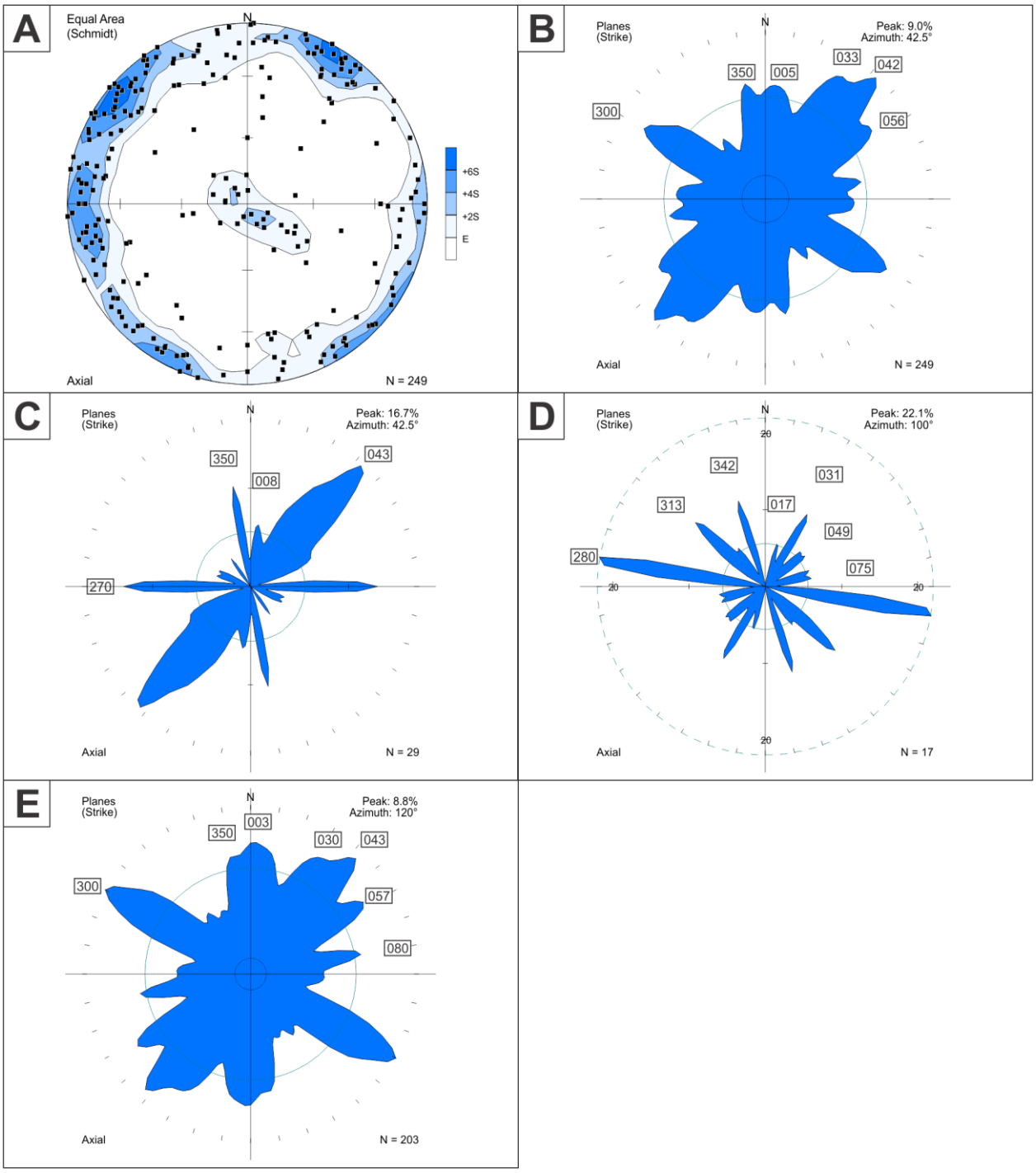

Figure 5.2.13: Fourbay Lake Pluton Area – Joint Orientation Data

A: All joints displayed as equal area lower hemisphere stereonet plot of poles to planes. (n=249).
B: All joints displayed as rose diagram of trends of planes with orientation of all peaks greater than the expected value E (n=249).
C: All joints with a dip ≤ 30 degrees displayed as rose diagram of trends of planes (n=29).
D: All joints with a dip between 31 - 60 degrees displayed as rose diagram of trends of planes (n=17).
E: All joints with a dip > 60 degrees displayed as rose diagram of trends of planes (n=203).

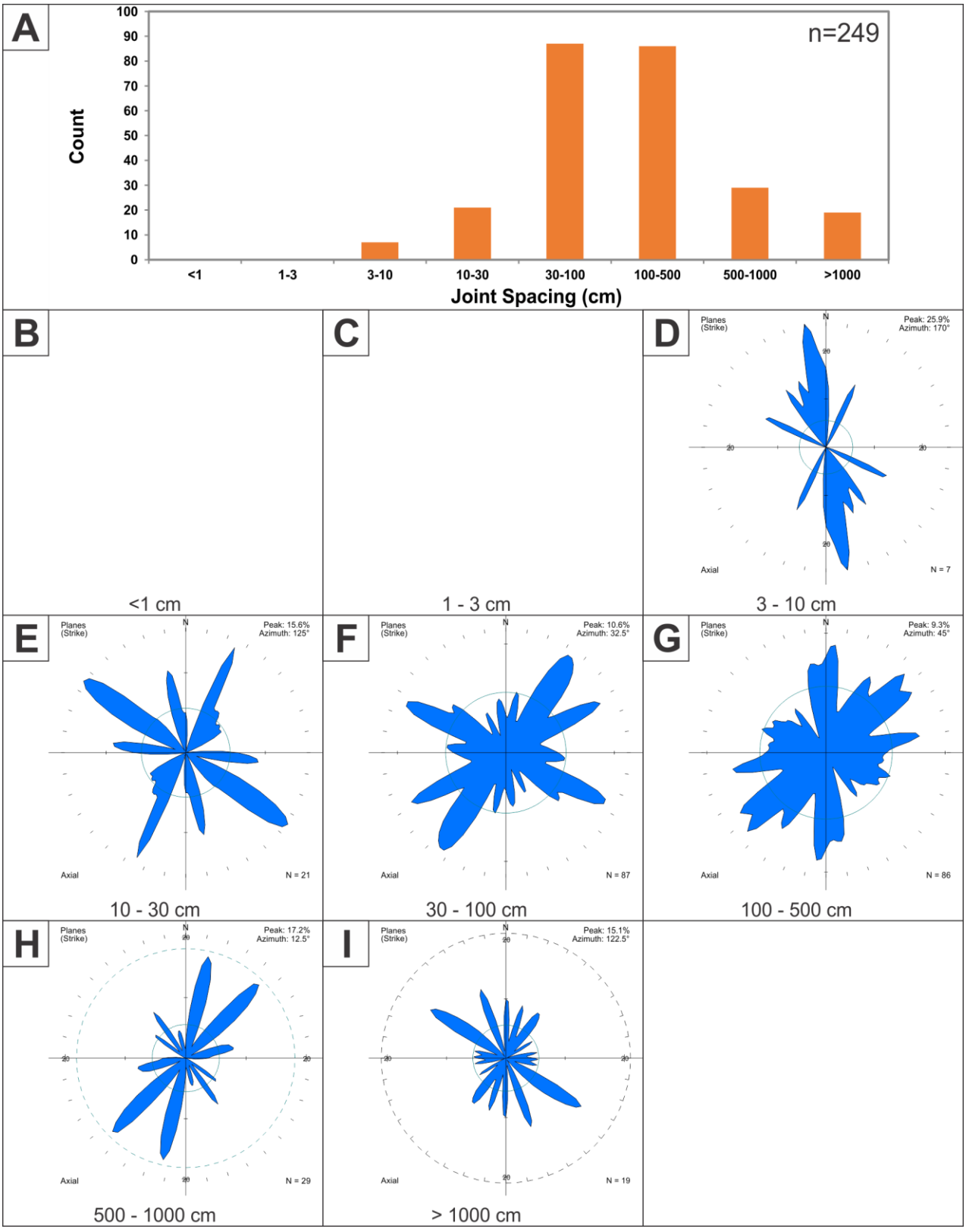

Figure 5.2.14: Fourbay Lake Pluton Area – Joint Spacing Summary

A: Histogram showing frequency distribution of joint spacing for all orientations and rock types (n=249).
B – I: Joints with the given joint spacing displayed as rose diagram of trends of planes. Any missing figures indicate no joints with that spacing were measured in this area.

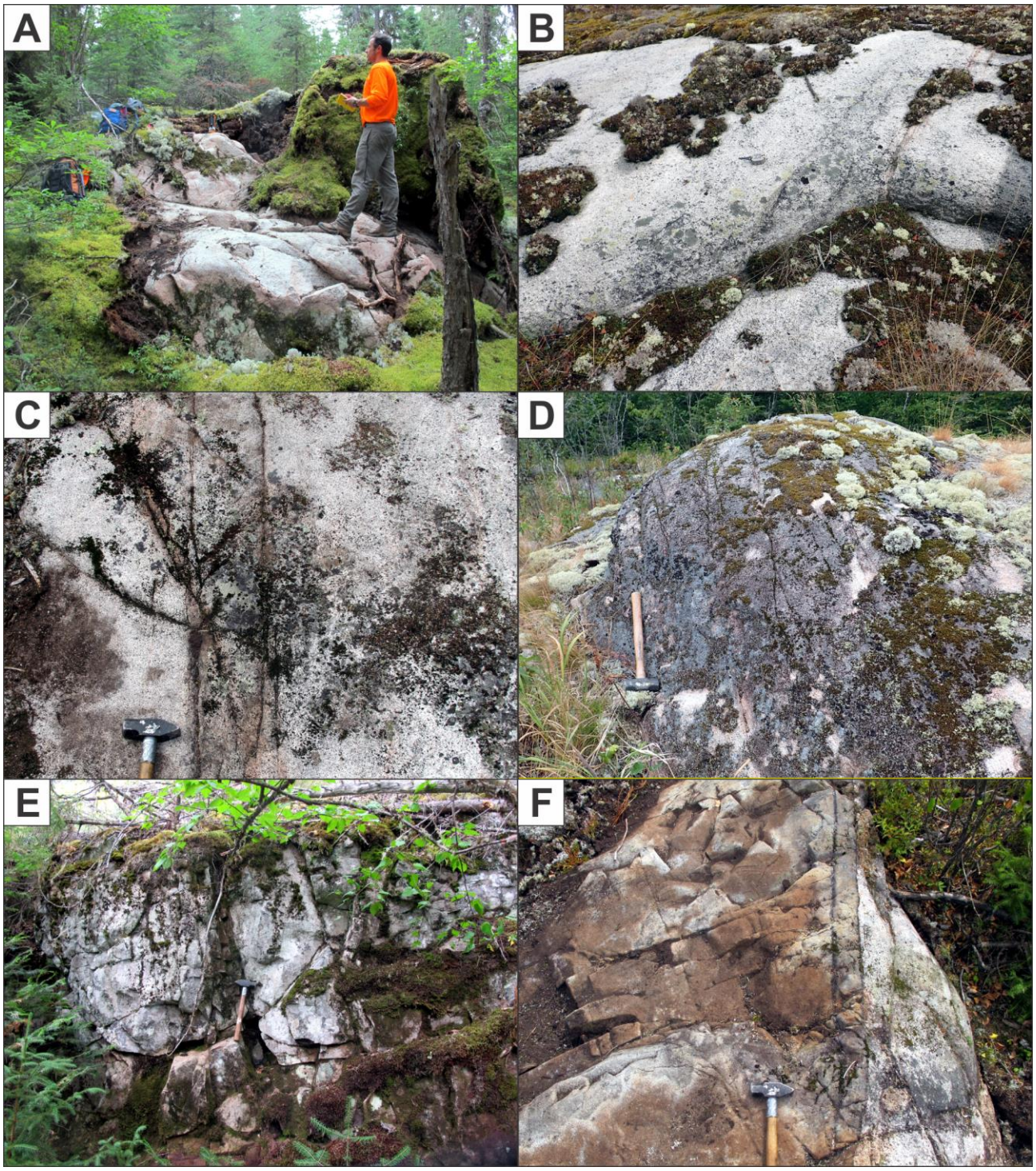

Figure 5.2.15: Fourbay Lake Pluton Area – Field Examples of Joints

A: Example of sub horizontal joint set with wide spacing cutting diorite (Stn 16CN0033, looking N, person for scale).
B: Example of wide joint spacing in diorite (Stn 16BH0209, looking E, compass for scale).
C: Example of moderate joint spacing in diorite (Stn 16CN0063, looking NW, hammer for scale).
D: Example of tight joint spacing in granodiorite (Stn 16BH0149, looking W, hammer for scale).
E: Example of multiple joint sets cutting diorite (Stn 16CN0062, section looking NW, hammer for scale).
F: Preferential development of joints proximal to contact and in a Marathon dyke cutting diorite (Stn 16CN0066, looking S, hammer for scale).

560000
570000
580000
5430000
5420000

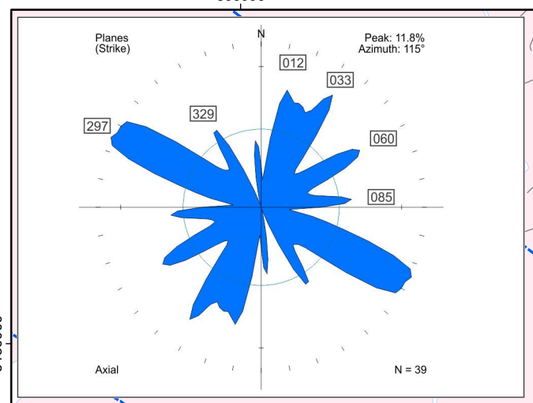

FOURBAY LAKE PLUTON

GAFFHOOK LAKE ROAD

BAREHEAD ROAD

BAREHEAD ROAD

Barehead L.

Fourbay Lake

Cirrus L.

614

8

9

13

9

N

LEGEND

- Withdrawal Area
- Main Road
- Local Road
- Waterbody
- Observation - Outcrop (51)
- Observation - Overburden (8)
- Fault - Sinistral (10)
- Fault - Dextral (8)
- Fault - Unknown (21)
- Slickenline (4)

Bedrock Geology

- Geological Boundary
- Mapped Fault
- Fold (syncline)
- Fold (anticline)
- 13: Granite-granodiorite
- 9: Gneissic tonalite suite
- 8: Gabbro
- 3: Felsic and intermediate metavolcanic rocks
- 2: Mafic metavolcanic Rocks
- Iron Formation

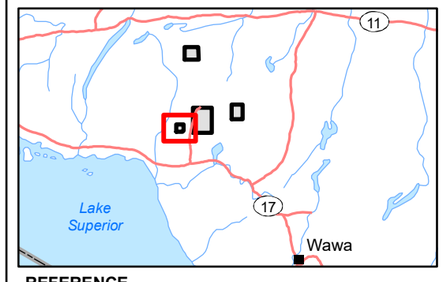

REFERENCE

Base Data: Land Information Ontario (obtained 2015);
CanVec Topography (obtained 2015)

Bedrock Geology: MRD 126-REV1 (Ontario Geological Survey, 2011);
Ontario Geological Survey Map 2665 (Santaguida, 2001);
Map 2666 (Santaguida, 2001);
Map 2667 (Johns, McIlraith and Stott, 2003);
Map 2668 (Johns and McIlraith, 2003)

0 2 km

srk consulting

PROJECT
DETAILED MAPPING REPORT
Manitouwadge Area, Ontario

TITLE
Fourbay Lake Pluton Area
Faults

DESIGN	KR	02 SEP 2014	**Figure 5.2.16**	REVISION 2
GIS	JA	02 AUG 2017		UTM ZONE 16N
CHECK	CN	02 AUG 2017		NAD 1983
REVIEW	JPS	02 AUG 2017		1:80,000

File: SRK_NWMO_ManStudy_AreaB_Fig5.2.16

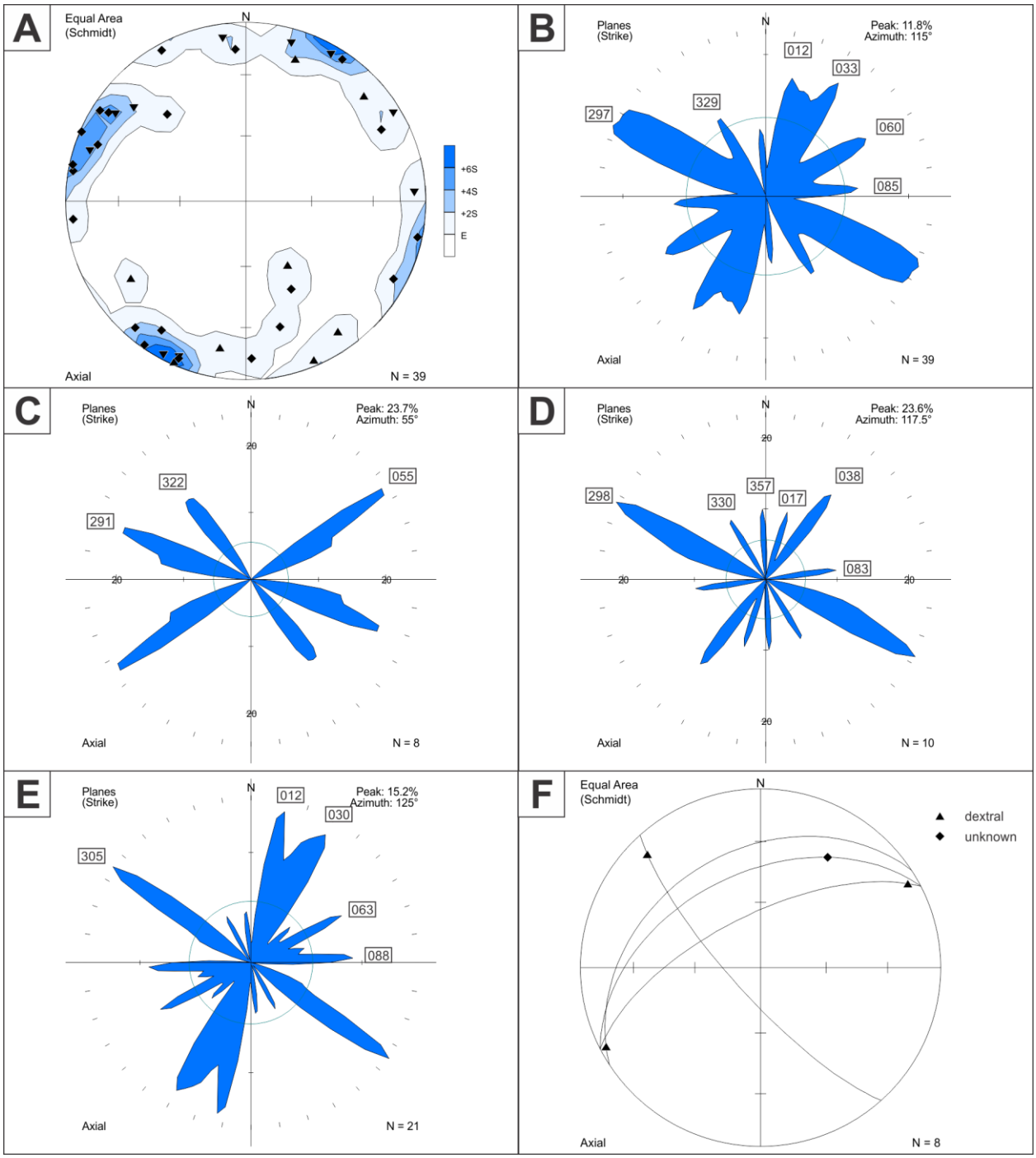

Figure 5.2.17: Fourbay Lake Pluton Area – Fault Orientation Data

A: All faults displayed as equal area lower hemisphere stereonet plot of poles to planes. Dextral faults: filled triangles (n=8). Sinistral faults: filled inverted triangles (n=10). Other or unknown movement sense faults: filled diamond (n=21).
B: All faults displayed as rose diagram of trends of planes with orientation of all peaks greater than the expected value E (n=39).
C: Dextral faults displayed as rose diagram of trends of planes (n=8).
D: Sinistral faults displayed as rose diagram of trends of planes (n=10).
E: Other or unknown movement sense brittle faults displayed as rose diagram of trends of planes (n=21).
F: Slickenline data displayed as equal area lower hemisphere stereonet plot of lineation points and great circles of the respective brittle faults on which they were measured. Lineation plotted as rake calculated from measured trend and plunge.

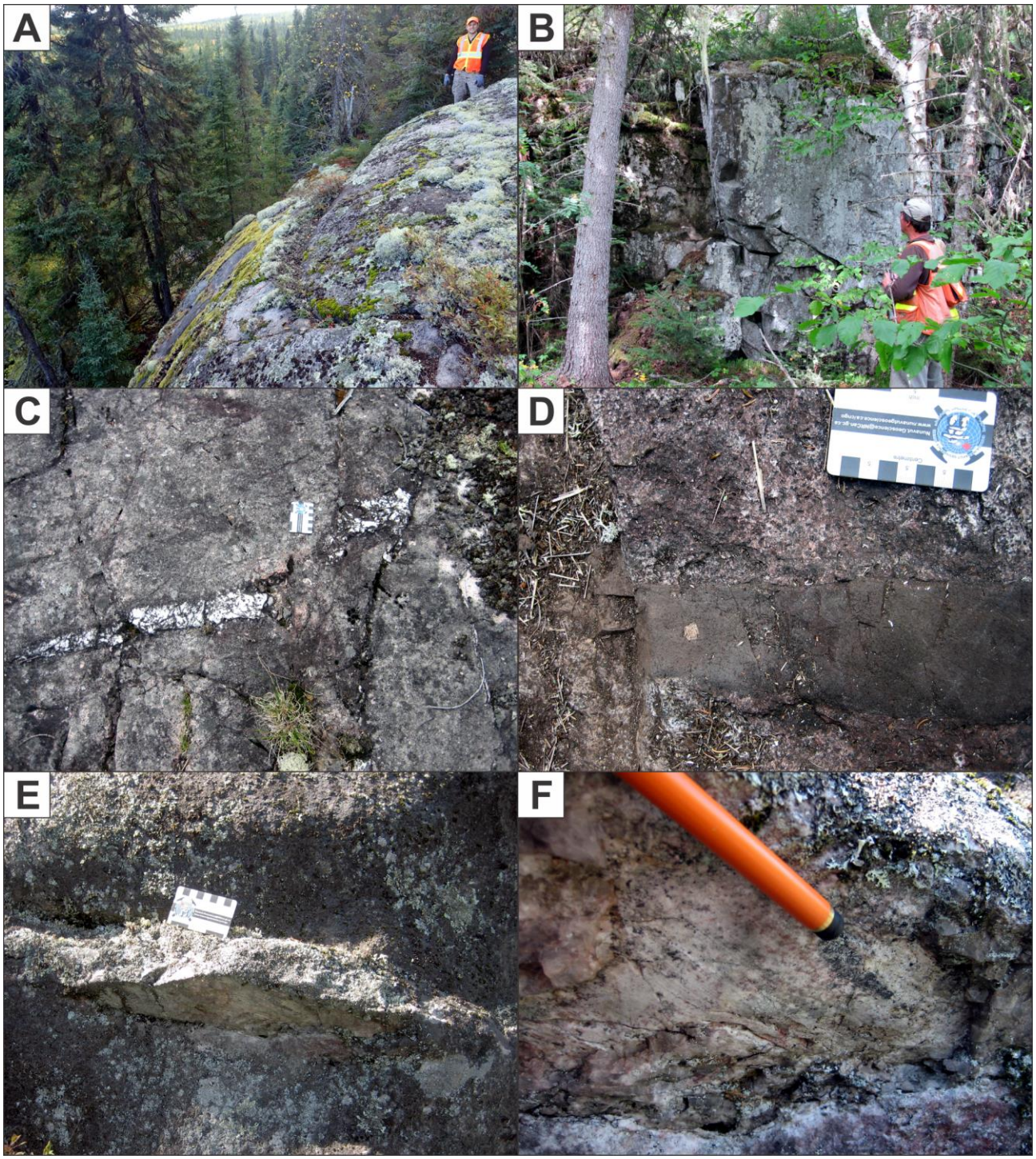

Figure 5.2.18: Fourbay Lake Pluton Area – Field Examples of Faults

A: Major SW-trending scarp parallel to surficial lineament (Stn 16BH0210, looking SW, person for scale).
B: Discrete, NW-striking, steeply NE-dipping fault (Stn 16CN0062, looking NW, person for scale).
C: Multiple, discrete, WNW-trending, sinistral strike-separation faults offsetting a quartz vein (Stn 16JK0154, looking NW, card for scale).
D: Discrete, WNW-trending, dextral strike-separation fault offsetting narrow mafic dyke (Stn 16JK0129, looking NW, card for scale).
E: Discrete fault with quartz vein fill and oblique slickenlines (Stn 16JK0130, looking NW, card for scale).
F: Moderately plunging slickenlines without steps indicate oblique slip on fault (Stn 16JK0130, looking N, pen for scale).

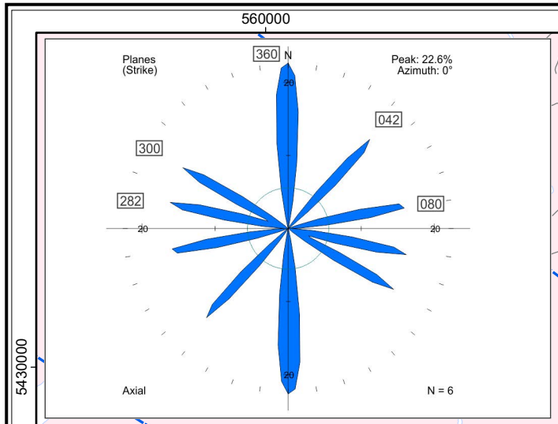

560000 570000 580000

5430000

5420000

N

FOURBAY LAKE PLUTON

GAFFHOOK LAKE ROAD

BAREHEAD ROAD

BAREHEAD ROAD

Barehead L.

614

Fourbay Lake

Cirrus L.

82 81 79 72 77 50

13

8

9

9

LEGEND

- Withdrawal Area
- Main Road
- Local Road
- Waterbody
- Observation - Outcrop (64)
- Observation - Overburden (8)
- Extension Vein (5)
- Shear Vein (1)

Bedrock Geology

- Geological Boundary
- Mapped Fault
- Fold (syncline)
- Fold (anticline)
- 13: Granite-granodiorite
- 9: Gneissic tonalite suite
- 8: Gabbro
- 3: Felsic and intermediate metavolcanic rocks
- 2: Mafic metavolcanic Rocks
- Iron Formation

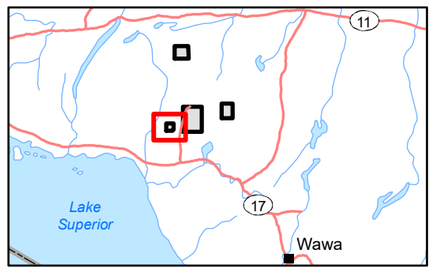

REFERENCE

Base Data: Land Information Ontario (obtained 2015);
CanVec Topography (obtained 2015)

Bedrock Geology: MRD 126-REV1 (Ontario Geological Survey, 2011);
Ontario Geological Survey Map 2665 (Santaguida, 2001);
Map 2666 (Santaguida, 2001);
Map 2667 (Johns, McIlraith and Stott, 2003);
Map 2668 (Johns and McIlraith, 2003)

0 2 km

srk consulting

PROJECT
DETAILED MAPPING REPORT
Manitouwadge Area, Ontario

TITLE
Fourbay Lake Pluton Area
Veins

DESIGN	KR	02 SEP 2014	**Figure 5.2.19**	REVISION 2
GIS	JA	02 AUG 2017		UTM ZONE 16N
CHECK	CN	02 AUG 2017		NAD 1983
REVIEW	JPS	02 AUG 2017		1:80,000

File: SRK_NWMO_ManStudy_AreaB_Fig5.2.19

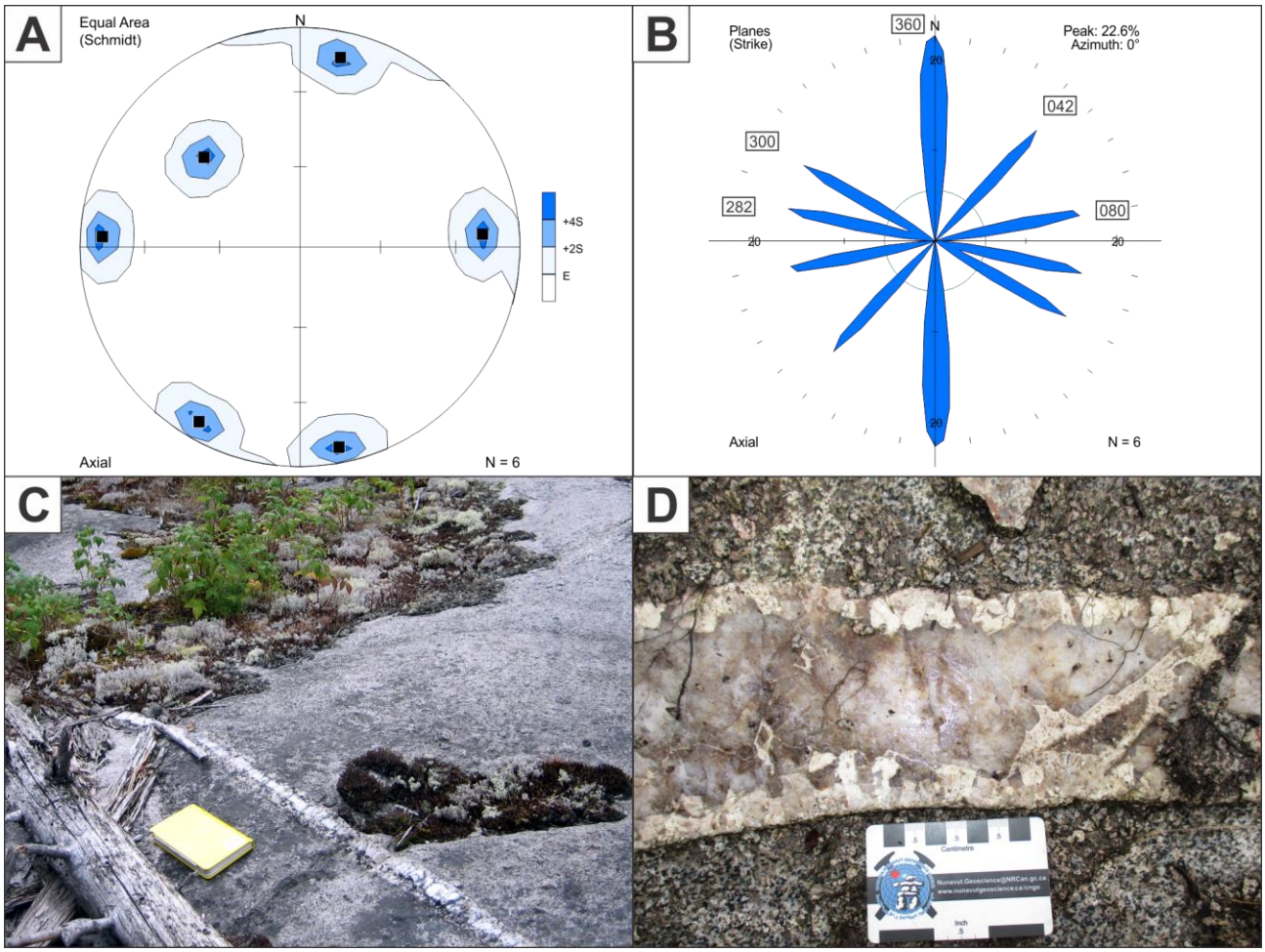

Figure 5.2.20: Fourbay Lake Pluton Area – Vein Orientation Data and Field Examples

A: All veins displayed as equal area lower hemisphere stereonet plot of poles to planes. (n=6).
B: All veins displayed as rose diagram of trends of planes with orientation of all peaks greater than the expected value E (n=6).
C: Straight quartz-feldspar vein (Stn 16JK0153, looking W, book for scale).
D: Close up of straight quartz-feldspar vein (Stn 16JK0212, looking SE, card for scale).

560000
570000
580000
5430000
5420000
N
FOURBAY LAKE PLUTON
GAFFHOOK LAKE ROAD
BAREHEAD ROAD
BAREHEAD ROAD
Barehead L.
614
Fourbay Lake
Cirrus L.
8
9
13
9

LEGEND

- Withdrawal Area
- Main Road
- Local Road
- Waterbody
- Observation - Outcrop (68)
- Observation - Overburden (8)
- Alteration - Hematite
- Alteration - Quartz
- Alteration - Epidote
- Alteration - Chlorite

Bedrock Geology

- Geological Boundary
- Mapped Fault
- Fold (syncline)
- Fold (anticline)
- 13: Granite-granodiorite
- 9: Gneissic tonalite suite
- 8: Gabbro
- 3: Felsic and intermediate metavolcanic rocks
- 2: Mafic metavolcanic Rocks
- Iron Formation

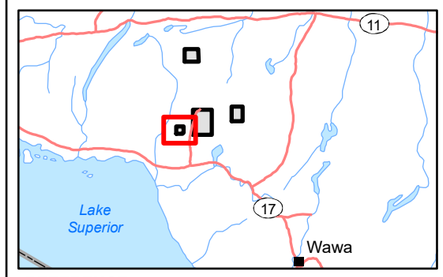

REFERENCE

Base Data: Land Information Ontario (obtained 2015);
CanVec Topography (obtained 2015)

Bedrock Geology: MRD 126-REV1 (Ontario Geological Survey, 2011);
Ontario Geological Survey Map 2665 (Santaguida, 2001);
Map 2666 (Santaguida, 2001);
Map 2667 (Johns, McIlraith and Stott, 2003);
Map 2668 (Johns and McIlraith, 2003)

0 2 km

srk consulting

PROJECT
DETAILED MAPPING REPORT
Manitouwadge Area, Ontario

TITLE
Fourbay Lake Pluton Area
Secondary Minerals and Alteration

DESIGN	KR	02 SEP 2014	**Figure 5.2.21**	REVISION 2
GIS	JA	02 AUG 2017		UTM ZONE 16N
CHECK	CN	02 AUG 2017		NAD 1983
REVIEW	JPS	02 AUG 2017		1:80,000

File: SRK_NWMO_ManStudy_AreaB_Fig5.2.21

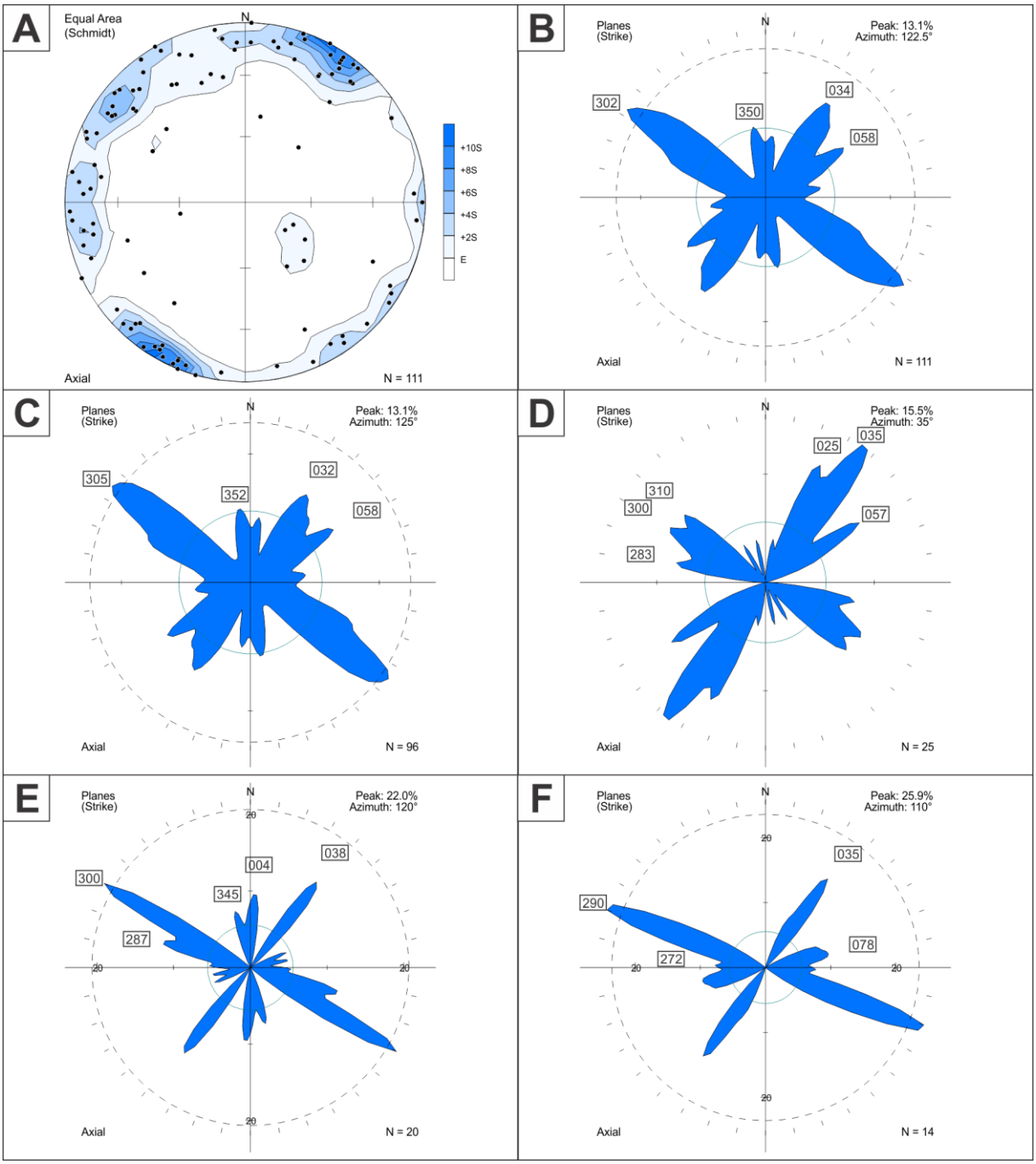

Figure 5.2.22: Fourbay Lake Pluton Area – Secondary Minerals and Alteration Orientation Data

A: All structures with visible alteration displayed as equal area lower hemisphere stereonet plot of poles to planes. (n=111).

B: All structures with visible alteration displayed as rose diagram of trends of planes with orientation of all peaks greater than the expected value E (n=111).

C: All structures with visible hematite alteration displayed as rose diagram of trends of planes with orientation of all peaks greater than the expected value E (n=96).

D: All structures with visible epidote alteration displayed as rose diagram of trends of planes with orientation of all peaks greater than the expected value E (n=25).

E: All structures with visible quartz alteration displayed as rose diagram of trends of planes with orientation of all peaks greater than the expected value E (n=20).

F: All structures with visible chlorite alteration displayed as rose diagram of trends of planes with orientation of all peaks greater than the expected value E (n=14).

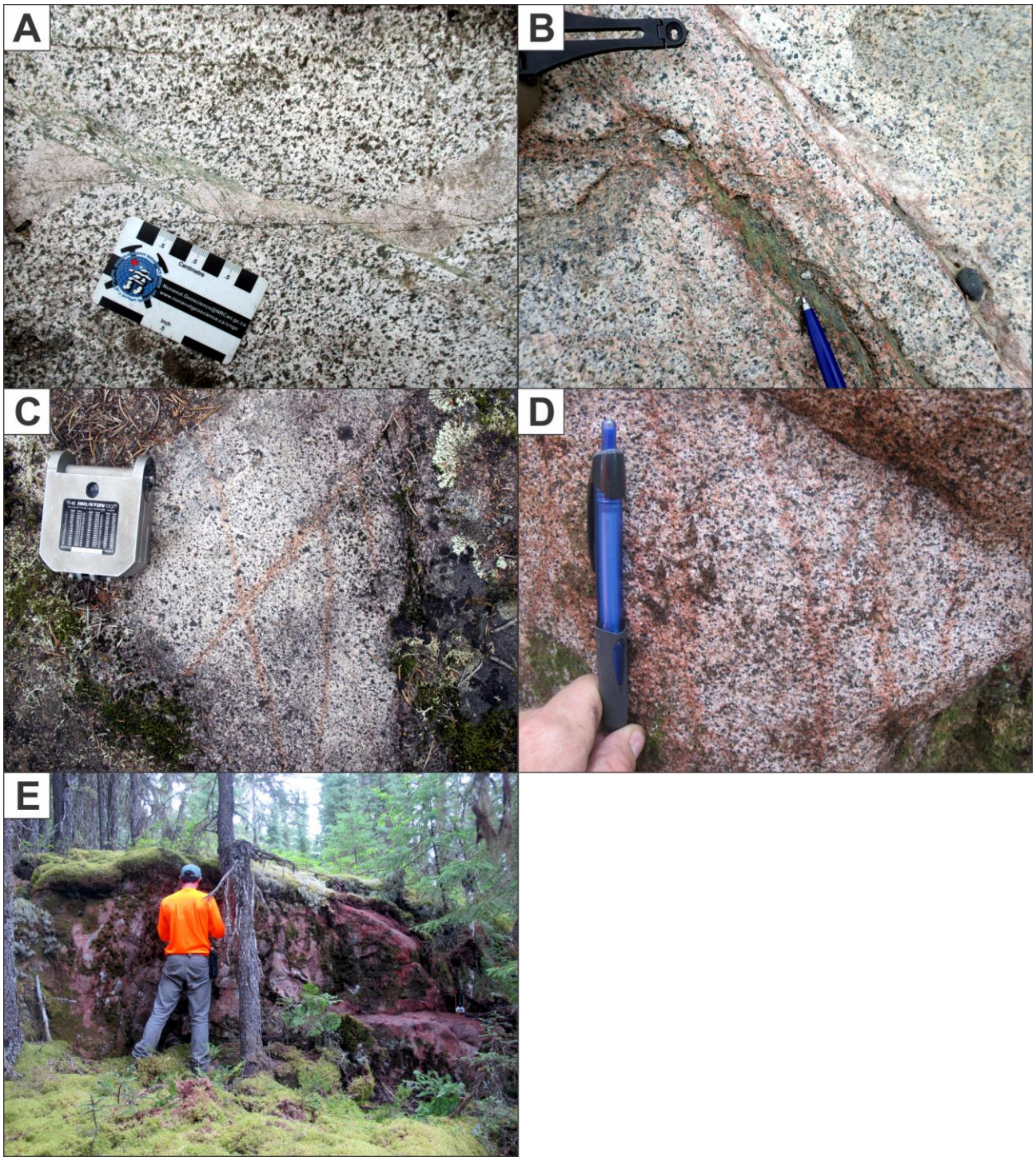

Figure 5.2.23: Fourbay Lake Pluton Area – Field Examples of Secondary Minerals and Alteration

A: Epidote-chlorite veins and weak chloritization of hornblende in granodiorite associated with dextral fault (Stn 16JK0212, looking SE, card for scale).
B: Epidote ±chlorite filled fault with hematite alteration and staining of feldspar (Stn 16BH0107, looking W, compass for scale).
C: Discrete hematite alteration halos around NE- and E-trending joints (Stn 16CN0034, looking NE, compass for scale).
D: Stronger hematite alteration halos around NE- and E-trending joints and weak pervasive hematite alteration of feldspar (Stn 16CN0036, looking E, pen for scale).
E: Pervasive hematite staining in same outcrop (Stn 16CN0036, looking NW, person for scale).

580000 590000 600000

5440000 5430000

N

LEGEND

- Withdrawal Area
- Main Road
- Local Road
- Waterbody
- Observation - Outcrop (217)
- Observation - Overburden (25)
- Predicted Outcrop

Bedrock Geology

- Geological Boundary
- Mapped Fault
- 13: Granite-granodiorite
- 9: Gneissic tonalite suite
- 8: Gabbro
- 2: Mafic metavolcanic Rocks

Barehead L. Kaginu L. Morley L. Agonzon Lake

BAREHEAD ROAD CAMP 60 ROAD AGONZON LK ROAD LAMPSON ROAD TWIST RD

9 8

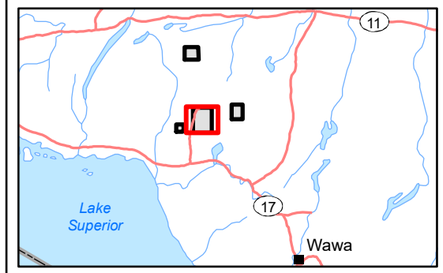

REFERENCE

Base Data: Land Information Ontario (obtained 2015); CanVec Topography (obtained 2015)

Bedrock Geology: MRD 126-REV1 (Ontario Geological Survey, 2011); Ontario Geological Survey Map 2665 (Santaguida, 2001); Map 2666 (Santaguida, 2001); Map 2667 (Johns, McIlraith and Stott, 2003); Map 2668 (Johns and McIlraith, 2003)

0 2 km

srk consulting

PROJECT
DETAILED MAPPING REPORT
Manitouwadge Area, Ontario

TITLE
Black-Pic Batholith Area West
Mapping Observation Locations

DESIGN	KR	02 SEP 2014	**Figure 5.3.1**	REVISION 2
GIS	JA	02 AUG 2017		UTM ZONE 16N
CHECK	CN	02 AUG 2017		NAD 1983
REVIEW	JPS	02 AUG 2017		1:81,000

File: SRK_NWMO_ManStudy_AreaC_Fig5.3.1

Figure 5.3.2: Black-Pic Batholith Area - West – Field Examples of Accessibility and Bedrock Exposure

A: Paved road provides excellent access along Highway 614 (Stn 16BH0079, looking NW, person for scale).
B: Aerial view of cliff face along lake marking strong NNE-trending surface lineament (Stn 16BH0235, looking SE, no scale).
C: Large, clean tonalite outcrop at helicopter accessible outcrop (Stn 16JK0239, looking NE, helicopter for scale).
D: Good outcrop exposure along lake accessible traverses (Stn 16JK0189, looking E, person for scale).
E: Large esker covered in light coloured moss can be mistaken for outcrop (Stn 16BH0255, looking S, person for scale).
F: Dense, young forest regrowth in older logged areas inhibits foot access (Stn 16BH0021, looking W, person for scale).

580000
590000
600000
5440000
5430000
N
8
9
614
Barehead L.
Kaginu L.
Morley L.
AGONZON LK ROAD
TWIST RD
CAMP 60 ROAD
Agonzon Lake
BAREHEAD ROAD
ROAD
LAMPSON ROAD
TWIST

LEGEND

- Withdrawal Area
- Main Road
- Local Road
- Waterbody
- Observation - Outcrop

Bedrock Geology

- Geological Boundary
- Mapped Fault
- 13: Granite-granodiorite
- 9: Gneissic tonalite suite
- 8: Gabbro
- 2: Mafic metavolcanic Rocks

Main Lithology

- Tonalite (190)

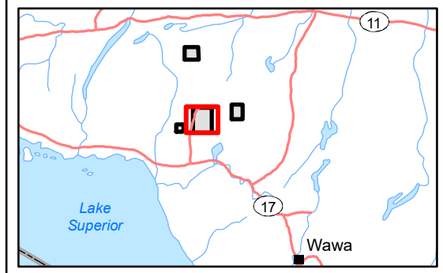

REFERENCE

Base Data: Land Information Ontario (obtained 2015);
CanVec Topography (obtained 2015)

Bedrock Geology: MRD 126-REV1 (Ontario Geological Survey, 2011);
Ontario Geological Survey Map 2665 (Santaguida, 2001);
Map 2666 (Santaguida, 2001);
Map 2667 (Johns, McIlraith and Stott, 2003);
Map 2668 (Johns and McIlraith, 2003)

0 2 km

srk consulting

PROJECT
DETAILED MAPPING REPORT
Manitouwadge Area, Ontario

TITLE
Black-Pic Batholith Area West
Main Lithological Units

DESIGN	KR	02 SEP 2014	**Figure 5.3.3**	REVISION 2
GIS	JA	02 AUG 2017		UTM ZONE 16N
CHECK	CN	02 AUG 2017		NAD 1983
REVIEW	JPS	02 AUG 2017		1:81,000

File: SRK_NWMO_ManStudy_AreaC_Fig5.3.3

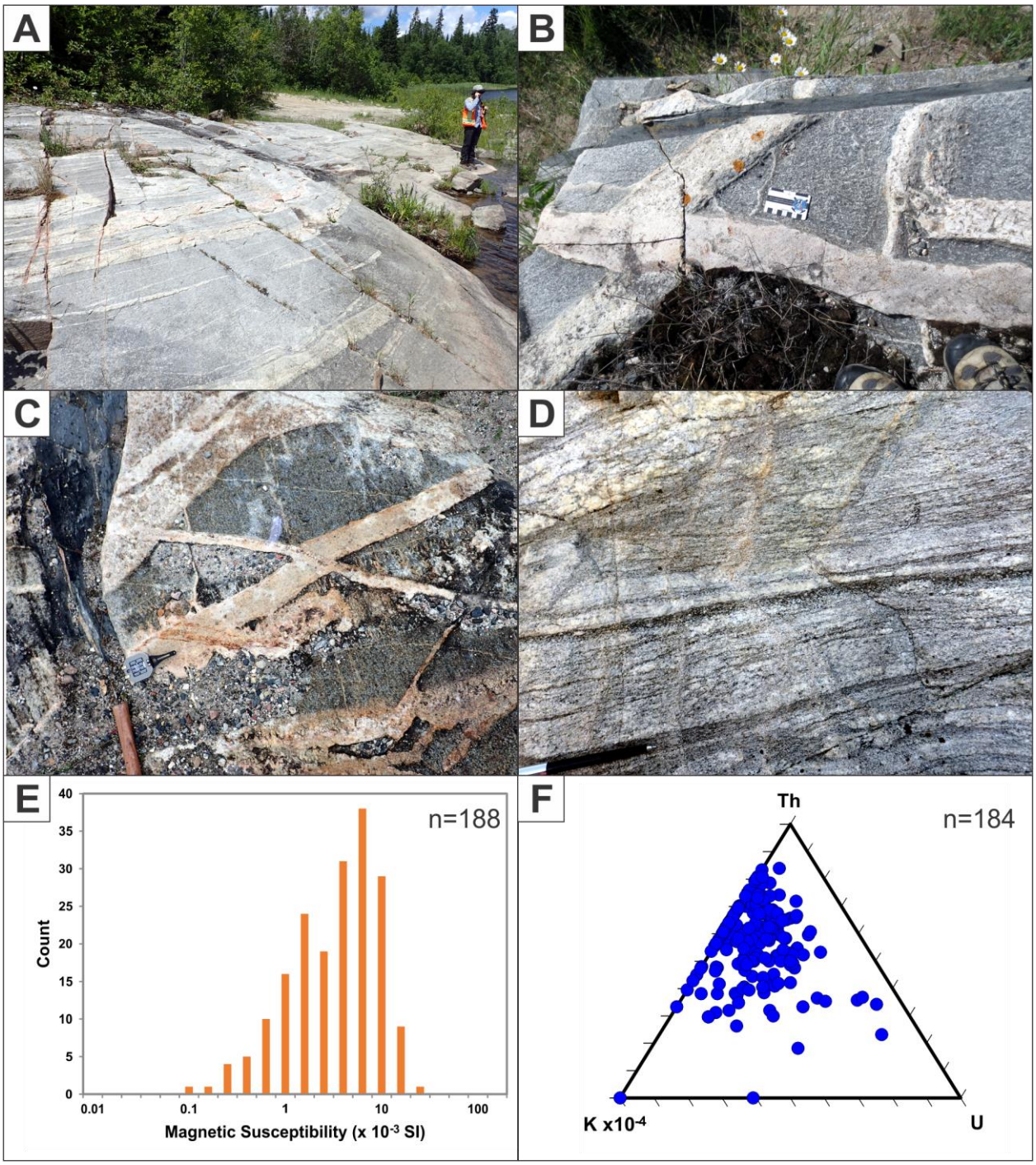

Figure 5.3.4 Black-Pic Batholith Area - West – Field Examples of Main Lithology: Tonalite

A: Representative shallow-dipping tonalite gneiss (Stn 16BH0011, looking NW, person for scale).
B: Foliated tonalite with multiple cross-cutting mafic and felsic dykes (Stn 16JK0054, looking NE, card for scale).
C: Foliated to weakly gneissic tonalite with multiple cross-cutting mafic and felsic dykes (Stn 16BH0064, looking W, compass for scale).
D: Close-up of tonalite gneiss showing mineral composition and texture (Stn 16BH0272, looking E, pen for scale).
E: Logarithmic histogram plot of magnetic susceptibility for foliated and gneissic tonalite.
F: Ternary plot of gamma ray spectrometer data for foliated and gneissic tonalite.

580000
590000
600000
5440000
5430000
N
8
9
614
Barehead L.
Kaginu L.
Morley L.
AGONZON LK ROAD
CAMP 60 ROAD
TWIST RD
Agonzon Lake
BAREHEAD ROAD
ROAD
LAMPSON ROAD
TWIST

LEGEND

- Withdrawal Area
- Main Road
- Local Road
- Waterbody
- Observation - Outcrop

Bedrock Geology

- Geological Boundary
- Mapped Fault
- 13: Granite-granodiorite
- 9: Gneissic tonalite suite
- 8: Gabbro
- 2: Mafic metavolcanic Rocks

Minor Lithology

- Diorite to Granodiorite (35)
- Granite (44)
- Foliated to Gneissic Mafic Rocks (6)
- Gabbro (19)

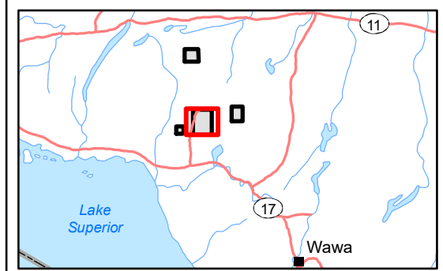

REFERENCE

Base Data: Land Information Ontario (obtained 2015);
CanVec Topography (obtained 2015)

Bedrock Geology: MRD 126-REV1 (Ontario Geological Survey, 2011);
Ontario Geological Survey Map 2665 (Santaguida, 2001);
Map 2666 (Santaguida, 2001);
Map 2667 (Johns, McIlraith and Stott, 2003);
Map 2668 (Johns and McIlraith, 2003)

0 2 km

srk consulting

PROJECT
DETAILED MAPPING REPORT
Manitouwadge Area, Ontario

TITLE
Black-Pic Batholith Area West
Minor Lithological Units

DESIGN	KR	02 SEP 2014	**Figure 5.3.5**	REVISION 2
GIS	JA	02 AUG 2017		UTM ZONE 16N
CHECK	CN	02 AUG 2017		NAD 1983
REVIEW	JPS	02 AUG 2017		1:81,000

File: SRK_NWMO_ManStudy_AreaC_Fig5.3.5

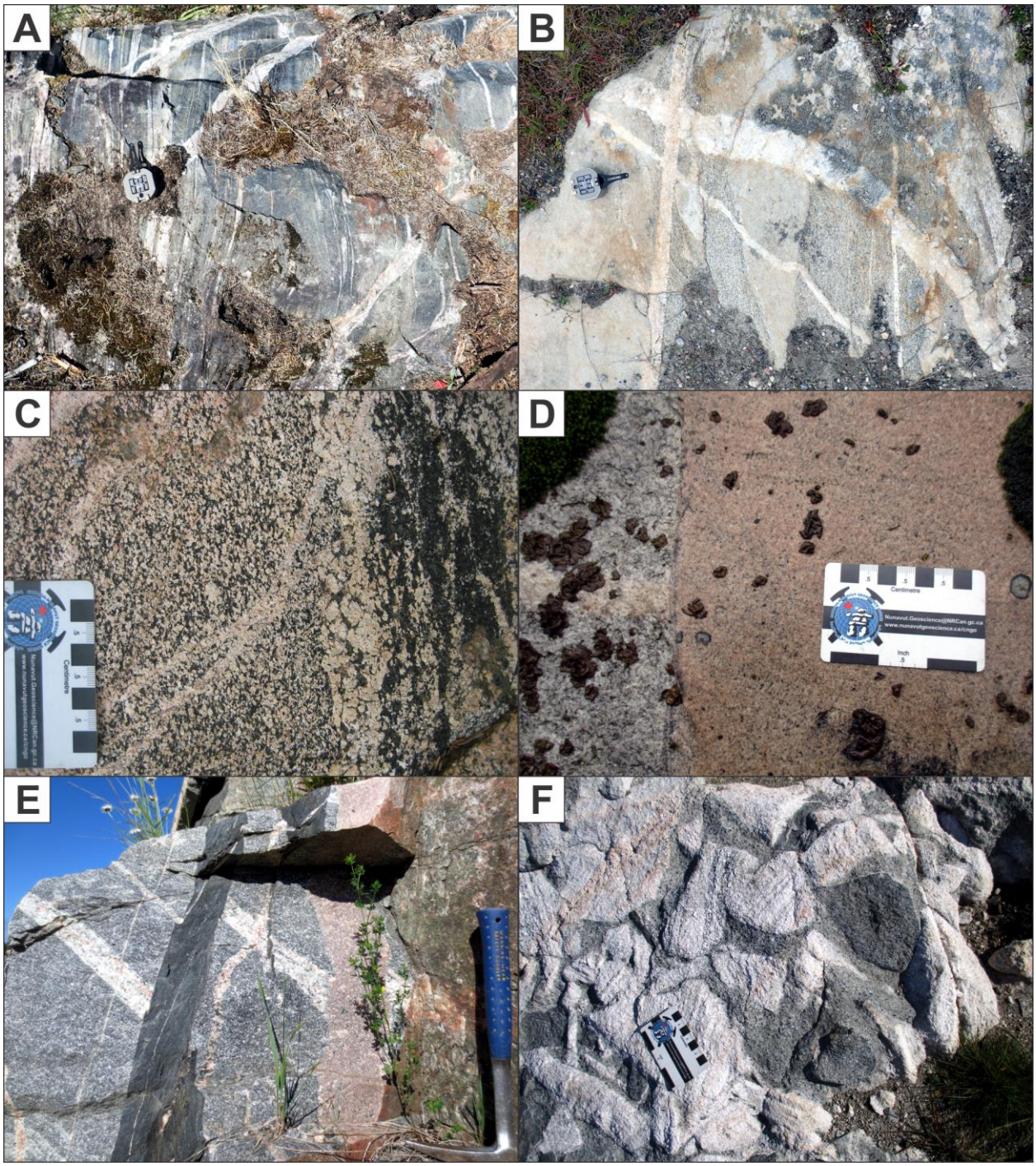

Figure 5.3.6: Black-Pic Batholith Area - West – Field Examples of Minor Lithological Units

A: Fine-grained mafic gneiss panel within domain of predominantly tonalite gneiss (Stn 16BH0034, looking N, compass for scale).
B: Multiple generations of felsic dykes cutting foliated tonalite and diorite (Stn 16BH0061, looking W, compass for scale).
C: Foliated diorite to gabbro intrusion cut by white felsic dykes (Stn 16JK0190, looking W, card for scale).
D: Wide, pink felsic dyke cutting older, narrow white felsic dyke and host foliated tonalite (Stn 16JK0202, looking NW, card for scale).
E: Multiple cross-cutting felsic dykes including a foliated mafic gabbroic dyke (Stn 16JK0054, looking W, hammer for scale).
F: Magmatic breccia dominated by randomly oriented gneissic tonalite clasts (Stn 16JK0238, looking SE, card for scale).

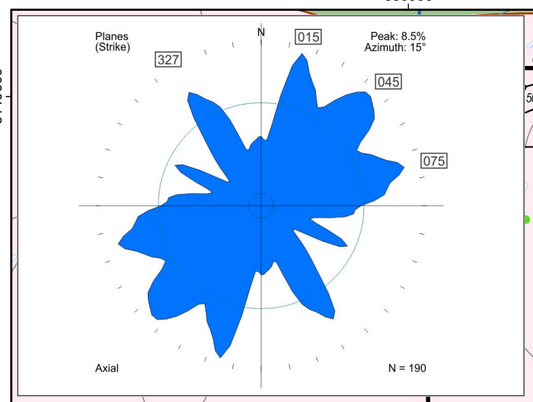

580000 590000 600000

5440000 5430000

Barehead L. Kaginu L. Morley L. Agonzon Lake

BAREHEAD ROAD CAMP 60 ROAD AGONZON LK ROAD LAMPSON ROAD TWIST RD

614 614

9

LEGEND

- Withdrawal Area
- Main Road
- Local Road
- Waterbody
- Observation - Outcrop (36)
- Observation - Overburden (25)
- Foliation (93)
- Gneissic Layering (97)
- Fold Axial Plane (3)
- Fold Axis (5)
- Mineral Lineation (9)

Bedrock Geology

- Geological Boundary
- Mapped Fault
- 13: Granite-granodiorite
- 9: Gneissic tonalite suite
- 8: Gabbro
- 2: Mafic metavolcanic Rocks

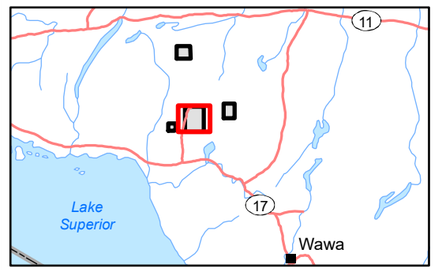

REFERENCE

Base Data: Land Information Ontario (obtained 2015);
CanVec Topography (obtained 2015)

Bedrock Geology: MRD 126-REV1 (Ontario Geological Survey, 2011);
Ontario Geological Survey Map 2665 (Santaguida, 2001);
Map 2666 (Santaguida, 2001);
Map 2667 (Johns, McIlraith and Stott, 2003);
Map 2668 (Johns and McIlraith, 2003)

0 2 km

srk consulting

PROJECT
DETAILED MAPPING REPORT
Manitouwadge Area, Ontario

TITLE
Black-Pic Batholith Area West
Tectonic Foliation

DESIGN	KR	02 SEP 2014	**Figure 5.3.7**	REVISION 2
GIS	JA	02 AUG 2017		UTM ZONE 16N
CHECK	CN	02 AUG 2017		NAD 1983
REVIEW	JPS	02 AUG 2017		1:81,000

File: SRK_NWMO_ManStudy_AreaC_Fig5.3.7

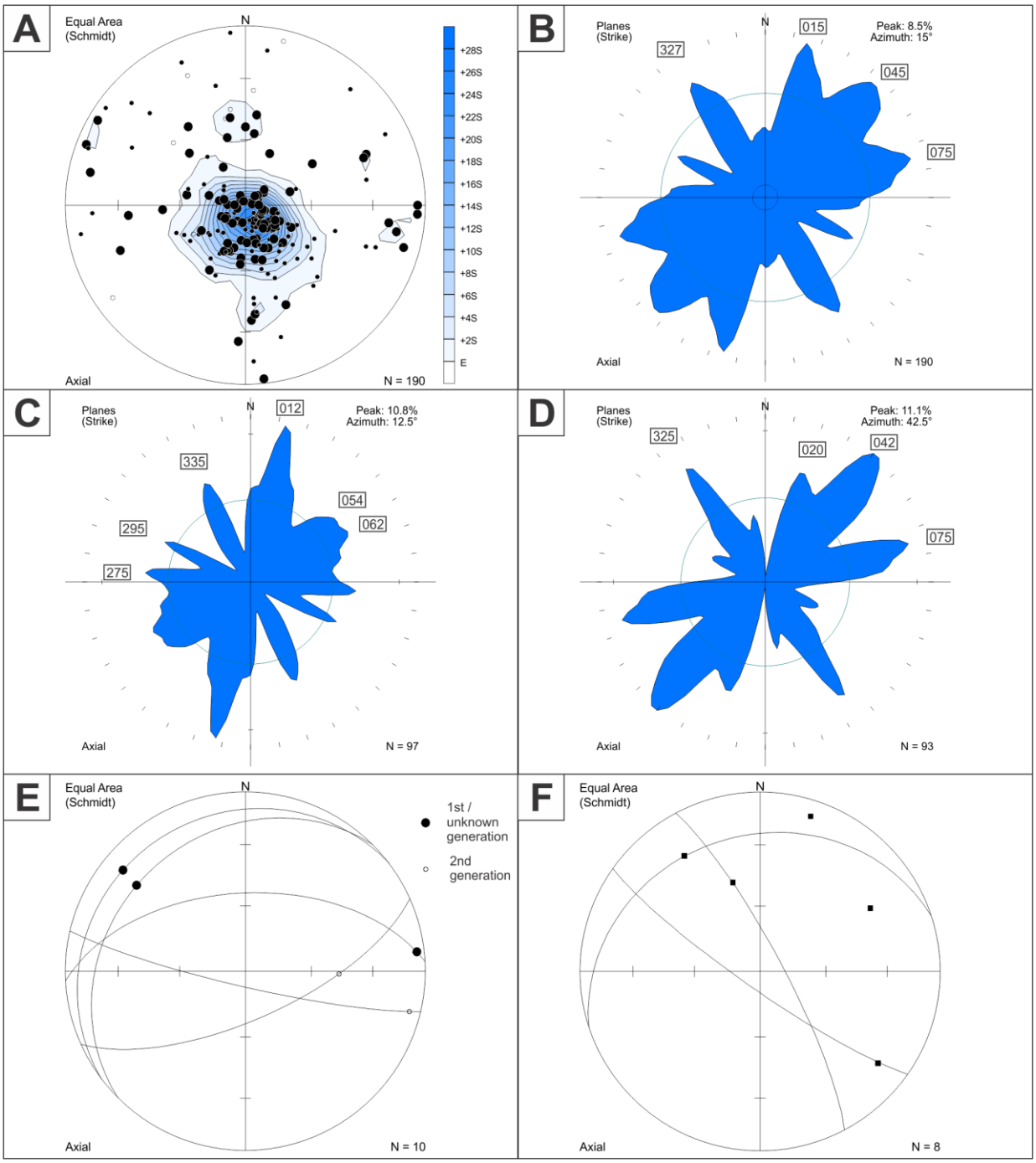

Figure 5.3.8: Black-Pic Batholith Area - West – Tectonic Foliation Orientation Data

A: All main gneissic layering and tectonic foliation displayed as equal area lower hemisphere stereonet plot of poles to planes. Gneissic layering: large circles (n=97). Mineral foliation: First/unknown generation - small circles (n=85); Second generation – open circles (n=8).

B: All main gneissic layering and tectonic foliation displayed as rose diagram of trends of planes with orientation of all peaks greater than the expected value E (n=190).

C: Gneissic layering displayed as rose diagram of trends of planes (n=97).

D: Mineral foliation displayed as rose diagram of trends of planes (n=93).

E: Mineral lineation data displayed as equal area lower hemisphere stereonet plot of lineation points and great circles of respective gneissic layering or foliation planes in the same outcrops. Lineation plotted as rake calculated from measured trend and plunge.

F: Fold axis and axial plane data displayed as equal area lower hemisphere stereonet plot of fold axis points and great circles of axial planes.

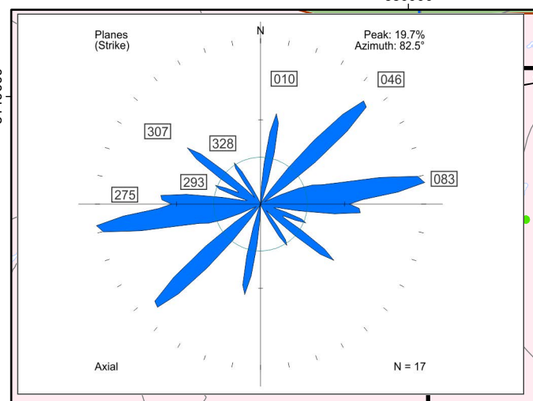

580000 590000 600000

5440000 5430000

N

8

TWIST RD

Kaginu L.

Morley L.

AGONZON LK ROAD

Barehead L.

CAMP 60 ROAD

Agonzon Lake

BAREHEAD ROAD

ROAD

LAMPSON ROAD

TWIST

614

9

LEGEND

- Withdrawal Area
- Main Road
- Local Road
- Waterbody
- Observation - Outcrop (207)
- Observation - Overburden (25)
- Brittle-Ductile Shear Zone (5)
- Ductile Shear Zone - Sinistral (1)
- Ductile Shear Zone - Dextral (4)
- Ductile Shear Zone - normal slip (4)
- Ductile Shear Zone - unknown slip (3)

Bedrock Geology

- Geological Boundary
- Mapped Fault
- 13: Granite-granodiorite
- 9: Gneissic tonalite suite
- 8: Gabbro
- 2: Mafic metavolcanic Rocks

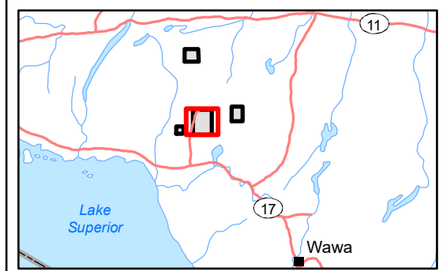

REFERENCE

Base Data: Land Information Ontario (obtained 2015);
CanVec Topography (obtained 2015)

Bedrock Geology: MRD 126-REV1 (Ontario Geological Survey, 2011);
Ontario Geological Survey Map 2665 (Santaguida, 2001);
Map 2666 (Santaguida, 2001);
Map 2667 (Johns, McIlraith and Stott, 2003);
Map 2668 (Johns and McIlraith, 2003)

0 2 km

srk consulting

PROJECT
DETAILED MAPPING REPORT
Manitouwadge Area, Ontario

TITLE
Black-Pic Batholith Area West
Ductile and Brittle-Ductile Shear Zones

DESIGN	KR	02 SEP 2014	**Figure 5.3.9**	REVISION 2
GIS	JA	02 AUG 2017		UTM ZONE 16N
CHECK	CN	02 AUG 2017		NAD 1983
REVIEW	JPS	02 AUG 2017		1:81,000

File: SRK_NWMO_ManStudy_AreaC_Fig5.3.9

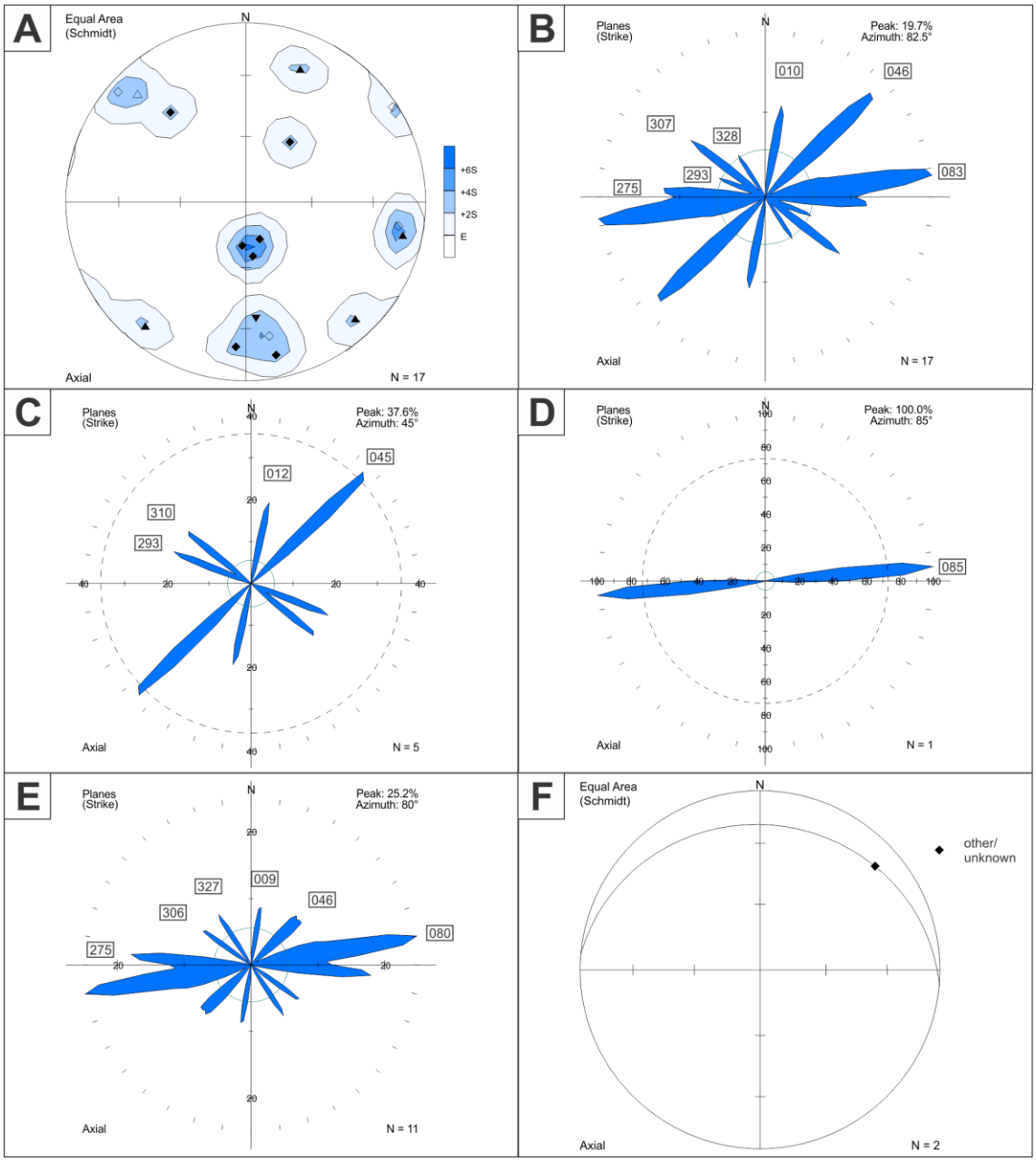

Figure 5.3.10: Black-Pic Batholith Area - West – Ductile and Brittle-Ductile Shear Zone Orientation Data

A: All ductile and brittle-ductile shear zones displayed as equal area lower hemisphere stereonet plot of poles to planes. Dextral shear zone: filled upright triangle (n=4). Dextral brittle-ductile shear zone: open upright triangle (n=1).Sinistral shear zone: filled inverted triangle (n=1). Other or unknown movement sense shear zones: filled diamond (n=7). Other or unknown movement sense brittle-ductile shear zone: open diamond (n=4).

B: All ductile and brittle-ductile shear zones displayed as rose diagram of trends of planes with orientation of all peaks greater than the expected value E (n=17).

C: Dextral shear zones and brittle-ductile shear zones displayed as rose diagram of trends of planes (n=5).

D: Sinistral shear zone displayed as rose diagram of trend of plane (n=1).

E: Other or unknown movement sense ductile and brittle-ductile shear zones displayed as rose diagram of trends of planes (n=11).

F: Mineral lineation data displayed as equal area lower hemisphere stereonet plot of lineation point and great circle of the ductile shear zone on which it was measured. Lineation plotted as rake calculated from measured trend and plunge.

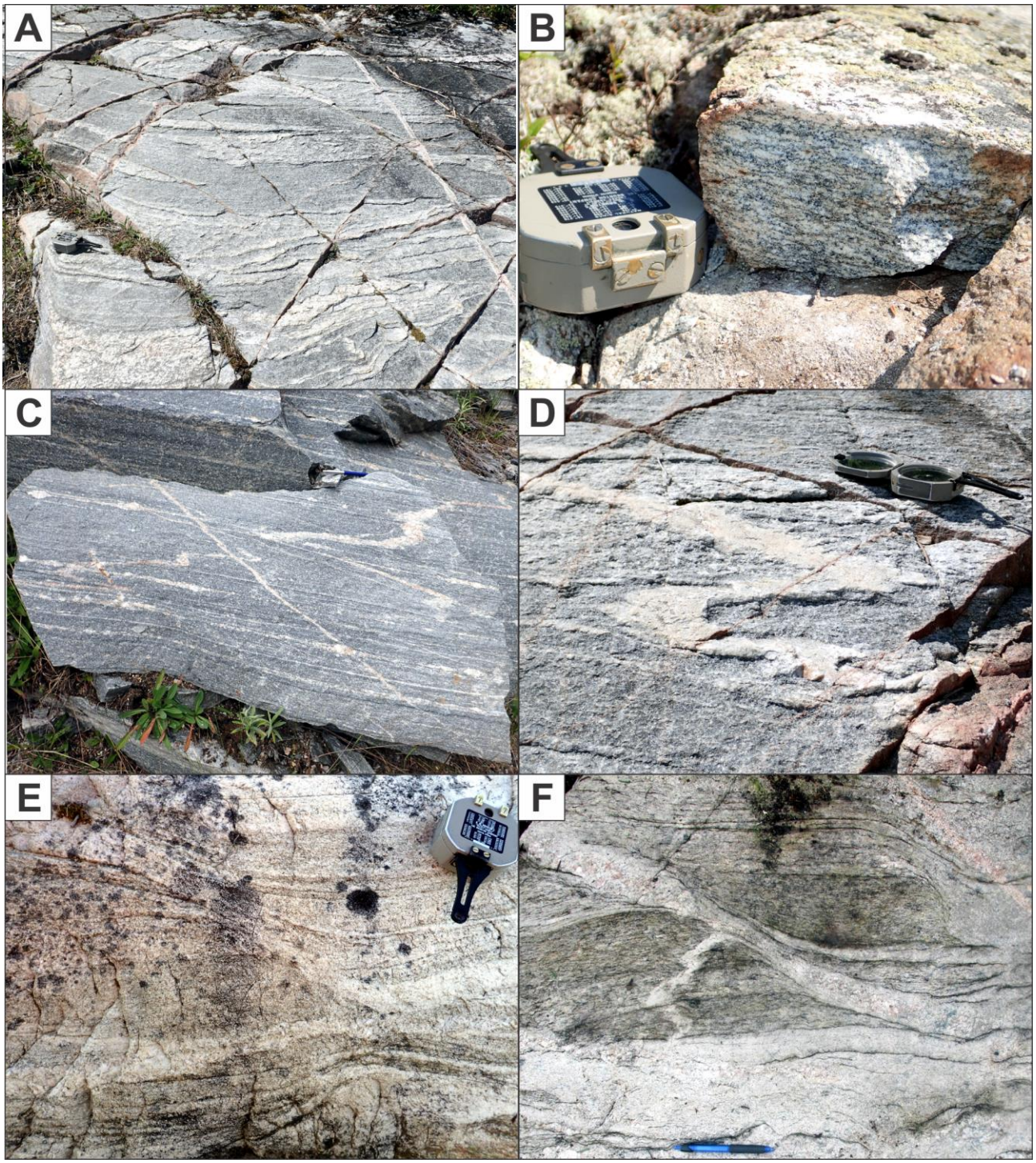

Figure 5.3.11: Black-Pic Batholith Area - West – Field Examples of Ductile Structures

A: Shallow-dipping gneissosity in tonalite gneiss (Stn 16BH0011, looking SW, compass for scale).
B: Close up of shallow-dipping foliation to weak gneissosity (Stn 16BH0017, looking N, compass for scale).
C: Straight gneissosity in domain of high ductile strain (Stn 16BH0079, looking NW, compass for scale).
D: Recumbent, shallowly plunging early folded and foliated felsic dyke in tonalite gneiss (Stn 16BH0011, looking SW, compass for scale).
E: Extensional, dextral strike-separation, moderate-dipping ductile shear zone (Stn 16BH0250, looking SE, compass for scale).
F: Extensional, dextral strike-separation ductile shear zone with associated boudinaged felsic dyke (Stn 16CN0120, looking S, pen for scale)

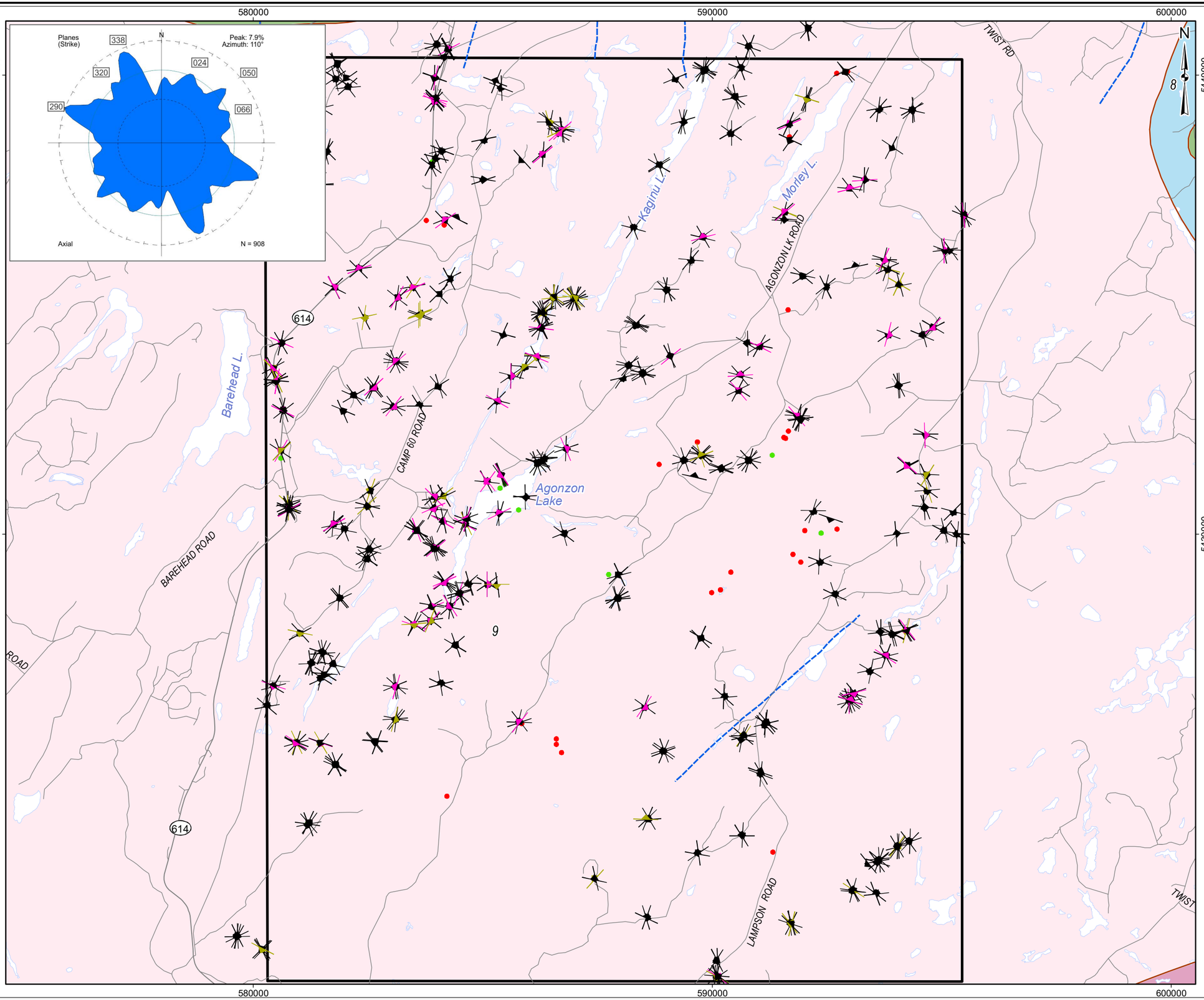

LEGEND

- Withdrawal Area
- Main Road
- Local Road
- Waterbody
- Observation - Outcrop (10)
- Observation - Overburden (25)
- Sub horizontal joint: 0-30° (80)
- Intermediate joint: 31-60° (60)
- Sub vertical joint: 61-90° (768)

Bedrock Geology

- Geological Boundary
- Mapped Fault
- 13: Granite-granodiorite
- 9: Gneissic tonalite suite
- 8: Gabbro
- 2: Mafic metavolcanic Rocks

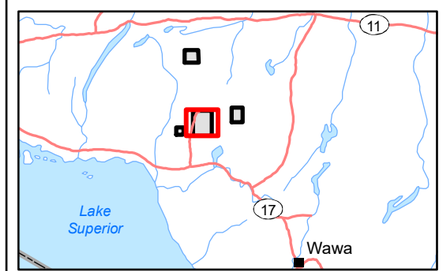

REFERENCE

Base Data: Land Information Ontario (obtained 2015);
CanVec Topography (obtained 2015)

Bedrock Geology: MRD 126-REV1 (Ontario Geological Survey, 2011);
Ontario Geological Survey Map 2665 (Santaguida, 2001);
Map 2666 (Santaguida, 2001);
Map 2667 (Johns, McIlraith and Stott, 2003);
Map 2668 (Johns and McIlraith, 2003)

0 2 km

srk consulting

PROJECT
DETAILED MAPPING REPORT
Manitouwadge Area, Ontario

TITLE
Black-Pic Batholith Area West Joints

DESIGN	KR	02 SEP 2014	**Figure 5.3.12**	REVISION 2
GIS	JA	02 AUG 2017		UTM ZONE 16N
CHECK	CN	02 AUG 2017		NAD 1983
REVIEW	JPS	02 AUG 2017		1:81,000

File: SRK_NWMO_ManStudy_AreaC_Fig5.3.12

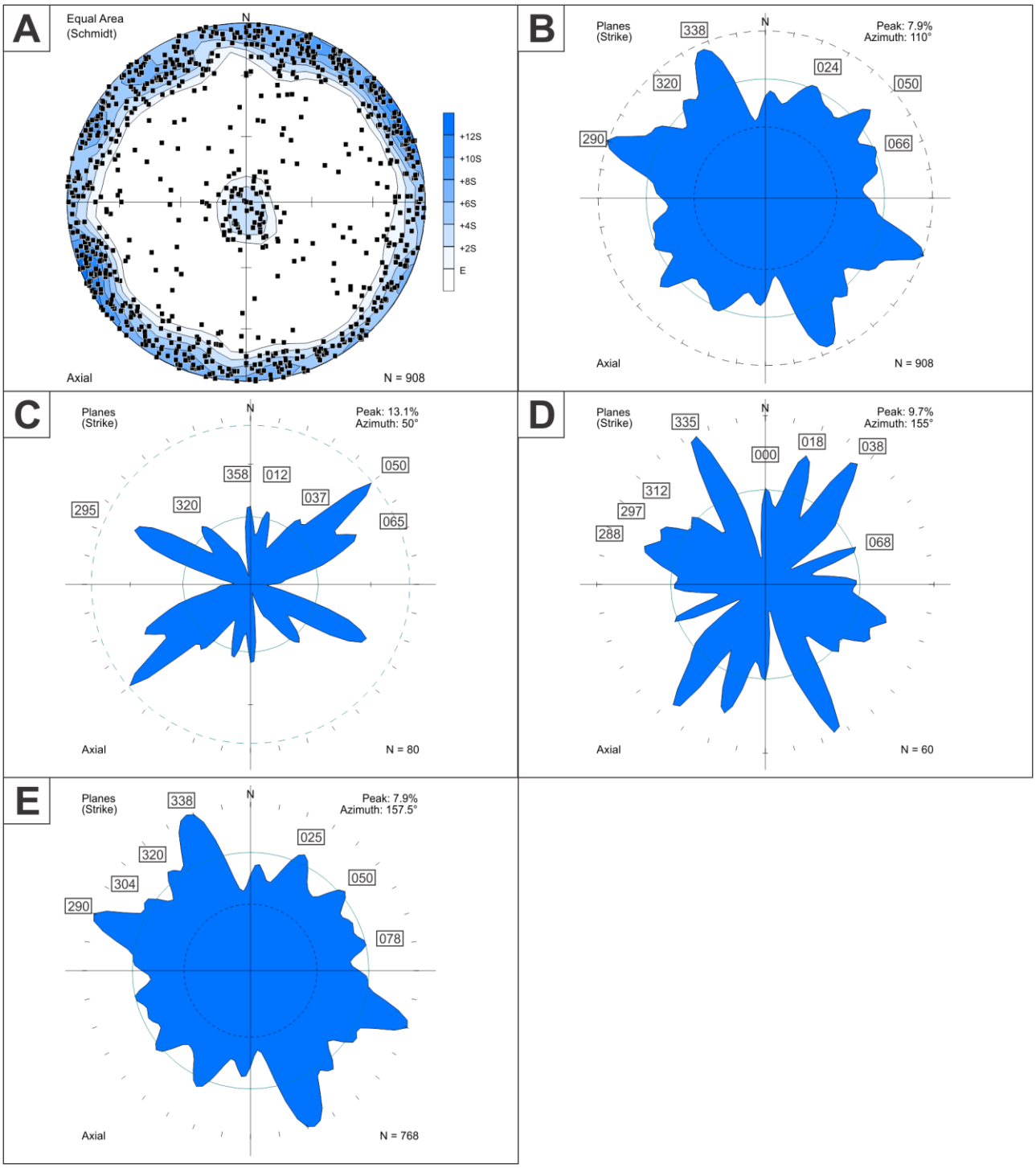

Figure 5.3.13: Black-Pic Batholith Area - West – Joint Orientation Data

A: All joints displayed as equal area lower hemisphere stereonet plot of poles to planes. (n=908).
B: All joints displayed as rose diagram of trends of planes with orientation of all peaks greater than the expected value E (n=908).
C: All joints with a dip ≤ 30 degrees displayed as rose diagram of trends of planes (n=80).
D: All joints with a dip between 31 - 60 degrees displayed as rose diagram of trends of planes (n=60).
E: All joints with a dip > 60 degrees displayed as rose diagram of trends of planes (n=768).

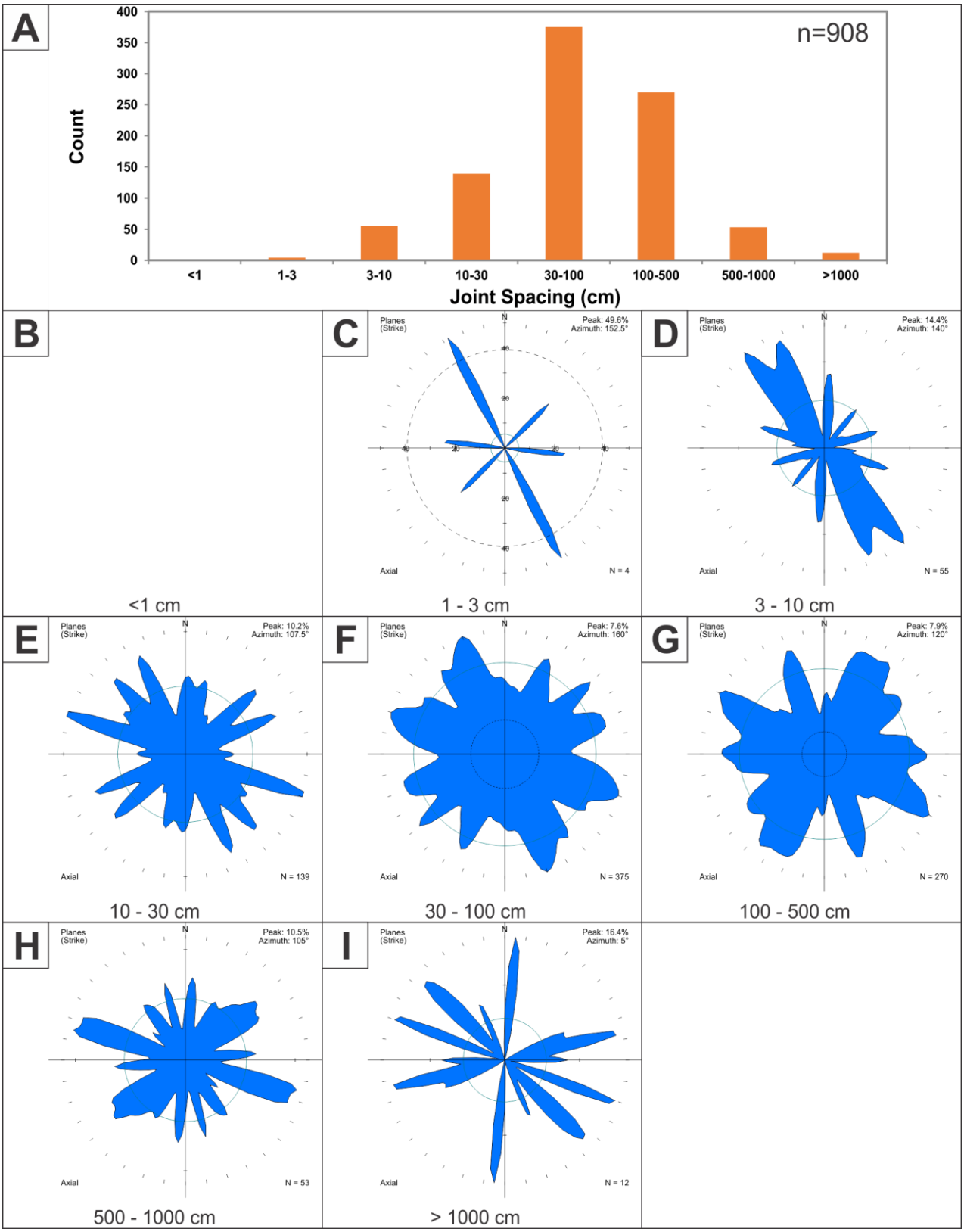

Figure 5.3.14: Black-Pic Batholith Area - West – Joint Spacing Summary

A: Histogram showing frequency distribution of joint spacing for all orientations and rock types (n=908).
B – I: Joints with the given joint spacing displayed as rose diagram of trends of planes. Any missing figures indicate no joints with that spacing were measured in this area.

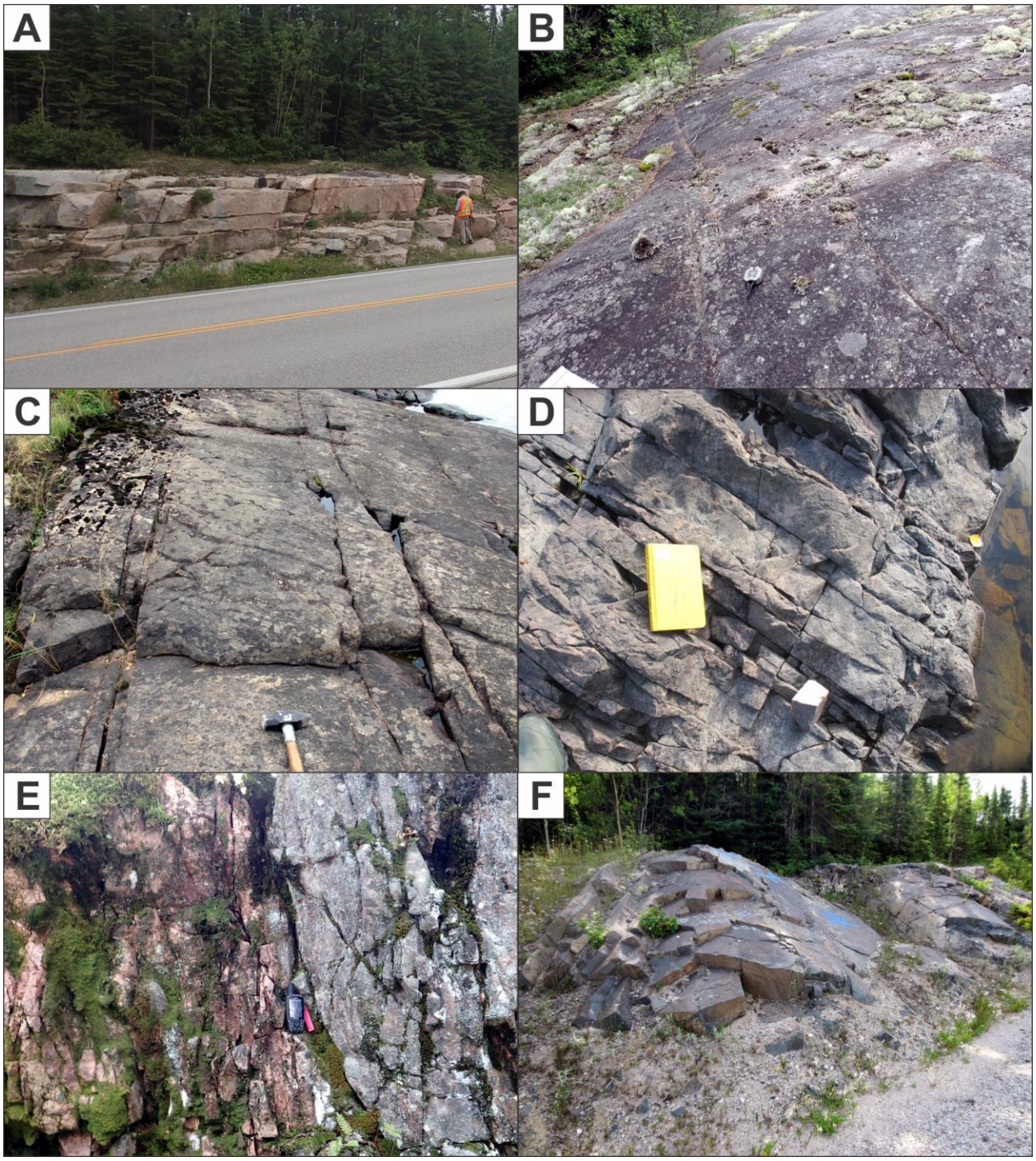

Figure 5.3.15: Black-Pic Batholith Area - West Field Examples of Joints

A: Example of sub horizontal joint set cutting tonalite gneiss (Stn 16BH0064, looking SE, person for scale).
B: Example of wide joint spacing in tonalite gneiss (Stn 16BH0041, looking S, compass for scale).
C: Example of moderate joint spacing in tonalite gneiss (Stn 16CN0063, looking E, hammer for scale).
D: Example of tight joint spacing in granite (Stn 16CN0127, looking N, book for scale).
E: Example of multiple, tight, irregular joint sets in granite (Stn 16BH0117, section looking W, GPS for scale).
F: Unusual, curviplanar exfoliation joint set parallel to outcrop surface in mafic dyke (Stn 16JK0059, looking SE, no scale).

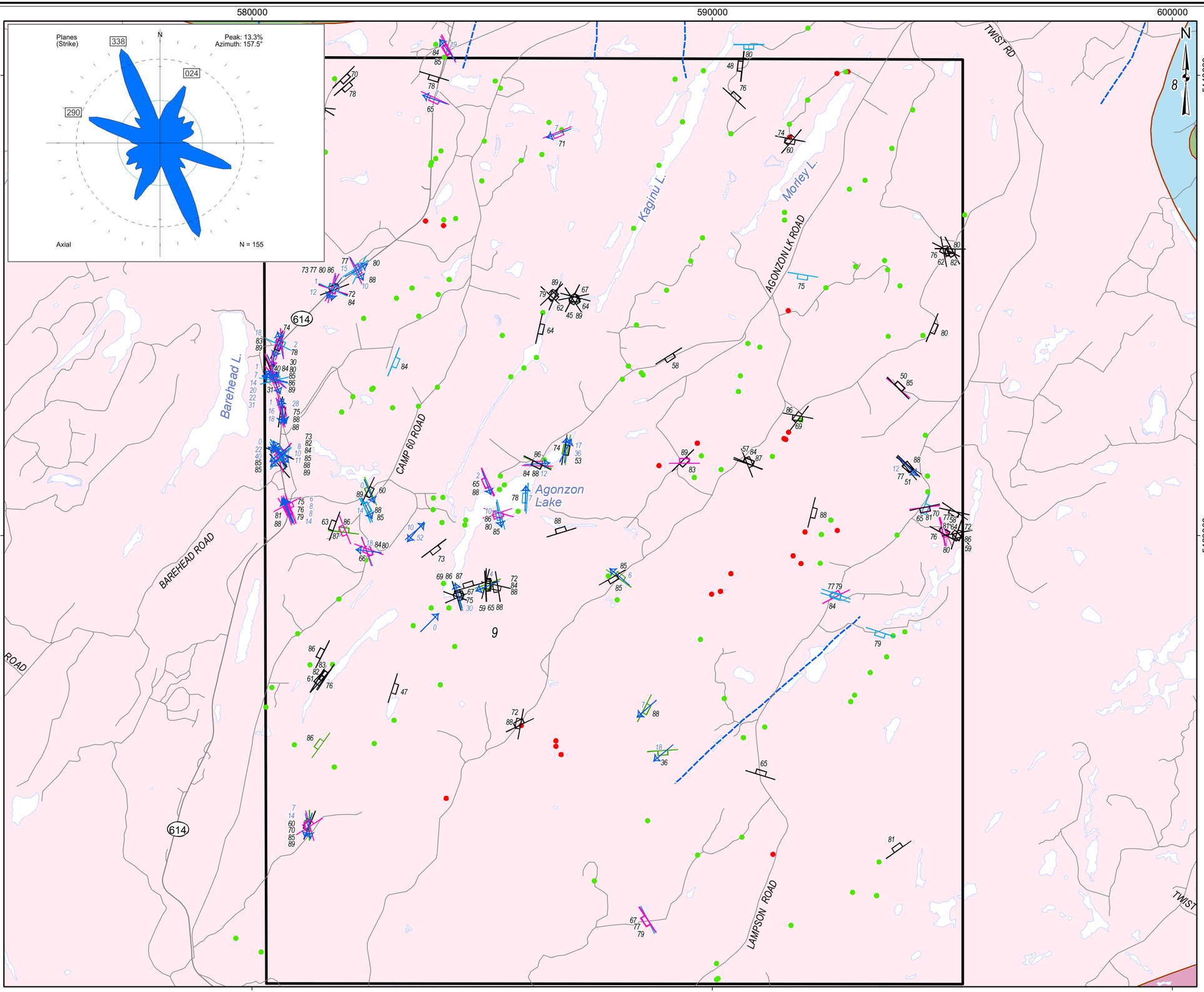

LEGEND

- Withdrawal Area
- Main Road
- Local Road
- Waterbody
- Observation - Outcrop (140)
- Observation - Overburden (25)
- Fault - Sinistral (23)
- Fault - Dextral (42)
- Fault - Strike (10)
- Fault - Unknown (80)
- Slickenline (49)

Bedrock Geology

- Geological Boundary
- Mapped Fault
- 13: Granite-granodiorite
- 9: Gneissic tonalite suite
- 8: Gabbro
- 2: Mafic metavolcanic Rocks

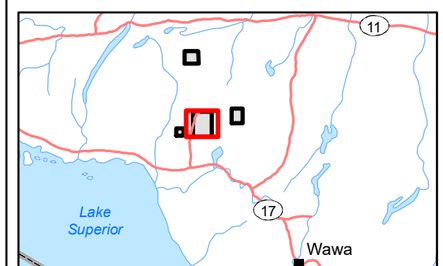

REFERENCE

Base Data: Land Information Ontario (obtained 2015); CanVec Topography (obtained 2015)

Bedrock Geology: MRD 126-REV1 (Ontario Geological Survey, 2011); Ontario Geological Survey Map 2665 (Santaguida, 2001); Map 2666 (Santaguida, 2001); Map 2667 (Johns, McIlraith and Stott, 2003); Map 2668 (Johns and McIlraith, 2003)

0 2 km

srk consulting

PROJECT: DETAILED MAPPING REPORT
Manitouwadge Area, Ontario

TITLE: **Black-Pic Batholith Area West Faults**

DESIGN	KR	02 SEP 2014	**Figure 5.3.16**	REVISION 2
GIS	JA	02 AUG 2017		UTM ZONE 16N
CHECK	CN	02 AUG 2017		NAD 1983
REVIEW	JPS	02 AUG 2017		1:81,000

File: SRK_NWMO_ManStudy_AreaC_Fig5.3.16

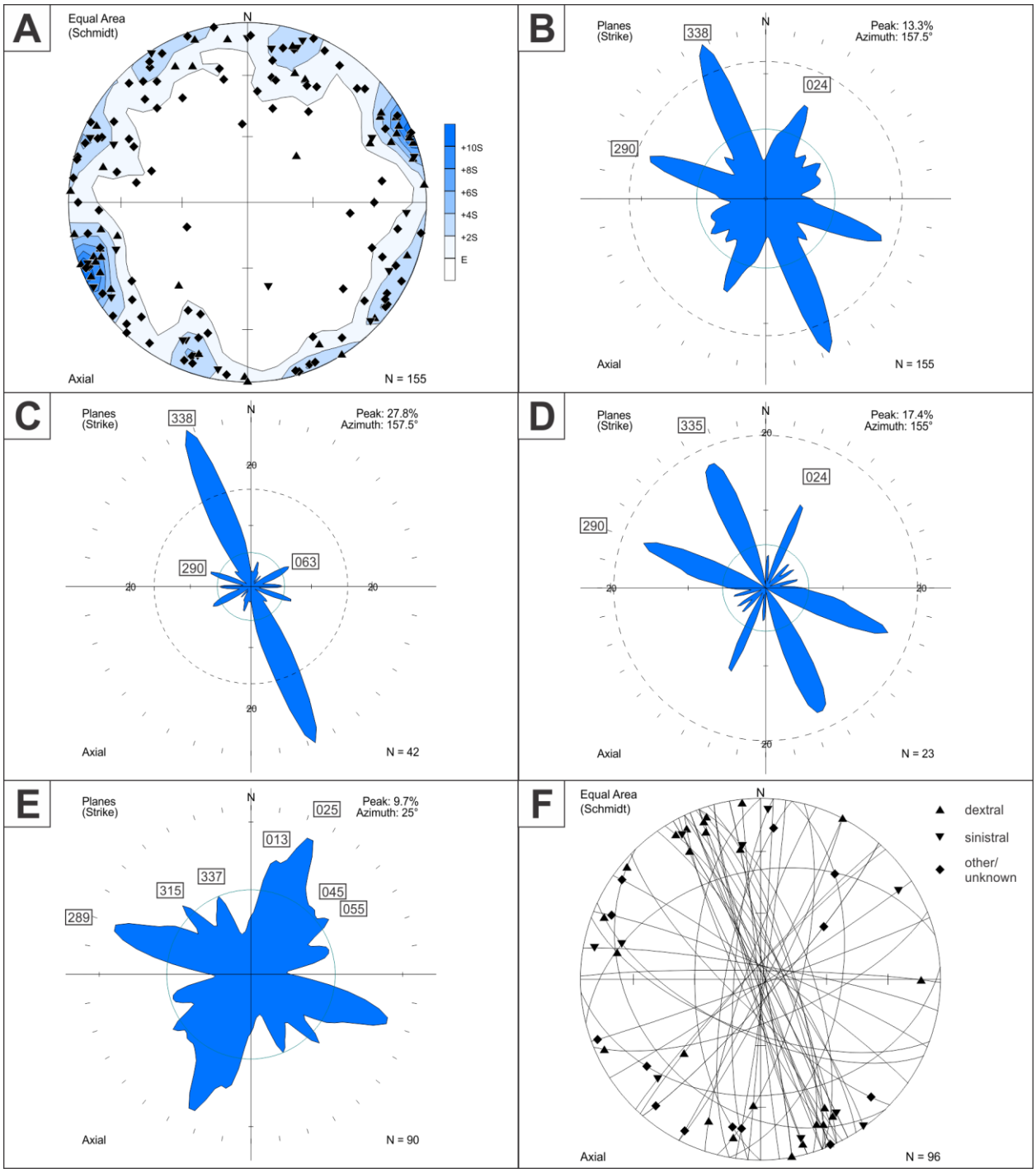

Figure 5.3.17: Black-Pic Batholith Area - West – Fault Orientation Data

A: All faults displayed as equal area lower hemisphere stereonet plot of poles to planes. Dextral faults: filled upright triangles (n=42). Sinistral faults: filled inverted triangles (n=23). Other or unknown movement sense faults: filled diamond (n=90).
B: All faults displayed as rose diagram of trends of planes with orientation of all peaks greater than the expected value E (n=155).
C: Dextral faults displayed as rose diagram of trends of planes (n=42).
D: Sinistral faults displayed as rose diagram of trends of planes (n=23).
E: Other or unknown movement sense faults displayed as rose diagram of trends of planes (n=90).
F: Slickenline data displayed as equal area lower hemisphere stereonet plot of lineation points and great circles of the respective faults on which they were measured. Lineation plotted as rake calculated from measured trend and plunge.

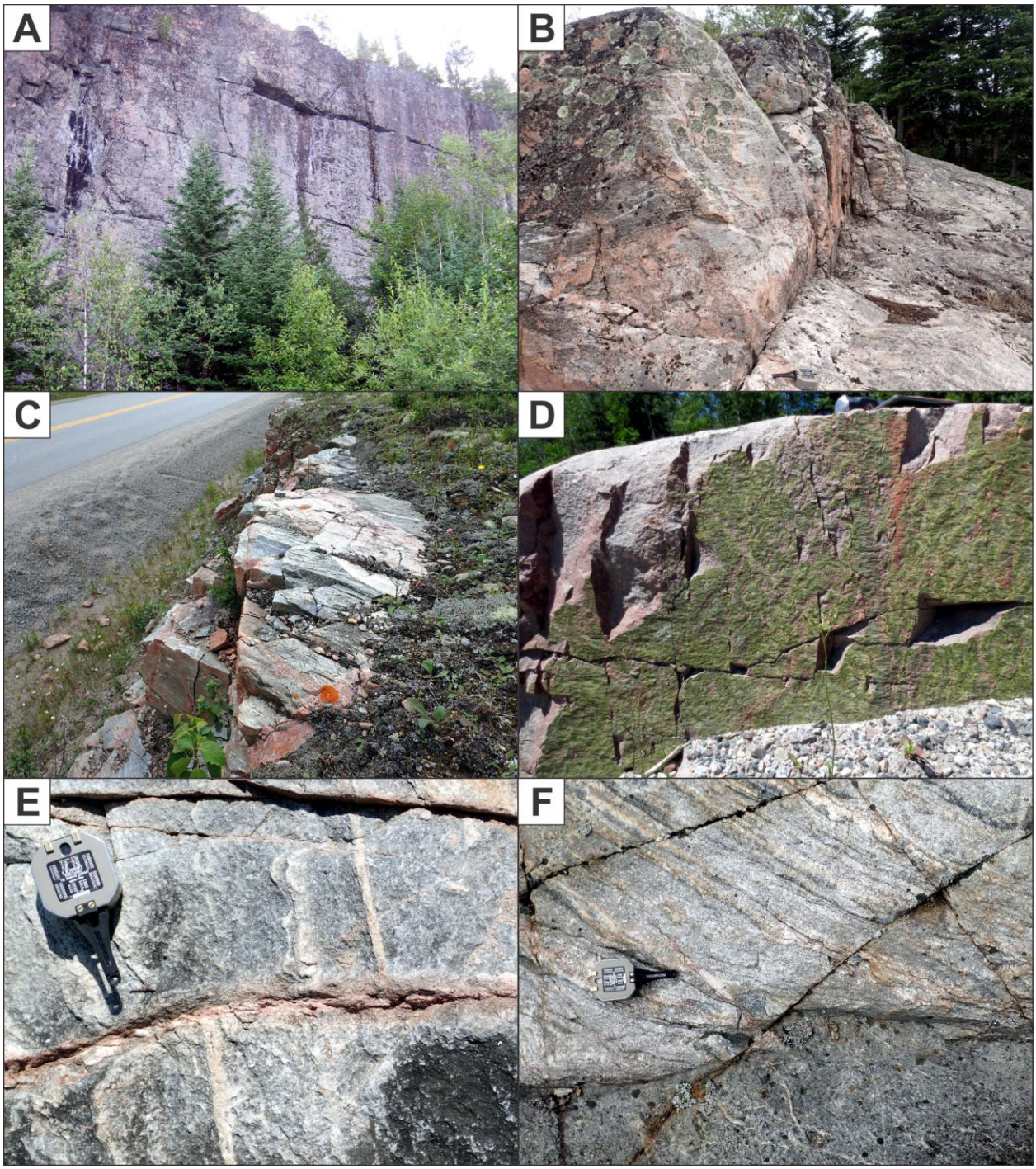

Figure 5.3.18: Black-Pic Batholith Area - West – Field Examples of Faults

A: Cliff edge coincident with major NNW to NNE-trending surficial lineament (Stn 16JK0132, looking SE, trees for scale).
B: Discrete, SE-trending fault with dextral kinematic indicators (Stn 16BH0025, looking SE, compass for scale).
C: Domain of discrete, NNW-trending, strongly altered dextral faults (Stn 16BH0079, looking NW, compass for scale).
D: Epidote slickenlines and steps indicate dextral slip on NNW-trending fault (Stn 16JK0055, looking W, hammer for scale).
E: Discrete E-trending dextral strike-separation fault with associated hematite alteration (Stn 16BH0011, looking S, compass for scale).
F: Discrete NW-trending sinistral strike-separation fault with little associated alteration (Stn 16BH0154, looking W, compass for scale).

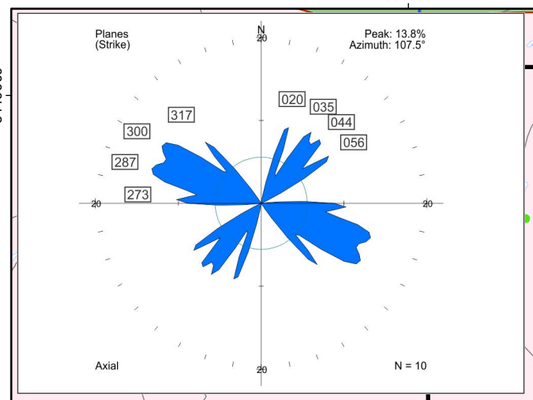

580000 590000 600000

5440000 5430000

N

8

TWIST RD

Kaginú L.

Morley L.

AGONZON LK ROAD

74

84

81

614

Barehead L.

CAMP 60 ROAD

Agonzon Lake

80

78

BAREHEAD ROAD

ROAD

9

53

37

48

77

52

614

LAMPSON ROAD

TWIST

580000 590000 600000

5440000 5430000

LEGEND

- Withdrawal Area
- Main Road
- Local Road
- Waterbody
- Observation - Outcrop (209)
- Observation - Overburden (25)
- Extension Vein (8)
- Shear Vein (2)

Bedrock Geology

- Geological Boundary
- Mapped Fault
- 13: Granite-granodiorite
- 9: Gneissic tonalite suite
- 8: Gabbro
- 2: Mafic metavolcanic Rocks

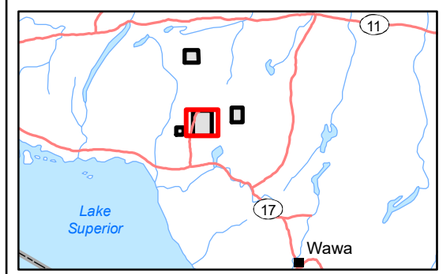

REFERENCE

Base Data: Land Information Ontario (obtained 2015);
CanVec Topography (obtained 2015)

Bedrock Geology: MRD 126-REV1 (Ontario Geological Survey, 2011);
Ontario Geological Survey Map 2665 (Santaguida, 2001);
Map 2666 (Santaguida, 2001);
Map 2667 (Johns, McIlraith and Stott, 2003);
Map 2668 (Johns and McIlraith, 2003)

0 2 km

srk consulting

PROJECT

DETAILED MAPPING REPORT
Manitouwadge Area, Ontario

TITLE

Black-Pic Batholith Area West Veins

DESIGN	KR	02 SEP 2014	**Figure 5.3.19**	REVISION 2
GIS	JA	02 AUG 2017		UTM ZONE 16N
CHECK	CN	02 AUG 2017		NAD 1983
REVIEW	JPS	02 AUG 2017		1:81,000

File: SRK_NWMO_ManStudy_AreaC_Fig5.3.19

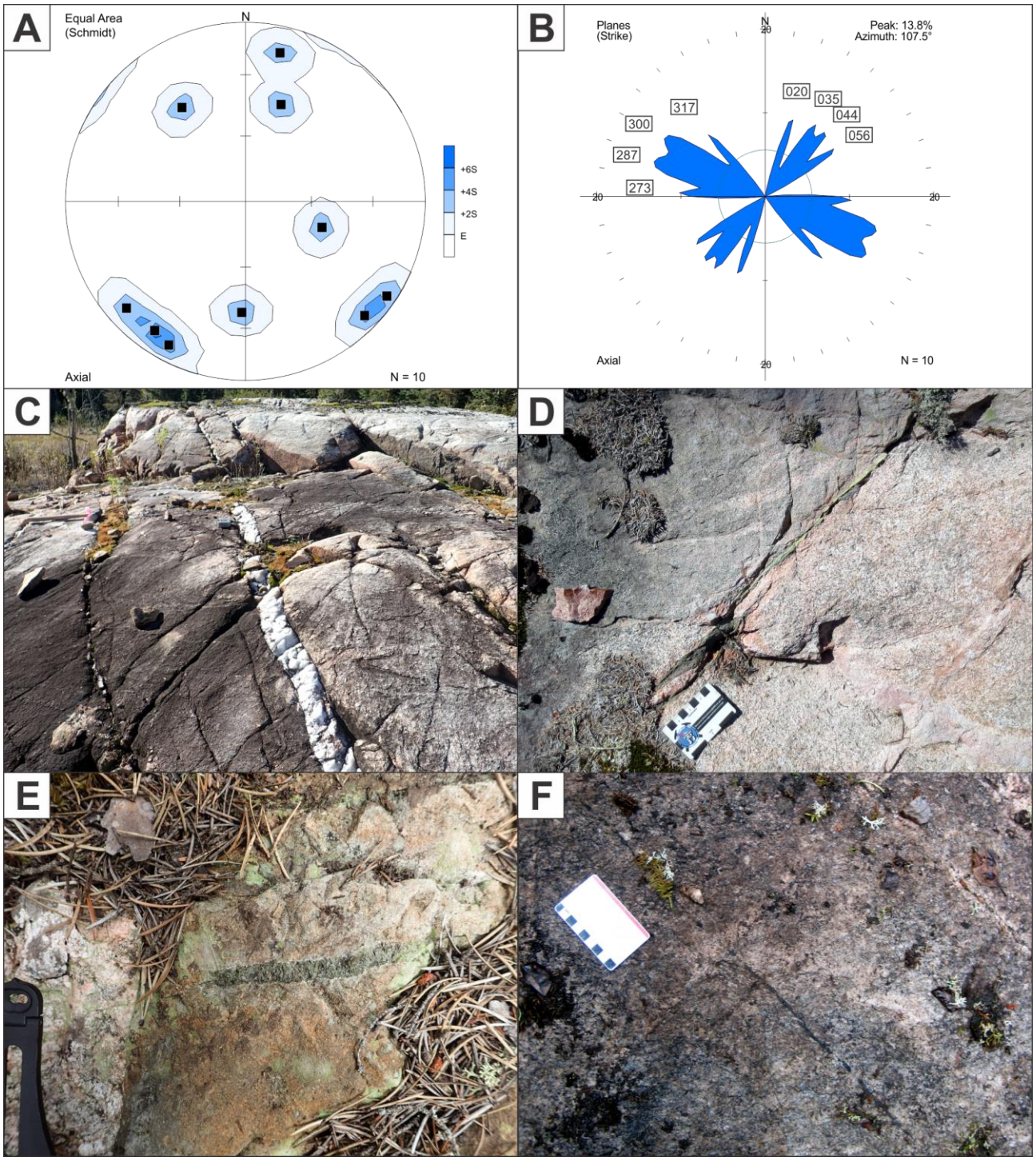

Figure 5.3.20: Black-Pic Batholith Area - West – Vein Orientation Data and Field Examples

A: All veins displayed as equal area lower hemisphere stereonet plot of poles to planes. (n=10).
B: All veins displayed as rose diagram of trends of planes with orientation of all peaks greater than the expected value E (n=10).
C: SW-trending straight quartz vein set (Stn 16BH0258, looking W, compass for scale).
D: Narrow, epidote shear vein (Stn 16JK0010, looking S, card for scale).
E: Narrow, epidote extension vein (Stn 16BH0040, looking N, compass for scale).
F: Narrow chlorite vein (Stn 16JK0167, looking E, card for scale).

580000 590000 600000

5440000 5430000

N

8 9

614

Barehead L. Kaginù L. Morley L. Agonzon Lake

AGONZON LK ROAD CAMP 60 ROAD BAREHEAD ROAD TWIST RD LAMPSON ROAD

LEGEND

- Withdrawal Area
- Main Road
- Local Road
- Waterbody
- Observation - Outcrop (217)
- Observation - Overburden (25)
- Alteration - Hematite
- Alteration - Quartz
- Alteration - Epidote
- Alteration - Chlorite

Bedrock Geology

- Geological Boundary
- Mapped Fault
- 13: Granite-granodiorite
- 9: Gneissic tonalite suite
- 8: Gabbro
- 2: Mafic metavolcanic Rocks

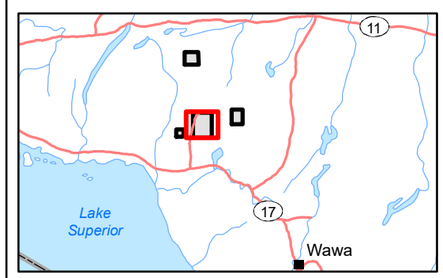

REFERENCE

Base Data: Land Information Ontario (obtained 2015); CanVec Topography (obtained 2015)

Bedrock Geology: MRD 126-REV1 (Ontario Geological Survey, 2011); Ontario Geological Survey Map 2665 (Santaguida, 2001); Map 2666 (Santaguida, 2001); Map 2667 (Johns, McIlraith and Stott, 2003); Map 2668 (Johns and McIlraith, 2003)

0 2 km

srk consulting

PROJECT

DETAILED MAPPING REPORT
Manitouwadge Area, Ontario

TITLE

Black-Pic Batholith Area West
Secondary Minerals and Alteration

DESIGN	KR	02 SEP 2014	**Figure 5.3.21**	REVISION 2
GIS	JA	02 AUG 2017		UTM ZONE 16N
CHECK	CN	02 AUG 2017		NAD 1983
REVIEW	JPS	02 AUG 2017		1:81,000

File: SRK_NWMO_ManStudy_AreaC_Fig5.3.21

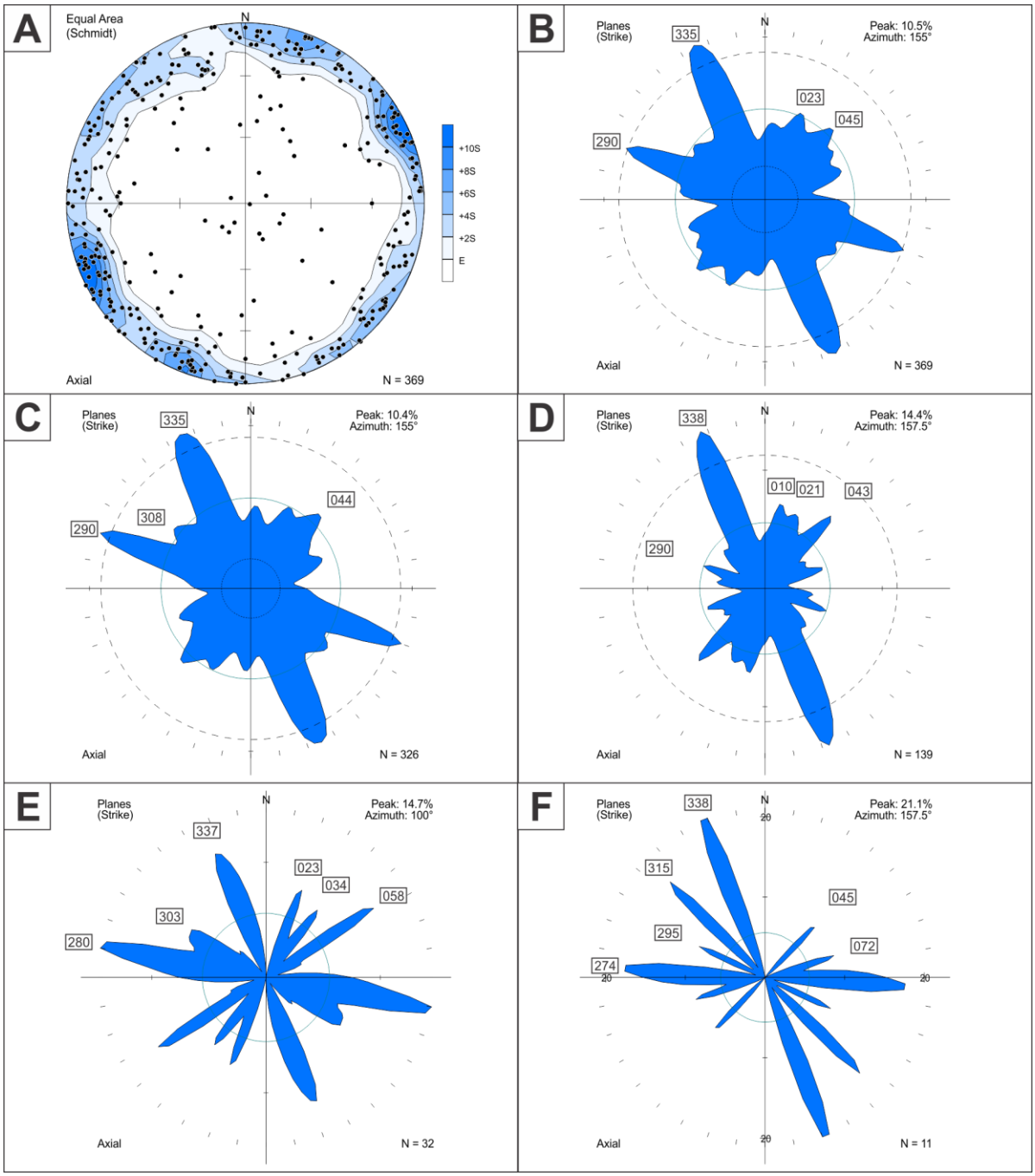

Figure 5.3.22: Black-Pic Batholith Area - West – Secondary Minerals and Alteration Orientation Data

A: All structures with visible alteration displayed as equal area lower hemisphere stereonet plot of poles to planes. (n=369).

B: All structures with visible alteration displayed as rose diagram of trends of planes with orientation of all peaks greater than the expected value E (n=369).

C: All structures with visible hematite alteration displayed as rose diagram of trends of planes with orientation of all peaks greater than the expected value E (n=326).

D: All structures with visible epidote alteration displayed as rose diagram of trends of planes with orientation of all peaks greater than the expected value E (n=139).

E: All structures with visible quartz alteration displayed as rose diagram of trends of planes with orientation of all peaks greater than the expected value E (n=32).

F: All structures with visible chlorite alteration displayed as rose diagram of trends of planes with orientation of all peaks greater than the expected value E (n=11).

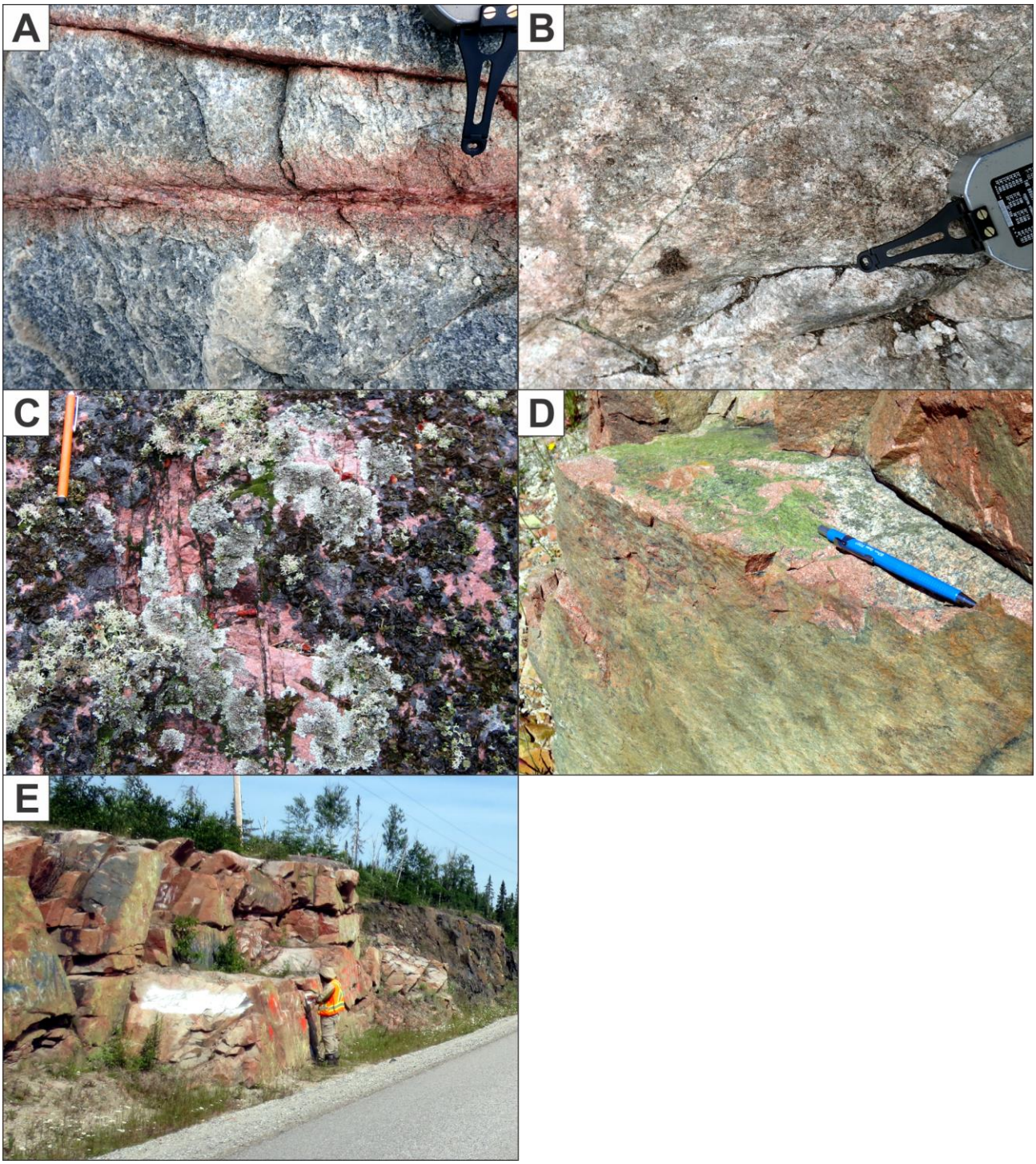

Figure 5.3.23: Black-Pic Batholith Area - West – Field Examples of Secondary Minerals and Alteration

A: Hematite staining and bleaching around joints and discrete faults (Stn 16BH0011, looking S, compass for scale).
B: Narrow epidote filled, weakly hematite stained joints (Stn 16BH0032, looking SE, compass for scale).
C: Pervasive hematite alteration associated with narrow spaced joint set (Stn 16JK0162, looking N, pen for scale).
D: Strong epidote and hematite alteration on multiple joint set surfaces (Stn 16JK0056, looking E, pen for scale).
E: Strong epidote and hematite alteration associated with domain of discrete NNW-trending faults adjacent to Marathon dyke (Stn 16JK0059, looking N, person for scale).

610000
620000
5440000
5430000
N

FARIES-
MOSHKINABI
INTRUSION

BLACK-PIC
BATHOLITH

Macutagon
Lake
Longnega
Granitehill L.
Sunderland
Lake
Garnham
Lake
Jembi
L.

400 ROAD
ICE LAKE RD.
ICE SOUTH ROAD

13
8
7
2
9

16JK0205 16JK0204 16JK0206 16JK0207 16JK0209 16JK0208
16BH0124 16BH0204 16BH0203 16BH0239 16BH0202 16BH0240 16BH0205 16BH0238
16CN0145 16CN0144 16BH0125 16CN0074 16BH0126 16BH0127 16JK0078 16CN0073 16CN0075
16JK0077 16CN0076 16JK0076 16JK0075 16JK0074 16CN0077 16JK0072 16JK0071
16BH0242 16BH0243 16BH0244 16CN0014 16BH0066 16CN0015 16JK0073 16BH0067
16CN0016 16BH0068 16BH0069 16BH0245 16BH0170 16BH0172 16BH0171 16BH0173 16BH0174 16BH0070 16BH0290
16CN0140 16CN0139 16CN0138 16BH0177 16BH0176 16BH0291 16BH0246 16BH0214 16BH0213 16BH0247
16BH0212 16BH0288 16BH0248 16JK0174 16CN0137 16BH0075 16CN0142 16BH0074 16JK0173 16BH0263
16JK0170 16BH0261 16BH0264 16JK0172 16JK0171 16BH0073 16BH0262 16CN0141 16JK0178 16BH0072
16CN0115 16JK0177 16JK0176 16JK0179 16JK0086 16CN0114 16CN0113 16JK0085 16JK0180
16BH0228 16JK0233 16JK0234 16BH0227 16BH0225 16BH0224 16BH0226 16JK0232
16JK0199 16JK0198 16JK0084 16BH0229 16JK0194 16BH0230
16CN0117 16CN0116 16JK0230 16JK0197 16JK0195 16JK0229 16JK0196 16JK0228 16JK0231
16JK0087 16JK0082 16CN0083 16JK0083 16CN0082 16CN0081 16CN0084 16JK0081 16CN0079 16CN0080
16JK0080
16JK0218 16JK0216 16JK0217

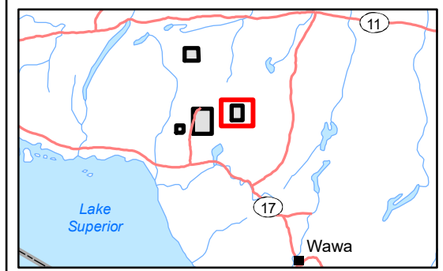

LEGEND

- Withdrawal Area
- Local Road
- Waterbody
- Observation - Outcrop (123)
- Observation - Overburden (4)
- Predicted Outcrop

Bedrock Geology

- Geological Boundary
- Mapped Fault
- 13: Granite-granodiorite
- 9: Gneissic tonalite suite
- 8: Gabbro
- 7: Ultramafic plutonic rocks
- 2: Mafic metavolcanic Rocks

REFERENCE

Base Data: Land Information Ontario (obtained 2015);
CanVec Topography (obtained 2015)

Bedrock Geology: MRD 126-REV1 (Ontario Geological Survey, 2011);
Ontario Geological Survey Map 2665 (Santaguida, 2001);
Map 2666 (Santaguida, 2001);
Map 2667 (Johns, McIlraith and Stott, 2003);
Map 2668 (Johns and McIlraith, 2003)

0 2 km

srk consulting

PROJECT
DETAILED MAPPING REPORT
Manitouwadge Area, Ontario

TITLE
Black-Pic Batholith Area East
Mapping Observation Locations

DESIGN	KR	02 SEP 2014	**Figure 5.4.1**	REVISION 2
GIS	JA	02 AUG 2017		UTM ZONE 16N
CHECK	BH	02 AUG 2017		NAD 1983
REVIEW	JPS	02 AUG 2017		1:80,000

File: SRK_NWMO_ManStudy_AreaD_Fig5.4.1

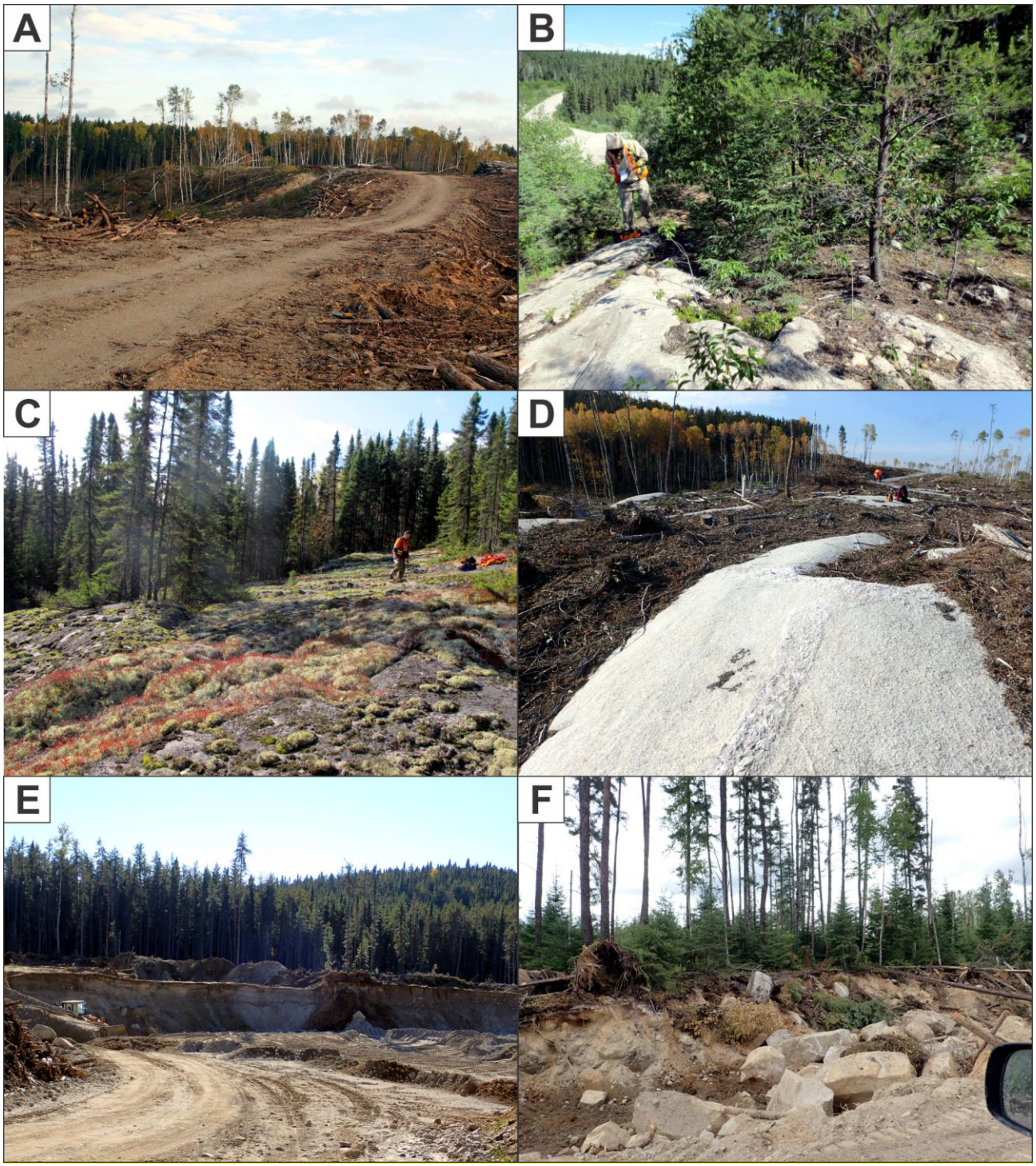

Figure 5.4.2: Black-Pic Batholith Area - East – Field Examples of Accessibility and Bedrock Exposure

A: New logging road access following large esker (Stn 16BH0242, looking N, no scale).
B: Typical rolling terrain and main logging road access (Stn 16JK0081, looking N, person for scale).
C: Large, partly moss and overburden covered outcrop (Stn 16CN0138, looking SW, person for scale).
D: Well-exposed, completely clean outcrops in area of recent logging (Stn 16BH0243, looking SW, person for scale).
E: Gravel pit showing thick section of glacial overburden (Stn 16BH0213, looking SW, loader for scale).
F: Large boulders in thick, poorly sorted glacial overburden (Stn 16BH0174, looking S, truck mirror for scale).

610000
620000
5440000
5430000
N

FARIES-
MOSHKINABI
INTRUSION

BLACK-PIC
BATHOLITH

13
7
2
9
8
400 ROAD
ICE LAKE RD.
ICE SOUTH ROAD
Macutagon
Lake
Longnega L.
Granitehill L.
Garnham
Lake
Jembi
L.
Sunderland
Lake

LEGEND

- Withdrawal Area
- Local Road
- Waterbody
- Observation - Outcrop

Bedrock Geology

- Geological Boundary
- Mapped Fault
- 13: Granite-granodiorite
- 9: Gneissic tonalite suite
- 8: Gabbro
- 7: Ultramafic plutonic rocks
- 2: Mafic metavolcanic Rocks

Main Lithology

- Granodiorite (34)
- Tonalite (78)

REFERENCE

Base Data: Land Information Ontario (obtained 2015);
CanVec Topography (obtained 2015)

Bedrock Geology: MRD 126-REV1 (Ontario Geological Survey, 2011);
Ontario Geological Survey Map 2665 (Santaguida, 2001);
Map 2666 (Santaguida, 2001);
Map 2667 (Johns, McIlraith and Stott, 2003);
Map 2668 (Johns and McIlraith, 2003)

0 2 km

srk consulting

PROJECT
DETAILED MAPPING REPORT
Manitouwadge Area, Ontario

TITLE
Black-Pic Batholith Area East
Main Lithological Units

DESIGN	KR	02 SEP 2014	**Figure 5.4.3**	REVISION 2
GIS	JA	02 AUG 2017		UTM ZONE 16N
CHECK	BH	02 AUG 2017		NAD 1983
REVIEW	JPS	02 AUG 2017		1:80,000

File: SRK_NWMO_ManStudy_AreaD_Fig5.4.3

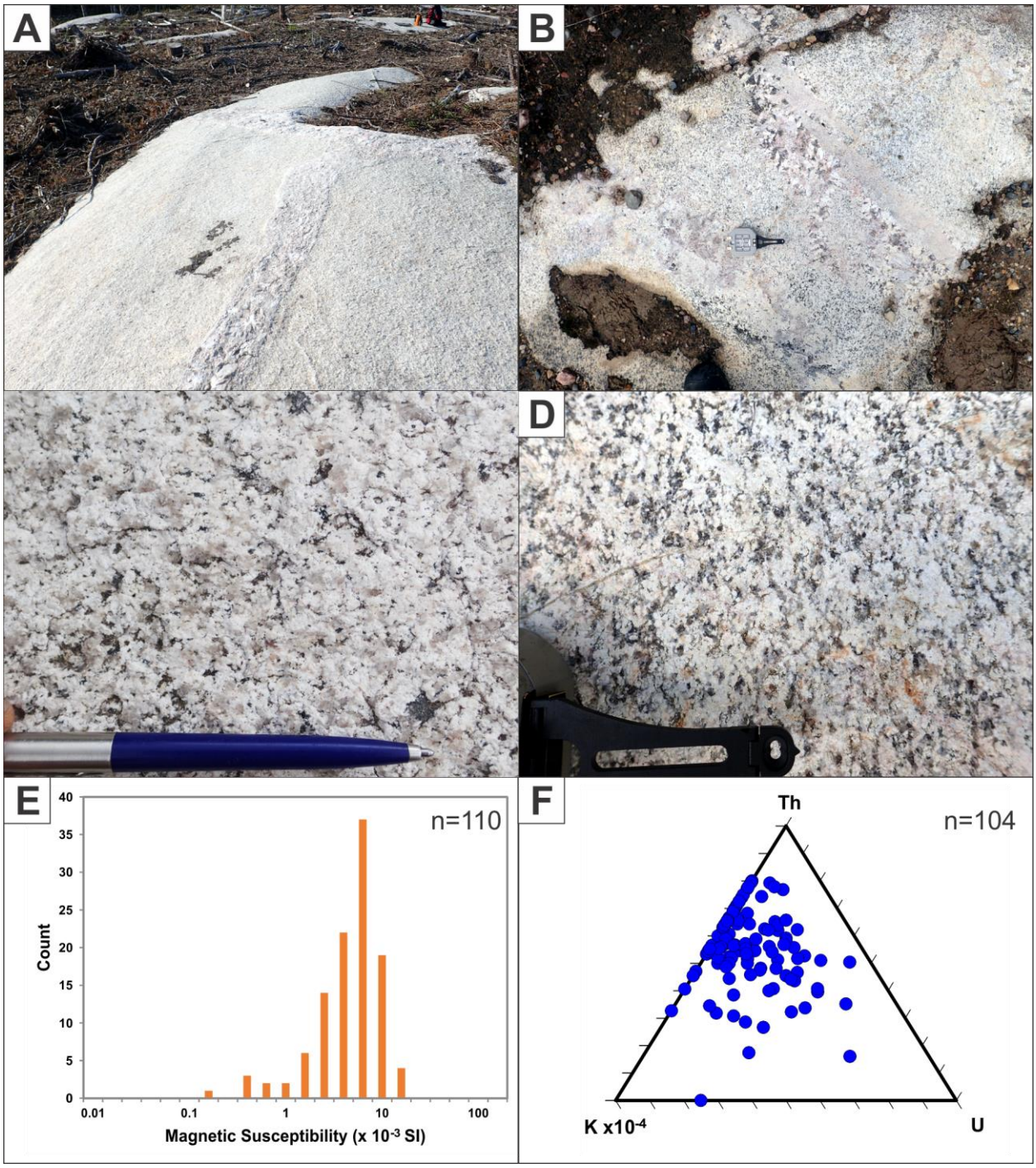

Figure 5.4.4: Black-Pic Batholith Area - East – Field Examples of Main Lithology: Tonalite to Granodiorite

A: Homogeneous tonalite cut by light pink pegmatite dykes (Stn 16BH0243, looking SW, pack for scale).
B: Homogeneous granodiorite cut by light pink pegmatite and fine grained felsic dykes (Stn 16BH0066, looking W, compass for scale).
C: Close-up of tonalite showing mineral composition and texture (Stn 16BH0176, looking S, pen for scale).
D: Close-up of granodiorite showing mineral composition and texture (Stn 16BH0066, looking W, compass for scale).
E: Logarithmic histogram plot of magnetic susceptibility for tonalite and granodiorite rocks.
F: Ternary plot of gamma ray spectrometer data for tonalite and granodiorite rocks.

610000
620000
5440000
5430000
N

FARIES-
MOSHKINABI
INTRUSION

BLACK-PIC
BATHOLITH

13
7
2
9
8
400 ROAD
ICE LAKE RD.
ICE SOUTH ROAD
Macutagon
Lake
Longnega L.
Granitehill L.
Garnham
Lake
Jembi
L.
Sunderland
Lake

LEGEND

- Withdrawal Area
- Local Road
- Waterbody
- Observation - Outcrop

Bedrock Geology

- Geological Boundary
- Mapped Fault
- 13: Granite-granodiorite
- 9: Gneissic tonalite suite
- 8: Gabbro
- 7: Ultramafic plutonic rocks
- 2: Mafic metavolcanic Rocks

Minor Lithology

- Diorite to Granodiorite (7)
- Granite (19)
- Gabbro (3)
- Migmatitic Metasedimentary Rock (1)

REFERENCE

Base Data: Land Information Ontario (obtained 2015);
CanVec Topography (obtained 2015)

Bedrock Geology: MRD 126-REV1 (Ontario Geological Survey, 2011);
Ontario Geological Survey Map 2665 (Santaguida, 2001);
Map 2666 (Santaguida, 2001);
Map 2667 (Johns, McIlraith and Stott, 2003);
Map 2668 (Johns and McIlraith, 2003)

0 2 km

srk consulting

PROJECT
DETAILED MAPPING REPORT
Manitouwadge Area, Ontario

TITLE
Black-Pic Batholith Area East
Minor Lithological Units

DESIGN	KR	02 SEP 2014	**Figure 5.4.5**	REVISION 2
GIS	JA	02 AUG 2017		UTM ZONE 16N
CHECK	BH	02 AUG 2017		NAD 1983
REVIEW	JPS	02 AUG 2017		1:80,000

File: SRK_NWMO_ManStudy_AreaD_Fig5.4.5

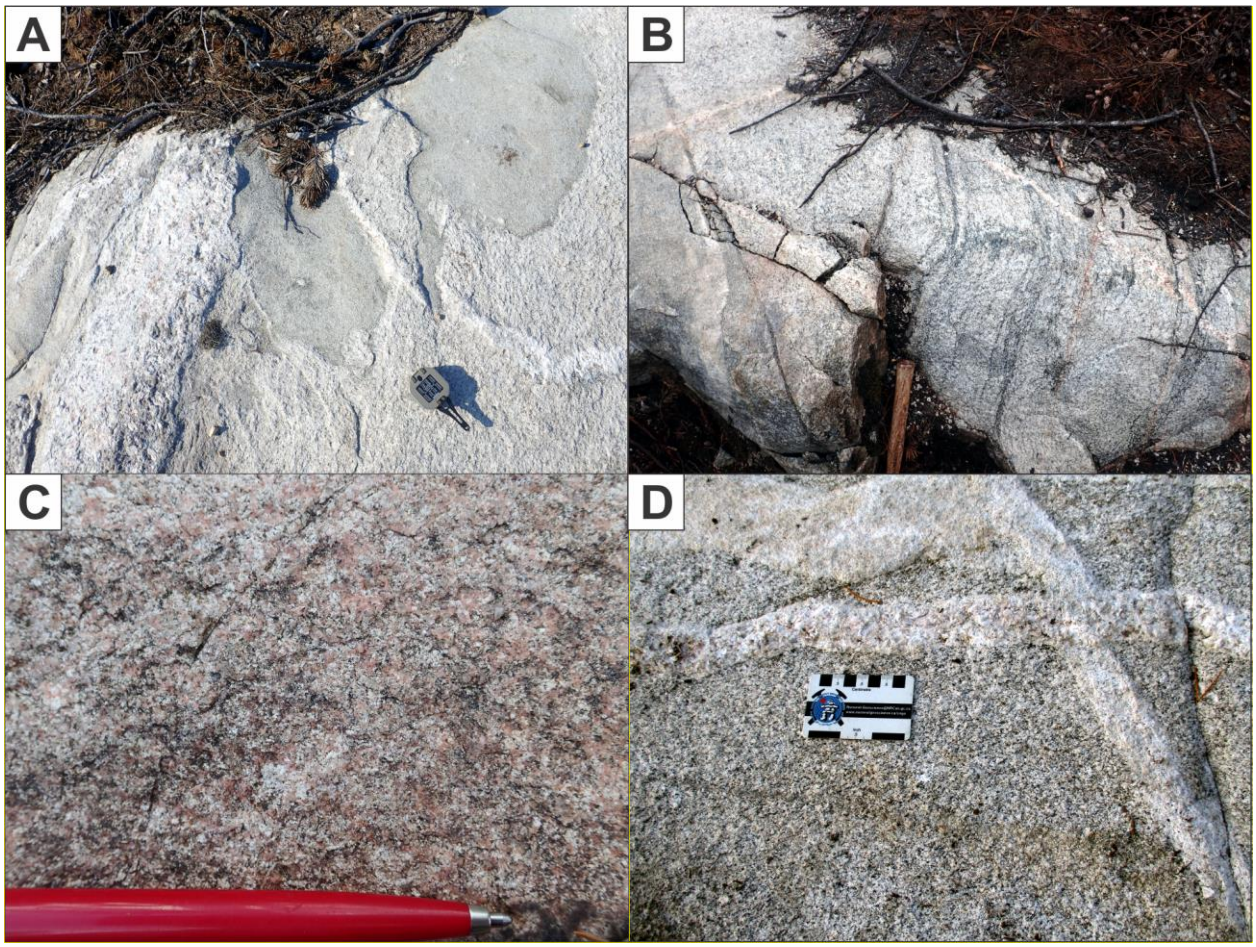

Figure 5.4.6: Black-Pic Batholith Area - East – Field Examples of Minor Lithological Units

A: Irregular diorite xenoliths in homogeneous tonalite (Stn16BH0243, looking SW, compass for scale).
B: Rare gneissic layering in homogeneous tonalite (Stn16BH0290, looking NW, hammer for scale).
C: Distinct red, leucocratic, fine-grained granite forms map scale intrusion (Stn16BH0126, looking SW, pen for scale).
D: Homogeneous tonalite host rock cut by fine-grained leucocratic felsic dyke and pink pegmatite felsic dyke (Stn16JK0209, looking NW, card for scale).

610000
620000
5440000
5430000
N

FARIES-
MOSHKINABI
INTRUSION

BLACK-PIC
BATHOLITH

Macutagon
Lake
Garnham
Lake
Jembi
L.
Longnega L.
Granitehill L.
Sunderland
Lake

400 ROAD
ICE LAKE RD.
ICE SOUTH ROAD

13
9
8
7
2

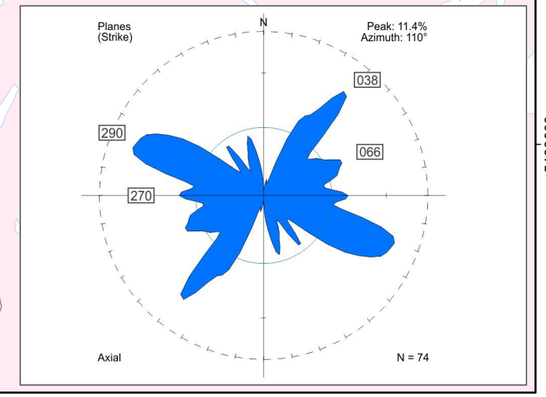

LEGEND

- Withdrawal Area
- Local Road
- Waterbody
- Observation - Outcrop (56)
- Observation - Overburden (4)
- Foliation (73)
- Gneissic Layering (2)
- Mineral Lineation

Bedrock Geology

- Geological Boundary
- Mapped Fault
- 13: Granite-granodiorite
- 9: Gneissic tonalite suite
- 8: Gabbro
- 7: Ultramafic plutonic rocks
- 2: Mafic metavolcanic Rocks

REFERENCE

Base Data: Land Information Ontario (obtained 2015);
CanVec Topography (obtained 2015)

Bedrock Geology: MRD 126-REV1 (Ontario Geological Survey, 2011);
Ontario Geological Survey Map 2665 (Santaguida, 2001);
Map 2666 (Santaguida, 2001);
Map 2667 (Johns, McIlraith and Stott, 2003);
Map 2668 (Johns and McIlraith, 2003)

0 2 km

srk consulting

PROJECT
DETAILED MAPPING REPORT
Manitouwadge Area, Ontario

TITLE
Black-Pic Batholith Area East
Tectonic Foliation

DESIGN	KR	02 SEP 2014	**Figure 5.4.7**	REVISION 2
GIS	JA	02 AUG 2017		UTM ZONE 16N
CHECK	BH	02 AUG 2017		NAD 1983
REVIEW	JPS	02 AUG 2017		1:80,000

File: SRK_NWMO_ManStudy_AreaD_Fig5.4.7

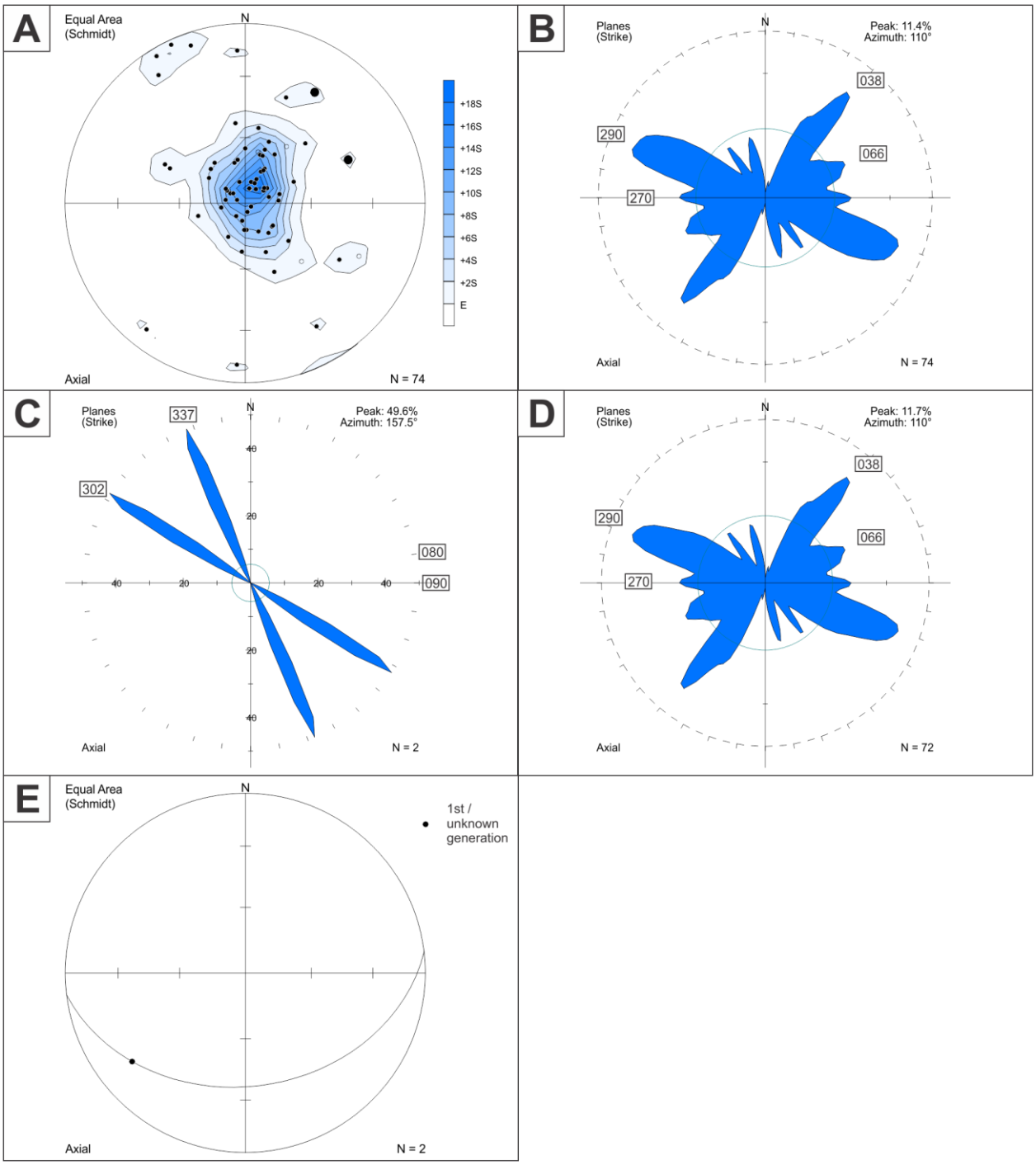

Figure 5.4.8: Black-Pic Batholith Area - East – Tectonic Foliation Orientation Data

A: All main gneissic layering and tectonic foliation displayed as equal area lower hemisphere stereonet plot of poles to planes. Gneissic layering: large circles (n=2). Mineral foliation: small circles (n=72).
B: All main gneissic layering and tectonic foliation displayed as rose diagram of trends of planes with orientation of all peaks greater than the expected value E (n=74).
C: Gneissic layering displayed as rose diagram of trends of planes (n=2).
D: Mineral Foliation displayed as rose diagram of trends of planes (n=72).
E: Mineral lineation data displayed as equal area lower hemisphere stereonet plot of lineation points and great circles of respective foliation planes in the same outcrops. Lineation plotted as rake calculated from measured trend and plunge.

610000
620000
5440000
5430000
N

FARIES-
MOSHKINABI
INTRUSION

BLACK-PIC
BATHOLITH

13
7
2
9
8

400 ROAD
ICE LAKE RD.
ICE SOUTH ROAD

Macutagon
Lake
Longnega L.
Granitehill L.
Garnham
Lake
Jembi
L.
Sunderland
Lake

86
60
16

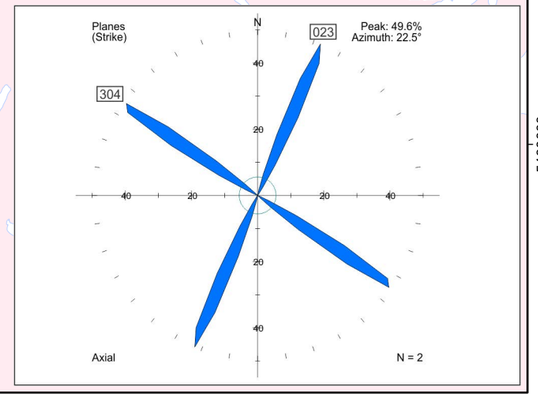

LEGEND

- Withdrawal Area
- Local Road
- Waterbody
- Observation - Outcrop (122)
- Observation - Overburden (4)
- Brittle-Ductile Shear Zone (1)
- Ductile Shear Zone - Sinistral (1)

Bedrock Geology

- Geological Boundary
- Mapped Fault
- 13: Granite-granodiorite
- 9: Gneissic tonalite suite
- 8: Gabbro
- 7: Ultramafic plutonic rocks
- 2: Mafic metavolcanic Rocks

REFERENCE

Base Data: Land Information Ontario (obtained 2015);
CanVec Topography (obtained 2015)

Bedrock Geology: MRD 126-REV1 (Ontario Geological Survey, 2011);
Ontario Geological Survey Map 2665 (Santaguida, 2001);
Map 2666 (Santaguida, 2001);
Map 2667 (Johns, McIlraith and Stott, 2003);
Map 2668 (Johns and McIlraith, 2003)

0 2 km

srk consulting

PROJECT
DETAILED MAPPING REPORT
Manitouwadge Area, Ontario

TITLE
Black-Pic Batholith Area East
Ductile and Brittle-Ductile Shear Zones

DESIGN	KR	02 SEP 2014	**Figure 5.4.9**	REVISION 2
GIS	JA	02 AUG 2017		UTM ZONE 16N
CHECK	BH	02 AUG 2017		NAD 1983
REVIEW	JPS	02 AUG 2017		1:80,000

File: SRK_NWMO_ManStudy_AreaD_Fig5.4.9

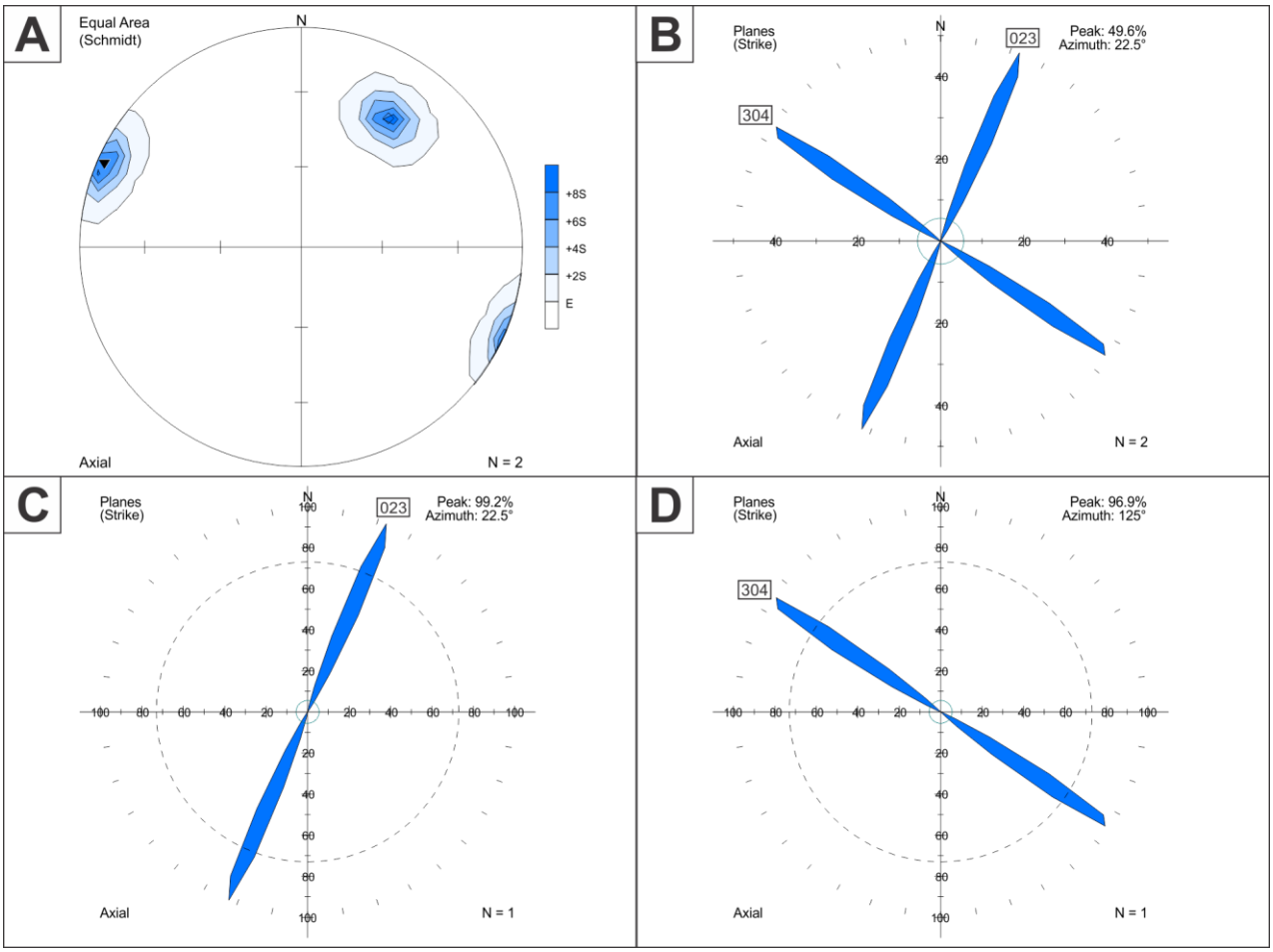

Figure 5.4.10: Black-Pic Batholith Area - East – Ductile and Brittle-Ductile Shear Zone Orientation Data

A: All ductile and brittle-ductile shear zones displayed as equal area lower hemisphere stereonet plot of poles to planes. Sinistral shear zones: filled inverted triangles (n=1). Other or unknown movement sense brittle-ductile shear zone: open diamond (n=1).

B: All ductile and brittle-ductile shear zones displayed as rose diagram of trends of planes with orientation of all peaks greater than the expected value E (n=2).

C: Sinistral shear zone displayed as rose diagram of trends of planes (n=1).

D: Other or unknown movement sense brittle-ductile shear zone displayed as rose diagram of trends of planes (n=1).

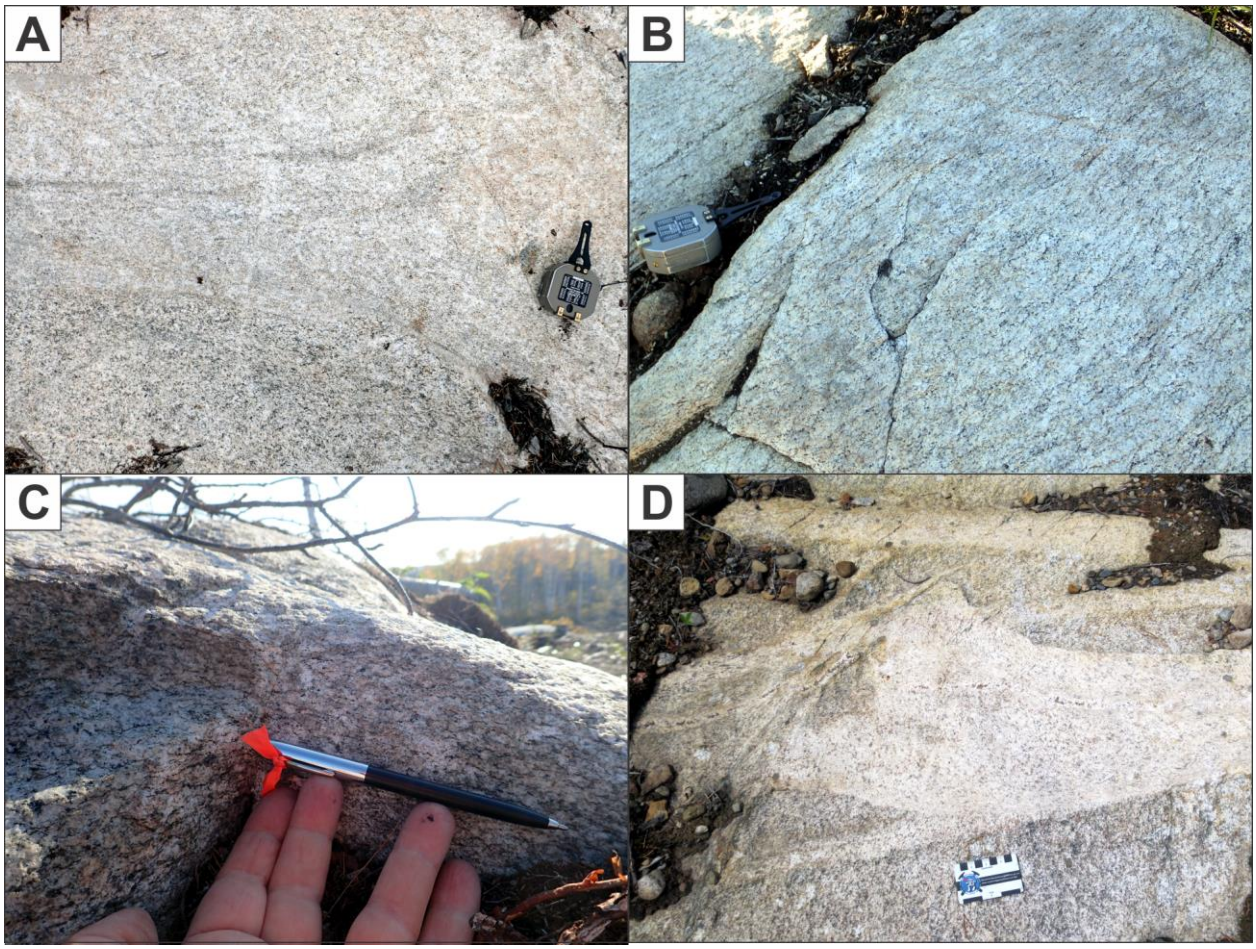

Figure 5.4.11: Black-Pic Batholith Area - East – Field Examples of Ductile Structures

A: Weak foliation developed in tonalite (Stn 16BH0124, looking N, compass for scale).
B: Shallow-dipping, moderately developed foliation in tonalite (Stn 16BH0214, looking N, compass for scale).
C: Shallow-dipping foliation in tonalite defined by slight flattening of quartz grains and alignment of biotite (Stn 16BH0179, looking W, compass for scale).
D: Foliation and dykes rotated counter clockwise into narrow, sinistral shear zone (Stn 16JK0073, looking NW, card for scale).

610000
620000
5440000
5430000
N

FARIES-
MOSHKINABI
INTRUSION

BLACK-PIC
BATHOLITH

13
7
2
9
8

400 ROAD
ICE LAKE RD.
ICE SOUTH ROAD

Macutagon
Lake
Longnega L.
Granitehill L.
Sunderland
Lake
Garnham
Lake
Jembi
L.

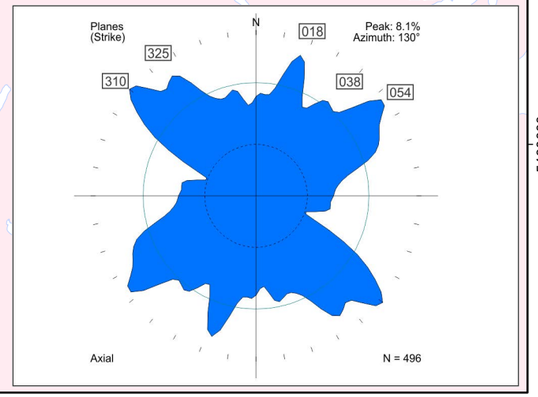

LEGEND

- Withdrawal Area
- Local Road
- Waterbody
- Observation - Outcrop (5)
- Observation - Overburden (4)
- Sub horizontal joint: 0-30° (35)
- Intermediate joint: 31-60° (30)
- Sub vertical joint: 61-90° (431)

Bedrock Geology

- Geological Boundary
- Mapped Fault
- 13: Granite-granodiorite
- 9: Gneissic tonalite suite
- 8: Gabbro
- 7: Ultramafic plutonic rocks
- 2: Mafic metavolcanic Rocks

REFERENCE

Base Data: Land Information Ontario (obtained 2015);
CanVec Topography (obtained 2015)

Bedrock Geology: MRD 126-REV1 (Ontario Geological Survey, 2011);
Ontario Geological Survey Map 2665 (Santaguida, 2001);
Map 2666 (Santaguida, 2001);
Map 2667 (Johns, McIlraith and Stott, 2003);
Map 2668 (Johns and McIlraith, 2003)

0 2 km

srk consulting

PROJECT
DETAILED MAPPING REPORT
Manitouwadge Area, Ontario

TITLE
Black-Pic Batholith Area East
Joints

DESIGN	KR	02 SEP 2014	**Figure 5.4.12**	REVISION 2
GIS	JA	02 AUG 2017		UTM ZONE 16N
CHECK	BH	02 AUG 2017		NAD 1983
REVIEW	JPS	02 AUG 2017		1:80,000

File: SRK_NWMO_ManStudy_AreaD_Fig5.4.12

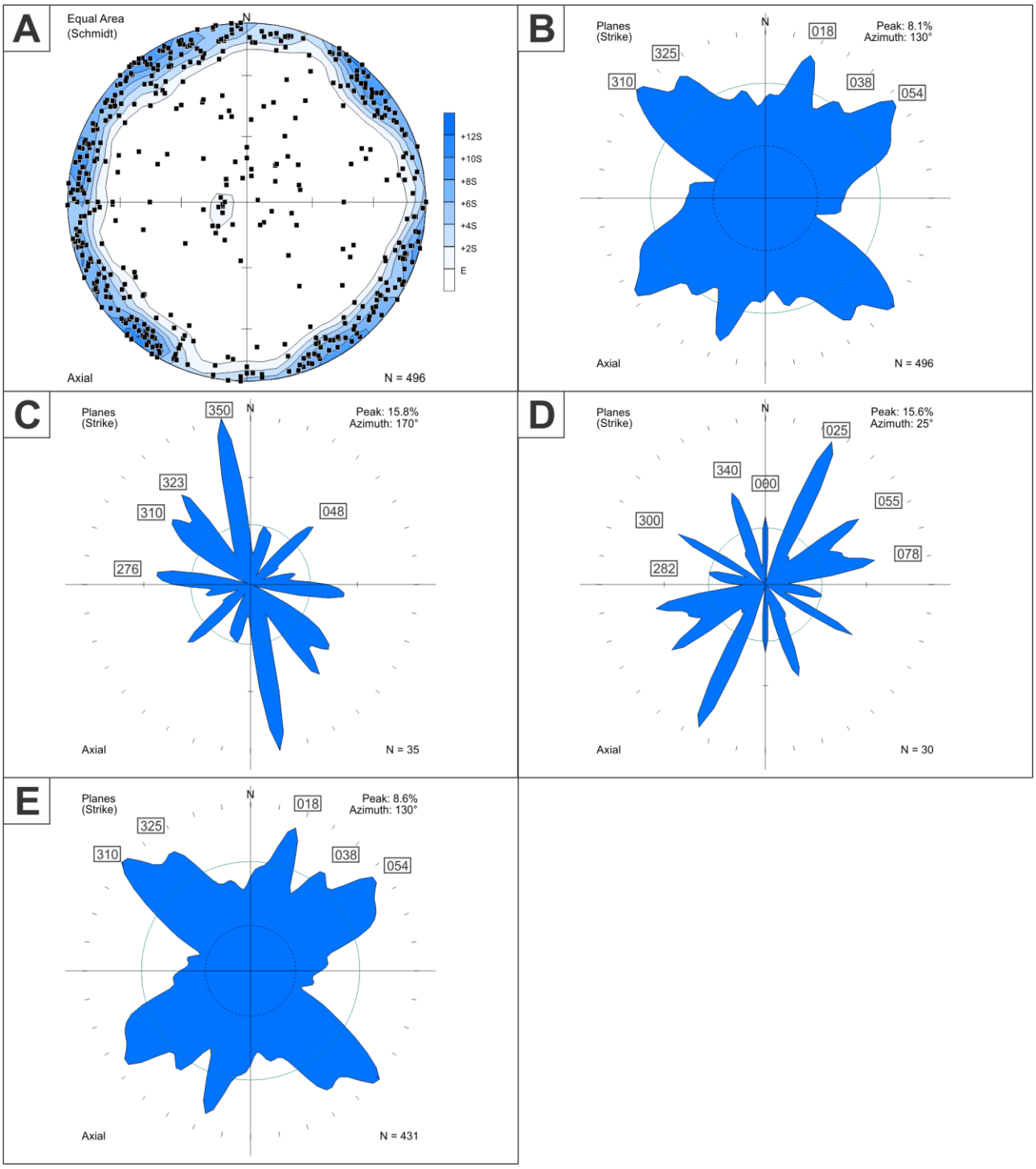

Figure 5.4.13: Black-Pic Batholith Area - East – Joint Orientation Data

A: All joints displayed as equal area lower hemisphere stereonet plot of poles to planes. (n=496).
B: All joints displayed as rose diagram of trends of planes with orientation of all peaks greater than the expected value E (n=496).
C: All joints with a dip ≤ 30 degrees displayed as rose diagram of trends of planes (n=35).
D: All joints with a dip between 31 - 60 degrees displayed as rose diagram of trends of planes (n=30).
E: All joints with a dip > 60 degrees displayed as rose diagram of trends of planes (n=431).

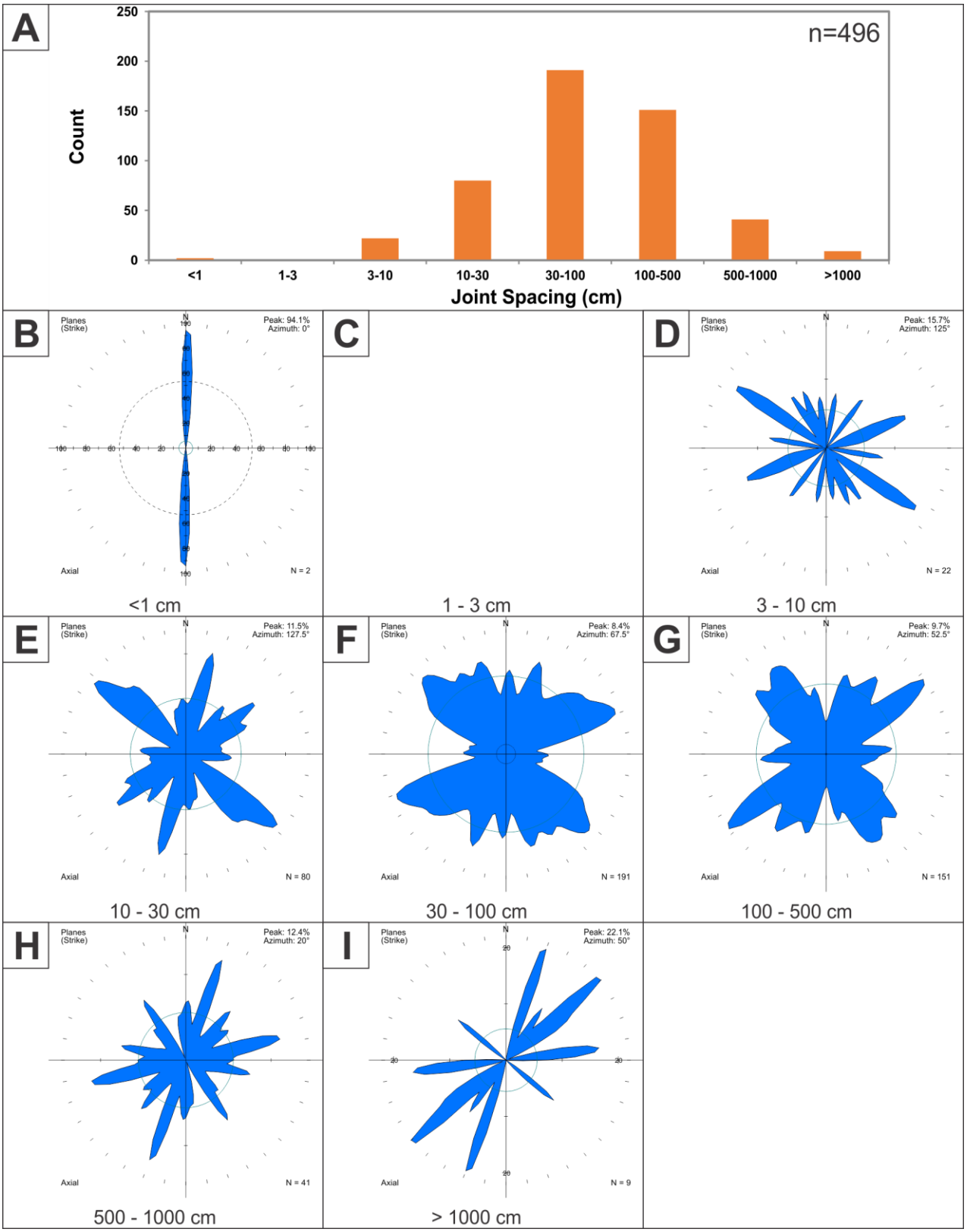

Figure 5.4.14: Black-Pic Batholith Area - East – Joint Spacing Summary

A: Histogram showing frequency distribution of joint spacing for all orientations and rock types (n=496).
B – I: Joints with the given joint spacing displayed as rose diagram of trends of planes. Any missing figures indicate no joints with that spacing were measured in this area.

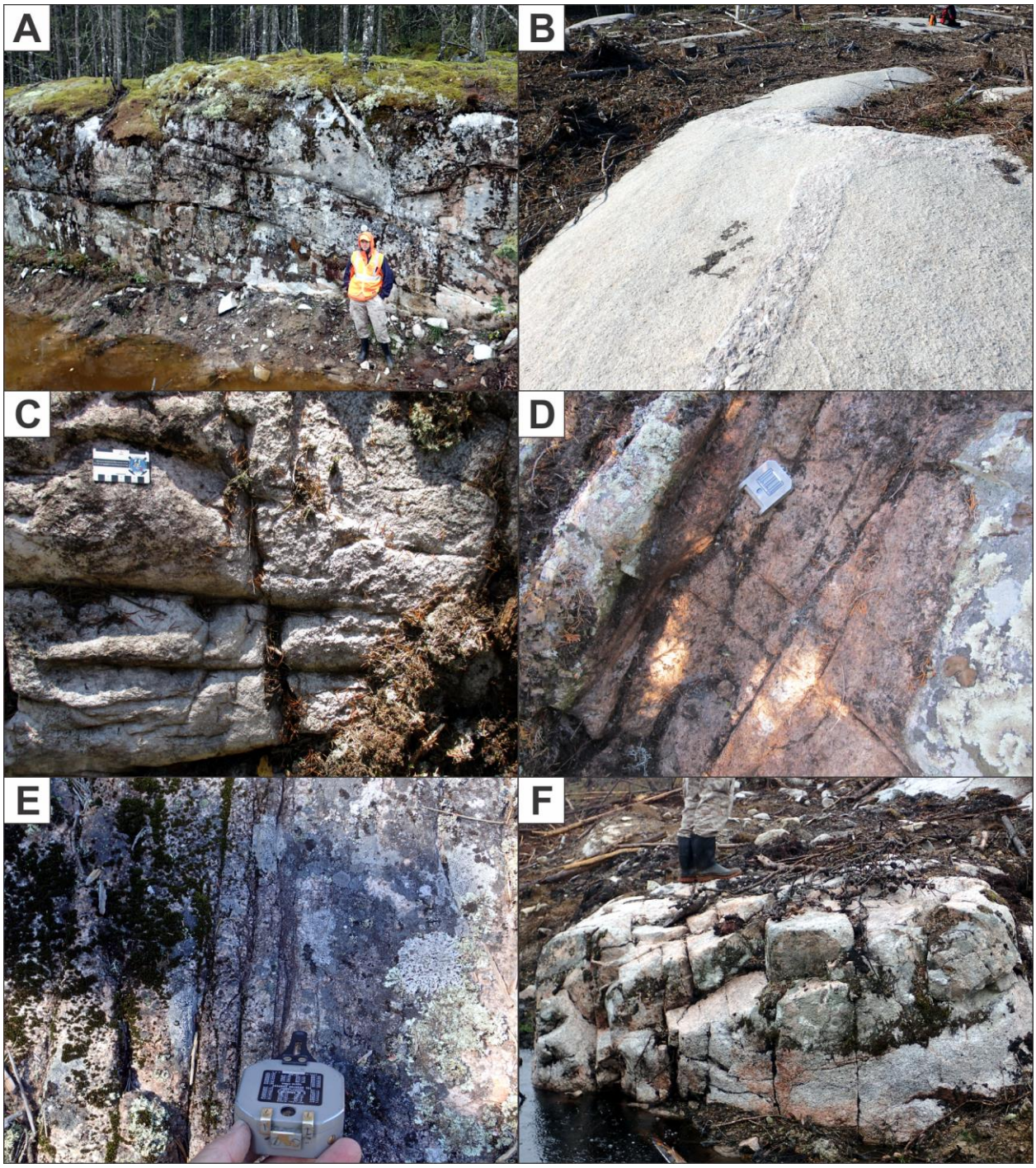

Figure 5.4.15: Black-Pic Batholith Area - East – Field Examples of Joints

A: Example of sub horizontal joint set with wide spacing cutting tonalite (Stn16BH0264, looking SW, person for scale).
B: Example of very wide joint spacing (none in view) in tonalite (Stn 16BH0243, looking SW, pack for scale).
C: Example of moderate to tight joint spacing in granodiorite (Stn 16JK0232, looking SW, card for scale).
D: Example of tight joint spacing in granodiorite proximal to interpreted lineament (Stn 16CN0140, looking N, compass for scale).
E: Example of narrow domain of tight joint spacing parallel to interpreted lineament (Stn 16BH0229, section looking N, compass for scale).
F: Three well-defined joint sets cutting tonalite (Stn 16BH0261, looking NW, person for scale).

610000

620000

5440000

5430000

FARIES-
MOSHKINABI
INTRUSION

BLACK-PIC
BATHOLITH

Macutagon
Lake

Garnham
Lake

Jembi
L.

Longnega L.

Granitehill L.

Sunderland
Lake

400 ROAD

ICE LAKE RD.

ICE SOUTH ROAD

N

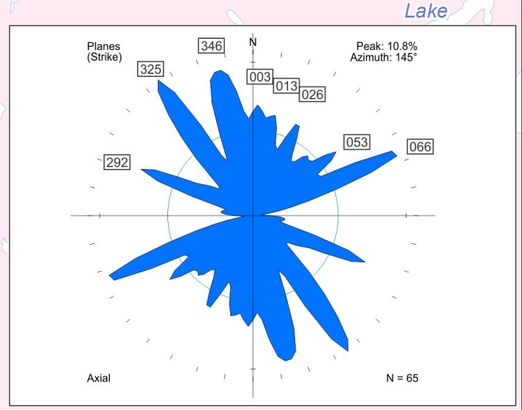

LEGEND

- Withdrawal Area
- Local Road
- Waterbody
- Observation - Outcrop (85)
- Observation - Overburden (4)
- Fault - Sinistral (6)
- Fault - Dextral (8)
- Fault - Strike (2)
- Fault - Unknown (49)
- Slickenline (8)

Bedrock Geology

- Geological Boundary
- Mapped Fault
- 13: Granite-granodiorite
- 9: Gneissic tonalite suite
- 8: Gabbro
- 7: Ultramafic plutonic rocks
- 2: Mafic metavolcanic Rocks

REFERENCE

Base Data: Land Information Ontario (obtained 2015);
CanVec Topography (obtained 2015)

Bedrock Geology: MRD 126-REV1 (Ontario Geological Survey, 2011);
Ontario Geological Survey Map 2665 (Santaguida, 2001);
Map 2666 (Santaguida, 2001);
Map 2667 (Johns, McIlraith and Stott, 2003);
Map 2668 (Johns and McIlraith, 2003)

0 2 km

srk consulting

PROJECT
DETAILED MAPPING REPORT
Manitouwadge Area, Ontario

TITLE
**Black-Pic Batholith Area East
Faults**

DESIGN	KR	02 SEP 2014	**Figure 5.4.16**	REVISION 2
GIS	JA	02 AUG 2017		UTM ZONE 16N
CHECK	BH	02 AUG 2017		NAD 1983
REVIEW	JPS	02 AUG 2017		1:80,000

File: SRK_NWMO_ManStudy_AreaD_Fig5.4.16

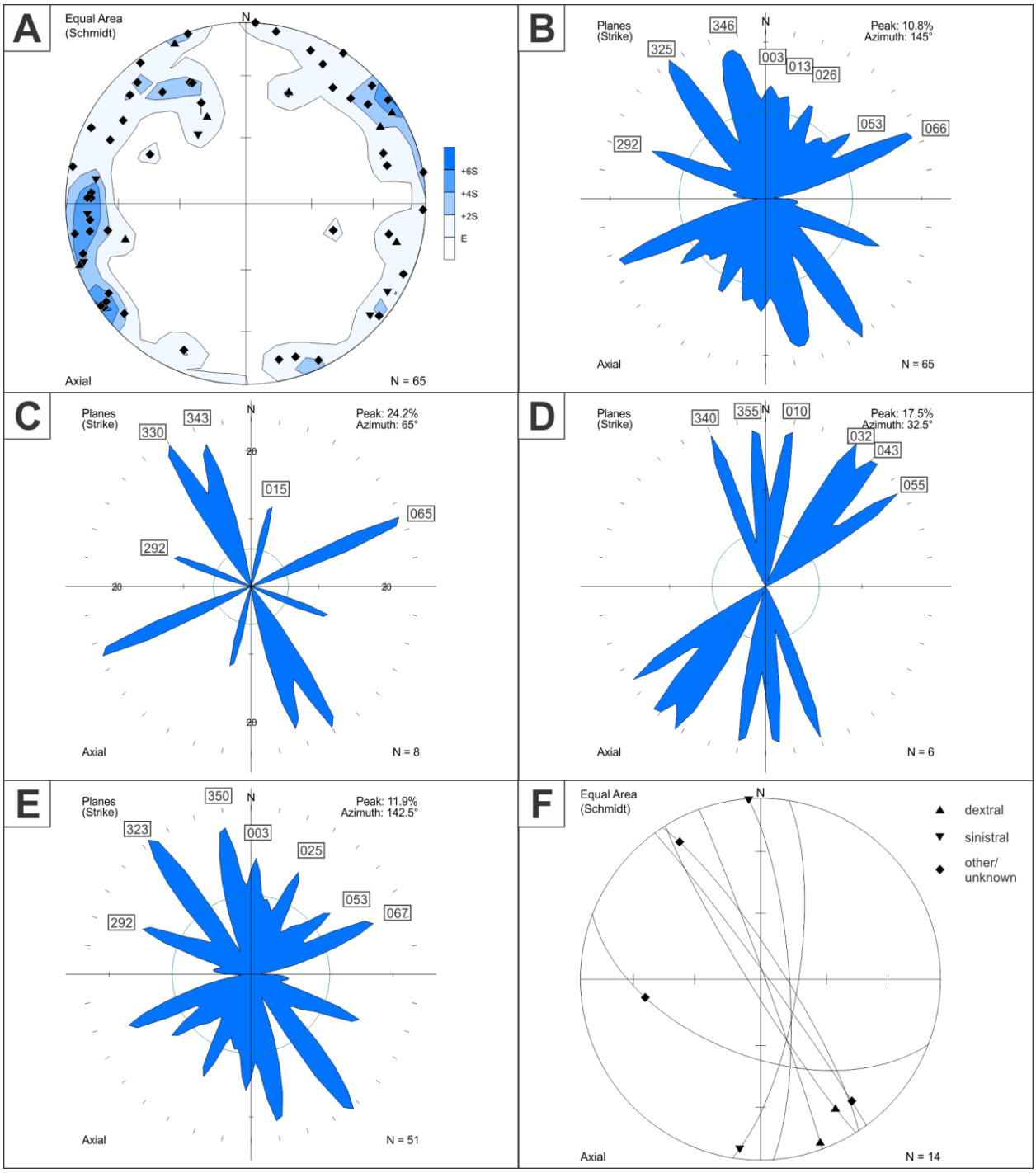

Figure 5.4.17: Black-Pic Batholith Area - East – Fault Orientation Data

A: All faults displayed as equal area lower hemisphere stereonet plot of poles to planes. Dextral brittle faults: filled triangles (n=8). Sinistral brittle faults: filled inverted triangles (n=6). Other or unknown movement sense brittle faults: filled diamond (n=51).
B: All faults displayed as rose diagram of trends of planes with orientation of all peaks greater than the expected value E (n=65).
C: Dextral brittle faults displayed as rose diagram of trends of planes (n=8).
D: Sinistral brittle faults displayed as rose diagram of trends of planes (n=6).
E: Other or unknown movement sense brittle faults displayed as rose diagram of trends of planes (n=51).
F: Slickenline data displayed as equal area lower hemisphere stereonet plot of lineation points and great circles of the respective brittle faults on which they were measured. Lineation plotted as rake calculated from measured trend and plunge.

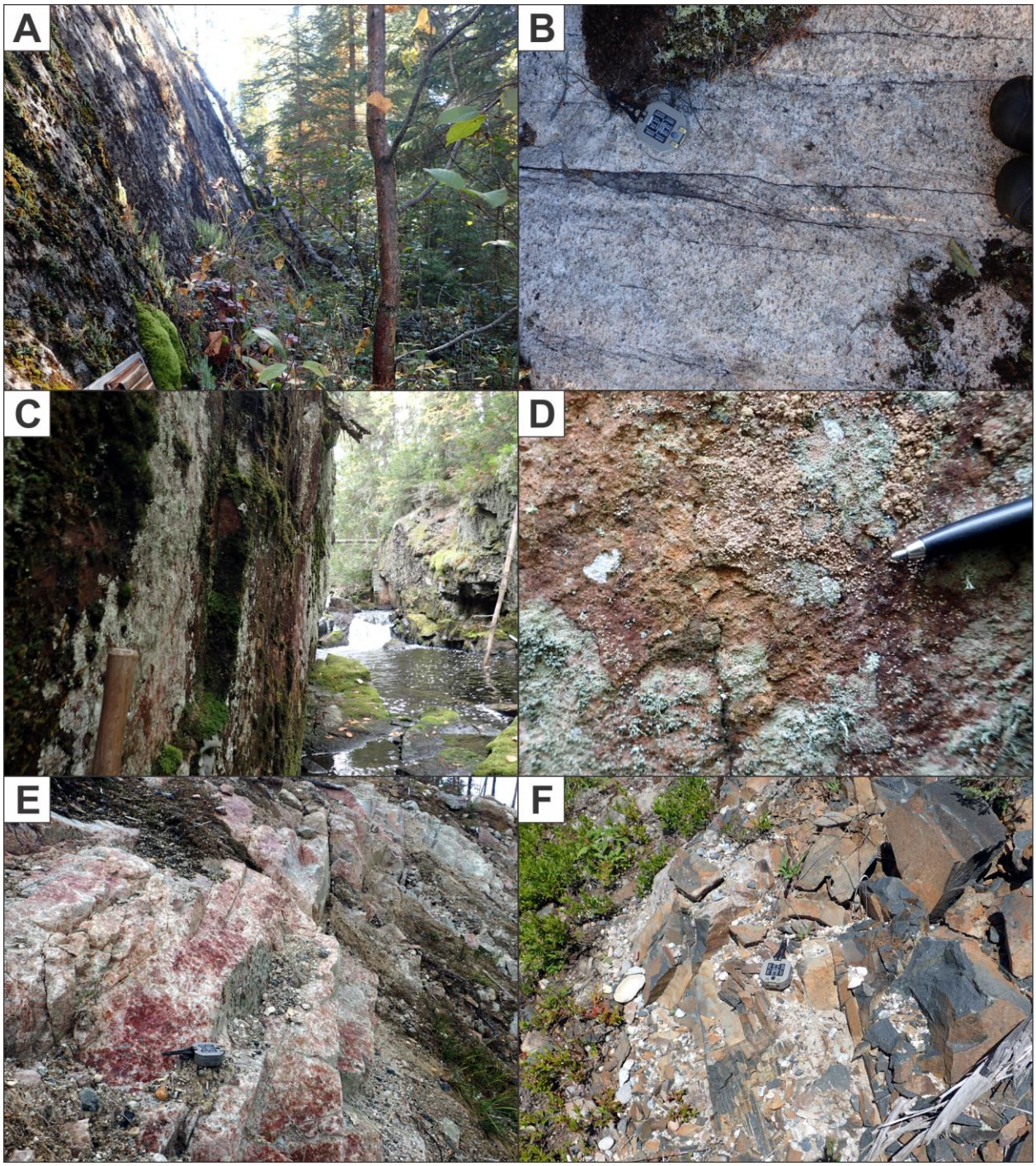

Figure 5.4.18: Black-Pic Batholith Area - East – Field Examples of Faults

A: SE-striking, moderately SW-dipping fault scarp (Stn 16BH0226, looking SE, clipboard for scale).
B: Discrete, SE-striking, moderately dipping fault adjacent to scarp in photo A with an oblique joint set consistent with dextral movement (Stn 16BH0226, looking NE, compass for scale).
C: Steep sided gorge marks overturned, SE-striking, steeply SW-dipping fault (Stn 16BH0238, looking NW, hammer for scale).
D: Weak but consistent slickenlines and steps define an oblique dextral movement on fault in Photo C (Stn 16BH0238, looking SW, pen for scale).
E: Strong hematite and epidote alteration associated with strongly jointed fault coincident with magnetic and surficial SE-trending lineament (Stn 16BH0248, looking E, compass for scale).
F: Tightly spaced, NNW-trending joint set in Matachewan dyke parallel to a mapped fault with sinistral offset of the dyke (Stn 16BH0074, looking N, compass for scale).

610000
620000
5440000
5430000
N

FARIES-
MOSHKINABI
INTRUSION

BLACK-PIC
BATHOLITH

13
7
2
9
8
86

400 ROAD
ICE LAKE RD.
ICE SOUTH ROAD

Macutagon
Lake
Longnega L.
Granitehill L.
Garnham
Lake
Jembi
L.
Sunderland
Lake

Planes
(Strike)
Peak: 100.0%
Azimuth: 45°
045
340
Axial
N = 1

LEGEND

- Withdrawal Area
- Local Road
- Waterbody
- Observation - Outcrop (122)
- Observation - Overburden (4)
- Extension Vein (1)

Bedrock Geology

- Geological Boundary
- Mapped Fault
- 13: Granite-granodiorite
- 9: Gneissic tonalite suite
- 8: Gabbro
- 7: Ultramafic plutonic rocks
- 2: Mafic metavolcanic Rocks

11
17
Wawa
Lake
Superior

REFERENCE

Base Data: Land Information Ontario (obtained 2015);
CanVec Topography (obtained 2015)

Bedrock Geology: MRD 126-REV1 (Ontario Geological Survey, 2011);
Ontario Geological Survey Map 2665 (Santaguida, 2001);
Map 2666 (Santaguida, 2001);
Map 2667 (Johns, McIlraith and Stott, 2003);
Map 2668 (Johns and McIlraith, 2003)

0 2 km

srk consulting

PROJECT
DETAILED MAPPING REPORT
Manitouwadge Area, Ontario

TITLE
**Black-Pic Batholith Area East
Veins**

DESIGN	KR	02 SEP 2014	**Figure 5.4.19**	REVISION 2
GIS	JA	02 AUG 2017		UTM ZONE 16N
CHECK	BH	02 AUG 2017		NAD 1983
REVIEW	JPS	02 AUG 2017		1:80,000

File: SRK_NWMO_ManStudy_AreaD_Fig5.4.19

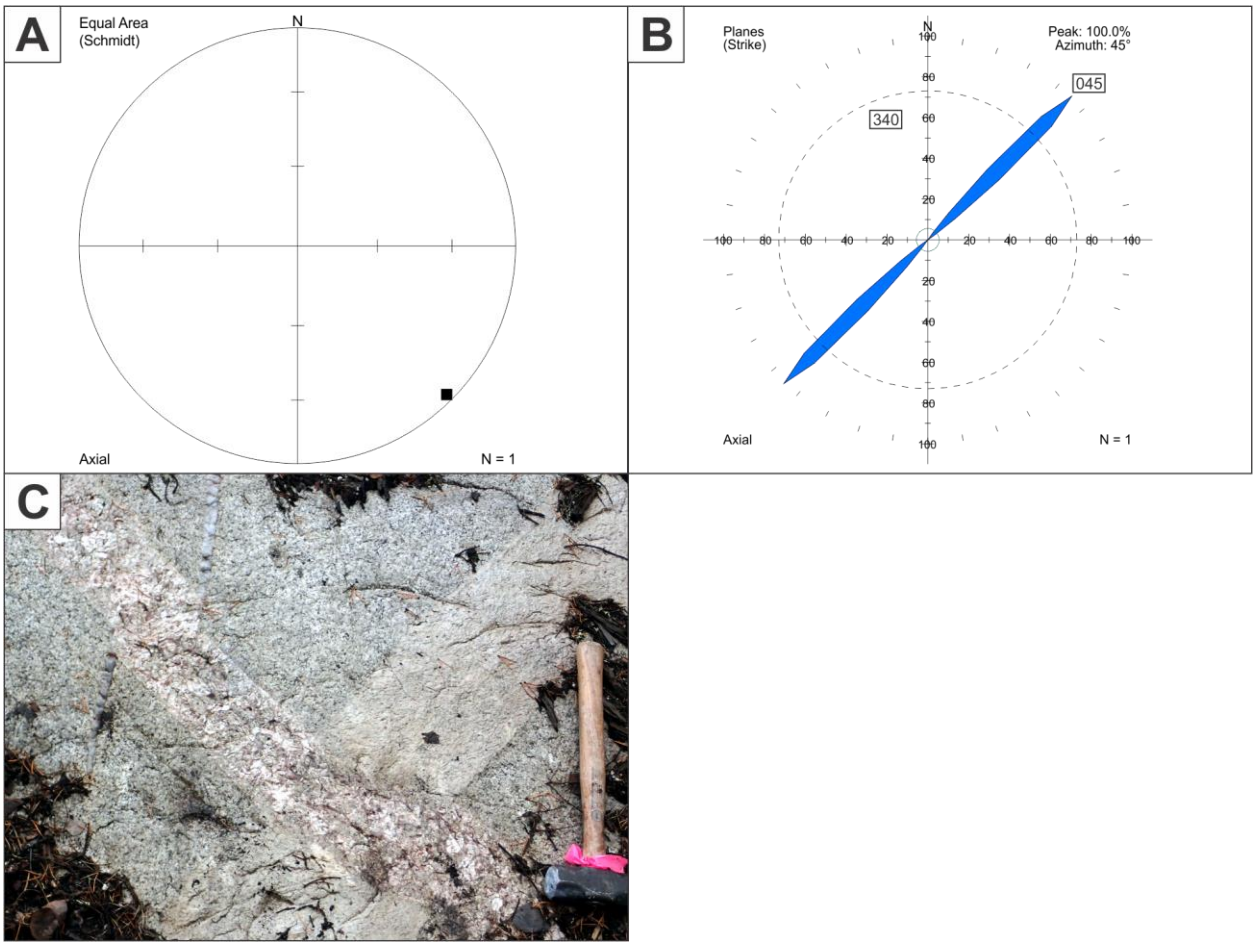

Figure 5.4.20: Black-Pic Batholith Area - East – Vein Orientation Data and Field Examples

A: Single vein measurement displayed as equal area lower hemisphere stereonet plot of pole to planes. Narrow veins were typically measured as filled joints or faults (n=1).

B: Single vein measurement displayed as rose diagram of trend of planes with orientation of all peaks greater than the expected value E (n=1).

C: NE-trending quartz vein and older white felsic dyke cut by younger pink felsic dyke (Stn 16BH0263, looking SW, hammer for scale).

610000
620000
5440000
5430000
N
FARIES-
MOSHKINABI
INTRUSION
BLACK-PIC
BATHOLITH
13
7
2
9
8
400 ROAD
ICE LAKE RD.
ICE SOUTH ROAD
Macutagon
Lake
Longnega L.
Granitehill L.
Garnham
Lake
Jembi
L.
Sunderland
Lake
LEGEND
Withdrawal Area
Local Road
Waterbody
Observation - Outcrop (123)
Observation - Overburden (4)
Alteration - Hematite
Alteration - Quartz
Alteration - Epidote
Alteration - Chlorite
Bedrock Geology
Geological Boundary
Mapped Fault
13: Granite-granodiorite
9: Gneissic tonalite suite
8: Gabbro
7: Ultramafic plutonic rocks
2: Mafic metavolcanic Rocks
11
17
Lake
Superior
Wawa
REFERENCE
Base Data: Land Information Ontario (obtained 2015);
CanVec Topography (obtained 2015)
Bedrock Geology: MRD 126-REV1 (Ontario Geological Survey, 2011);
Ontario Geological Survey Map 2665 (Santaguida, 2001);
Map 2666 (Santaguida, 2001);
Map 2667 (Johns, McIlraith and Stott, 2003);
Map 2668 (Johns and McIlraith, 2003)
0
2
km
srk consulting
PROJECT
DETAILED MAPPING REPORT
Manitouwadge Area, Ontario
TITLE
Black-Pic Batholith Area East
Secondary Minerals and Alteration
DESIGN KR 02 SEP 2014
GIS JA 02 AUG 2017
CHECK BH 02 AUG 2017
REVIEW JPS 02 AUG 2017
Figure
5.4.21
REVISION 2
UTM ZONE 16N
NAD 1983
1:80,000
File: SRK_NWMO_ManStudy_AreaD_Fig5.4.21

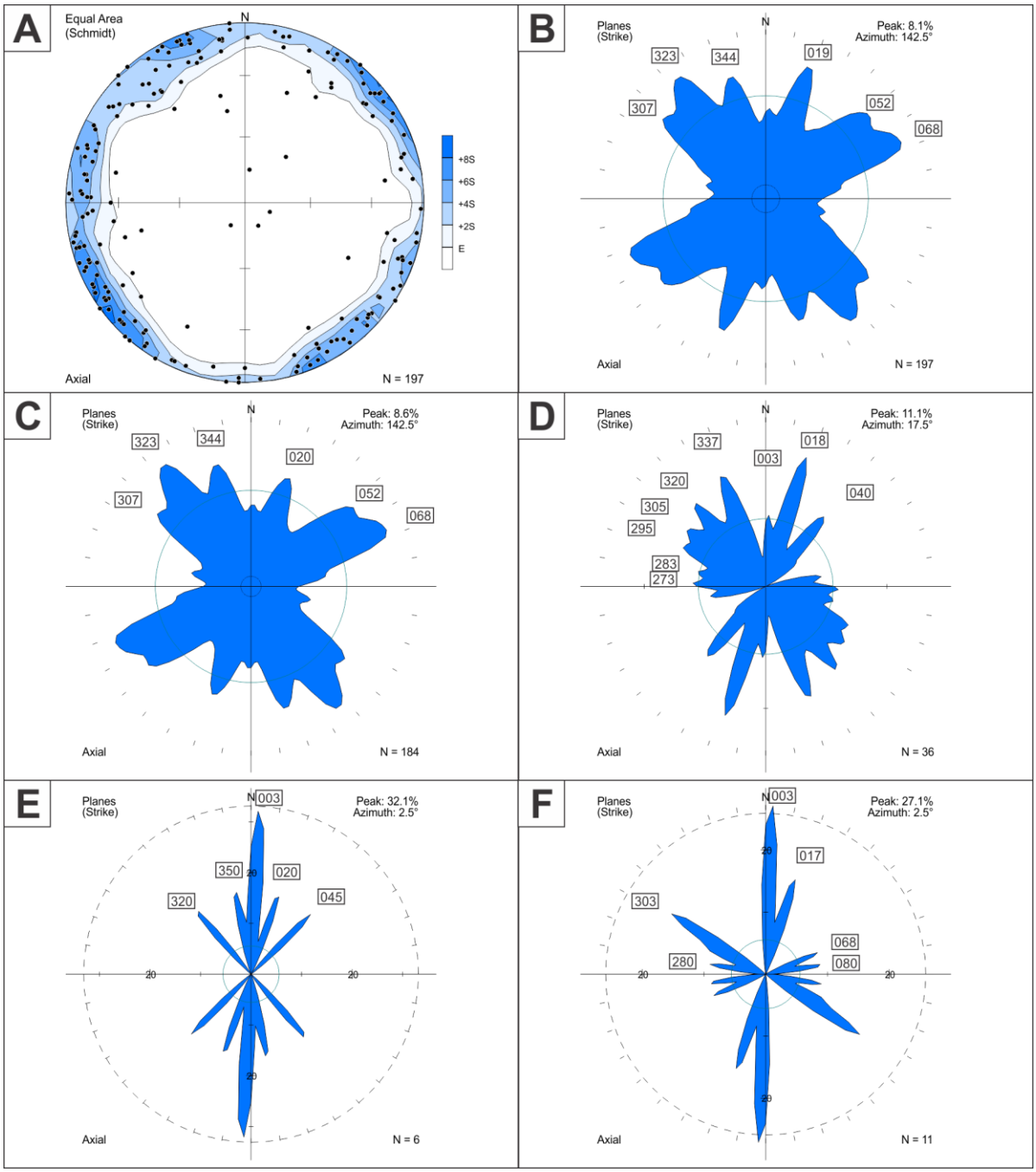

Figure 5.4.22: Black-Pic Batholith Area - East – Secondary Minerals and Alteration Orientation Data

A: All structures with visible alteration displayed as equal area lower hemisphere stereonet plot of poles to planes. (n=197).

B: All structures with visible alteration displayed as rose diagram of trends of planes with orientation of all peaks greater than the expected value E (n=197).

C: All structures with visible hematite alteration displayed as rose diagram of trends of planes with orientation of all peaks greater than the expected value E (n=184).

D: All structures with visible epidote alteration displayed as rose diagram of trends of planes with orientation of all peaks greater than the expected value E (n=36).

E: All structures with visible quartz alteration displayed as rose diagram of trends of planes with orientation of all peaks greater than the expected value E (n=6).

F: All structures with visible chlorite alteration displayed as rose diagram of trends of planes with orientation of all peaks greater than the expected value E (n=11).

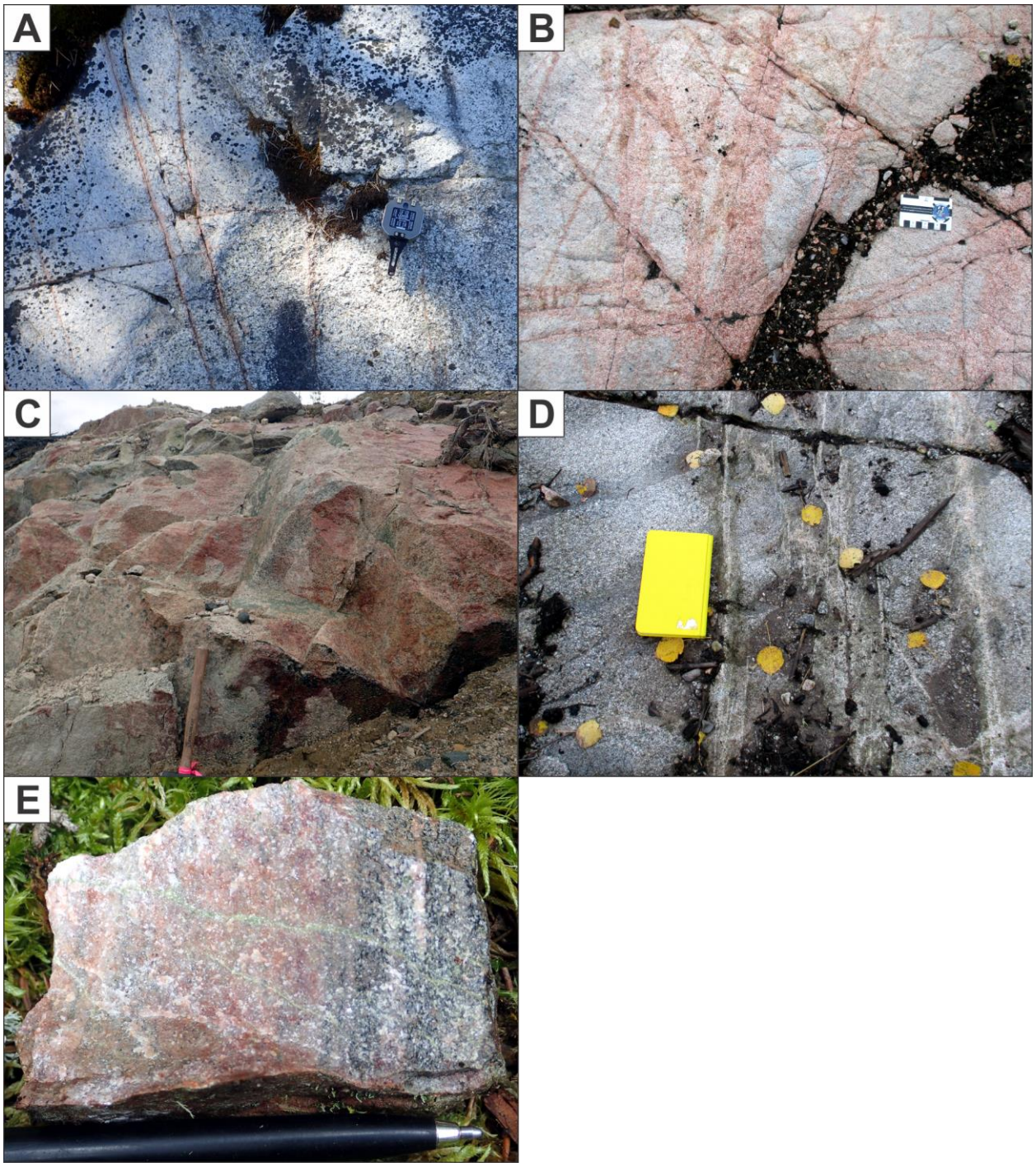

Figure 5.4.23: Black-Pic Batholith Area - East – Field Examples of Secondary Minerals and Alteration

A: Widely spaced jointing with weak hematite staining (Stn 16BH0072, looking S, compass for scale).
B: Cross cutting network of joints all with moderate hematite staining (Stn 16JK0207, looking SE, card for scale).
C: Well-defined epidote and hematite on all joint surfaces along interpreted fault coincident with well-defined SE-trending surficial lineament (Stn 16BH0248, looking N, hammer for scale).
D: Quartz and epidote ± chlorite in N-trending set of joints with bleached halo in country rock (Stn 16JK0208, looking S, card for scale).
E: Thin epidote veinlets in pervasive silica and hematite altered tonalite hand sample from NW-trending fault zone (Stn 16BH0238, pen for scale).

560000 570000 580000 590000 600000 610000 620000 630000

5490000 5480000 5470000 5460000 5450000 5440000 5430000 5420000

Quetico Area

METASEDIMENTARY ROCKS

QUETICO SUBPROVINCE

WAWA SUBPROVINCE

NAMA CREEK PLUTON

LOKEN LAKE PLUTON

FARIES-MOSHKINABI INTRUSION

MANITOUWADGE GREENSTONE BELT

RAWLUK LAKE PLUTON

BLACK-PIC BATHOLITH

FOURBAY LAKE PLUTON

DOTTED LAKE PLUTON

Black-Pic Batholith Area - East

Black-Pic Batholith Area - West

Fourbay Lake Pluton Area

HILLSPORT

CN Rail

MANITOUWADGE

Eino L.
Laurie L.
Stilwell Lake
Mann L.
Phillip L.
Fran Lake
Mustela Lake
White Otter L.
Osawin R.
Bound L.
Foch R.
Nagagami Lake
Anthony L.
Waboosekon L.
Beavercross Lake
Flanders Lake
Osawin Lake
White Otter R.
Kagiano R.
Upper Flanders Lake
Everest L.
Michal L.
Island L.
Foch L.
Linbarr Lake
Kern Lake
Rabbitskin Lake
Wowun L.
Loken Lake
Waskisk Lake
Mose Lake
Pic River
Manitouwadge L.
Obakamiga Lake
Longmega L.
Macutagon Lake
Granitehill L.
Shekak Lake
Tocheri Lake
Sunderland Lake
Xagimu L.
Morley L.
Barehead Lake
Agonzon Lake
Garnham Lake
Jembi L.
Twist Lake
Black R.
Pickle L.
McGill
Shabotik R.
Matthews Lake

614

N

LEGEND

- Withdrawal Area
- Main Road
- Local Road
- Railway
- Waterbody

Field Station

- Mafic Dyke - Contact Observed
- Mafic Dyke - Contact Not Observed

Mafic Dyke

- Biscotasing
- Marathon
- Matachewan

Bedrock Geology

- Geological Boundary
- Subprovince Boundary
- Fold (syncline)
- Fold (anticline)
- 13: Granite-granodiorite
- 11: Granite-granodiorite
- 10: Foliated tonalite suite
- 9: Gneissic tonalite suite
- 8: Gabbro
- 7: Ultramafic plutonic rocks
- 5: Metasedimentary rocks
- 4: Felsic volcanic rocks
- 3: Felsic and intermediate metavolcanic rocks
- 2: Mafic metavolcanic Rocks
- Iron Formation

REFERENCE

Base Data: Land Information Ontario (obtained 2015); CanVec Topography (obtained 2015)

Bedrock Geology: MRD 126-REV1 (Ontario Geological Survey, 2011); Ontario Geological Survey Map 2665 (Santaguida, 2001); Map 2666 (Santaguida, 2001); Map 2667 (Johns, McIlraith and Stott, 2003); Map 2668 (Johns and McIlraith, 2003)

0 10 km

srk consulting

PROJECT: DETAILED MAPPING REPORT
Manitouwadge Area, Ontario

TITLE: **Manitouwadge Area**
Distribution of Proterozoic Mafic Dykes

DESIGN	KR	02 SEP 2014	**Figure 5.5.1**	REVISION 2
GIS	JA	02 AUG 2017		UTM ZONE 16N
CHECK	CN	02 AUG 2017		NAD 1983
REVIEW	JPS	02 AUG 2017		1:280,000

File: SRK_NWMO_ManStudy_Fig5.5.1_mafic

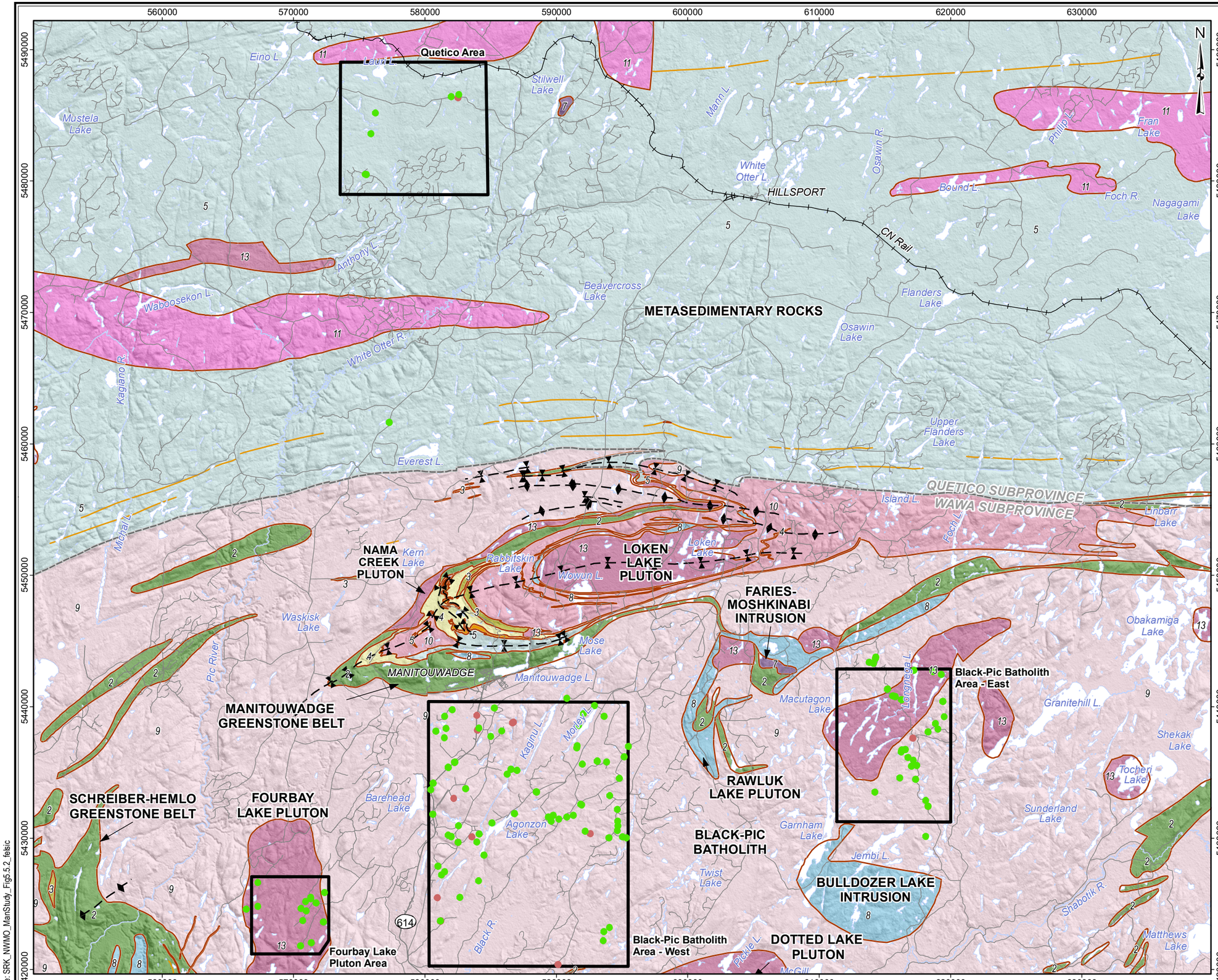
Quetico Area
METASEDIMENTARY ROCKS
HILLSPORT
CN Rail
QUETICO SUBPROVINCE
WAWA SUBPROVINCE
NAMA CREEK PLUTON
LOKEN LAKE PLUTON
FARIES-MOSHKINABI INTRUSION
MANITOUWADGE
MANITOUWADGE GREENSTONE BELT
SCHREIBER-HEMLO GREENSTONE BELT
FOURBAY LAKE PLUTON
Fourbay Lake Pluton Area
RAWLUK LAKE PLUTON
BLACK-PIC BATHOLITH
Black-Pic Batholith Area - East
Black-Pic Batholith Area - West
BULLDOZER LAKE INTRUSION
DOTTED LAKE PLUTON
Eino L.
Stilwell Lake
Mann L.
White Otter L.
Osawin R.
Phillip L.
Fran Lake
Bound L.
Foch R.
Nagagami Lake
Mustela Lake
Anthony L.
Waboosekon L.
White Otter R.
Kagiano R.
Beavercross Lake
Flanders Lake
Osawin Lake
Upper Flanders Lake
Everest L.
Michal L.
Island L.
Foch L.
Linbarr Lake
Kern Lake
Rabbitskin Lake
Wowun L.
Loken Lake
Waskisk Lake
Pic River
Mose Lake
Manitouwadge L.
Obakamiga Lake
Longnose L.
Macutagon Lake
Granitehill L.
Shekak Lake
Tocheri Lake
Sunderland Lake
Barehead Lake
Agonzon Lake
Kagimu L.
Moberly L.
Black R.
Garnham Lake
Jembi L.
Twist Lake
Shabotik R.
Pickle L.
McGill
Matthews Lake
614
N
LEGEND
Withdrawal Area
Main Road
Local Road
Railway
Waterbody
Bedrock Geology
Geological Boundary
Subprovince Boundary
Fold (syncline)
Fold (anticline)
13: Granite-granodiorite
11: Granite-granodiorite
10: Foliated tonalite suite
9: Gneissic tonalite suite
8: Gabbro
7: Ultramafic plutonic rocks
5: Metasedimentary rocks
4: Felsic volcanic rocks
3: Felsic and intermediate metavolcanic rocks
2: Mafic metavolcanic Rocks
Iron Formation
Felsic Dyke
Mafic Dyke
Thunder Bay
CAN
USA
Wawa
Lake Superior
Sudbury
Sault Ste. Marie
REFERENCE
Base Data: Land Information Ontario (obtained 2015); CanVec Topography (obtained 2015)
Bedrock Geology: MRD 126-REV1 (Ontario Geological Survey, 2011); Ontario Geological Survey Map 2665 (Santaguida, 2001); Map 2666 (Santaguida, 2001); Map 2667 (Johns, McIlraith and Stott, 2003); Map 2668 (Johns and McIlraith, 2003)
0
10
km
srk consulting
PROJECT
DETAILED MAPPING REPORT
Manitouwadge Area, Ontario
TITLE
Manitouwadge Area
Distribution of Felsic and Mafic Dykes
DESIGN KR 02 SEP 2014
GIS JA 15 NOV 2017
CHECK CN 15 NOV 2017
REVIEW JPS 15 NOV 2017
Figure 5.5.2
REVISION 2
UTM ZONE 16N
NAD 1983
1:280,000
File: SRK_NWMO_ManStudy_Fig5.5.2_felsic

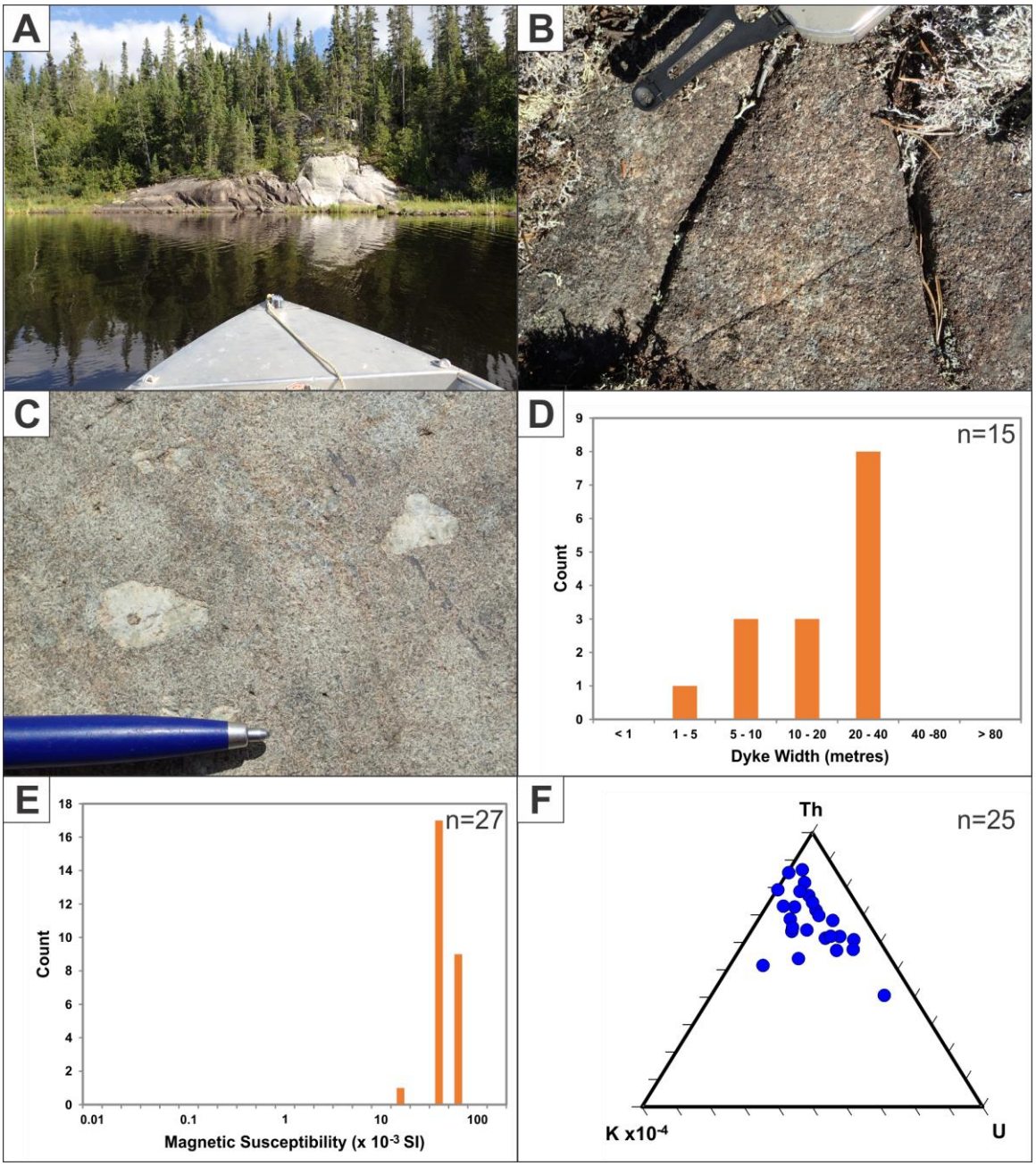

Figure 5.5.1.1: Matachewan Dykes – General Properties

A: Overview of Matachewan dyke in contact with host tonalite on the shore of Agonzon Lake (Stn 16BH0195, looking SE, boat and shoreline for scale).

B: Typical brown weathering texture of Matachewan dyke (Stn 16BH0035, looking SE, compass for scale).

C: Slightly weathered Matachewan dyke exhibiting plagioclase phenocrysts within a matrix of acicular plagioclase and fine grained mafic minerals (Stn 16BH0070, looking SE, pen for scale).

D: Histogram showing frequency distribution of Matachewan dyke width (n=15).

E: Logarithmic histogram plot of magnetic susceptibility for Matachewan dykes (n=27).

F: Ternary plot of gamma ray spectrometer data for Matachewan dykes (n=25).

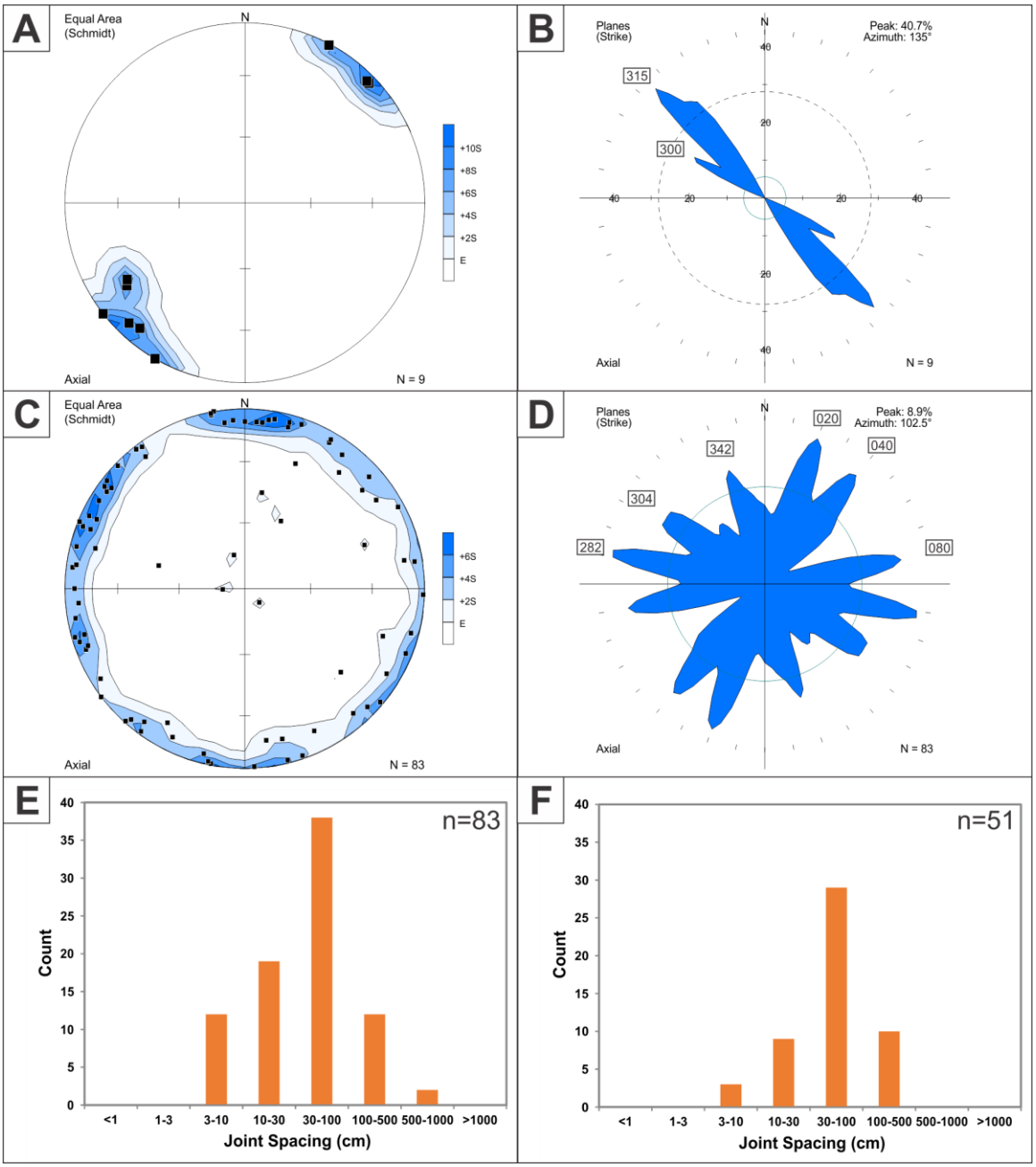

Figure 5.5.1.2: Matachewan Dykes – Structures

A: All mapped Matachewan dyke contact orientations displayed as equal area lower hemisphere stereonet plot of poles to planes (n=9).

B: All mapped Matachewan dyke contact orientations displayed as rose diagram of trends of planes with orientation of all peaks greater than the expected value E (n=9).

C: All joints measured in Matachewan dykes displayed as equal area lower hemisphere stereonet plot of poles to planes (n=83).

D: All joints measured in Matachewan dykes displayed as rose diagram of trends of planes with orientation of all peaks greater than the expected value E (n=83).

E: Histogram showing frequency distribution of joint spacing in Matachewan dykes (n=83).

F: Histogram showing frequency distribution of joint spacing in host rocks adjacent to Matachewan dykes (n=51).

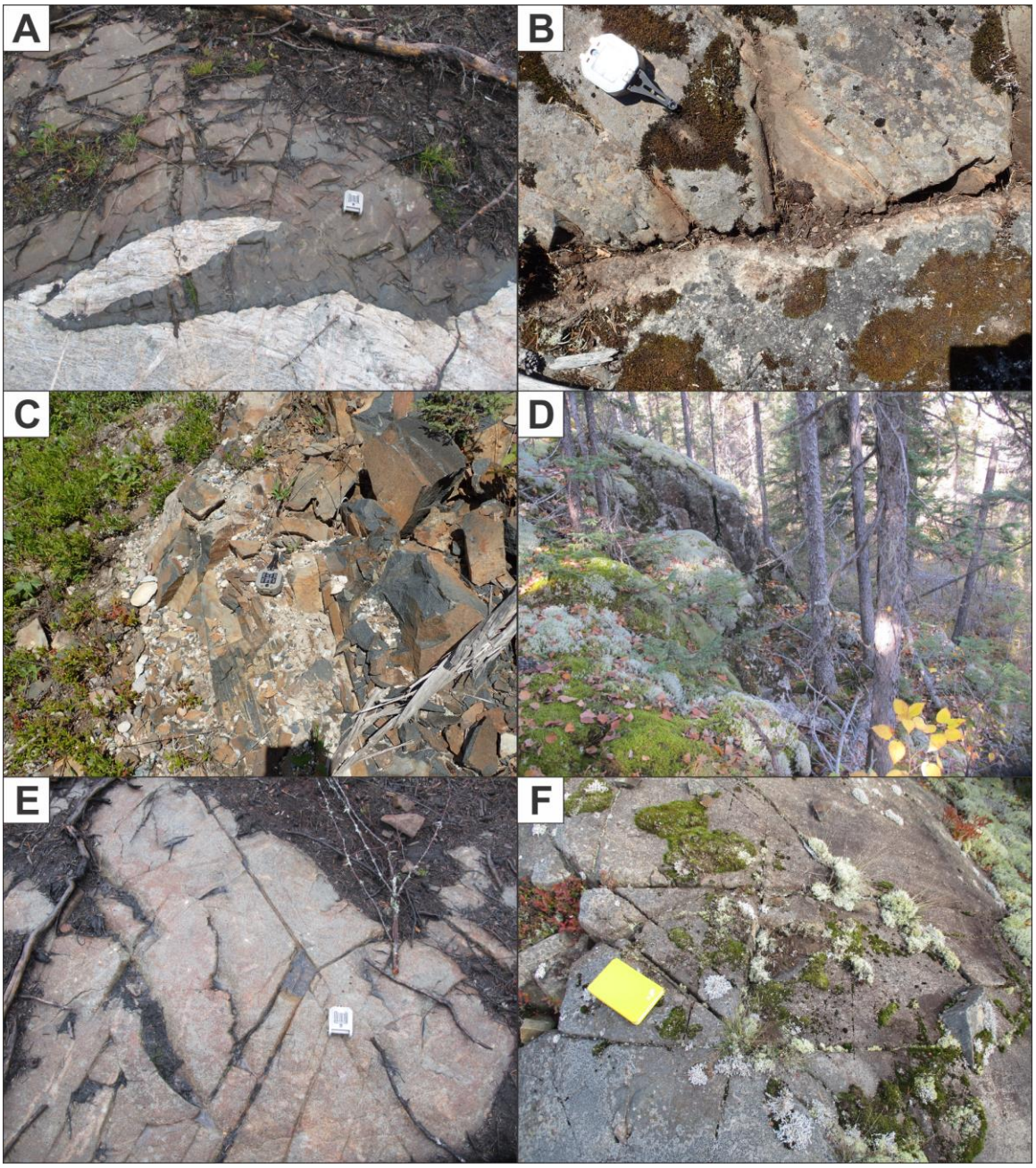

Figure 5.5.1.3: Matachewan Dykes – Field Examples of Structural Features

A: Matachewan dyke intruding tonalite with chilled dyke margins and no brittle structures along dyke contacts. Also note closely spaced joints within dyke, and a lack of joints within the host tonalite adjacent to the dyke (Stn 16CN0119, looking W, compass for scale).

B: Dyke (upper portion of photo) intruding tonalite, and exhibiting a sharp, altered, recessive but not structurally re-activated dyke contact. Note hematite alteration in joints within dyke (Stn 16BH0074, looking SW, compass for scale).

C: Close-spaced joints associated with a northwest-trending brittle fault cutting the dyke at a low angle (Stn 16BH0074, looking N, compass for scale).

D: Multi-metre tall scarp and adjacent valley developed along dyke contact (Stn 16CN0139, looking NW, no scale).

E: Representative closely spaced joints within Matachewan dyke (Stn 16CN0119, looking N, compass for scale).

F: Representative closely spaced joints within Matachewan dyke (Stn 16JK0251, looking N, book for scale).

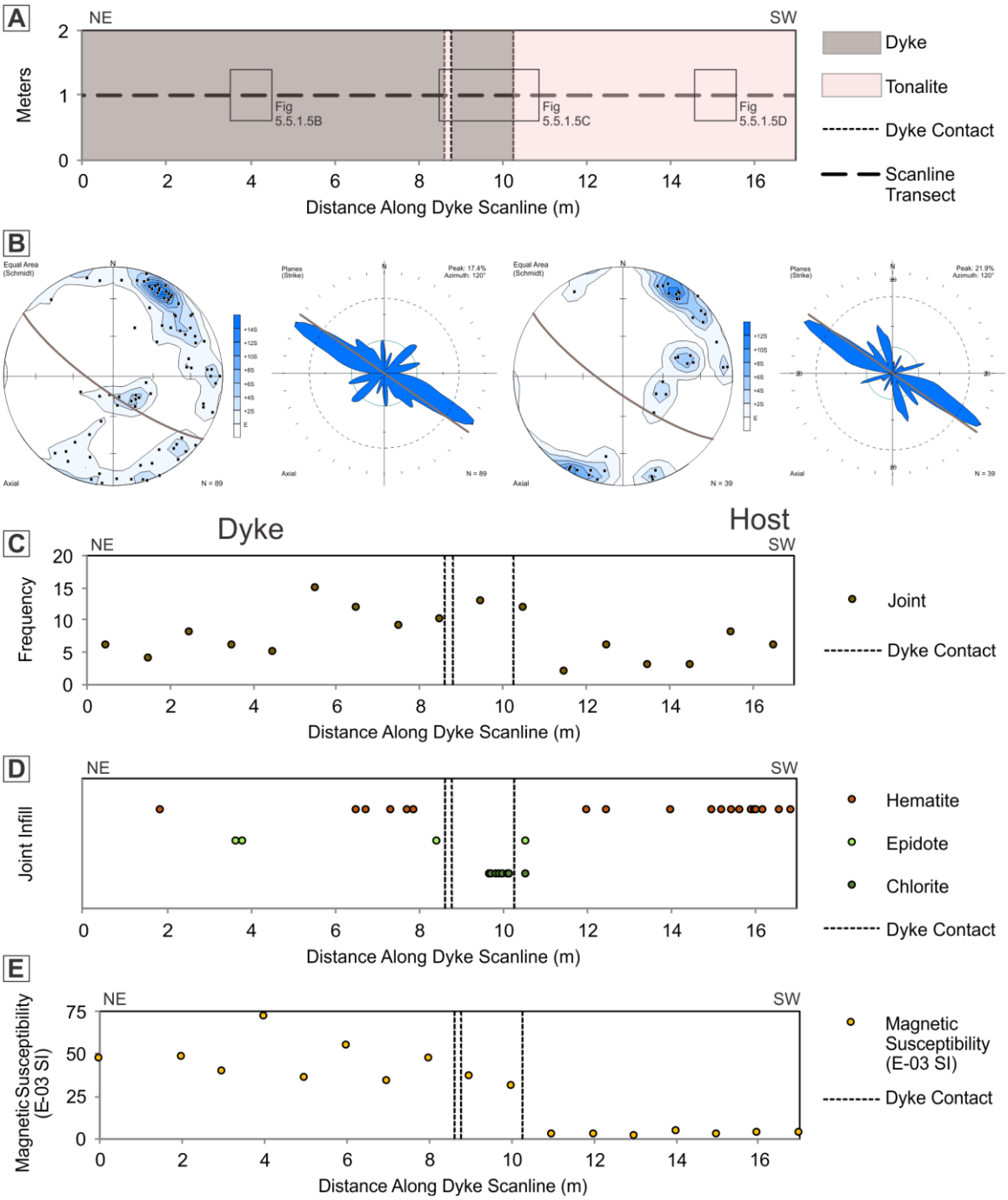

Figure 5.5.1.4: Matachewan Dykes - Composite Summary of Scanline Results

A: Schematic overview of the Matachewan scanline transect showing dyke, host rock and dyke contacts and location of field photographs.

B: All mapped joints in Matachewan dyke and host rock displayed as stereonet (equal area lower hemisphere stereonet plot of poles to planes) and rose diagrams (trends of planes with orientation of all peaks greater than the expected value). Contact of dyke displayed as brown line.

C: Frequency of joints per meter interval along the scanline transect.

D: Distribution of alteration minerals along the scanline transect.

E: Magnetic susceptibility measurements along the scanline transect.

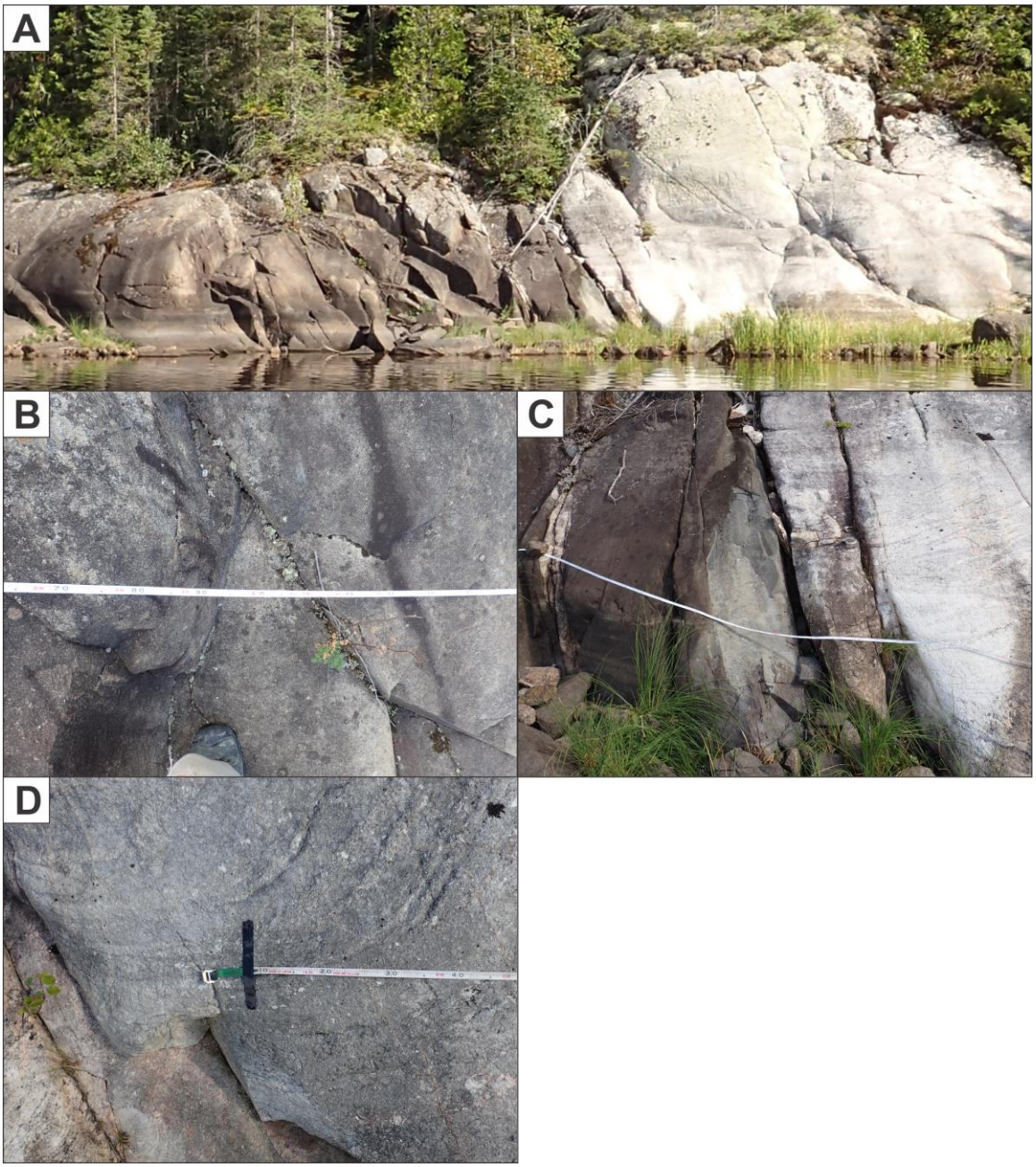

Figure 5.5.1.5: Matachewan Dykes – Field Photographs from Scanline Exercise

A: Overview of the Matachewan scanline section, corresponds to schematic overview in Figure 5.5.1.4A (looking SE, no scale).

B: Representative segment of the Matachewan dyke along the scanline. Locations of photos in Figure 5.5.1.4A (looking SE, tape measure for scale).

C: Contact between the Matachewan dyke and host tonalite (looking SE, tape measure for scale).

D: Representative segment of the host tonalite along the scanline (looking SE, tape measure for scale).

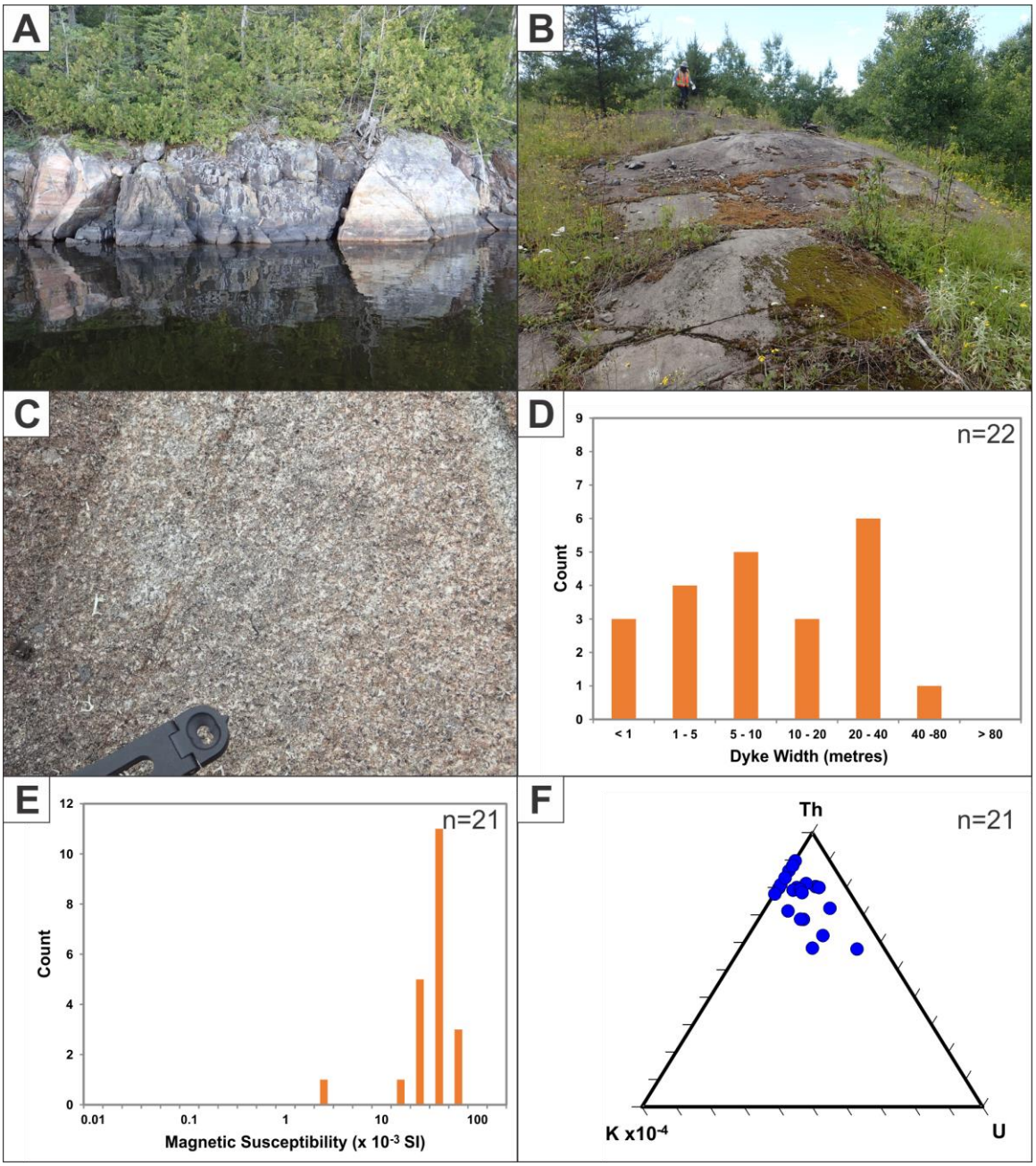

Figure 5.5.2.1: Marathon Dykes – General Properties

A: Overview of Marathon dyke in contact with host tonalite on the shore of Agonzon Lake (Stn 16BH0196, looking N, no scale).

B: Typical outcrop exposure of Marathon dyke exhibiting a rounded geometry and brown weathered colour (Stn 16BH0085, looking SW, person for scale).

C: Representative texture and composition of Marathon dyke, exhibiting a matrix of acicular plagioclase and fine grained mafic minerals, and a grey to brown weathering colour (Stn 16BH0024, looking NW, compass for scale).

D: Histogram showing frequency distribution of Marathon dyke width (n=22).

E: Logarithmic histogram plot of magnetic susceptibility for Marathon dykes (n=21).

F: Ternary plot of gamma ray spectrometer data for Marathon dykes (n=21).

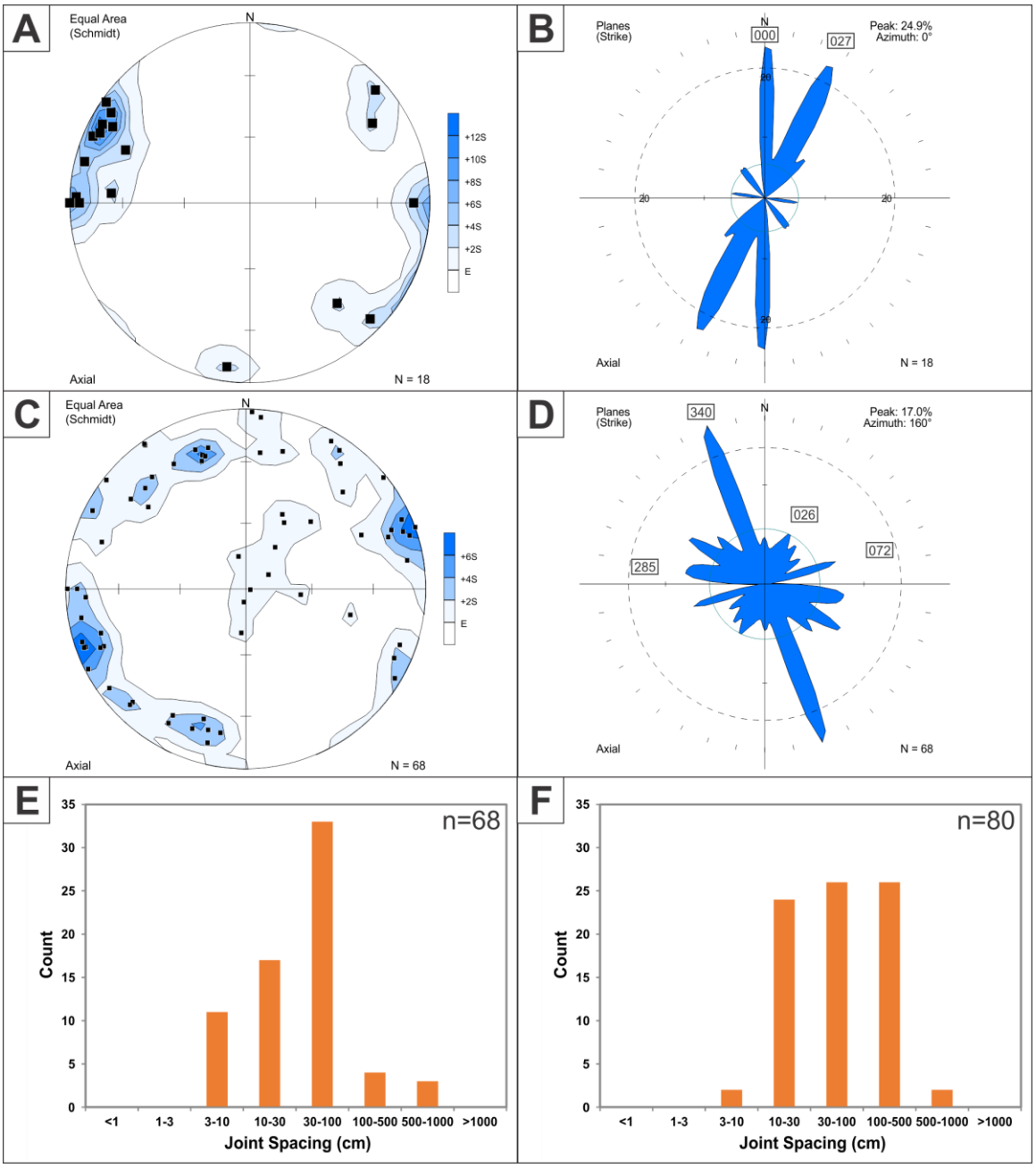

Figure 5.5.2.2: Marathon Dykes – Structures

A: All mapped Marathon dyke contact orientations displayed as equal area lower hemisphere stereonet plot of poles to planes. (n=18).

B: All mapped Marathon dyke contact orientations displayed as rose diagram of trends of planes with orientation of all peaks greater than the expected value E (n=18).

C: All joints measured in Marathon dykes displayed as equal area lower hemisphere stereonet plot of poles to planes. (n=68).

D: All joints measured in Marathon dykes displayed as rose diagram of trends of planes with orientation of all peaks greater than the expected value E (n=68).

E: Histogram showing frequency distribution of joint spacing in Marathon dykes (n=68).

F: Histogram showing frequency distribution of joint spacing in host rocks adjacent to Marathon dykes (n=80).

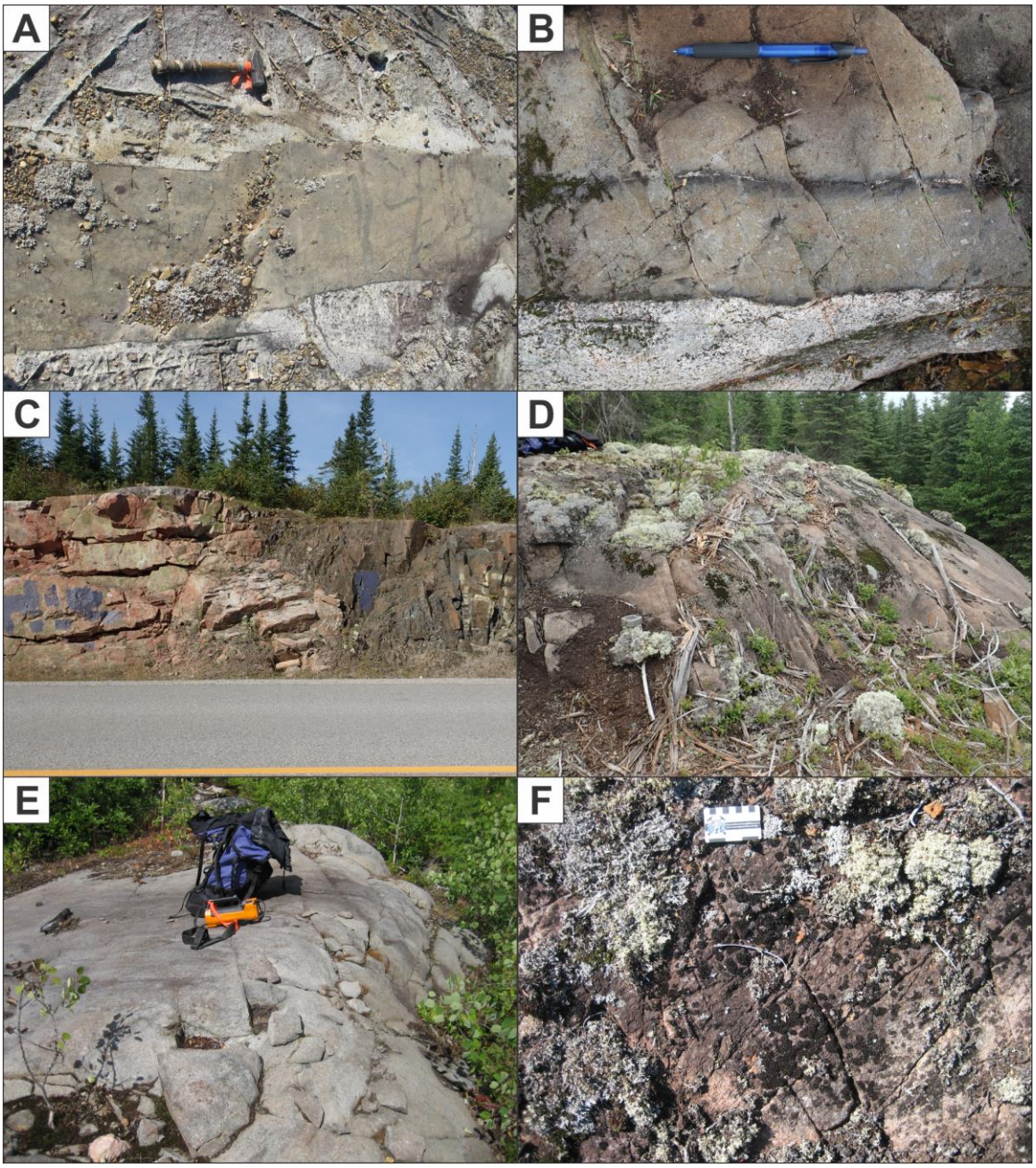

Figure 5.5.2.3: Marathon Dykes – Field Examples of Structural Features

A: Marathon dyke intruding tonalite, exhibiting chilled margins and undeformed dyke contacts. Note deviation in dyke geometry, as it steps to the west, but is not offset along fault (Stn 16CN0007, looking W, hammer for scale).

B: Multiple chilled margins of Marathon dyke, indicating multiple dyke intrusion pulses. Note undeformed dyke contact and closely spaced joints within dyke (likely cooling joints), but not within host diorite (Stn 16CN0066, looking W, pen for scale).

C: Matachewan dyke intruding tonalite in the Barehead Lake fault zone. Both units exhibit intense brittle deformation and pervasive closely spaced jointing (Stn 16BH00193, looking W, highway for scale).

D: Domain of more closely spaced northwest-trending joints within and oblique to Marathon dyke (Stn 16BH0024, looking NW, backpack for scale).

E: Pervasive moderately spaced jointing within Marathon dyke (Stn 16JK0138, looking N, backpack for scale).

F: Pervasive close-spaced jointing within Marathon dyke (Stn 16JK0191, looking NW, scale card for scale).

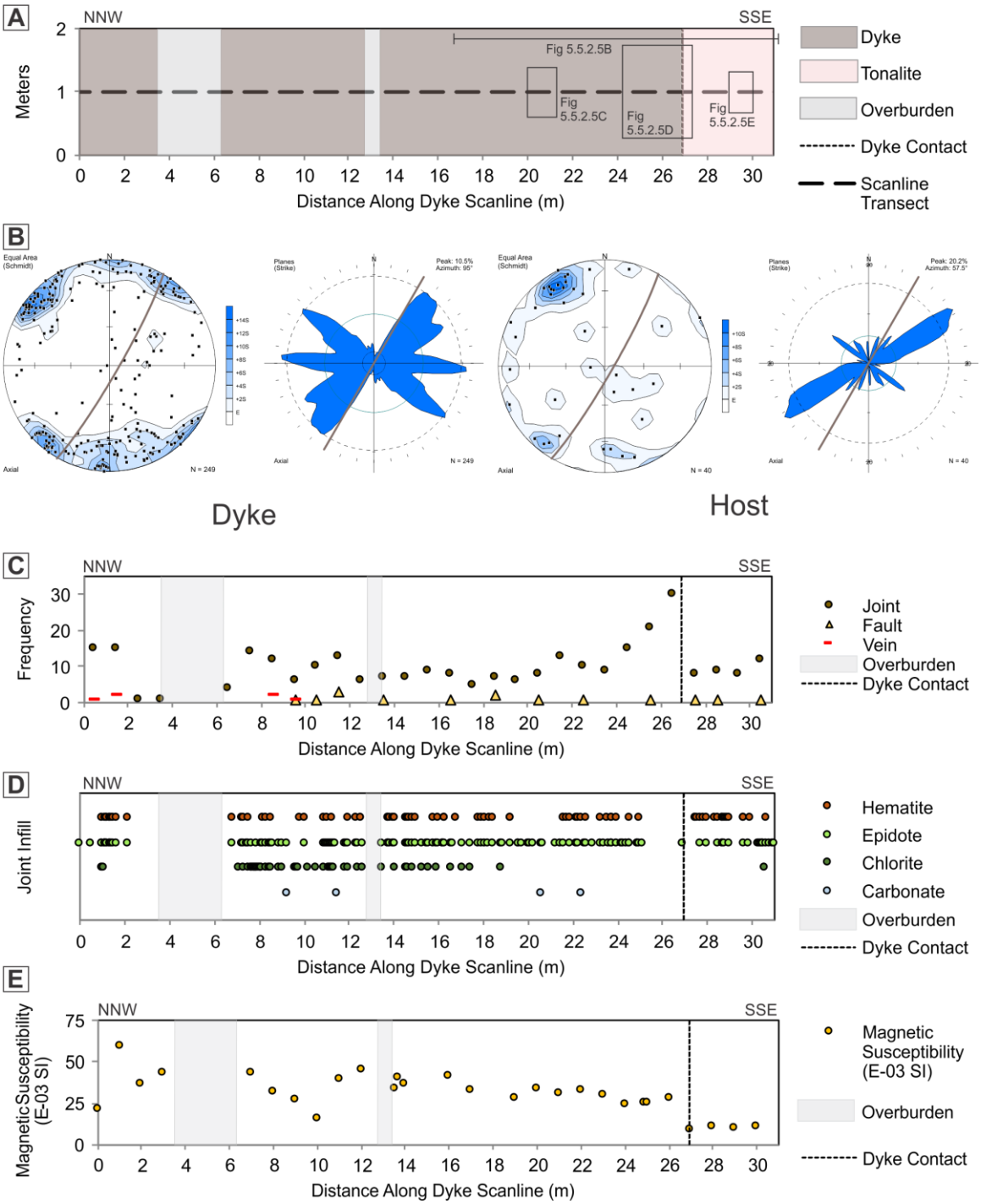

Figure 5.5.2.4: Marathon Dykes – Composite Summary of Scanline Results

A: Schematic overview of the Marathon scanline transect showing dyke, host rock and dyke contacts and location of field photographs.

B: All mapped joints in Marathon dyke and host rock displayed as stereonet (equal area lower hemisphere stereonet plot of poles to planes) and rose diagrams (trends of planes with orientation of all peaks greater than the expected value). Contact of dyke displayed as brown line.

C: Frequency of joints per meter interval along the scanline transect.

D: Distribution of alteration minerals along the scanline transect.

E: Magnetic susceptibility measurements along the scanline transect.

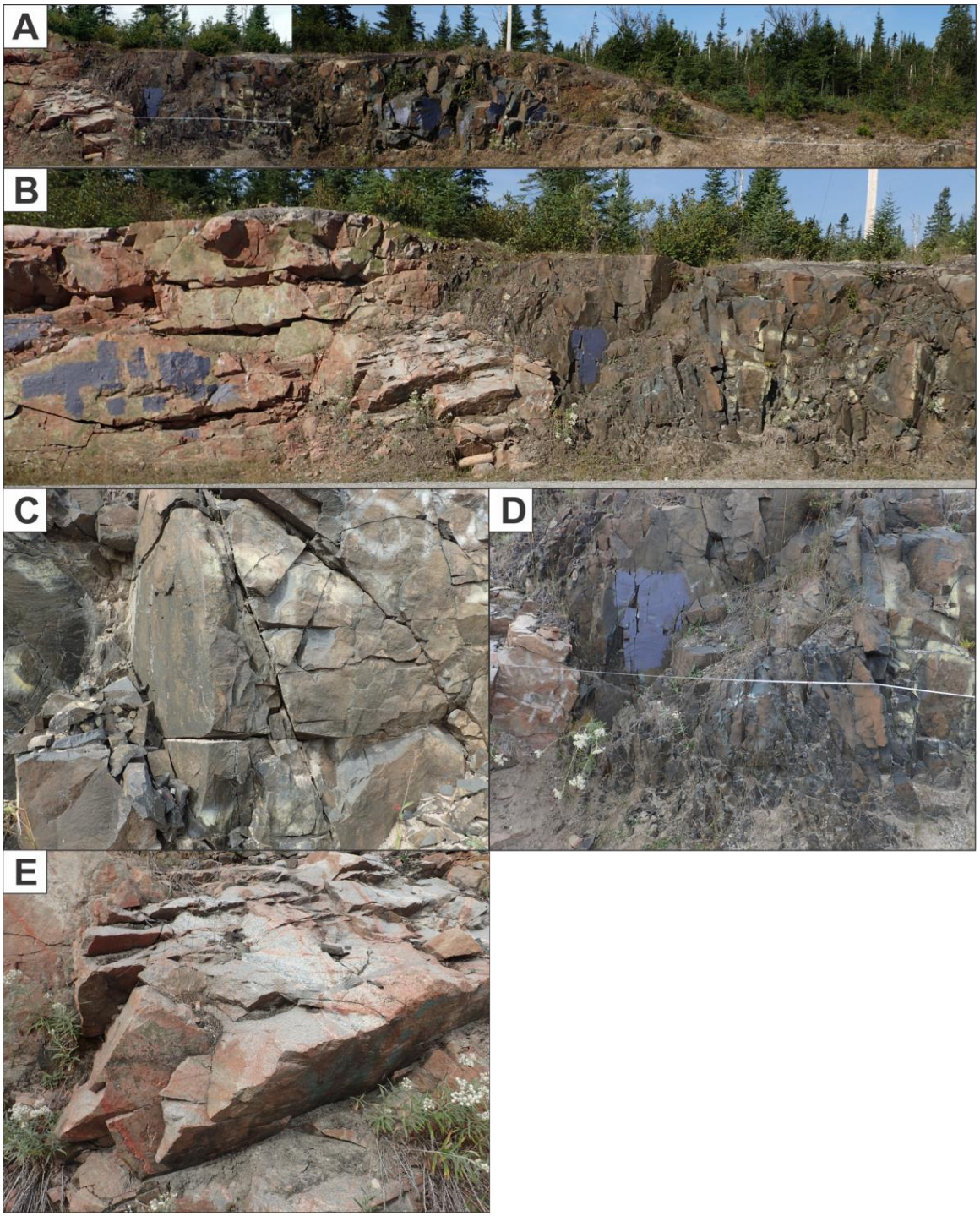

Figure 5.5.2.5: Marathon Dykes – Field Photographs from Scanline Exercise

A: Overview of the Marathon scanline section, corresponding to schematic overview in Fig 5.5.2.4. Photograph has N on the right, opposite to the perspective of the schematic overview (looking WSW, tape measure for scale).

B: Overview of Marathon dyke - host tonalite contact, exhibiting pervasive brittle deformation. Locations of photos in Figure 5.5.2.4A (looking WSW, no scale).

C: Representative pervasively jointed Marathon dyke along the scanline (looking WSW, no scale).

D: Contact between Marathon dyke and host tonalite, exhibiting closely spaced pervasive jointing. (looking WSW, tape measure for scale).

E: Representative pervasively jointed host tonalite along the scanline (looking WSW, no scale).

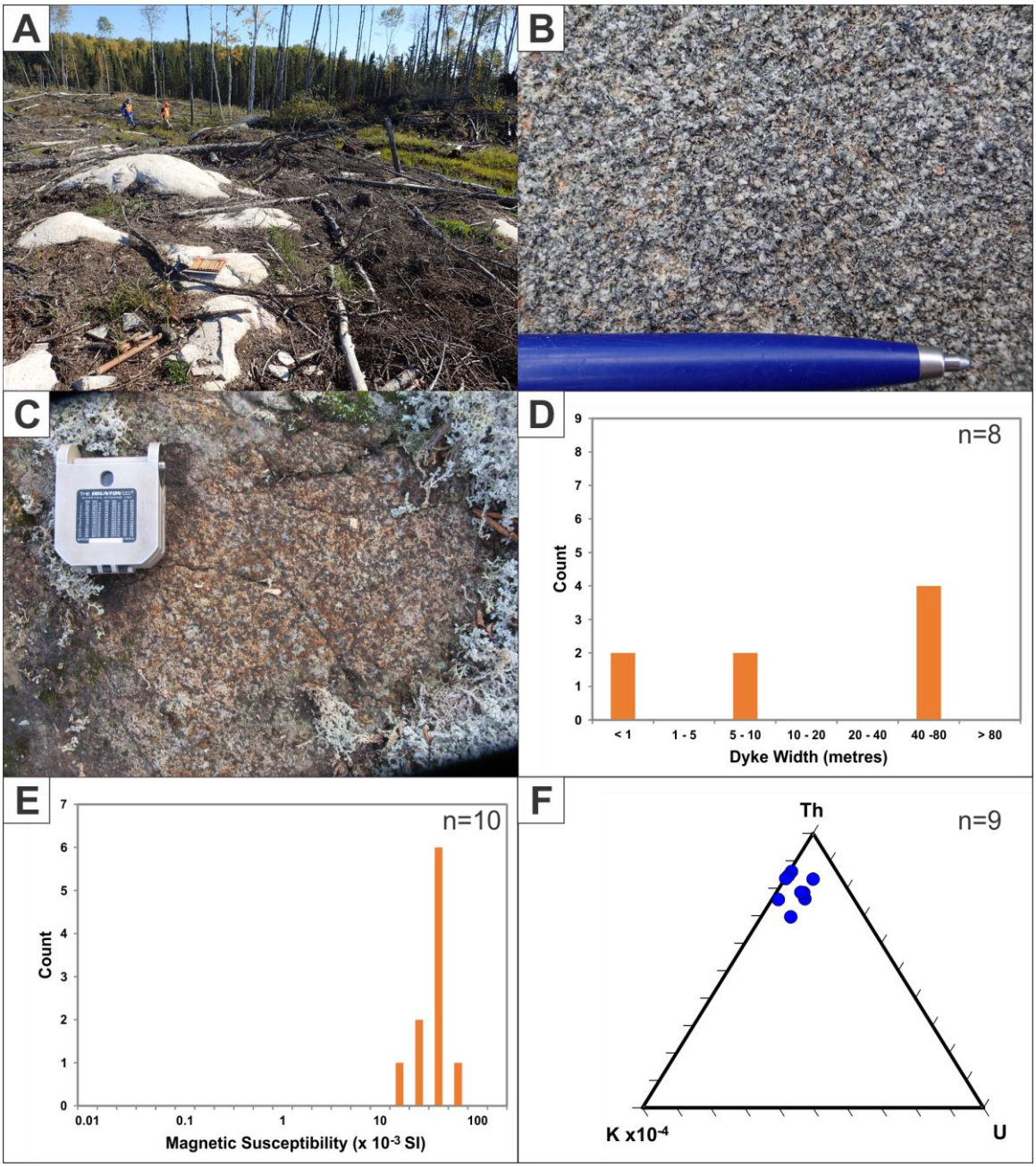

Figure 5.5.3.1: Biscotasing Dykes – General Properties

A: Typical outcrop exposure of Biscotasing dyke forming a series of rounded outcrops. (Stn 16BH0212, looking SE, people for scale).

B: Representative texture and composition of Biscotasing dyke, exhibiting a matrix of acicular plagioclase and fine grained mafic minerals, and a grey to brown lightly weathering colour. (Stn 16BH0075, looking NE, pen for scale).

C: Representative weathered surface of Biscotasing dyke, exhibiting the same texture as described in (B), but a more prominent brown weathered colour. (Stn 16CN0105, looking SW, compass for scale).

D: Histogram showing frequency distribution of Biscotasing dyke width (n=8).

E: Logarithmic histogram plot of magnetic susceptibility for Biscotasing dykes (n=10).

F: Ternary plot of gamma ray spectrometer data for Biscotasing dykes (n=9).

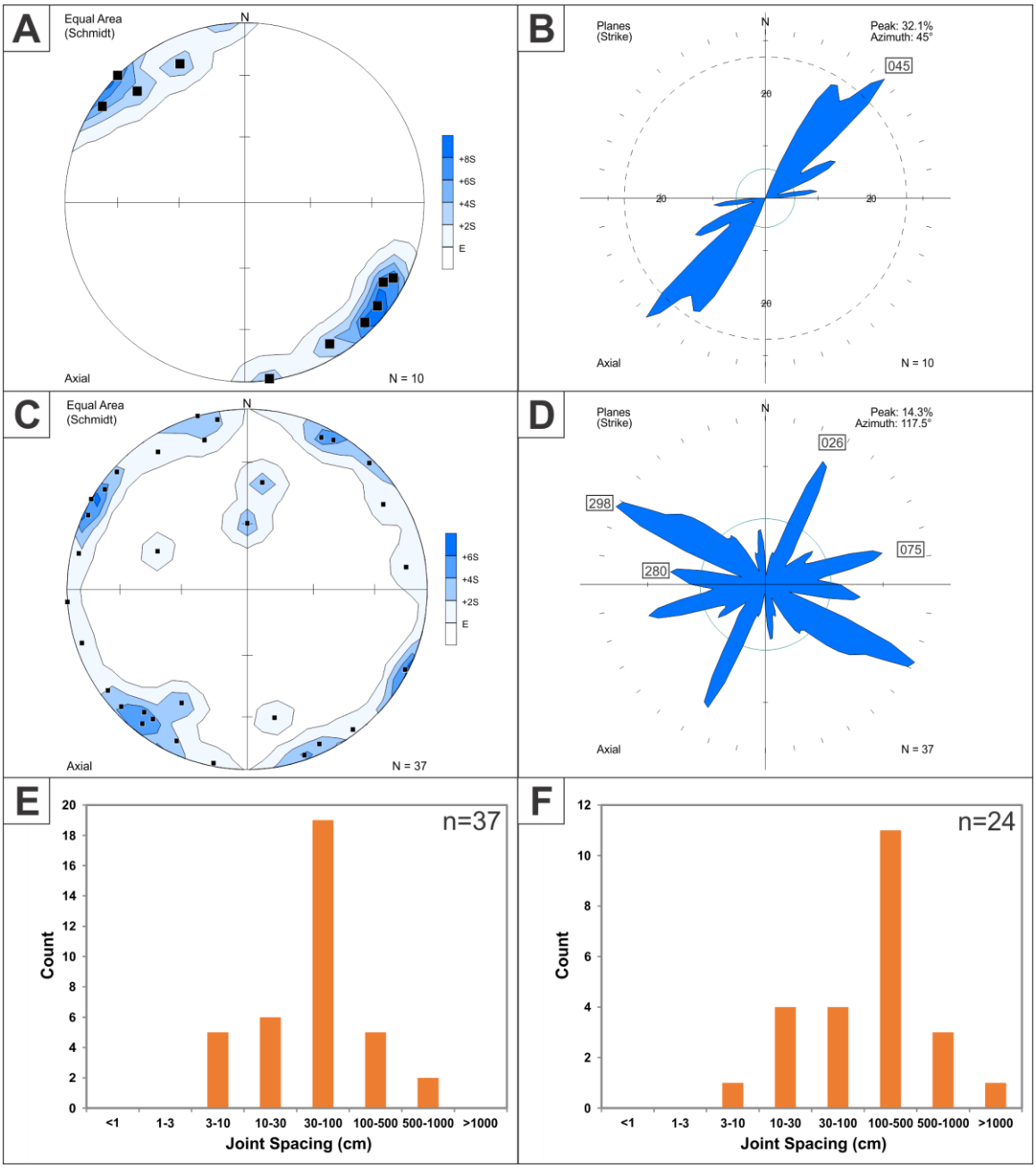

Figure 5.5.3.2: Biscotasing Dykes – Structures

A: All mapped Biscotasing dyke contact orientations displayed as equal area lower hemisphere stereonet plot of poles to planes. (n=10).

B: All mapped Biscotasing dyke contact orientations displayed as rose diagram of trends of planes with orientation of all peaks greater than the expected value E (n=10).

C: All joints measured in Biscotasing dykes displayed as equal area lower hemisphere stereonet plot of poles to planes. (n=37).

D: All joints measured in Biscotasing dykes displayed as rose diagram of trends of planes with orientation of all peaks greater than the expected value E (n=37).

E: Histogram showing frequency distribution of joint spacing in Biscotasing dykes (n=37).

F: Histogram showing frequency distribution of joint spacing in host rocks adjacent to Biscotasing dykes (n=24).

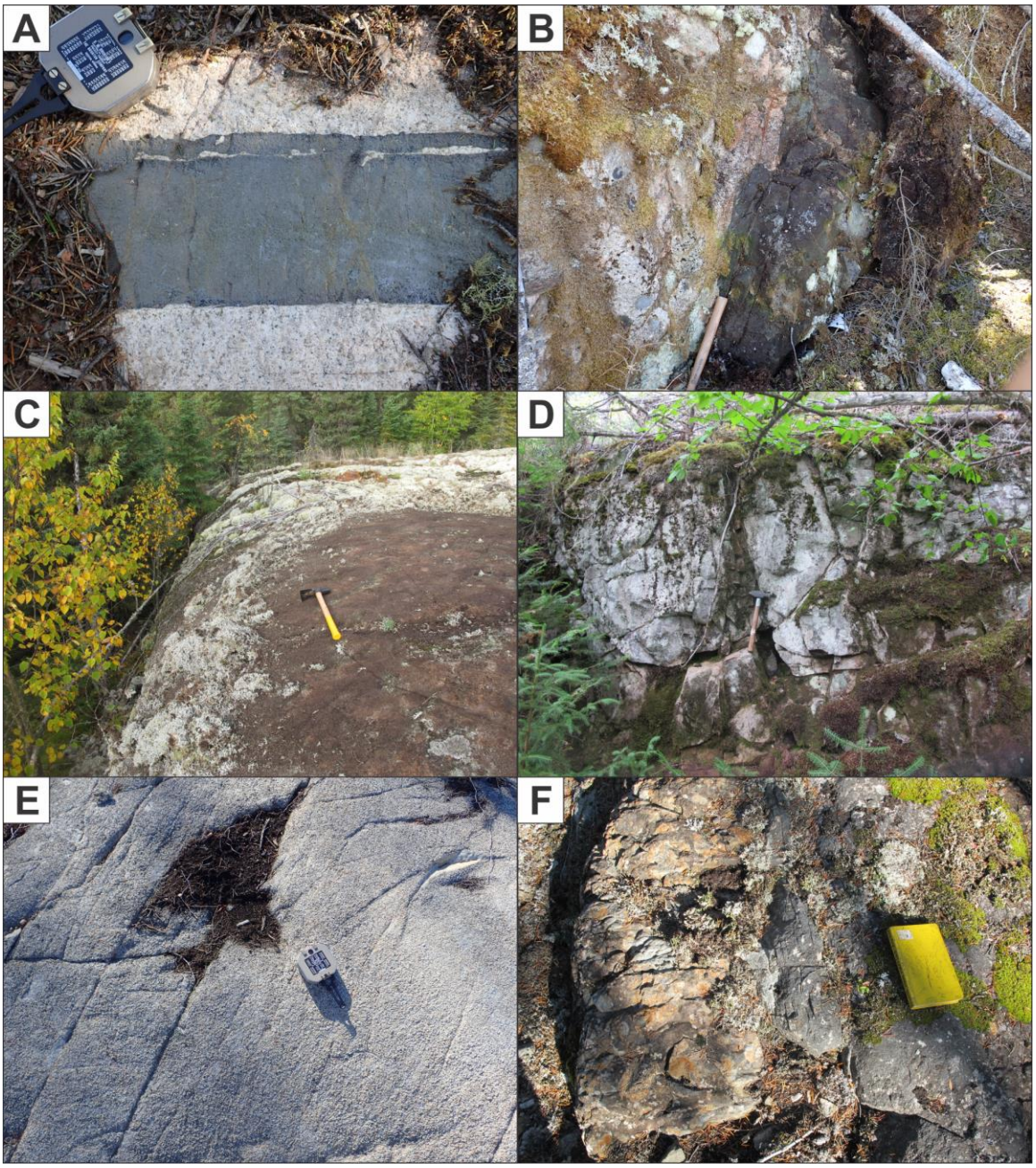

Figure 5.5.3.3: Biscotasing Dykes – Field Examples of Structural Features

A: Chilled, non-deformed margins along contacts of narrow subsidiary Biscotasing dyke intruding tonalite (Stn 16BN0075, looking SE, compass for scale).

B: Sharp jagged contact of Biscotasing dyke with host tonalite, with no brittle deformation or reactivation (Stn 16BH0075, looking SW, hammer for scale).

C: Edge of Biscotasing dyke forming multi-metre tall northeast-trending ridge (Stn 16CN0105, looking NE, hammer for scale).

D: Biscotasing dyke cut by northwest-trending fault (going into page), expressed as closely spaced joints centred around the fault (Stn 16CN0062, looking NW, hammer for scale).

E: Representative Biscotasting dyke exhibiting multiple relatively closely spaced joint sets (relative to the host rock), likely associated with cooling (Stn 16BH0212, looking SW, compass for scale).

F: Increased northeast-oriented fracture frequency in host tonalite (grey rock) within 30 centimetres directly adjacent to dyke (brown rock) and increased jointing in the dyke relative to the host tonalite (Stn 16CN0117, looking NE, book for scale).

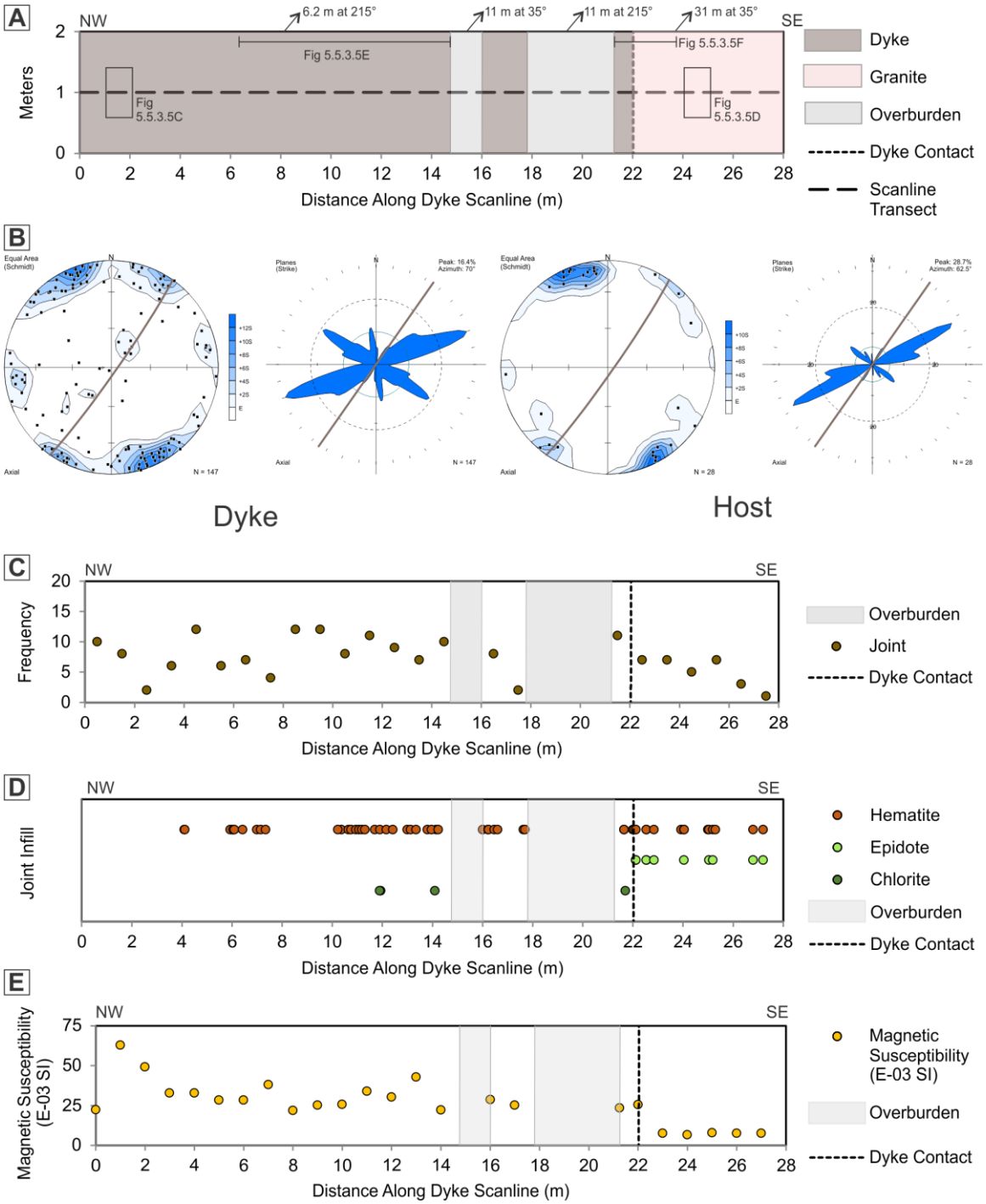

Figure 5.5.3.4: Biscotasing Dykes – Composite Summary of Scanline Results

A: Schematic overview of the Biscotasing scanline transect showing dyke, host rock and dyke contacts and location of field photographs.

B: All mapped joints in Biscotasing dyke and host rock displayed as stereonet (equal area lower hemisphere stereonet plot of poles to planes) and rose diagrams (trends of planes with orientation of all peaks greater than the expected value). Contact of dyke displayed as brown line.

C: Frequency of joints per meter interval along the scanline transect.

D: Distribution of alteration minerals along the scanline transect.

Magnetic susceptibility measurements along the scanline transect.

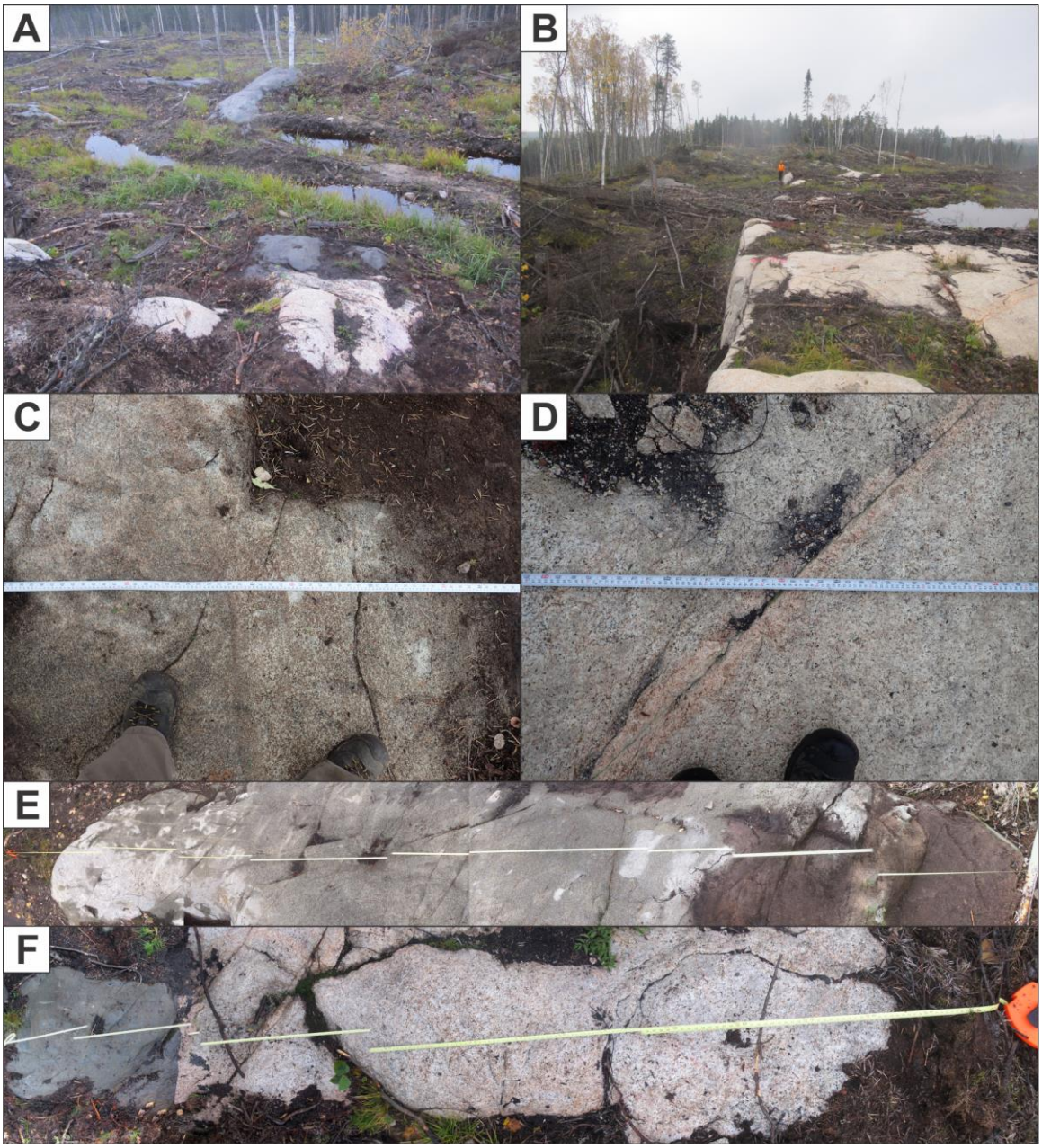

Figure 5.5.3.5: Biscotasing Dykes – Field Photographs from Scanline Transect

A: Overview of portions of the Biscotasing scanline section (looking SE, no scale).

B: Overview of contact of Biscotasing dyke with host granodiorite, forming metre tall scarp along the granite contact (looking SW, no scale).

C: Representative Biscotasing dyke along the scanline. Locations of photos in Figure 5.5.3.4A (looking SW, tape measure for scale).

D: Representative host granodiorite along the scanline, exhibiting hematite alteration along joint (looking SW, tape measure for scale).

E: Representative section of Biscotasing dyke along the scanline (looking SW, tape measure for scale).

F: Contact between Biscotasing dyke and host granodiorite along the scanline (looking SW, tape measure for scale).

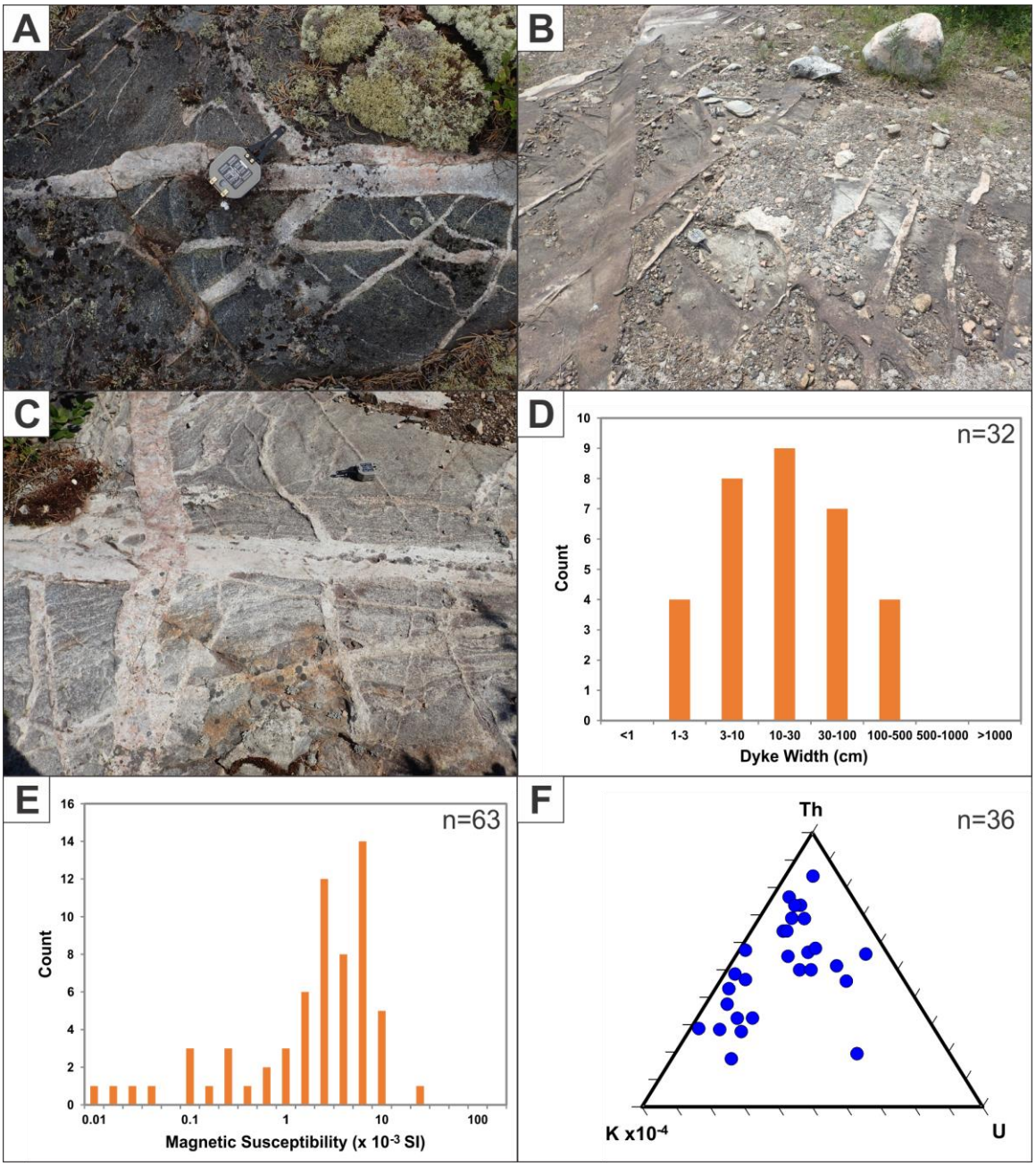

Figure 5.5.4.1: Felsic Dykes – General Properties

A: Outcrop exposure of three sets of felsic granitic dykes intruding gabbro and cut by minor hematite altered fault (Stn 16BH0043, looking NW, compass for scale).

B: Network of three sets of felsic granitic dykes intruding tonalite gneiss (Stn 16BH0058, looking SW, compass for scale).

C: Multiple sets of felsic granitic dykes intruding tonalite gneiss and cut by minor hematite altered fault. Note that the east-trending dyke set both cuts and is cut by the north-trending dyke set (Stn 16BH0121, looking E, compass for scale).

D: Histogram showing frequency distribution of granitoid dyke width (n=32).

E: Logarithmic histogram plot of magnetic susceptibility for granitoid dykes (n=63).

F: Ternary plot of gamma ray spectrometer data for granitoid dykes (n=36).

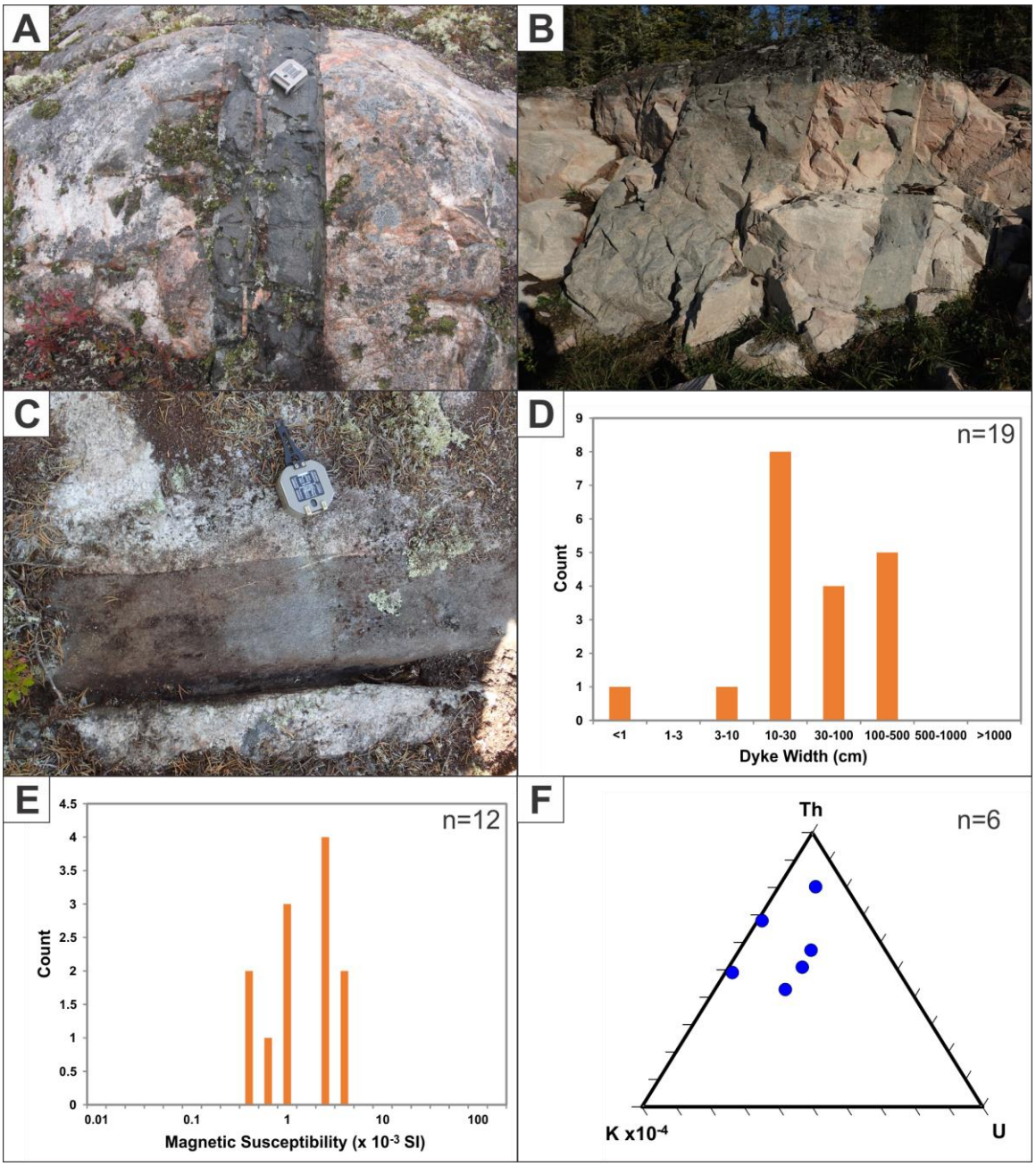

Figure 5.5.4.2: Mafic Dykes – General Properties

A: Dark green to black mafic gabbro dyke intruding tonalite (Stn 16CN0147, looking NE, compass for scale).

B: Outcrop overview of multiple gabbro dykes intruding tonalite (Stn 16BH0259, looking SE, compass for scale).

C: Foliated dark green to black mafic gabbro dyke intruding tonalite (Stn 16BH0115, looking N, compass for scale).

D: Histogram showing frequency distribution of gabbro dyke width (n=19).

E: Logarithmic histogram plot of magnetic susceptibility for gabbro dykes (n=12).

F: Ternary plot of gamma ray spectrometer data for gabbro dykes (n=6).

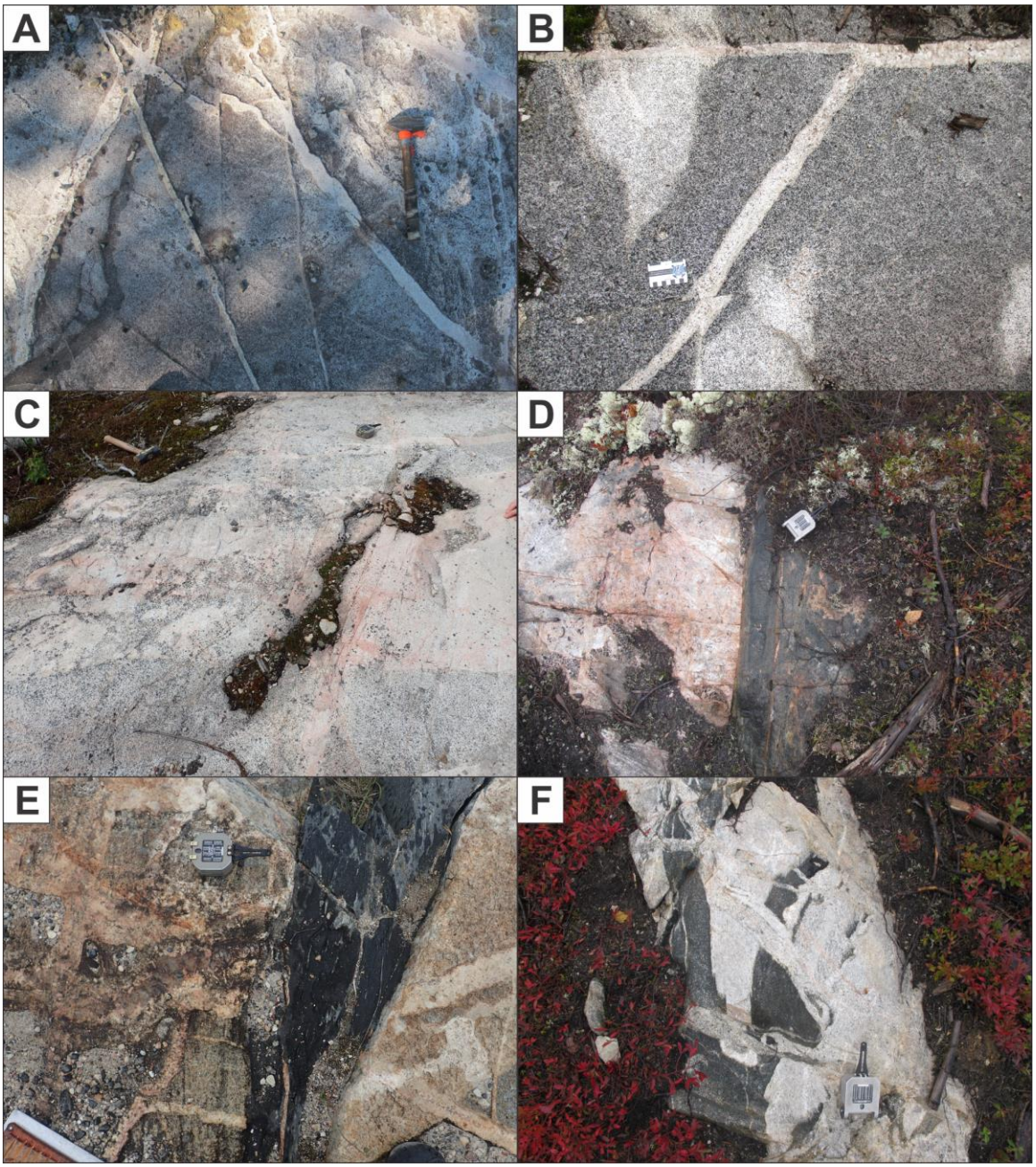

Figure 5.5.4.3: Felsic and Mafic Dykes – Field Examples of Structural Features

A: Network of felsic granitic dykes offset by minor fault with sinistral kinematics (Stn 16CN0007, looking NE, hammer for scale).

B: Felsic granitic dyke offset by epidote chlorite altered minor fault with sinistral kinematics. (Stn 16JK0212, looking SE, scale card for scale).

C: Increased density of joints within felsic dyke relative to host granodiorite. (Stn 16BH0105, looking NW, hammer for scale).

D: Well-foliated contact of gabbro mafic dyke cutting tonalite. (Stn 16CN0147, looking NE, compass for scale).

E: Strongly foliated gabbro mafic dyke intruding tonalite. (Stn 16BH0064, looking W, compass for scale).

F: Sub-angular fragments of gabbro representing a pulled apart gabbro mafic dyke within tonalite. (Stn 16CN0147, looking E, compass for scale).